Protein Engineering of an Industrially-used Lipase

by Ann Kennedy BSc

Thesis submitted to the University of Nottingham for the degree of Doctor of Philosophy, June 2000

To Fred

Contents

Table of Contents.....i
Table of Figures.....v
Abstract.....viii
Acknowledgements.....ix
Abbreviations.....x

CHAPTER 1 Introduction.....1
1.1 Interaction with Lipids.....2
1.1.1 Physical Properties of Lipase Substrates.....2
1.1.2 Interfacial Activation.....4
1.2 Lipase Structure.....7
1.2.1 The α/β Hydrolase Fold.....7
1.2.1.2 Evolutionary Relationships.....10
1.2.2 The Lid.....11
1.2.2.1 Conformational Change.....11
1.2.2.2 Structural basis for substrate selectivity.....12
1.3 Catalytic Mechanism.....14
1.3.1 The Oxyanion Hole.....16
1.4 Substrate Binding Site.....17
1.4.1.1 The binding site of Rhizomucor miehei *and related fungal lipases*.....18
1.4.1.2 The binding site of Candida rugosa *lipase*.....18
1.4.1.3 The binding site of human pancreatic lipase.....18
1.5 Substrate Specificities.....20
1.5.1 Structural Basis for Lipase Enantioselectivity.....21
1.6 Industrial Applications of Lipases.....24
1.6.1 Lipases in Bread Making.....25
1.6.1.1 Making bread.....25
1.6.1.2 Bread staling.....26
1.6.1.3 Lipase as an ingredient in bread.....27
1.6.2 Lipases in the Dairy Industry.....28
1.6.3 Lipases in Detergents.....28
1.6.4 Lipases in the Oleochemical Industry.....29
1.6.4.1 Preparation of soaps and fatty acids.....29
1.6.4.2 Synthesis of structured fats.....29
1.6.4.3 Production of monoacylglycerols.....30
1.6.5 Lipases as Biocatalysts in Organic Synthesis.....31
1.6.6 Protein Engineering of Industrial Lipases.....32
1.7 Research Objectives.....32

CHAPTER 2 Materials and Methods.....34
2.1 General Molecular Biology Methods.....35
2.1.1 Growth and Storage of *E. coli* Bacteria.....35
2.1.2 Alkaline Lysis Fast 'Mini-prep' Method for Preparation of Plasmid DNA.....35
2.1.3 Alkaline Lysis/PEG Precipitation 'Mini-prep.' Method for Preparation of Plasmid DNA Suitable for ABI Sequencing.....36
2.1.4 Alkaline Lysis 'Maxi-prep' Procedure for Isolation of Plasmid DNA.....36
2.1.5 Agarose Gel Electrophoresis.....37
2.1.6 Spectrophotometric Determination of Nucleic Acid Concentration and Purity.....37
2.1.7 Preparation of 'Competent' *E. coli* Cells.....38
2.1.8 Transformation of Competent *E. coli* Cells.....38

2.1.8.1 *Blue/white screening* *38*
2.1.9 Gel Purification of DNA Fragments 39
2.1.10 Restriction Digest of DNA 39
2.1.11 Treatment with Calf intestinal phosphatase 39
2.1.12 Ligation Reaction 40
2.1.13 DNA Sequencing 40
2.1.13.2 *Cycle Sequencing* *41*
2.1.13.3 *Purification of extension products* *42*
2.1.13.4 *Electrophoresis of extension products* *42*
2.2 Generation of Lipase Mutants **42**
2.2.1 RNA Extraction 42
2.2.2 Preparation of cDNA 43
2.2.2.1 *DNase treatment of RNA* *43*
2.2.2.2 *Reverse Transcriptase-PCR* *44*
2.2.2.3 *PCR (of genomic clone)* *45*
2.2.2.4 *TOPO TA Cloning® of cDNA* *45*
2.2.3 Site-Directed Mutagenesis 46
2.2.3.1 *Production of single-stranded DNA* *46*
2.2.3.2 *Phosphorylation of primers* *47*
2.2.3.3 *Annealing conditions* *48*
2.2.3.4 *Synthesis of the complementary DNA Strand* *48*
2.3 Expression of Lipases **49**
2.3.1 Transformation into *Pichia Pastoris* GS115 49
2.3.1.1 *Preparation of DNA* *49*
2.3.1.2 *Spheroplast Transformation Method* *50*
2.3.1.3 *EasyComp transformation method into* Pichia pastoris *51*
2.3.2 Screening Transformants 52
2.3.2.1 *Screening for* AOX1*-disrupted transformants* *52*
2.3.2.2 *Screening for lipase expression on Rhodamine B plates* *52*
2.3.3 Small Scale Expression of Lipase 53
2.3.4 Large Scale Expression of Lipase 53
2.3.4.1 *Expression of* Mut$^+$ *transformants.* *53*
2.3.4.2 *Expression of* Mut^s *transformants* *53*
2.3.5 Preparation of Frozen stocks 54
2.4 Purification of Lipases **54**
2.4.1 Anion-Exchange Chromatography 54
2.4.2 SDS-Polyacrylamide Gel Electrophoresis (PAGE) 54
2.4.2.1 *Sample Preparation* *54*
2.4.2.2 *Gel Electrophoresis* *54*
2.4.2.3 *Western Blotting* *55*
2.4.2.4 *Electro-blot for N-terminal sequencing* *56*
2.4.3 Protein Quantitation 56
2.5 Lipase Activity Assays **57**
2.5.1 Resorufin Ester Assay 57
2.5.2 *para*-Nitrophenyl Acetate (*p*-NPA) Assay 57
2.5.3 Olive Oil Emulsion Assay 57
2.5.4 Measurement of Emulsion Surface Area 58
2.6 Data Analysis **59**

CHAPTER 3 Molecular Modelling and Design of Mutants of Danisco's Lipase 3 ..61
3.1 Introduction **62**
3.1.1 Homology Modelling 62
3.1.2 Modelling Electrostatic Interactions 63
3.1.2.1 *Calculating Electrical Potentials* *64*
3.2 Design of Mutants of Lipase 3 ..... **65**
3.2.1 The Homology Model of Lipase 3 65

3.2.2 Design of 'Glycosylation' Mutants 66
3.2.3 Design of 'Activity Mutants' 67
3.2.3.1 Lipase substrates in dough *67*
3.2.3.2 Stabilisation of the Active Enzyme *67*
3.2.3.3 Stabilisation of Transition State *69*

CHAPTER 4 Production of Genes Coding for Variants of Danisco's Lipase 3 by Site-Directed-Mutagenesis 76
4.1 Introduction 77
4.1.1 Site-Directed *in vitro* Mutagenesis Using Uracil-Containing Single-Stranded DNA 77
4.1.1.1 Isolation of Single-Stranded DNA *77*
4.1.1.2 The dut⁻ ung⁻ *method of mutagenesis* *79*
4.2 Mutagenesis 80
4.2.1 Cloning the Lipase Gene into pBS-KS 80
4.2.2 Isolation of cDNA Coding for Danisco Lipase 3 81
4.2.2.1 RNA extraction *81*
4.2.2.2 Reverse Transcriptase-PCR *82*
4.2.2.3 PCR of genomic clone *82*
4.2.2.4 Cloning Lipase cDNA into the Pichia pastoris *expression vector pHIL-D2* *84*
4.2.3 Site-Directed-Mutagenesis 85
4.2.3.1 Preparation of Uss pHILcLip and pBSLip DNA *85*
4.2.3.2 Synthesis of the mutagenic strand *86*

CHAPTER 5 Expression and Purification of Danisco Lipase 3 Variants from *Pichia pastoris* 90
5.1 Introduction 91
5.1.1 The *Pichia pastoris* Expression System 91
5.1.1.1 Recombination events with GS115 ..... *92*
5.1.1.2 Transformation into Pichia pastoris *95*
5.1.2 MALDI-TOF mass spectrometry 96
5.2 Expression of Lipases 96
5.2.1 Transformation and Expression of Wild-Type Lipase in *Pichia pastoris* 96
5.2.1.1 Spheroplast transformation of wild type pHILcLip and screening of His⁺ recombinants 96
5.2.1.2 Expression of wild type lipase and screening of expression levels from His⁺ recombinant strains 97
5.2.2 Transformation and Expression of Mutant Lipases in *Pichia pastoris* 99
5.2.2.1 Spheroplast transformation of 'activity' mutant pHILcLip DNA and selection for multiple-integrants using 3-AT *99*
5.2.2.2 Expression of 'activity' mutants, and comparison of transformants from EasyComp™ and spheroplast methods of transformation *101*
5.2.2.3 Spheroplast transformation and expression of 'glycosylation' mutants *102*
5.2.3 Large Scale Expression of Lipases 103
5.3 Purification of Lipases 106
5.4 Mass Spectrometry of Lipases 111
5.5 Discussion 119
5.5.1 Purification of 'Glycosylation' Mutant Lipases 120
5.5.2 Mass Spectrometry Analysis of Wild Type and 'Glycosylation' Mutants 120
5.5.2.1 Glycosylation of secreted proteins *120*
5.5.2.2 Mass spectrometry of wild-type Lipase 3 ..... *122*
5.5.2.3 Mass spectrometry of 'glycosylation' mutants of Lipase 3 ..... *123*

CHAPTER 6 Characterisation of Wild type and Mutant Lipases Expressed in *Pichia pastoris* 125
6.1 Introduction 126
6.1.1 Lipase assays 126

6.1.1.1 *Activity in solution (p-NPA assay)* *126*
6.1.1.2 *Activity at the lipid-water interface* *127*
6.2 Assay Conditions **128**
6.2.1 Stability of Olive Oil Emulsions 128
6.2.2 Effect of Calcium Chloride 128
6.2.3 Determination of pH Optima 129
6.2.3.1 *Soluble substrate* *129*
6.2.3.2 *Insoluble substrate* *130*
6.2.4 The Effect of Temperature on Lipase Activity 132
6.3 Specific Activities of Lipases **133**
6.3.1 'Activity' Mutants 134
6.3.2 'Glycosylation' Mutants 135
6.3.3 Wild type *A. niger* 135
6.4 Discussion **135**

CHAPTER 7 Kinetic Analysis of Lipase 3 Variants Expressed in *Pichia pastoris*. 137
7.1 Introduction **138**
7.1.1 Steady-State Kinetics 138
7.1.2 Lipase Kinetics at the Interface 140
7.1.2.1 *Kinetic Constants* *142*
7.1.2.2 *Monolayer Conditions* *143*
7.2 Results **144**
7.2.1 Lipase Activity at the Interface 144
7.2.1.1 *'Activity' mutants with interfacial substrate* *151*
7.2.1.2 *'Glycosylation' mutants with interfacial substrate* *151*
7.3 Discussion **151**
7.3.1 'Activity' mutants 152
7.3.1.1 *T112D E114Q* *152*
7.3.1.2 *W116A and W116A I113W* *153*
7.3.1.3 *H225D* *155*
7.3.2 'Glycosylation' mutants 156
7.3.3 The sigmoidal relationship between initial rates and interfacial surface area 157
7.3.3.1 *Co-operativity* *157*
7.3.3.2 *Co-operativity of lipases?* *162*

CHAPTER 8 Analysis of Danisco's 'Glycosylation' Mutants Expressed in *Aspergillus niger* **168**
8.1 Introduction **169**
8.2 Analysis of 'Glycosylation' Mutants Expressed in *Aspergillus niger* **170**
8.2.1 Specific Activities 170
8.2.2 Kinetic Analysis 171
8.3 Discussion **173**
8.3.1 Kinetic Analysis of 'Glycosylation' Mutants Expressed using *Aspergillus niger* 173
8.3.2 Analysis of Wild Type Lipase 3 Expressed using *Pichia pastoris* 173
8.3.2.1 *Sigmoidal kinetics* *176*
8.3.3 Comparison of Lipases Expressed in *Pichia pastoris* and *Aspergillus niger* 176
8.3.3.1 *Comparison of wild type enzymes* *178*
8.3.3.2 *Co-operativity* *178*

CHAPTER 9 Results of Baking Trials and Final Discussion **182**
9.1 Introduction **183**
9.2 Evaluation of Lipase Mutants Expressed by *Pichia pastoris* in Model Dough Systems and Baking Trials **183**
9.2.1 'Glycosylation' mutants tested in dough and bread 184
9.2.1.1 *Free fatty acid release in dough* *184*
9.2.1.2 *Baking tests* *185*

9.2.2 The T112D E114Q 'activity' lipase mutant tested in dough and bread 187
9.2.3 The *Pichia pastoris* Yeast System for Expressing Lipase 3 Variants 188
9.3 Future Work 189
9.3.1 Kinetic analysis 189
9.3.2 Glycosylation 189
9.3.3 Further Mutants of Lipase 3 190

APPENDIX A Materials, Media and Solutions 193
A1 Suppliers 193
A2 Strain Genotypes 193
A2.1 *E.coli* strains 193
A2.2 *Pichia pastoris* Yeast Strain 193
A3 Media 194
A3.1 Bacterial Media 194
A3.2 Stock Solutions for preparing Yeast Media 194
A3.3 Yeast Media 195
A3.4 Media Additives 196
A4 Solutions for Alkaline Lysis DNA Preparation 197
A5 Agarose Gel Electrophoresis Buffers 197
A6 Restriction Digest Buffers 198
A7 Site-Directed-Mutagenesis Buffers 198
A8 SDS-PAGE Solutions 198

APPENDIX B Lipase3 cDNA Sequence 200

References 202

Table of Figures

Figure 1.1 Aggregation of lipid molecules in aqueous media 4
Figure 1.2 The 'interfacial activation' of a lipase. 5
Figure 1.3 Diagrammatic representation of *Rhizomucor miehei* lipase structures illustrating conformational changes on 'lid-opening'. 6
Figure 1.4 Canonical α/β hydrolase fold and the folds of two lipases. 8
Figure 1.5 (a) The structure of the *Humicola lanuginosa* fungal lipase (*Hl*L) in its native (closed) state, and (b) A Cα diagram of the 'nucleophile elbow' of *Hl*L. 9
Figure 1.6 A diagram of a triacylglycerol molecule showing the stereospecifically numbered carbon atoms of glycerol, labelled sn-1, sn-2 and sn-3. 21
Figure 1.7 The empirical rule for enantiorecognition by *Candida rugosa* lipase: a schematic diagram of the favoured enantiomer for secondary alcohols. 21
Figure 1.8 Phosphonate esters linked to nucleophilic serine mimic the transition state of the acylation step in the lipase reaction mechanism. 22
Figure 2.1 The pCR –TOPO vector. 46
Figure 3.1 Sequence alignment of Danisco Lipase 3 (Lip3) & *Humicola lanuginosa* lipase (*Hl*L). 71
Figure 3.2 Homology modelling of Danisco Lipase 3. 72

Figure 3.3 The α-carbon backbone of the Danisco Lipase 3 homology model and potential sites for N-glycosylation. 73
Figure 3.4 Mutants of Danisco Lipase 3 designed to improve activity by pushing equilibrium towards an 'open' lid. 74
Figure 3.5 A diagram of the Danisco Lipase 3 homology model showing the potential field of a simple transition state model. 75
Figure 4.1 Synthesis of phagemid single-stranded DNA. 78
Figure 4.2 Restriction map of Danisco's primary *lipA* clone (pLIP4). 80
Figure 4.3 The pBluescript vector from Stratagene. 81
Figure 4.4 Agarose gel electrophoresis of RNA extracted from *Aspergillus niger* mycelia that over-expresses Danisco's Baking Lipase 3. 82
Figure 4.5 Agarose gel electrophoresis of RT-PCR reactions showing the isolation of lipase cDNA. 83
Figure 4.6 The pHIL-D2 *Pichia pastoris* expression vector. 85
Figure 4.7 Agarose gel of uracil-rich single-stranded DNA preparations of (a) pHILcLip and (b) pBSLip. ..86
Figure 4.8 Agarose gel electrophoresis of mutagenesis reactions using pBSLip single-stranded DNA and 'glycosylation' mutant primers. 88
Figure 5.1 The generic structure of a *Pichia* expression vector. 93
Figure 5.2 Gene insertion at *his4*. 94
Figure 5.3 Gene replacement at *AOX1* in GS115. 94
Figure 5.4 SDS-PAGE of supernatants from small-scale expression of wild-type lipase *in Pichia pastoris* GS115. 99
Figure 5.5 Rhodamine B plate assay for detection of His^+ GS115 transformants expressing lipase. 101
Figure 5.6 SDS-PAGE of *Pichia pastoris* supernatants from large-scale expression of mutant and wild-type Lipase 3. 105
Figure 5.7 SDS-PAGE of anion-exchange chromatography fractions 31-45 from the purification of wild type Lipase 3. 107
Figure 5.8 FPLC HiTrap Q anion-exchange separation of wild type lipase from *Pichia pastoris* culture supernatant. 108
Figure 5.9 FPLC HiTrap Q anion-exchange separation of a 'glycosylation' mutant of Lipase 3 from *Pichia pastoris* culture supernatant. 108
Figure 5.10 SDS-PAGE of anion-exchange chromatography fractions from purification of 'activity' mutants of Lipase 3. 109
Figure 5.11 SDS-PAGE of anion-exchange chromatography fractions from purification of 'glycosylation' mutants of Lipase 3. 110
Figure 5.12 MALDI-TOF Mass Spectrometry of wild type and 'glycosylation' mutants of Danisco's Lipase 3. 112

Figure 5.13 The structures of typical glycosylation groups attached to proteins. 122
Figure 6.1 Effect of pH on hydrolytic activity of (a) wild type and 'activity' mutant lipases and (b) 'glycosylation' mutant lipases with soluble substrate. 130
Figure 6.2 Effect of pH on hydrolytic activity of (a) wild type and 'activity' mutant lipases and (b) 'glycosylation' mutant lipases with insoluble, emulsified substrate. 131
Figure 6.3 The effect of temperature on activity of wild type Lipase 3 (in *Pichia pastoris* supernatant). 132
Figure 6.4 The effect of temperature on activity of wild type Lipase 3 iso-forms separated by anion exchange chromatography. 133
Figure 7.1 Proposed model for the action of a soluble enzyme at an interface. 141
Figure 7.2 A kinetic model for lipase catalysis. 141
Figure 7.3 Typical graphs for measurement of lipase initial rates with emulsified olive oil using a pH-stat controller. 146
Figure 7.4 Kinetic analysis of lipase variants using olive oil emulsion substrate. 147
Figure 7.5 A Lineweaver–Burk plot for wild-type Lipase 3 (expressed in *Pichia pastoris*) with olive oil substrate. 149
Figure 7.6 A Hill plot for wild-type lipase (expressed in *Pichia pastoris)* with olive oil substrate. 150
Figure 7.7 Analysis of kinetic curves, using three different concentrations of wild type Lipase 3 (from expression in *Pichia pastoris*). 166
Figure 13.1 Effect of varying the surface area of an olive oil emulsion substrate on the activity of Danisco's 'glycosylation mutants' (expressed in *A. niger*) and wild type lipases (expressed in *Pichia pastoris* and *A. niger*). 171
Figure 13.2 Effect of varying the amount of olive oil emulsion substrate on activity of wild type lipase expressed in *Pichia pastoris,* where average emulsion particle size = 0.93 μm. 175
Figure 13.3 Effect of varying the amount of olive oil emulsion substrate on activity of wild type lipase expressed in *Pichia pastoris,* where average emulsion particle size = 0.43 μm. 175
Figure 13.4 Hill plots for the wild type lipases expressed in *Pichia pastoris* and *Aspergillus niger.* 180
Figure 14.1 Fatty acid release in model dough with *Pichia* expressed lipase mutants. 185
Figure 14.2 Fatty acid release in model dough with *Pichia* expressed wild type and T112D E114Q mutant lipase. 187

Abstract

Lipase 3 is a fungal lipase produced industrially for use as a dough-conditioning enzyme in bread making. Mutants of Lipase 3 were designed to improve enzyme specific activity and to prevent N-linked glycosylation, which was found to cause a drop in activity on industrial-scale production. These were based on three-dimensional model structures of Lipase 3 in 'open' and 'closed' conformational states derived from crystallographic data of fungal lipases sharing high sequence homology.

Lipase variants were expressed and secreted by *Pichia pastoris* yeast and purified by anion-exchange chromatography, which allowed the separation of two active isoforms. Analysis of the 'glycosylation' mutants by SDS-PAGE and MALDI-TOF mass spectrometry implied that mutation of N-linked glycosylation sites prevented attachment of oligosaccharide groups to these sites. Mutants were characterised by measurement of specific activities with soluble and emulsified substrates and determination of kinetic constants with emulsified substrate. None of the 'activity' mutants showed improved activity over wild type, and the significant drop in activity with emulsified substrate on mutation of a 'lid' tryptophan residue indicated that this residue was required for interaction with long-chain triacylglycerol substrates. Specific activities and kinetic constants measured for the 'glycosylation' mutants did not differ significantly from those of the wild type enzyme.

Sigmoidal kinetic curves were observed for lipases expressed in *Pichia pastoris* and *Aspergillus niger* with emulsified substrate. Co-operativity was measured using the Hill plot and found to be positive. The possibility of a kinetic mechanism, rather than an allosteric mechanism (involving interactions between ligand binding sites), for co-operativity is discussed.

Acknowledgements

I would firstly like to thank my project supervisors, Ian Connerton and Jim Warwicker for their help and guidance throughout my PhD. Secondly my sponsors Danisco, who provided the opportunity for me to work on this project. Also, the people in the Protein Engineering department of the IFR who taught me several of the techniques I needed, in particular Niki Cummings and Mark Taylor. I am very grateful to the people at Danisco who were involved with the project and provided valuable help when required; Susan Madrid, Jørn Mikkelsen, Charlotte Poulson and Jørn Børch Søe.

Finally, many thanks to my family (Mum, Dad, Mark, Angela, Julie, John and Helena) and friends for their support, and most thanks of all to Fred.

Abbreviations

°C	degrees Celsius
A	Alanine (one-letter code)
Ala	Alanine (three-letter code)
AMV	Avian Myeloblastosis Virus
APS	ammonium persulphate
Arg	Arginine (three-letter code)
Asp	Aspartic acid (three-letter code)
ATP	adenosine triphosphate
BCIP	5-bromo-4-chloro-3-indolyl phosphate
bp	base pair
BSA	bovine serum albumin
C	Cysteine (one-letter code)
cccDNA	covalently closed circular DNA
cDNA	complementary DNA
CIP	calf intestinal phosphatase
*Cr*L	*Candida rugosa* lipase
C-terminus	carboxyl terminus of a protein
CTP	cytidine triphosphate
Cys	Cysteine (three-letter code)
d	2' deoxy
D	Aspartatic acid (one-letter code)
Da	Dalton
ddNTP	dideoxynucleotide triphosphate
DEPC	diethylpyrocarbonate
dH2O	distilled water
DMSO	dimethyl sulphoxide
DNA	deoxyribonucleic acid
DNase	deoxyribonuclease
dNTP	2' deoxyribonucleotide 5' triphosphate
ds	double stranded (DNA)
DTT	dithiothreitol
dut	mutation of *E. coli* host strain, resulting in inactivation of dUTPase
E	Glutamic acid (one-letter code)
E. coli	*Esherichia coli*

Eco RI	restriction enzyme cutting at G˘AATTC
EDTA	ethylene diamine tetra-acetic acid
g	gram
g	gravity (Relative Centrifugal Force)
Gal	galactose
GalNAc	N-acetylgalactosamine
Gln	Glutamine (three-letter code)
Glu	Glutamic acid (three-letter code)
GTP	guanosine triphosphate
H	Histidine (one-letter code)
HCl	hydrochloric acid
His	Histidine (three-letter code)
$His^{+/-}$	Phenotype of *Pichia pastoris* referring to histidinol dehydrogenase activity.
*Hl*L	*Humicola lanuginosa* lipase
HPLC	high pressure liquid chromatography
HRP	horse radish peroxidase
I	Isoleucine (one-letter code)
Ile	Isoleucine (three-letter code)
IPTG	isopropyl-ß-D-thiogalactoside
ITP	inosine triphosphate
kb	kilobase pair
k_{cat}	catalytic constant (or turnover number)
KCl	potassium chloride
kD	kilodalton
KH_2PO_4	potassium di-hydrogen orthophosphate
Km	Michaelis constant
L	Leucine (one-letter code)
lacZ	β-galactosidase gene
Leu	Leucine (three-letter code)
LipA	Danisco Lipase 3 gene
M	molar
Man	mannose
mA	milliamperes
MCS	multiple cloning site
$MgCl_2$	magnesium chloride
ml	millilitre

mol	mole
MOPS	3-[N-Morpholino] propanesulphonic acid
mRNA	messenger RNA
$Mut^{+/S}$	Methanol utilisation phenotype of *Pichia pastoris* GS115.
Na_2HPO_4	disodium hydrogen orthophosphate
NaCl	sodium chloride
NBT	nitroblue tetrazolium
NC-IUBMB	Nomenclature Committee of the International Union of Biochemistry and Molecular Biology.
Not I	restriction enzyme cutting at GC˅GGCCGC
N-terminus	amino terminus of a protein
oc	open circular DNA
PAGE	polyacrylamide gel electrophoresis
PBS	phosphate buffered saline
PCR	polymerase chain reaction
PEG	polyethylene glycol
phage	bacteriophage
p-NPA	*para*-nitrophenyl acetate
Pst I	restriction enzyme cutting at CTGCA˅G
PVDF	polyvinylidene difluoride
Q	Glutamine (one-letter code)
R	Arginine (one-letter code)
*Rd*L	*Rhizopus delemar* lipase
resorufin ester	1,2-O-Dilauryl-rac-glycero-3-glutaric acid-resorufin ester
RF	replicative form
*Rm*L	*Rhizopus miehei* lipase
RNA	ribonucleic acid
RNase	ribonuclease
*Ro*L	*Rhizopus oryzae* lipase
rpm	revolutions per minute
RT	reverse transcriptase
S.A.	sialic acid
Sac I	restriction enzyme cutting at GAGCT˅C
SDS	sodium dodecyl sulphate
ss	single stranded (DNA)
T	Threonine (one-letter code)

TAE	tris acetate EDTA buffer
TBE	tris borate EDTA buffer
TEMED	N,N,N',N'-tetramethyl ethylene diamine
Thr	Threonine (one-letter code)
Tm	melting temperature
Tris	tris (hydroxymethyl) aminomethane
Trp	Tryptophan (three-letter code)
TTP	thymidine triphosphate
U	uracil
ung⁻	mutation of *E. coli* host strain, resulting in inactivation of uracil N-glycosylase
UV	ultraviolet
v	initial velocity
V	volt
V_{max}	maximum velocity
v/v	volume for volume
W	Tryptophan (one-letter code)
w.t.	wild type
w/v	weight for volume
XGal	5-bromo-4-chloro-3-indoyl-β-D-galactopyranoside
$ZnCl_2$	zinc chloride

CHAPTER 1 Introduction

Lipases (EC 3.1.1.3) are carboxylic ester hydrolases. Whilst they are able to accept a wide range of different carboxylic esters, they show higher specific activities toward glyceridic substrates and have the systematic name 'triacylglycerol acylhydrolase' [assigned by the Nomenclature Committee of the International Union of Biochemistry and Molecular Biology (NC-IUBMB): http://www.chem.qmw.ac.uk/iubmb/enzyme/], (Sarda and Desnuelle, 1958, Ferrato *et al.* 1997).

Lipases are present in animals, plants and micro-organisms where they are responsible for the breakdown of triacylglycerols used to store chemical energy (Desnuelle, 1972). They can catalyse the hydrolysis or transesterification of triacylglycerol molecules depending on the solvent system used (Scheme 1) and are able to accept a wide range of unnatural substrates (Schmid and Verger, 1998). A unique feature of these enzymes is the ability to act at lipid-water interfaces, as their usual substrates (neutral lipids) are often insoluble (Desnuelle, 1972). Their versatility and high regio- and enantio-selectivities have led to a number of potential applications in industry and make them useful biocatalysts in organic syntheses (Jaeger and Reetz, 1998). Lipases are ideal enzymes for industrial use as they can be produced in large quantities from both natural and recombinant sources, particularly fungal and microbial. More recently, genetic engineering techniques have allowed optimisation of expression levels and of lipase properties to specialise them for particular uses (Schmid and Verger, 1998).

Scheme 1 Hydrolysis and esterification reactions catalysed by lipases. Hydrolysis of triacylglycerols results in the generation of diacylglycerols, which are hydrolysed to monoacylglycerols and then glycerol.

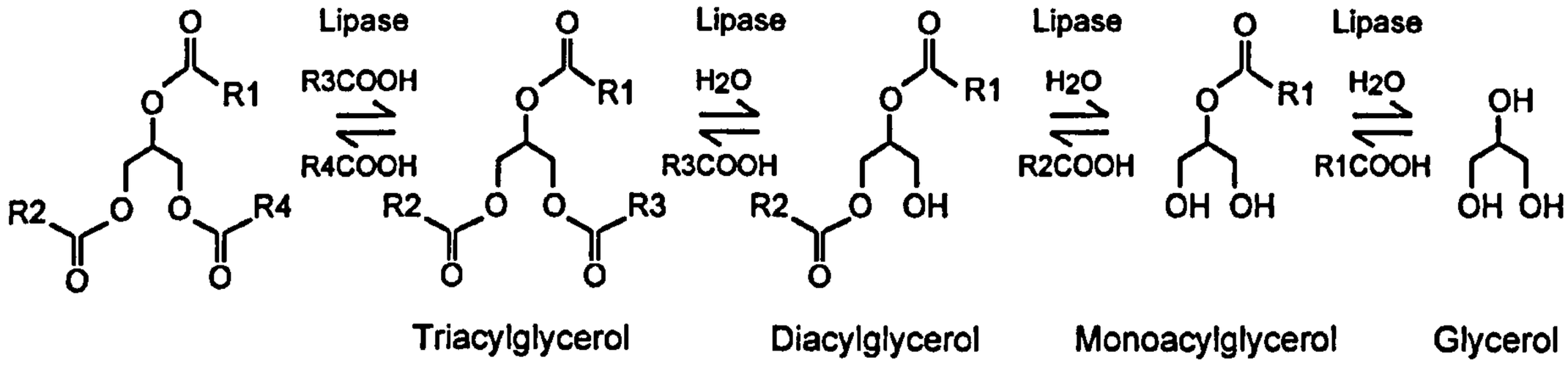

1.1 Interaction with Lipids

1.1.1 Physical Properties of Lipase Substrates

The usual substrates of lipases are neutral lipids, in particular long-chain triacylglycerols. Triacylglycerols are amphiphilic due to the presence of polar groups that give part of the molecule a degree of hydrophilicity, despite their being essentially hydrophobic. These

polar groups are ester bonds in acylglycerols and the hydroxy groups of mono- and di-acylglycerols. 'Polar lipids' tend to orientate in water so that the polar groups associate with water molecules while the non-polar 'tails' associate with each other by hydrophobic interactions. The primary driving force for the insolubility of lipids in water is the large positive free energy associated with the transfer of hydrocarbon moieties from an aqueous solution to a non-aqueous phase ("the hydrophobic effect"). The diversity of phase structures displayed by biological lipids are determined by many other interactions including van der Waals interactions, hydrogen bonding and electrostatic interactions, as well as their basic insolubility. Lipids have been classified according to their behaviour in water, and polar lipids divided into three classes (Small, 1968).

Class I polar lipids are insoluble, non-swelling amphiphilic lipids. Long chain tri- and di-acylglycerols (with acyl chains of 12 or more carbon atoms) are in this class. The predominance of hydrophobic chains in their structure means they are almost completely non-polar and so tend to associate in water to form oil droplets where the surface area is minimal. On the surface they can be spread to form stable monomolecular films. They do not swell in water, as they are virtually insoluble, but possess some surface solubility as demonstrated by their ability to form stable monolayers. Polar lipids (or proteins) introduced into such a system can act as 'surface active agents' by burying their hydrophobic groups in the triacylglycerol droplets with their polar groups at the surface, preventing the droplets from coalescing and creating a more stable, emulsion.

Class II consists of insoluble, swelling amphiphilic lipids. Fatty acids and monoacylglycerols are in this class. On the surface of water they can spread to form stable monolayers, and in bulk they become hydrated (swell) to form well-defined liquid crystalline phases such as lamellar, hexagonal and cubic structures. The predominant phase depends on water content and temperature. Swelling only occurs at temperatures high enough to render the hydrocarbon chains partly liquid and will depend on the chain length, saturation, branching and substitution.

Class III polar lipids are soluble amphiphiles and include short chain triacylglycerols, and ionised fatty acids. These are partly soluble in water and can aggregate to form micelles in equilibrium with monomers. Above a critical micellar concentration (CMC) the number and size of these aggregates increases without significantly altering the concentration of single molecules. This class of polar lipid are capable of solubilizing other classes of

lipids. They form unstable monolayers at the air-water interface and demonstrate an equilibrium between molecules in the bulk phase and those on the surface.

Lipase substrates can therefore exist in aqueous environments either as an isotropic solution in the form of monomers, micelles and adsorbed monolayers, or, as a turbid emulsion, which appears beyond the solubility limit (Figure 1.1). Monomeric and aggregated forms of lipase substrate usually coexist in a complex equilibrium (Ferrato *et al.* 1997).

Figure 1.1 Aggregation of lipid molecules in aqueous media. Schematic representation of various physicochemical states of lipase substrates in water. Monomers, micelles, emulsion and adsorbed monolayer co-exist in equilibrium. Lipid molecules are represented with polar 'heads' (filled circles) and hydrophobic 'tails' (straight lines). (Reproduced from Ferrato *et al.* 1997)

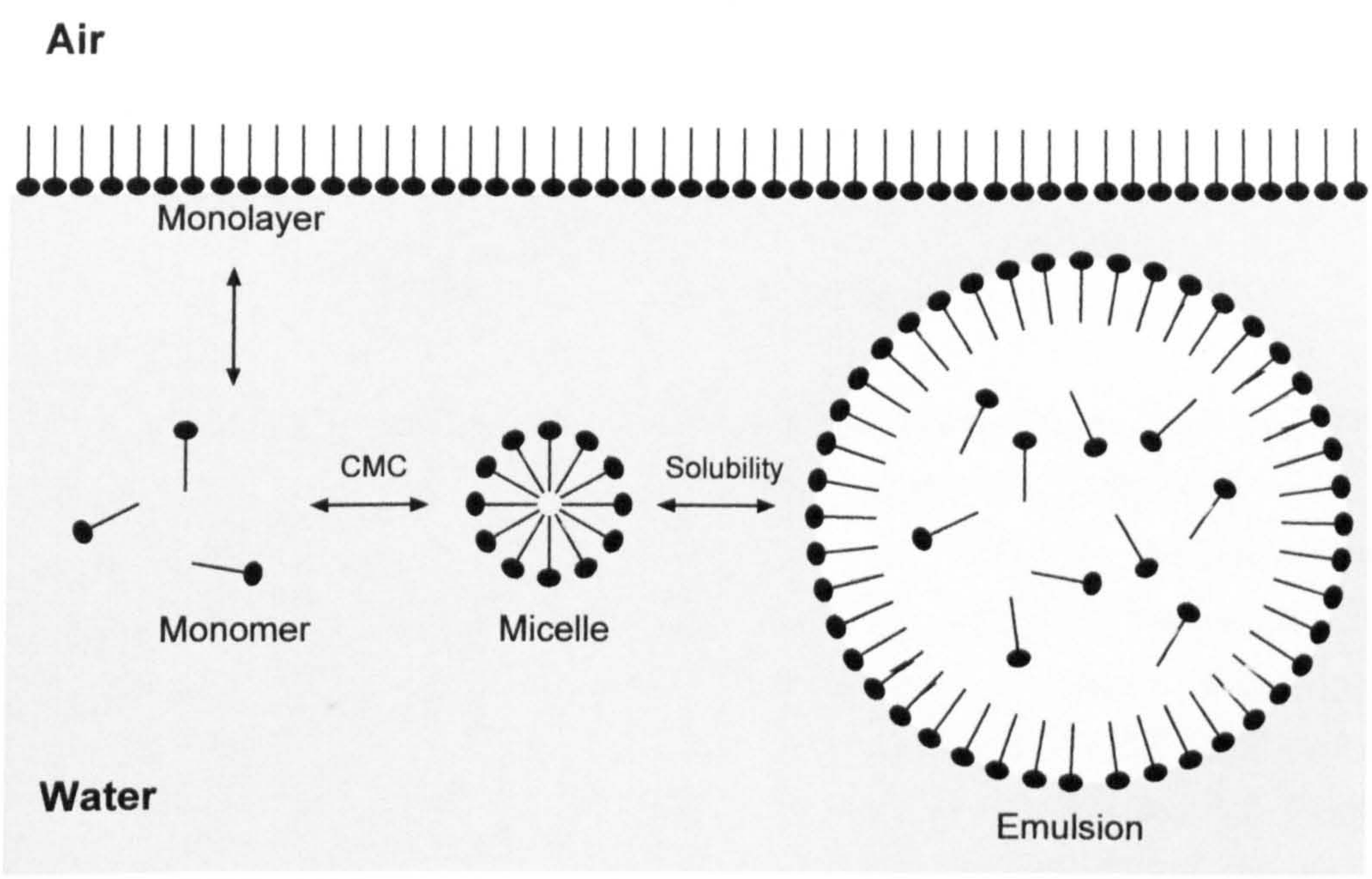

1.1.2 Interfacial Activation

Long before structural information from crystallographic studies became available, the adsorption of lipases to hydrophobic interfaces was observed and the phenomenon of 'interfacial activation' demonstrated (Sarda *et al.* 1957, Sarda and Desnuelle, 1958). Interfacial activation is the term given to the dramatic increase in lipase activity seen when substrate concentration exceeds its solubility limit and it is a characteristic feature of many lipases (Figure 1.2). The ability of lipases to catalyse ester hydrolysis at lipid-water interfaces distinguishes them from esterases (which catalyse the hydrolysis of water soluble esters only).

Figure 1.2 The 'interfacial activation' of a lipase. Comparison of the kinetic behaviours of an esterase (horse liver esterase) and a lipase (porcine pancreatic lipase) on catalysing the hydrolysis of a partly soluble triacylglycerol substrate (triacetin). Hydrolysis rate is shown as a function of substrate concentration, which is expressed in multiples of saturation. A line indicates the solubility limit of the substrate. (Reproduced from Sarda and Desnuelle, 1958)

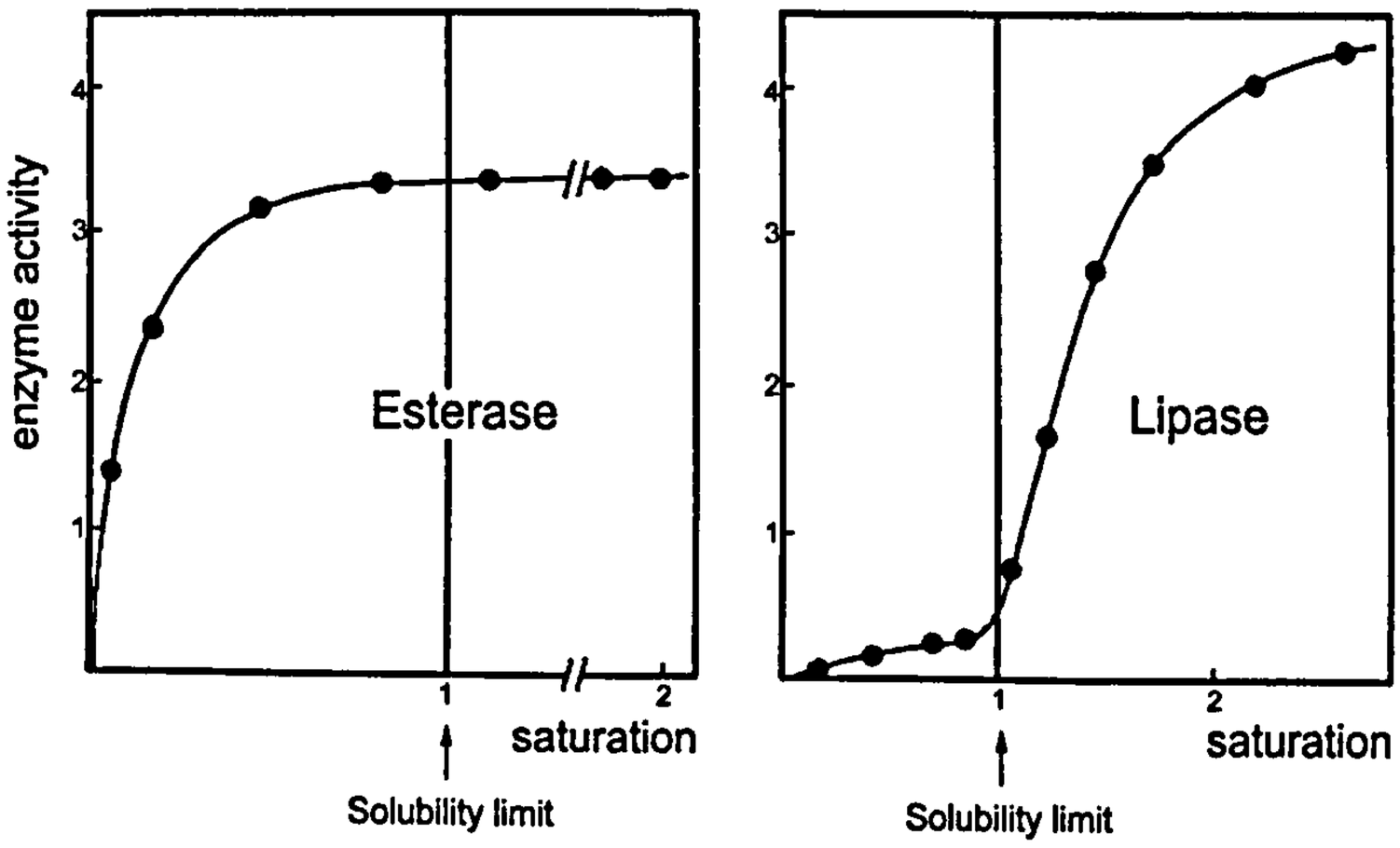

A structural explanation for interfacial activation was provided when lipase structures were solved by X-ray crystallography (Brady *et al.* 1990, Winkler *et al.* 1990). The presence of an amphiphilic loop or 'lid' covering the active site was observed. Comparison of native and inhibitor-bound lipase structures revealed that the lid undergoes a structural change on binding an inhibitor molecule, moving away from the active site (Brzozowski *et al.* 1991, Derewenda *et al.* 1992, van Tilbeurgh *et al.* 1993). Lid 'opening' exposed hydrophobic residues around the active site and lining the inner surface of the open lid (Figure 1.3). Interfacial activation is believed to occur as a result of this conformational change from the 'closed' form, in which access to the active site is blocked, to the 'open' conformation, in which the active site is exposed. Overall enzyme activity will depend on the relative stabilities of these two forms. In the presence of a lipid-water interface, lid-opening exposes buried hydrophobic residues allowing the enzyme to adsorb to the interface via hydrophobic interactions, which stabilise this conformation. In an aqueous environment the amphiphilic nature of the lid allows stabilisation of the 'closed' state as polar side chains on the outer lid surface are exposed and hydrophobic residues on the inner lid surface are buried.

Figure 1.3 Diagrammatic representation of *Rhizomucor miehei* lipase structures illustrating conformational changes on 'lid-opening'. The structures of (a) native *R. miehei* lipase and (b) in complex with the inhibitor *n*-hexylphosphonate ethyl ester are drawn with their α-carbon backbone. The catalytic triad, lid residue Trp 88, and the inhibitor are drawn with all atoms. The complete atomic structures of the native molecule (c), and the complex (d), are drawn with van der Waals radii. Non polar atoms are shaded. (Reproduced from Brzozowski *et al.* 1991).

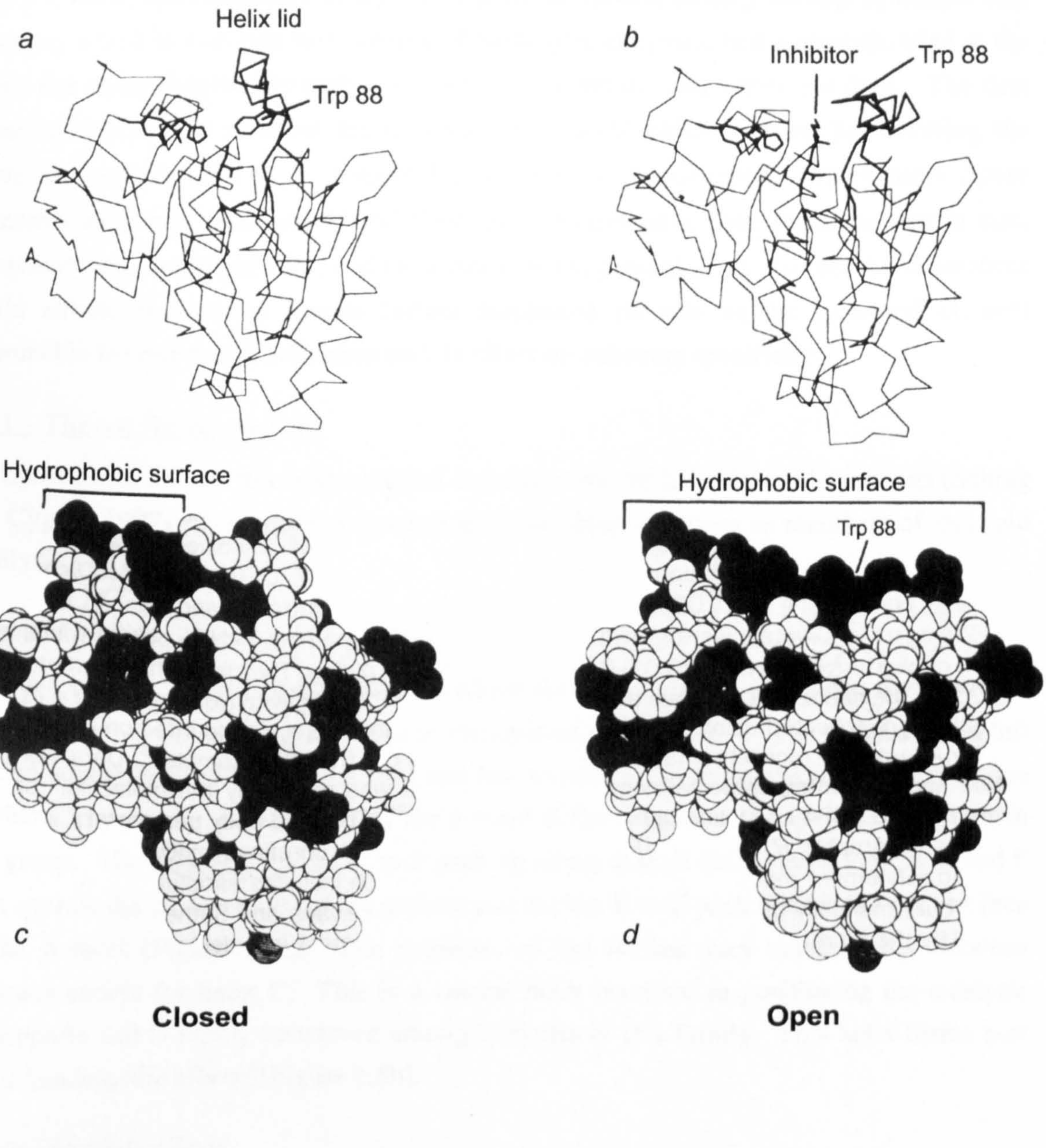

1.2 Lipase Structure

The first lipase structures to be solved by X-ray crystallography were of the fungal *Rhizomucor miehei* lipase (Brady *et al.* 1990) and human pancreatic lipase (Winkler *et al.* 1990) shortly followed by the *Geotrichum candidum* fungal lipase (Schrag et al. 1991). They revealed structural features that are typical of lipases, namely the α/β hydrolase fold structure, which is common to a number of hydrolytic enzymes, and a catalytic triad at the active site consisting of aspartate (or glutamate), histidine and serine residues. The first lipase structures also revealed the presence of an amphiphilic loop or 'lid' covering the active site and thought to be responsible for interfacial activation. Many more lipase structures have now been solved and their lid structures have been found to vary in size, complexity and amphiphilicity, and for some, it is not present at all. In fact the differences in lid structures between lipases further emphasise its role as the structural element responsible for interfacial activation and its effect on substrate specificity.

1.2.1 The α/β Hydrolase Fold

All lipases with known three-dimensional structures are α/β hydrolase fold proteins (Schrag and Cygler, 1997). A number of features establish these enzymes as members of this fold family: -

A central β-sheet

This is a central, mostly parallel β-sheet where the β strands are connected by α-helices. The topology of the α/β fold structure is represented in Figure 1.4. The β-sheet has a left handed superhelical twist and the first and last strands cross at approximately 90° to one another. The degree of curvature of the β-sheet differs significantly between enzymes in this group. The helices, labelled A to F pack on either side of the β-sheet: helices A and F pack against the concave side of the β-sheet and helices B to E pack against the convex face of the β-sheet (Figure 1.5a). The positions of the helices vary considerably between enzymes except for helix C. This is a central helix involved in positioning the catalytic nucleophile and is highly conserved among enzymes of this family. This helix forms part of the 'nucleophile elbow' (Figure 1.5b).

The 'nucleophile elbow'

This is the most conserved feature of the fold. The catalytic site residues occur at the C-terminal ends of β-strands. The catalytic nucleophile (Nu) is located in a highly conserved pentapeptide, Gly-X-Nu-X-Gly where glycine (Gly) may be replaced by other small residues. In lipases the nucleophile is a serine residue (Ser). This pentapeptide forms a

Figure 1.4 Canonical α/β hydrolase fold and the folds of two lipases. Schematic representations of (a) the common α/β hydrolase fold structure, and the folds of (b) *Humicola lanuginosa* fungal lipase (strand β10, marked in grey, does not occur in all lipases in this family) and (c) pancreatic lipase. Numbering of β strands and naming of α helices are consistent with Ollis et al. (1992). Catalytic residues are marked: serine; S, histidine; H, aspartate; D and glutamate; E, and the lid regions are marked with grey areas. (Reproduced from Schrag and Cygler, 1997 and Cygler and Schrag, 1997)

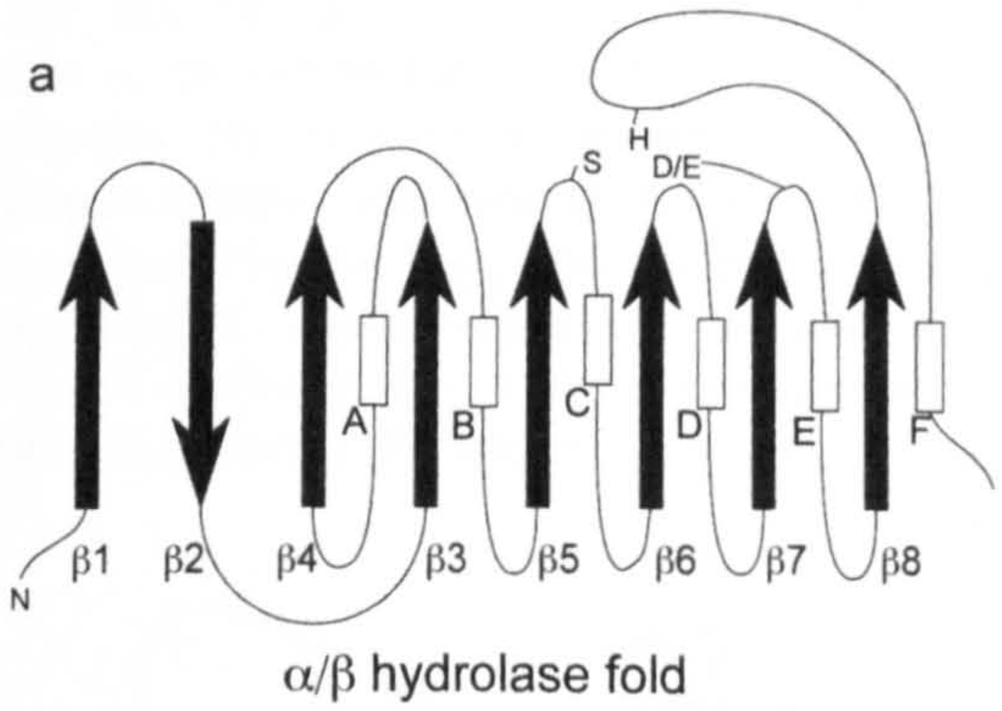

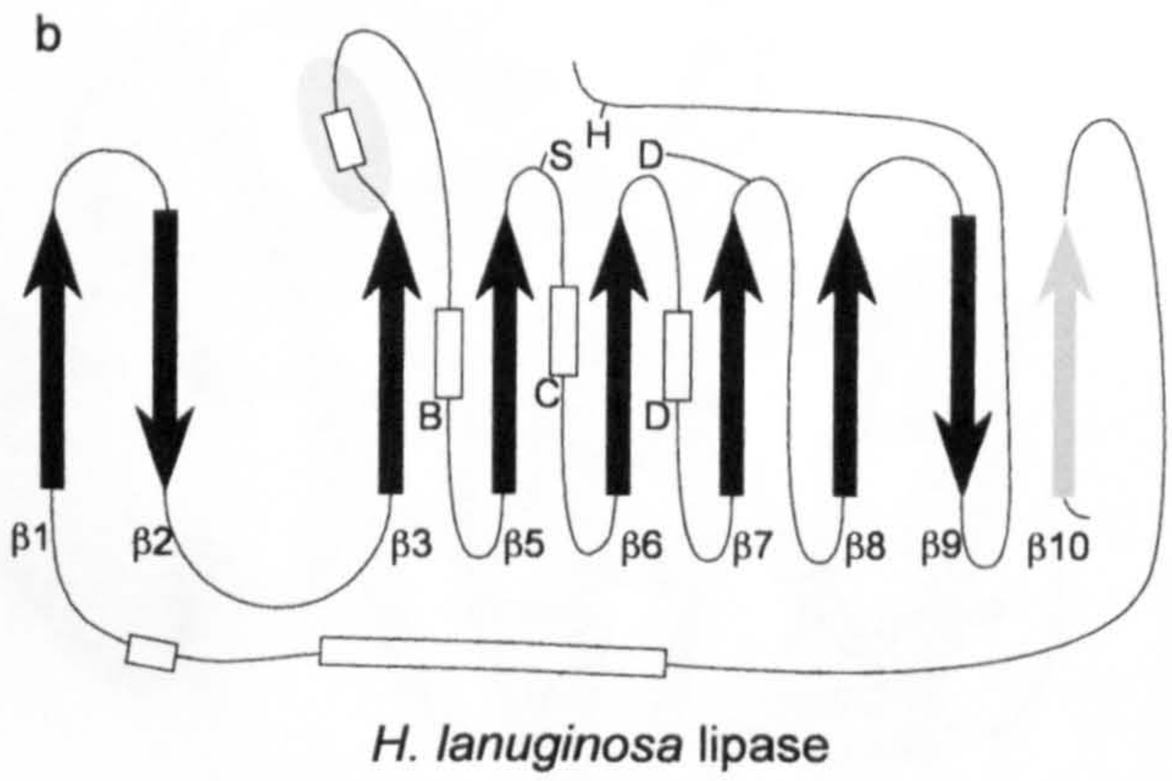

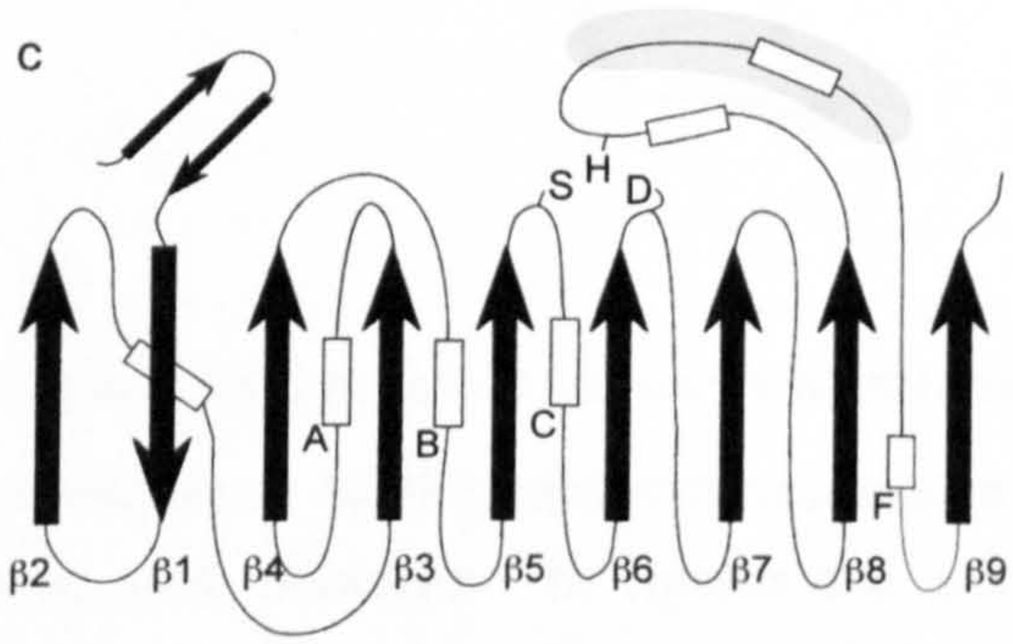

tight turn in a strand-turn-helix motif (Figure 1.5b), which forces the nucleophile to adopt unusual main-chain torsion angles. The strand is generally near the centre of the β sheet and for consistency is always termed the β5 strand (Figure 1.4). Helix C is the helix of the motif. Steric restrictions in forming this turn require a small side chain or no side chain at

positions Nu-2 and Nu+2 and are very often glycine residues. Nu+3 must also be small to prevent steric conflicts with the β4 strand.

Figure 1.5 (a) The structure of the *Humicola lanuginosa* fungal lipase (*Hl*L) in its native (closed) state, and (b) A Cα diagram of the 'nucleophile elbow' of *Hl*L. Side chains of the active site triad are shown in full (Asp 201, His 258 and Ser 146). (a) The tertiary structure of *Hl*L (see Figure 1.4b for a schematic representation of the α/β hydrolase fold). The side chain of a tryptophan residue within the lid is also indicated (Trp 89). This structure is representative of a group of related fungal lipases, including *Rhizomucor miehei*, *Rhizopus delemar*, and *Penicillium camembertii*. These lipases lack equivalents for helices A, E and F. They are replaced by one long helix that packs against the concave side of the β sheet with the helix axis roughly perpendicular to the β strands. (b) The active site serine residue is located at a hairpin loop between the β5 strand and α helix C. Co-ordinates were obtained from the Brookhaven Protein Database (code 1TIB) and modelled using Swiss PDB Viewer (Guex and Peitsch, 1997) and rendered with Pov-Ray PPC.

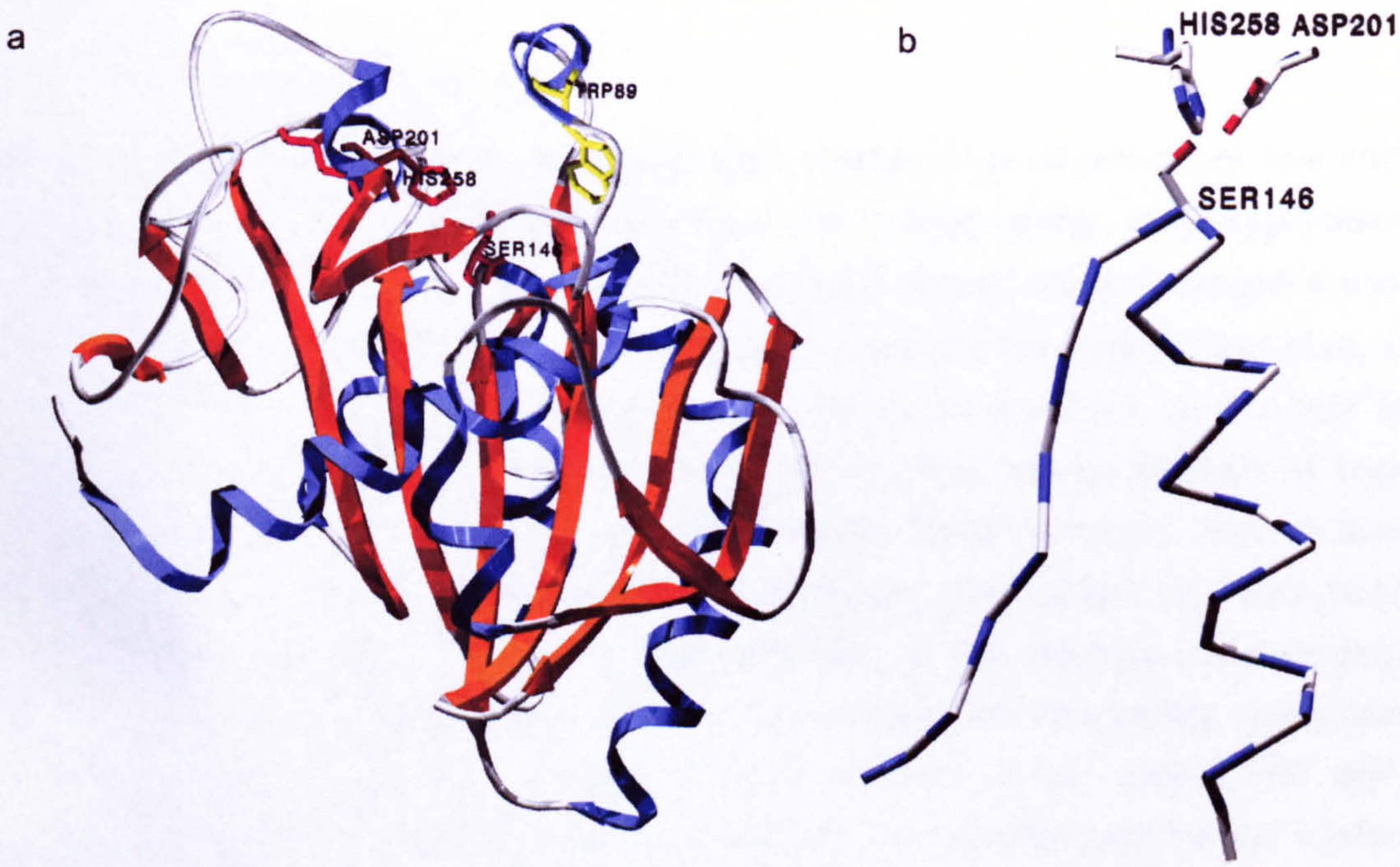

Sequence of catalytic residues (serine-acid-histidine)

The linear sequence of the catalytic residues in an α/β hydrolase fold protein is always nucleophile, acid, histidine. In lipases the active site is composed of a catalytic triad similar to that in serine proteases, consisting of serine, aspartate (or glutamate), and histidine. The nucleophile is present in the 'nucleophile elbow' between the β5 strand and the α helix C. The arrangement of the strands and loops following the 'elbow' allows the catalytic triad to assemble and permits the nucleophilic attack of substrate molecules by the serine. At the C-terminal end of the β6 strand, the main chain takes a sharp turn moving it away from the nucleophile at the end of the β5 strand. A residue with a small side chain is located at this bend. The C-terminal end of the β7 strand extends beyond the end of β6 by

at least one residue and the acid group is in this loop following the β7 strand. The catalytic histidine resides in a loop following the β8 strand, the length and conformation of which is variable.

Triad handedness

The twist of the β-sheet imposes a 'handedness' on the catalytic triad. This is the same in all lipases and corresponds to that of the canonical α/β-hydrolase fold. It is in fact a mirror image of the triad in serine proteases. Triad handedness defines the stereoselectivity of the reactions catalysed, and so nucleophilic attack on the ester bond of a lipase substrate occurs on the opposite face of the scissile bond relative to the attack of an amide bond by a serine protease.

1.2.1.2 Evolutionary Relationships

The α/β hydrolase fold was first described after a study of the structures of five enzymes (dienelactone hydrolase, haloalkane dehalogenase, wheat serine carboxypeptidase II, acetylcholinesterase and *Geotrichum candidum* fungal lipase) which revealed a common fold despite diverse substrate specificities and little sequence homology (Ollis *et al.* 1992). Several hydrolytic enzymes have since been identified as members of this fold family (Schrag and Cygler, 1997), all adopting the same core fold despite the lack of sequence homology. They also have a conserved sequence order for the catalytic triad residues and conserved loops that contain the triad and the oxyanion hole residues (for stabilisation of the oxyanion intermediate formed by the substrate in the reaction mechanism). In particular the loops that contain the catalytic triad residues are structurally well conserved and are able to accommodate various different residues at the nucleophile and acid positions (glutamate or aspartate may occur as the acid residue and serine, cysteine or aspartate as the nucleophile). This is an example of divergent evolution of enzymes whilst preserving the arrangement of catalytic residues. The α/β hydrolase fold is preserved, as it seems to provide an effective framework for catalytic triads, arranging them for efficient catalysis of hydrolysis reactions.

The α/β hydrolase fold enzymes are themselves related by convergent evolution to the trypsin family of serine proteases, subtilisin and cysteine proteases, as they all contain identically arranged catalytic triads despite having no similarity in their overall structures (Brenner, 1988, Ollis *et al.* 1992). The serine/cysteine residues are within hydrogen-bonding distance of a ring nitrogen (Nε2) of histidine. The other ring nitrogen (Nδ1) is hydrogen-bonded to the carboxylate group of the aspartate or glutamate residue that is

buried (which is unusual for acid groups in proteins, suggesting an important role for this residue). If the histidine rings of these enzymes are superimposed, the hydrogen-bonded atoms of the nucleophile group and the acid carboxylate group are also superimposed. This is a geometrical consequence of strong hydrogen bonding (Blow, 1990). Consequently these enzymes have very similar mechanisms of action. However, the fold, the sequential order of the catalytic triad and the positions of the oxyanion hole residues are very different.

1.2.2 The Lid

1.2.2.1 Conformational Change

As mentioned already, many lipases have one or more surface loops that cover the active site to form a lid and which undergo a conformational change allowing access of substrate molecules to the active site. It is 'lid-opening' that is believed to be responsible for the interfacial activation of lipases. Usually the lid is amphiphilic and it is often α-helical. This is the case for *Rhizomucor miehei* lipase where the lid is made up of a single α-helix, and for the *Geotrichum candidum* lipase where α-helices from two different surface loops cover the active site.

A comparison of native and inhibitor-bound structures of *Rhizomucor miehei* lipase indicated that the conformational change involved a rigid hinge-like movement of the 15 residue long lid over 12 Å and as a result, exposed a hydrophobic area of approximately 750 $Å^2$ (Derewenda *et al.* 1992). However, resolution of further lipase structures demonstrated that this movement is not necessarily rigid and that these enzymes in fact appear to have an intrinsic conformational lability in the absence of stabilising effects from crystal contacts (Derewenda *et al.* 1994a,b). Earlier studies may not have reflected this, as enzyme conformations are influenced by the conditions of crystallisation and certain conformations may be selectively stabilised. This observed flexibility implies that even in the absence of a lipid-water interface the two conformations may exist in a subtle equilibrium.

An example of the complexity of structural changes that can occur in lipase activation is demonstrated by the structure of the human pancreatic lipase-procolipase complex in its activated state (van Tilbeurgh *et al.* 1993). Colipase is a small protein co-factor that enables pancreatic lipase to bind to bile salt-covered interfaces formed in the intestine. When co-crystallised with mixed micelles of phosphatidylcholine and bile salts, the

pancreatic lipase has an open lid structure. Comparison with the closed enzyme revealed that a complex alteration in structure had occurred on opening. An α-helical region of the 'closed' lid had partially unwound to form two new helices connected by a tight turn. Conformational changes also occurred in an active-site loop, termed the β5 loop (after the secondary structure nomenclature of Winkler *et al.* 1990). Whilst making van der Waals contacts exclusively with the lid when 'closed', when 'open' the β5 loop had folded back on the core of the protein to adopt a new conformation stabilised by many new polar interactions with residues from the protein core and lid. The lid itself, previously stabilised almost exclusively by non-polar interactions with the protein core in the closed conformation, was stabilised by many new hydrogen bonds and salt bridges with the protein surface, the β5-loop and the N-terminal region of procolipase on opening. The maximum main-chain movement on lid opening was 29 Å. These conformational changes served to increase the hydrophobicity of the region around the active site by exposure of hydrophobic side chains and burial of hydrophilic side chains, with a contribution from the hydrophobic side of the main amphiphilic helix of the lid. In particular a tryptophan residue located in the lid, which fills the active-site pocket in the closed structure, was moved to the surface of the molecule. The active site was thus made accessible to the substrate.

1.2.2.2 Structural basis for substrate selectivity

The experimentally determined three-dimensional structures and derived models thereof, have provided an insight into the relationship between the structure and function of lipases. In particular, substrate selectivity within the pancreatic lipase gene family has been related to the nature of the lid domain and two loops at the catalytic site (the β5 loop and the β9 loop) (Carrière *et al.* 1998). As described above, human pancreatic lipase (HPL) demonstrates interfacial activation and possesses a lid that covers the active site in the 'closed' enzyme, stabilised by van der Waals contacts with loops β5 and β9. For the substrate to gain access into the active site, the lid-domain and the β5 surface loop undergo conformational changes resulting in the exposure of the active site. It is the β9 loop and the lid domain that are responsible for the activity of HPL on insoluble substrates, as they are highly hydrophobic and allow enzyme adsorption onto lipid-water interfaces.

Guinea pig pancreatic (phospho)lipase shares high sequence homology (78 %) with HPL but has a much shortened lid domain (5 residues instead of 23 in pancreatic lipase). This enzyme does not display interfacial activation and is fully active on both soluble and insoluble substrates (Hjorth *et al.* 1993). This can be explained by the absence of a full lid

domain allowing direct access of monomeric substrate in solution to the active site. The guinea pig (phospho)lipase also demonstrates high activity on phospholipid substrates and is able to hydrolyse galactolipids. By calculating the ratio of the accessible surface of hydrophilic residues to the accessible surface of hydrophobic residues, the hydrophilic/lipophilic balance is found to be higher for the residues in the β5 surface loop and the (shortened) lid domain of guinea pig (phospho)lipase compared to the homologous loops in HPL (Carrière *et al.* 1998). The deletion in the lid therefore results in exposure of a large active site crevice, the surrounding loops of which are highly hydrophilic, allowing the accommodation of larger and more polar substrates. It follows that the suppression of phospholipase activity in HPL cannot only be attributed to the presence of a lid domain, but also to the hydrophobicity of the surface loops that surround the active site.

A pancreatic lipase from a species related to the guinea pig, the coypu (*Myocastor coypus*), also shows phospholipase activity, although not as high as that for the guinea pig (phospho)lipase, and the absence of interfacial activation, yet possesses a full-length lid domain (Thirstrup *et al.* 1994). This is probably due to the coypu pancreatic (phospho)lipase (CoPL-RP2) having an open lid in solution. A sequence comparison with human pancreatic lipase supports this theory. The lid regions of these enzymes share little sequence homology. To stabilise the open conformation of HPL, residues of the lid region are involved in hydrogen bonds and salt bridges with the core of the protein, the colipase and the β5 loop. In the coypu pancreatic (phospho)lipase, the corresponding residues are almost all different. In particular a tryptophan residue in the lid of HPL that interacts with the β5 loop is replaced by a leucine in CoPL-RP2, thus weakening these interactions and so facilitating the spontaneous opening of the lid. The lid of CoPL-RP2 would possess a higher degree of lability than that of HPL and so would make the active site more accessible to monomeric and charged substrates, such as phospholipid. It would seem that interfacial activation is not due solely to the presence of a lid that can block access of monomeric substrate to the active site, but rather to the ability of the lid to undergo a conformational change from a closed to an open conformation that can be maintained by stabilising interactions, in the presence of a lipid-water interface.

The importance of lid amphiphilicity on substrate selectivity has been demonstrated for HPL (Jennens and Lowe, 1994) and lipoprotein lipase (Dugi *et al.* 1992) by mutagenesis studies in which the amphiphilic properties of the lid were altered. The presence of the amphiphilic lid was essential for hydrolysis of emulsified long chain triacylglycerol substrates, but not of short chain substrates, such as tributyrin. Deletions in the lid resulted

in decreased activity against long chain substrates and enhanced activity against soluble substrate.

Crystal structures of cutinase, a lipolytic enzyme that degrades cutin (an insoluble polyester matrix covering the surface of plants) have been used to demonstrate the role of the lid in determining the size of substrate preferentially bound by lipases. This enzyme does not possess a lid structure and whilst capable of hydrolysing triacylglycerols is not interfacially activated, being able to hydrolyse both soluble and emulsified substrates. From the three-dimensional structure of the fungal *Fusarium solani pisi* cutinase, the active-site serine was seen to lie in a crevice and to be accessible to solvent (Martinez *et al.* 1992). The activity of cutinase was found to be maximal for substrates with acyl chains of three or four carbons but rapidly dropped with increasing chain length (Mannesse *et al.* 1995). The crystal structure of cutinase complexed to a tributyrin analogue, mimicking the first tetrahedral intermediate of the reaction pathway, provided a structural explanation for this preference as it revealed that the butyl chain of the scissile ester bond was accommodated in a small pocket at the active site crevice (Longhi *et al.* 1997). The inhibitor was almost completely embedded in the active site crevice, as would be a tributyrin molecule. The accessibility of the active site and the complete embedding of the substrate molecule in the catalytic crevice could account for cutinase activity on tributyrin in aqueous solution. Above CMC concentrations, the binding of tributyrin to the active site would completely remove it from the lipid phase. Longer chain molecules would protrude from the active site crevice and continue interacting with the lipid phase leading to lower activities with these substrates. Lipases with deep and broad active sites formed upon interaction with the interface would be expected to have a greater ability to extract such molecules. This appears to be the case for HPL, which has high activity on triolein (C18 alkyl chain) and its structure has shown that it is able to accommodate an inhibitor with a C11 alkyl chain (Egloff *et al.* 1995).

1.3 Catalytic Mechanism

The catalytic triad was first discovered at the active site of the serine proteases. Just over twenty years later, structure determinations revealed the same constellation of aspartate/glutamate, histidine and serine at the active site of lipases (Brady *et al.* 1990, Winkler *et al.* 1990). Serine proteases and lipases normally catalyse the hydrolysis of peptide bonds and ester bonds respectively by very similar reaction mechanisms proceeding through an acylenzyme intermediate (Fersht, 1985).

The acyl-transfer reaction mechanism of a lipase is shown in Scheme 2. After formation of

Scheme 2 The acyl-transfer mechanism of lipolysis. Hydrolysis of an ester substrate is through the formation of an acyl-enzyme intermediate. Both the acylation and deacylation of the catalytic serine residue involve tetrahedral intermediates. The amino acid numbering corresponds to the active site of lipase from *Rhizopus oryzae*, *Ro*L.

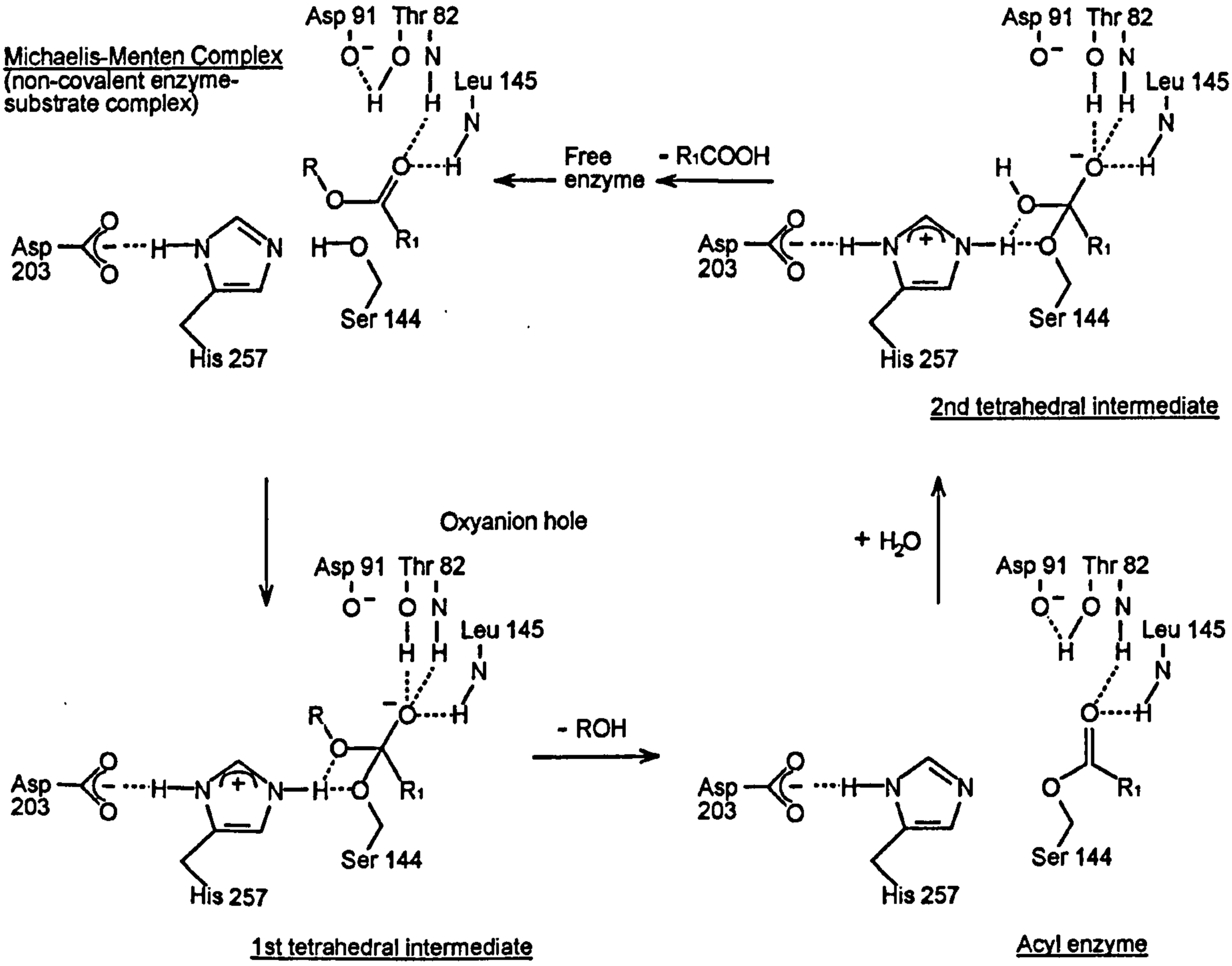

the non-covalent Michaelis complex between the enzyme and substrate, the reaction starts with the nucleophilic attack of the ester bond by the hydroxyl group of the active site serine. The catalytic histidine acts as a general base accepting a proton from the hydroxyl group of serine as it attacks the substrate carbonyl carbon. This leads to the formation of an unstable tetrahedral intermediate, or a transition state approximating such a structure, in which the substrate carbonyl group has formed a negative oxyanion (t^-) and the histidine has a positive charge due to its protonation (His^+). It is believed that rate acceleration in serine proteases is largely due to electrostatic stabilisation of the [$His^+ \ldots t^-$] ion pair (Warshel *et al.* 1989). The buried aspartate residue of the catalytic triad stabilises the transition state from the His^+ side, and the oxyanion side (t^-) is stabilised by hydrogen bonds from atoms in the 'oxyanion hole' of the protein. The tetrahedral transition state

collapses to the acylenzyme releasing the alcohol molecule, which accepts a proton from the protonated imidazole ring of histidine. The acylenzyme is then hydrolysed by a water molecule or cleaved by a competing nucleophile via a second tetrahedral intermediate as the above steps are reversed.

1.3.1 The Oxyanion Hole

The oxyanion hole stabilises the negative charge developed by the substrate carbonyl group in the reaction mechanisms of lipases and serine proteases. These reaction mechanisms involve a major change in charge distribution, from a neutral ground state to the tetrahedral transition state consisting of an ion pair [$His^{+}...t^{-}$]. Enzymes work as catalysts by lowering the activation free energy of the corresponding reaction pathway by stabilisation of the transition state (Lienhard, 1973, Fersht, 1985). For serine proteases and lipases this stabilisation seems to be achieved both by acting as a template to the tetrahedral geometry of the transition state and by electrostatically complementing the changes in charge distribution that occur during the reaction (Warshel *et al.* 1978, Warshel *et al.* 1981, Warshel *et al.* 1989). The buried aspartic group of the catalytic triad and the oxyanion hole provide such electrostatic interactions.

In serine proteases the oxyanion hole consists of an arrangement of backbone and side chain atoms that stabilise the oxyanion by hydrogen bonds. Effective charge stabilisation is achieved, as the dipoles of the oxyanion hole are pre-aligned toward the carbonyl oxygen; thus minimising 'reorganisation energy' usually associated with the polarisation of solvent molecules around charges. In lipases, the oxyanion hole is not always prearranged. Where a conformational change is necessary for substrate to gain access to the active site (such as lid opening), a second consequence is often the correct orientation of the oxyanion hole residues for catalysis. It was previously thought that cutinase, which has an exposed active site and no lid domain, has a pre-formed oxyanion hole, i.e. existing in the unbound enzyme (Martinez *et al.* 1992). However a recent investigation (Prompers *et al.* 1999) of the dynamics of cutinase through a structural comparison among different crystal forms of its variants (Longhi *et al* 1997) showed that while the core is highly rigid, the binding site including the oxyanion hole is mobile. As for all other lipases investigated so far, the oxyanion hole of cutinase is probably only correctly aligned upon binding of the substrate.

In the family of fungal lipases including *Humicola lanuginosa* (*HlL*), *Rhizomucor miehei* (*RmL*), *Rhizomucor oryzae* (*RoL*) and *Rhizomucor delemar* (*RdL*) that have similar tertiary structures (Figure 1.5), the residues that make up the oxyanion hole have been identified

(Derewenda *et al.* 1994, Joeger and Haas, 1994, Beer *et al.* 1996). The backbone amides of two residues and the hydroxyl side chain of one of these residues provide the hydrogen atoms that stabilise the three free electron pairs of the oxyanion oxygen via hydrogen bonding. The amide group and hydroxyl side chain of a serine or threonine (Ser 83 in *Hl*L, Ser 82 in *Rm*L, Thr 82 in *Ro*L and Thr 83 in *Rd*L), and the backbone amide of a leucine residue (at position 147 in *Hl*L and *Rd*L, 146 in *Rm*L and 145 in *Ro*L) form the oxyanion hole of these enzymes. The reaction mechanism for RoL is shown in Scheme 2 and includes the oxyanion hole residues. The serine/threonine residue belongs to the hinge region of the lipase lid, hence its reorientation on lid opening. The other oxyanion hole residue, leucine, is the next residue after the catalytic serine, in the nucleophile elbow.

In the closed structures of *Ro*L and *Rm*L the hydroxyl group of the Thr/Ser residue is hydrogen bonded to an aspartate residue (Asp 91). On formation of the first tetrahedral intermediate, the Thr/Ser side chain re-orientates to hydrogen bond to the oxyanion. Reformation of the hydrogen bond between Ser/Thr and Asp promotes the breakdown of the tetrahedral intermediate as an electron pair is released from hydrogen bond stabilisation by the oxyanion hole allowing the carbonyl carbon to return to the sp^2 hybrid state. The two electron pairs of the carbonyl oxygen are then stabilised by the backbone amides of Thr/Ser and Leu of the oxyanion hole. In *Hl*L an asparagine is present in the equivalent position (Asn 92). The hydrogen bond with threonine would be weaker and so would not increase reaction rate as effectively as aspartate in this position, as the reformation of the hydrogen bond between threonine and asparagine is less favourable. This has been supported by site-directed-mutagenesis (Beer *et al* 1996) of *Ro*L in which Asp 91 was replaced with an asparagine residue. Activity dropped to 7.2 % that of wild type and the Km (representing the affinity between substrate and enzyme in the non-covalent Michaelis complex) with triolein more than doubled. The effect on the Km was thought to be due to the weaker hydrogen bond with threonine resulting in a greater probability of asparagine adopting a conformation that blocks the hydrophobic substrate binding pocket.

1.4 Substrate Binding Site

X-ray crystallographic analysis of lipases bound to transition-state or substrate analogues, and molecular dynamics simulations of substrate binding, have enabled the identification of probable regions involved in substrate binding and the prediction of substrate molecule orientation at the active site. For example, the active site can be mapped through use of the program GRID which identifies protein regions that have the potential to interact with probes that mimic functional groups of the substrate (Pleiss *et al.* 1998, Hult and

Holmquist, 1997, Norin *et al.* 1994). The affinities of such probes are calculated by means of a molecular force field. A substrate can be divided into probes and used to determine how it can bind at the active site. The substrate binding sites of lipases have been found to range in shape from the shallow trough located near the protein surface of *Rhizomucor miehei* (Brzozowski *et al.* 1991) to the unique tunnel-like binding pocket of *Candida rugosa* (Grochulski *et al.* 1994). Some of the results of these studies are described below.

1.4.1.1 The binding site of Rhizomucor miehei *and related fungal lipases*

The crystal structure of *Rhizomucor miehei* lipase in complex with *n*-hexylphosphonate ethyl ester (Brzozowski *et al.* 1991) revealed the presence of a hydrophobic groove presumed to be the binding site of the leaving fatty acid of the triacylglycerol substrate. This binding site appeared to be created on lid displacement, only partly pre-existing in the native enzyme, and able to accommodate medium and long acyl-chains. For the related fungal lipase, that of *Humicola lanuginosa* complexed to a C12 inhibitor (dodecylethyl phosphate), the acyl chain of the inhibitor was seen to sit tightly in a hydrophobic channel (Lawson *et al.* 1994). Defined hydrophobic patches were observed around the active site, in addition to this area being generally non-polar for interfacial binding. These were presumed to function as binding sites for the remaining fatty acyl chains. In particular, a second shorter, shallow hydrophobic dent parallel to the hydrophobic crevice was observed in this lipase and also the homologous lipase from *Rhizopus oryzae*.

1.4.1.2 The binding site of Candida rugosa *lipase*

Crystal structures obtained from *Candida rugosa* lipase complexed with single alkyl chain inhibitors identified a unique hydrophobic binding tunnel (Grochulski *et al.* 1994). The alkyl chains bound to the enzyme in a long, narrow, hydrophobic tunnel projecting to the middle of the protein and then bending towards the protein surface in an 'L' shape. The tunnel was present in the closed protein although activation would require conformational changes to expose its mouth and small movements of side-chain residues lining the tunnel to accommodate the fatty acid chain. The tunnel could accommodate an acyl chain length of up to 18 carbons. Modelling of triacylglycerol binding revealed a "tuning fork" conformation in which the fatty acyl chain to be cleaved lies in the hydrophobic tunnel whilst the other acyl chains point towards the solvent.

1.4.1.3 The binding site of human pancreatic lipase

The crystal structure of the pancreatic lipase-colipase complex inhibited by a C11 alkyl phosphonate compound revealed a possible mode of substrate binding at the active site of this lipase (Egloff *et al* 1995). In the open enzyme two hydrophobic zones close to the

catalytic serine residue were exposed. The alkyl chain of an inhibitor molecule fitted into a hydrophobic groove, which start at the catalytic serine and runs toward the protein surface, away from the active site histidine. Van der Waals contacts were made with hydrophobic residues lining the floor of this groove. It was predicted that this chain represented the interaction of the leaving fatty acid of a triacylglycerol substrate, with this binding mode placing the carbonyl group in a suitable orientation for ester hydrolysis. The alkyl chain of a second inhibitor molecule interacted with a hydrophobic plateau formed by the hydrophobic half-sides of the two amphipathic lid helices, possibly indicating the binding site of a second alkyl chain of triacylglycerol substrate. No binding site could be defined for a third acyl chain, which may remain in the lipid layer. As observed for the *Candida rugosa* lipase (Grochulski *et al.* 1994) and *Fusarium solani* cutinase (Longhi *et al.* 1997), the triacylglycerol molecule appears to adopt a 'fork' conformation at the active site. It was noted that a hydrophilic pocket separated the two hydrophobic zones, which may interact with the polar atoms of the glycerol backbone of the substrate and could also harbour the water molecules necessary for hydrolysis.

In general the structures of inhibited lipases have revealed a pattern of hydrophobic and hydrophilic regions around the active site that are responsible for binding triacylglycerol substrate molecules (Beer *et al.* 1996, Kazlauskas, 1994). The ester substrate is bound at the catalytic site situated at the bottom of a binding pocket. The catalytic serine residue is located at a hairpin bend between a β strand and an α helix (the nucleophile elbow). From the structures resolved to date, it appears that the alcohol portion of the substrate rests on a floor formed by the end of the β strand, and the acyl chain points toward the α helix. The binding pocket can be divided into three regions: -

(1) A region above the β5 strand (of the nucleophile elbow) where the alcohol portion and small alcohol substituents of the substrate bind;
(2) a hydrophobic pocket which binds larger alcohol substituents; and
(3) a 'tunnel' above the α helix C, which varies considerably among lipases, that binds the acyl chain.

The α carbon of an acyl chain binds just below the large hydrophobic binding region of the alcohol binding-site and substituents at the α-carbon would extend into the hydrophobic pocket.

The orientation of the carbonyl oxygen and the scissile fatty acyl chain in relation to the catalytic triad residues appears to be similar in all the inhibited lipase structures solved (Cygler and Schrag, 1997). Binding sites for a second acyl chain of a substrate molecule

have been inferred from complexes where a second (single-chain) inhibitor molecule has bound nearby and in some cases has indicated that a 'tuning fork' conformation is adopted by the triacylglycerol molecule (Grochulski *et al.* 1994, Egloff *et al.* 1995). Lipases tend to have long hydrophobic binding sites for the leaving fatty acyl chain varying in length from 7.8 Å in cutinase to 22 Å in *Candida rugosa* and *Rhizomucor miehei* lipases (Pleiss *et al.* 1998), and substrate specificity appears to be reflected in the size of this site. The large hydrophobic binding sites of lipases are in contrast to those of esterases, which have small acyl binding pockets specific for their preferred substrate. Molecular modelling of substrate binding in lipases combined with site-directed-mutagenesis has identified hydrophobic residues that line the acyl binding site and interact with bound substrate (Holmquist *et al.* 1997, Martinelle *et al.* 1996, Chang *et al.* 1996, Beer *et al.* 1996, Holmquist *et al.* 1994, Joeger and Haas, 1994). Mutatagenesis of these residues based on their positions in relation to the fatty acyl chain has been used to alter the chain length specificities of these enzymes.

1.5 Substrate Specificities

Lipases are generally able to accept a wide range of substrates due to their large hydrophobic binding sites. However, they can be selective for certain types of substrate. For example, lipases can show preferences for tri-, di- or mono-acylglycerols such as the lipase from *Penicillium camembertii*, which specifically binds mono- and di-acylglycerols (Yamaguchi *et al.* 1996). More commonly, selectivity is observed for the length of acyl chain that can be cleaved. Lipases usually catalyse the hydrolysis of neutral lipids, however, some are also able to hydrolyse charged substrates such as phospholipids and show selectivity for this type of substrate. As discussed above, these substrate preferences are influenced by the size and shape of the substrate binding site and the balance between hydrophilic and hydrophobic residues around the active site. Overall, lipases display a broad range of specificities. They can also show positional specificities for the fatty acid that is to be cleaved. For example, the lipase from *Humicola lanuginosa* hydrolyses fatty acids from the sn-1 and sn-3 positions of a triacylglycerol molecule, with a tendency to prefer cleavage at the sn-1 position. This is due to the stereochemical non-equivalence of these two groups (Figure 1.6). A useful feature of lipases is that whilst being able to accept a broad range of substrates, they retain enantioselectivity for each one.

Figure 1.6 A diagram of a triacylglycerol molecule showing the stereospecifically numbered carbon atoms of glycerol, labelled sn-1, sn-2 and sn-3. The two primary hydroxyl groups are stereochemically distinct.

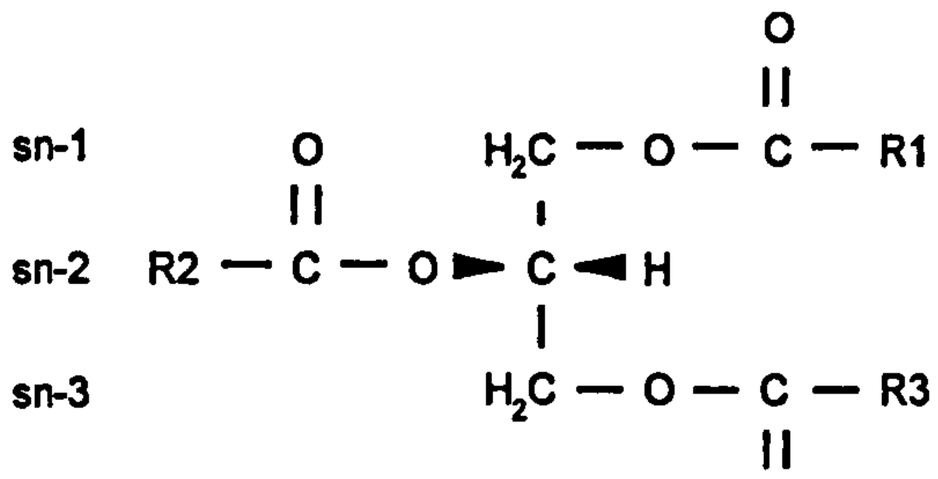

1.5.1 Structural Basis for Lipase Enantioselectivity

Based on the observed enantioselectivities of lipases towards hundreds of secondary alcohols for hydrolysis reactions, where the substrate is an ester, and for esterification reactions where the substrate is an alcohol, a general rule was formed that predicts which enantiomer of a secondary alcohol reacts faster in a lipase-catalysed reaction (Kazlauskas *et al.* 1991). The rule is based on the sizes of the substituents at the stereo-centre and is explained in Figure 1.7.

Figure 1.7 The empirical rule for enantiorecognition by *Candida rugosa* lipase: a schematic diagram of the favoured enantiomer for secondary alcohols. The hydroxyl group points forward out of the page, M represents a medium substituent and L represents a large substituent. In hydrolysis reactions, the substrate is the ester of the alcohol shown and in transesterification reactions the substrate is an alcohol. (Kazlauskas *et al.* 1991)

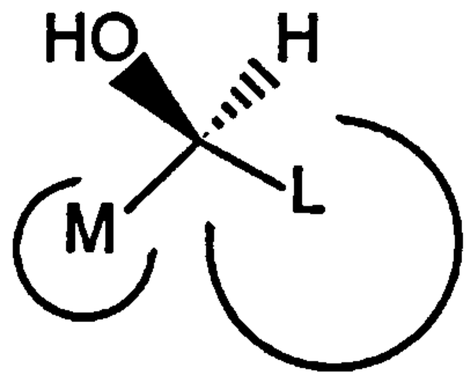

When the alcohol is drawn with the hydroxyl group pointing forward from the plane of the page, the favoured enantiomer bears a large substituent on the right and a medium substituent on the left. The size difference between these two groups is important in determining the degree of enantioselectivity shown by lipases and as a consequence the resolution of secondary alcohols is poor when the substituents are of a similar size (Kazlauskas *et al.* 1991). Although the degree of enantioselectivity also varies between lipases themselves and depends on the substrate bound, they all seem to prefer the enantiomer shown in Figure 1.7.

Cygler *et al.* (1994) attempted to identify a mechanism for the enantiorecognition demonstrated by lipases. As lipases followed the same empirical rule for enantiomer recognition, they presumed that the mechanism of recognition would also be similar and probably involve structural features common to lipases. To identify which structural features of lipases were involved in enantiorecognition, the group investigated structures of the lipase from *Candida rugosa* (*Cr*L) bound to transition state analogues of enantiomers of menthol. In the ester hydrolysis reaction catalysed by lipase the alcohol is released as the first tetrahedral intermediate collapses. Therefore, the transition state that determines enantioselectivity towards the secondary alcohol resembles this intermediate. To mimic this transition state, phosphonate inhibitors were bound at the active site (Figure 1.8).

Figure 1.8 Phosphonate esters linked to nucleophilic serine mimic the transition state of the acylation step in the lipase reaction mechanism. (1R)- and (1S)-menthyl hexylphosphonate covalently linked to active site serine mimic the fast- and slow- reacting enantiomers respectively in the hydrolysis of menthyl heptanoate and were used by Cygler *et al.* (1994) to identify how these esters orientate in the catalytic site.

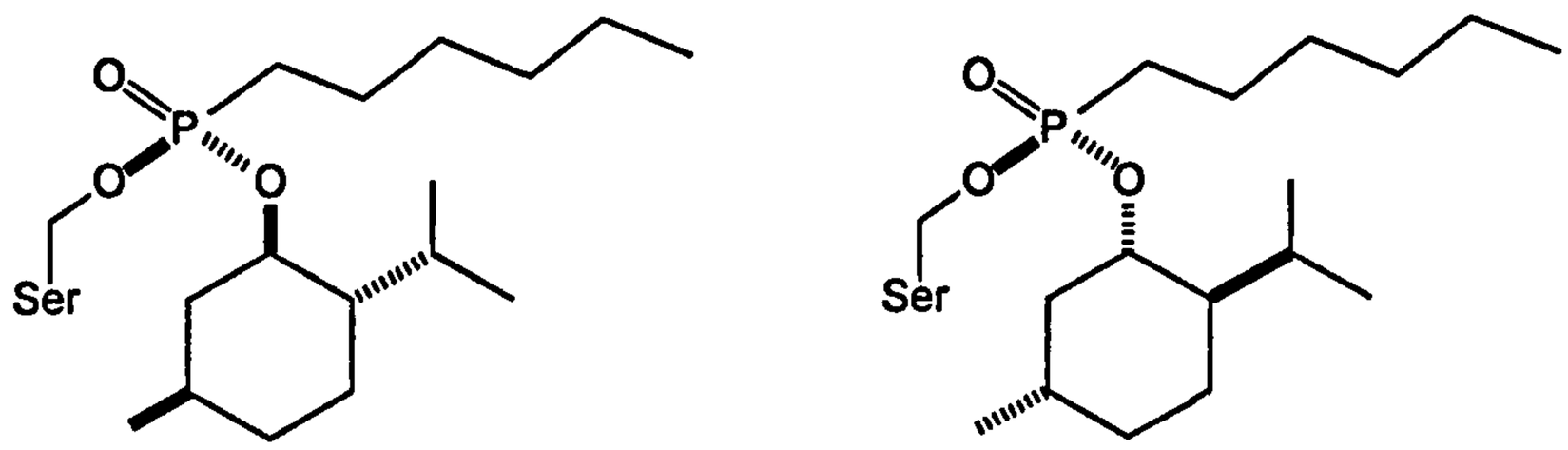

(1R)-menthyl hexylphosphonate (1S)-menthyl hexylphosphonate

A survey of the enantiopreferences shown by *Cr*L and several other lipases towards menthol esters were found to agree with the empirical rule shown in Figure 1.7. Enantiomers of the menthyl hexylphosphonate group were covalently linked to the catalytic serine of *Cr*L to mimic the transition states for the fast and slow reacting enantiomers in the hydrolysis of menthyl heptanoate, and their crystal structures provided a picture for the structural basis of enantio-selection. While the hexyl chain bound in a tunnel extending to the centre of the enzyme, the menthyl rings were at the entrance to the tunnel in a crevice exposed to the solvent. The shape of the binding crevice, which was to a large extent formed from the loops that assemble the catalytic triad and the oxyanion hole, was consistent with the model of the alcohol binding-site generalised from the empirical rule. The binding crevice was positioned on the C-terminal ends of the β-strands with the large substituent $-CH[CH(CH_3)_2]CH_2-$ pointing into a hydrophobic region and open to the solvent, and the medium substituent $-CH_2CH(CH_3)-$ resting on the floor of the crevice.

The most significant difference between the complexes of the two enantiomers was the orientation of the imidazole ring of the catalytic histidine. In the fast reacting enantiomer complex the orientation of the imidazole remained unchanged and formed a bifurcated hydrogen bond to the oxygen of the catalytic serine and oxygen of menthol (consistent with the proposed role of histidine in the catalytic mechanism, see Scheme 2). In contrast, the steric requirements of the large substituent of the slow reacting enantiomer forced the imidazole ring of histidine to rotate and break the hydrogen bond with the alcohol oxygen, resulting in the slower reaction of this enantiomer. As the menthol group requires protonation to leave, the absence of this hydrogen bond could slow this step.

The orientation of the leaving alcohol group is likely to be similar between lipases as the loops that form the binding site for this group also assemble the oxyanion hole and arrange the catalytic triad. These loops are part of the α/β hydrolase fold structure and so are highly conserved among lipases. The common fold structure also subjects the alcohol substituents of bound substrates to the same steric restrictions. The greatest restrictions result from limited space around the catalytic residues, the oxyanion hole, and the supporting β-sheet. These interactions, and the steric requirement for hydrogen bonding between the alcohol and catalytic histidine, all involve the catalytic machinery, thus providing a simple explanation for the common enantio-preferences shown by lipases toward secondary alcohols.

Whilst Cygler *et al.* (1994) have provided a structural explanation for the empirical rule for enantioselectivity shown by lipases towards secondary alcohols, based on their common tertiary structure and catalytic mechanism, there are still several unanswered questions regarding the stereoselectivity of lipases, such as whether this rule also applies to primary alcohols, whether the leaving fatty acyl group which can also bind in the hydrophobic pocket influences stereoselectivity towards alcohols and how lipases distinguish between enantiomeric carboxylic acids. The variability of the acyl binding-site between lipases may account for different enantioselectivity of lipases towards stereocentres in the acyl chain. There is no common rule to predict stereoselectivity toward triacylglycerol substrates, which differs between lipases and can depend on the substrate structure (Rogalska *et al.* 1993). High resolution of crystal structures of transition state analogues bound to lipases, combined with molecular dynamics simulations, is being used to gain a further understanding of the molecular basis of the stereopreferences shown by lipases.

Computer-aided modelling of substrate binding has been used to determine factors that influence stereoselectivity shown by the sn-1(3)-regioselective *Rhizopus oryzae* lipase toward triacylglycerols and analogues (Haalck et al. 1997, Holzwarth *et al.* 1997). More recently the design of lipase variants with modified stereoselectivity based on molecular modelling of substrate binding was used to improve this model and explain the influence of the sn-2 substituent (Schrieb *et al.* 1998). This substituent has been observed to play a crucial role in determining the stereoselectivity of *Ro*L and of other microbial lipases (Stadler *et al.* 1995). Two hydrophobic patches in the binding site of *Ro*L were assumed to bind the acyl chains of the substrate: a deep hydrophobic crevice binds the scissile sn-1(3) fatty acid chain and a shallow hydrophobic dent binds the non-hydrolysed sn-2 acyl chain. Molecular modelling showed that steric interactions occur between the substrate sn-2 group and the side chain of a leucine residue in the hydrophobic dent (Leu 258). The sn-2 group packs into a gap between the catalytic histidine (His 257) and the hydrophobic Leu 258. The restrictions imposed by this gap implied that small flexible groups would be better accommodated than rigid and bulky groups. When the functional sn-2 group was small and flexible (e.g. an ester or ether group) there were no steric repulsions in either orientation (with the sn-1 or sn-3 group bound at the hydrophobic crevice), and in this case stereopreference was for the sn-1 orientation. However, *Ro*L became more sn-3 selective as the chemical structure at sn-2 became more rigid and bulky (e.g. an amide or phenyl group), due to the steric repulsion between the side chain of Leu 258 and the rigid group at sn-2 when in the sn-1 orientation.

The model predicted that, depending on the substrate bound, repulsion by Leu 258 in the hydrophobic dent is one factor that governs whether the sn-1 or sn-3 chain binds in the hydrophobic crevice of *Ro*L lipase. Other factors that determine this stereopreference include a relaxed conformation of the glycerol backbone and stabilisation of the oxyanion by the side chain of Thr 83 (Scheme 2). Due to variability in structure of lipase binding-sites, this model cannot be extended to other lipases without resolution/modelling of their own three-dimensional structures.

1.6 Industrial Applications of Lipases

Lipases are industrially useful enzymes. Properties that are exploited in industrial applications include their broad range of substrate specificities, high regio- and enantio-specificities, stability in organic solvents and their ability to catalyse hydrolysis under mild conditions. The ease with which they can be purified in large quantities from natural and recombinant sources also makes them amenable to use in industry. Their most important

commercial use is as an additive to detergents. However, lipases are also widely used in the food industry, for the preparation of speciality fats and more recently as biocatalysts in biotransformations for the industrial scale synthesis of chiral intermediates in enantiomerically pure forms. Some examples of the current and potential industrial uses of lipases are discussed below.

1.6.1 Lipases in Bread Making

1.6.1.1 Making bread

A special feature of wheat flour is that on addition of water, a viscoelastic cohesive dough is formed that can be kneaded. During baking, this dough is transformed into an elastic bread. A major structural change occurs during this process in which gas cells expand into an open network of pores. Gas cell stabilisation and gas retention largely determine the crumb structure and volume of wheat bread. The baking and handling properties of the dough are influenced by processing conditions and by the dough ingredients (Autio and Laurikainen, 1997).

Wheat flour dough consists of two continuous and immiscible aqueous phases: the gluten phase, and a liquid phase containing water-soluble compounds and starch. While the starch component provides a source of fermentable sugars for the generation of carbon dioxide gas, the gluten is responsible for the dough elasticity and stability (Belitz and Grosch, 1999). Gluten is formed on the addition of water to wheat flour and mainly consists of proteins (90 %). The gluten proteins are responsible for the rheological properties that give the dough gas-holding capacity and an elastic crumb after baking. A model of dough expansion (Gan *et al*, 1995) suggests that at early stages of fermentation the expanding gas cells are embedded in a starch-protein matrix. At advanced stages of fermentation and the early stages of baking, the starch-protein matrix fails to enclose the gas cells completely, leaving areas with just a thin liquid film. With increasing fermentation time, the surface area of the liquid film increases and the stability of this film determines the behaviour of the dough. Surface-active materials, such as proteins and pentosans (arabinoxylan) dissolved in the dough aqueous phase and also wheat lipids, particularly polar lipids, stabilise the film so that it can expand across a larger area without rupturing. Wheat lipids closely associated with the liquid phase of dough probably represent the most significantly surface-active components in wheat flour dough. They can rapidly form a lipid monolayer at the gas/liquid interface. Surface active synthetic emulsifiers, such as diacetyl tartaric acid (DATA) esters of monoacylglycerols, can also improve gas retention. Gas cell

stabilisation and gas retention properties are therefore determined both by the liquid-film and by gluten proteins, as the extensibility of the starch–protein matrix is important for gas cell stabilisation. The relative significance of these two phases may vary amongst flours and if both are unsatisfactory then gas retention in the dough will be poor.

For industrial scale bread making, "dough should be acceptable for handling, including fast mechanical systems, and be able to initiate and sustain a gas production that will raise the volume while retaining a good structure, and not collapse or otherwise degrade when baked, or at some time after baking. There are also requirements of taste and texture, crumb and crust colour and the overall keeping properties to consider" (Godfrey, 1996). Additives and enzymes are used as ingredients in industrial bread making, mainly for dough conditioning or to reduce staling. The effect of enzymes on bread making enables their use in place of chemical additives, which are generally undesirable in terms of diet, and in some cases are no longer permitted. For example, the oxidant potassium bromate is now prohibited in bread in Europe. Enzymes are selected for their desired effect in bread and depending on the substrates available.

The use of enzymes in bread can improve the dough processing, the bread quality and reduce staling rate. Increased loaf volume and improved crumb structure result in a softer crumb, which gives the loaf an improved shelf-life by reducing crumb firmness during storage as well as improving the texture of the final product. Alternatively an anti-staling effect can be achieved by reducing starch retrogradation, the main cause of crumb staling. This involves the increased re-alignment of starch molecules from an amorphous to a semi-crystalline form. Cereal starch granules mainly consist of two glucans, amylose (25 %) and amylopectin (75 %), and have a semi-crystalline character, the crystalline regions consisting primarily of amylopectin. Amylose retrogradation occurs at a faster rate than amylopectin retrogradation, as indicated by a greater drop in solubility with time, and it is amylopectin recrystallization that seems to be the major cause of bread staling (Belitz and Grosch, 1987). The changes in the structure of starch during the baking process are summarised in the next section.

1.6.1.2 Bread staling

When suspended in water, starch granules swell. Amylose can be dissolved out of the granule without disturbing their crystalline character. In making dough, this swelling is limited, since the available water is limited. When the suspension is heated a pasty and sticky starch suspension is formed at the 'gelatinisatin' temperature (ca. 53 - 65 °C,

depending on starch origin) and consists of highly swollen intact granules dispersed in a solution of free amylose molecules. When a gelatinised starch paste is cooled rapidly, the starch paste sets to a gel. In the early cooling period after baking, amylose molecules start to form a gel structure in the crumb because of their ability to align and retrograde (the transition from the solubilised (swollen) state to an insoluble, shrunken, microcrystalline state by realignment of starch molecules). The crumb of fresh baked bread is therefore a network of amylose chains and embedded swollen starch granules, in which the hydrated amylopectin moiety is retained. During staling, changes occur in the swollen starch granules. This is due to starch retrogradation, in particular of amylopectin. Amylopectin molecules, which are separated by hydration, start to aggregate via their branches, thus reinforcing the swollen starch granules. As a result the crumb becomes firm, loses its elasticity and crumbles more easily.

1.6.1.3 Lipase as an ingredient in bread

Lipases used in making bread have been found to retard staling and also to confer positive dough conditioning effects (particularly 1,3-specific lipases). These effects are manifest by improved dough stability on over-fermentation, increased loaf volume and an improved more uniform crumb structure. Lipases can give a volume increase of 20 – 30 %, although overdose results in dough becoming dry and stiff with a reduced volume increase. The effect depends on the type of flour used and the baking formulation. In particular lipases have a significant effect on improving bread quality in fat-free formulations or those with added oil. It has no further improving effect when the recipe contains added hydrogenated shortening (Si, 1996).

Studies show that while the rheological properties of dough are not effected by addition of lipase, measurement of the rheological properties of gluten treated with lipase indicate an increase in gluten strength. Gluten from lipase-treated wheat flour dough is significantly stronger and more elastic. It is this increase in gluten strength that is responsible for the positive dough conditioning effects and improved dough stability on over-fermentation. Overdosing results in a too strong gluten complex, this gives too stiff a dough and a smaller volume increase. The exact nature of these extra cross-links within the gluten networks is still unclear (Si, 1997, Monfort *et al.* 1999).

The effect of lipases is thought to be due to hydrolysis of wheat lipids resulting in an *in situ* production of di- and mono- acylglycerols, which are effective emulsifiers. They strengthen gluten and decrease staling. They improve the ability of gluten to form a film

around the gas bubbles allowing them to expand and retain the generated gas. The result is increased dough strength and gas retention, which increases loaf volume and gives a better crumb structure. The improved keeping properties are due to the effects on loaf volume and crumb structure improving the crumb softness, rather than an effect on starch retrogradation (Si, 1997). It is known that emulsifiers and lipids form complexes with both constituents of starch to different extents during baking, that retards their retrogradation (Autio and Laurikainen, 1997). In fact as a rule, emulsifiers such as mono-acylglycerols are added to extend the shelf life of bread in this way. However, the amount of monoacylglycerols generated from wheat lipids in dough systems upon the addition of lipase would not account for the effects observed on loaf volume and crumb structure by an effect on starch retrogradation alone (Poldermans and Schoppink, 1999, Si, 1997).

As well as significant effects on improving dough stability and crumb structure, lipases do not result in dough stickiness, and therefore have good synergistic effects in improving bread quality when used with xylanases or amylases. When used with xylanase, the over-dosing of which can cause stickiness, non-sticky dough is achieved and a greater volume increase than when either of these enzymes are used alone.

1.6.2 Lipases in the Dairy Industry

Lipases are used for flavour enhancement in cheeses and to accelerate cheese ripening (Vulfson, 1994). The lipolysis of milk fat releases fatty acids, which give specific flavour characteristics. Traditionally the lipases used have been from animal tissues as rennet paste, but more recently have been substituted by lipases from microbial sources such as *Rhizomucor miehei*, *Aspergillus niger* and *Aspergillus oryzae*. Lipase cocktails can be used to create lipolytic flavour profiles. For example, hydrolysis of short chain fatty acids results in a sharp and tangy flavour, and the hydrolysis of medium chain fatty acids gives a soapy taste. They can be used to imitate sheep and goat's milk cheese, and also in the making of 'enzyme modified cheese' (EMC) to provide a concentrated cheese flavour.

1.6.3 Lipases in Detergents

There is interest in the use of enzymes in washing powders, to allow lower washing temperatures and reduce the use of chemical surfactants. Lipases were first screened for their ability to function in standard washing conditions of alkaline pH (around pH 10 - 11) and a temperature of 50 – 60 °C, but were found to only marginally improve the action of chemical surfactants already present in washing powders. However, they were later discovered to improve secondary washing behaviour as not only were fat stains removed,

but also their redeposition onto the washed materials seemed to be prevented. For this reason they are now widely used in detergent formulations. Novo Nordisk produced the first commercial lipase, Lipolase™, in 1994 for use as a detergent additive. Lipolase™ originates from the *Humicola lanuginosa* fungal lipase, the gene for which was cloned and expressed in *Aspergillus oryzae* (Jaeger and Reetz, 1998).

1.6.4 Lipases in the Oleochemical Industry

As well as their major use in food, fats and oils are also produced as a renewable chemical feedstock for non-food-related applications ('oleochemistry'), for example in the preparation of soap. The hydrolysis, glycerolysis and alcoholysis of lipids have in the past been carried out by a steam fat-splitting process that is very energy consuming and requires further purification of products by re-distillation. Enzymatic hydrolysis using lipases overcomes both of these difficulties.

1.6.4.1 Preparation of soaps and fatty acids

Triacylglycerols are used in the preparation of soap, mainly by chemical processes that operate continuously at 100 °C and which provide quantitative yields within minutes. Lipases can be used to hydrolyse triacylglycerols to make soap at 30 °C using stirred reactors (Schmid and Verger, 1998). While the process takes much longer, the advantages of this method are lower depreciation costs, a better colour of soap and generation of 20 % glycerol water as a by-product (instead of more dilute glycerol in the steam splitting process). At the moment only one company, Miyoshi Yushi in Japan, produces significant quantities of soap by lipase catalysed fat hydrolysis, using *Candida rugosa* lipases.

1.6.4.2 Synthesis of structured fats

The position, chain length and degree of unsaturation of acyl chains all influence the physical properties, the nutritional use and sensory values of triacylglycerols. Many lipases show *sn*-1,3 specificity and can be used to modify triacylglycerols by regioselective trans-esterification reactions. For example, changing the degree of saturation of acyl chains in a triacylglycerol to modify melting behaviour, such as in the preparation of margarines to improve spreadability. Another example would be the production of cocoa butter substitutes by the upgrading of cheaper oils. Cocoa butter has a desirable 'mouth feel' and is predominantly made up of triacylglycerols with oleic acid in the sn-2 position and stearic and palmitic acids in the sn-1 and sn-3 positions. Industrially, a company called Unichema produces 'chocolate fat' using a process that is patented by Unilever (Schmid and Verger, 1998). It involves the interesterification of high-oleic sunflower oil with stearic acid using immobilised sn-1,3-regioselective *Rhizomucor miehei* lipase as the catalyst (Scheme 3).

Scheme 3 Production of a cocoa-butter substitute by interesterification of a natural triacylglycerol using an sn-1,3-regioselective lipase. (Schmid and Verger, 1998)

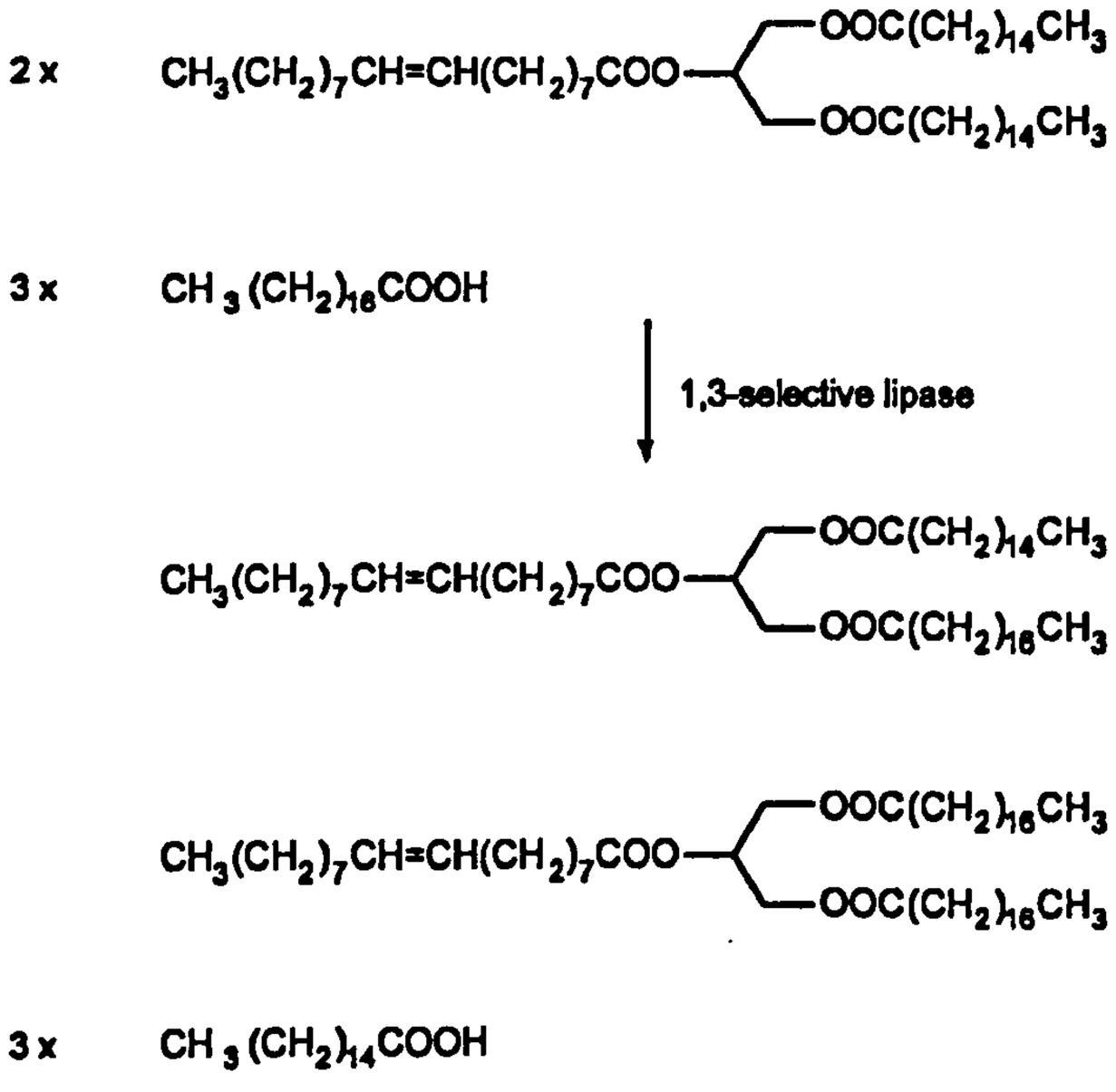

Lipoprotein lipase and pancreatic lipases are responsible for the hydrolysis of triacylglycerols in the blood stream and intestine respectively. Both are more efficient at hydrolysing esters of medium-chain fatty acids than esters of long-chain fatty acids. New types of fat emulsions based on triacylglycerols carrying medium- and long-chain fatty acids, designed to provide optimum nutrition for patients are being produced for parenteral and enteral administration using sn-1,3-specific lipases (Schmid and Verger, 1998, Björkling *et al.* 1991). These are hydrolysed at a rate between that of pure medium and long chain triacylglycerols and are cleared from the blood stream more rapidly than conventional emulsion products. Triacylglycerols of this type containing essential fatty acids have shown beneficial effects against cardiovascular and inflammatory diseases. They are preferentially prepared by interesterification using sn-1,3 lipases, as chemical methods can promote side reactions (such as oxidation, *cis-trans* isomerisation and double-bond migration)

1.6.4.3 Production of monoacylglycerols

Monoacylglycerols are used as emulsifiers in food, cosmetics, and drug preparations. They are usually produced by glycerolysis of triacylglycerols, followed by short-path distillation yielding monoacylglycerols of over 90 % purity. Monoacylglycerols can be prepared using lipases but, as with chemical manufacture, a mixture of di- and mono-acylglycerols is

produced. As yet the use of lipases for the commercial production of monoacylglycerols cannot compete with their chemical manufacture.

1.6.5 Lipases as Biocatalysts in Organic Synthesis

Lipases have been used by organic chemists to catalyse a wide variety of chemo-, regio- and stereoselective transformations for a long time. They can be used for the synthesis of optically pure compounds from prochiral substrates and for the kinetic resolution of racemates. A number of factors make lipases ideal for use as biocatalysts. As a consequence of their large substrate binding domains lipases are able to accept a wide range of compounds, whilst still showing regio-selectivity and/or enantiopreference. As well as alcohols and carboxylic-acid esters, lipases are able to bind diols, α and β hydroxy acids, cyanohydrins, chlorohydrins, diesters, lactones, amines, diamines, amino-alcohols and α and β amino-acid derivatives (Jaeger and Reetz, 1998). Lipases have evolved to withstand the denaturing effect of the lipid/water interface and so are stable in organic solvents. In non-aqueous media, lipases can be used for ester synthesis or interesterification reactions. The acyl-enzyme formed in the hydrolysis reaction can be considered an acylating agent. The wide substrate range accommodated by lipases also allows the acylation of nucleophiles other than those possessing hydroxy groups (e.g. hydroperoxides, amines and thiols)(Schmid and Verger, 1998).

Enantiomerically pure products and intermediates are necessary in the production of pharmaceuticals, agrochemicals and fine-chemicals. Despite the obvious potential for the use of lipases as industrial biocatalysts, the number of enantioselective processes catalysed by these enzymes in industry is limited (Jaeger and Reetz, 1998). One example is a key transformation in the synthesis of calcium antagonist Diltiazem™: lipase from *Serratia marcescens* is used to prepare a chiral intermediate by resolution of a racemate (Jaeger and Reetz, 1998, Schmid and Verger, 1998).

Generally, problems in using lipases as industrial biocatalysts arise from insufficient enantioselectivity, limited enzyme activity and difficulties in recycling the enzyme. There are also limitations in the kinetic resolution of racemates as the maximum conversion possible is 50 %. These problems are being overcome by recent technological developments. For example, new immobilisation techniques to enhance enzyme activity and stability, and dynamic kinetic resolution techniques enabling the complete conversion of a racemate to a single enantio-pure product. The latter requires a second catalyst, most often a transition-metal catalyst that is compatible with the lipase, to induce racemization of

the enantiomer not accepted by the enzyme (Jaeger and Reetz, 1998). *In vitro* evolution techniques can be used to improve lipase enantioselectivity. Random mutations are introduced into the lipase gene which is amplified, expressed and then screened for substrate selectivity by determination of enantiomeric excess (% ee). Using directed evolution, the enantioselectivity of hydrolysis of a chiral ester, catalysed by *Pseudomonas aeruginosa* lipase, was increased from 2 % ee to 81 % ee in four mutagenesis cycles. Sequencing of the mutated genes allowed structural identification of the mutants and further improvements in enantioselectivity by mutagenesis at the identified positions (Reetz and Jaeger, 1998 and Reetz and Jaeger, 1999). Directed evolution of enzyme catalysts has resulted in enzymes with improved thermostability, activity in organic solvents, and substrate specificity (Kuchner and Arnold, 1997). For successful engineering of an enzyme using this method, an established method of expression and secretion using a microbial host system is required, as well as a suitable and efficient screening system for the desired properties.

1.6.6 Protein Engineering of Industrial Lipases

To date, lipases from over 30 different biological sources have been cloned and expressed in host organisms and are available in pure form for commercial use. Most of these originate from fungi and bacteria. The structures of at least 13 lipases have been resolved so far by X-ray crystallography and with the exception of pancreatic lipase are all of microbial origin. Crystallographic studies have provided structural explanations for experimentally observed properties of lipases such as interfacial activation and substrate selectivity. The increasing availability of high-resolution structures combined with computer-aided molecular modelling provide a basis for the rational design of lipase variants, enabling the tailoring of properties for specific applications in industry. There is also potential for *in vitro* evolution, which has been used to improve lipase enantioselectivity, to modify and improve lipase functions or to create novel properties that could be useful in biotechnological applications (Kuchner and Arnold, 1997). At the moment, detergents are the most commercially important field of lipase applications, and most genetic engineering has been to enhance the stability and activity of lipases in a household detergent matrix (Schmid and Verger, 1998).

1.7 Research Objectives

The Ingredients Sector of Danisco is the world's largest producer of functional ingredients for the international food industry. Their product range includes enzymes, emulsifiers, flavourings, antioxidants, textural ingredients, fat replacers, pectin and animal feed

ingredients. Danisco produces Lipase 3 for use as an ingredient in bread making where it has a dough-conditioning effect. It is a fungal lipase originating from *Aspergillus niger* which Danisco also use to express Lipase 3 on an industrial scale. Protein engineering techniques can been used to modify enzyme properties and the aim of this project was to increase the specific activity of Lipase 3 using such methods. As over-production of Lipase 3 on an industrial scale was found to result in over-glycosylation of the enzyme with a subsequent drop in specific activity, it was also intended to prevent this post-translational modification in an attempt to restore the activity of the expressed enzyme to its original level.

The three-dimensional structure of Lipase 3 has not yet been determined. However a model structure can be made, based on available co-ordinates of lipase structures that share high sequence homology, using molecular modelling software. Such a model can then be used to study charge interactions within the structure and to predict the effects of altering residues in the design of lipase mutants.

Mutants of Lipase 3, designed from an homology model, can be generated by site-directed-mutagenesis of the lipase gene and expressed in a suitable host system. After production and purification, effects of the introduced mutations can be determined by kinetic analysis using the soluble esterase substrate, *para*-nitrophenyl acetate, to measure activity with monomeric substrate in solution, and long-chain triacylglycerol substrate (olive oil) in the form of an emulsion to assess lipase activity at a lipid-water interface.

CHAPTER 2 Materials and Methods

The suppliers of materials, the components of media and solutions, and strain genotypes referred to in this chapter are listed in Appendix A.

2.1 General Molecular Biology Methods

2.1.1 Growth and Storage of *E. coli* Bacteria

(Sambrook *et al.* 1989)

Bacteria were grown using sterile techniques in either L-broth liquid culture medium at 37 °C in a shaking incubator at 250 rpm overnight or on L-agar plates (solid culture medium) in an inverted position at 37 °C overnight. Liquid cultures were inoculated from single colonies from an L-agar plate or grown from overnight cultures diluted 1:100 in L-broth. Long term storage of bacteria was by addition of 10 % v/v glycerol to aliquots of overnight cultures followed by brief vortex-mixing, flash freezing in liquid nitrogen and storage at -70 °C. Frozen stocks were made of all transformed bacterial strains from which DNA was isolated and kept at least until the results of analysis, for example by restriction digest or DNA sequencing, were known.

2.1.2 Alkaline Lysis Fast 'Mini-prep' Method for Preparation of Plasmid DNA

(Sambrook *et al.* 1989)

The components of solutions A, B and C used in the Alkaline Lysis methods for preparing plasmid DNA are described in Appendix A (section A4).

A single colony was picked from an L-agar plate containing appropriate antibiotics for selection of plasmid DNA and cultured overnight in 10 ml L-broth also containing antibiotics for selection. Approximately 1.5 ml – 3 ml of the overnight culture was pelleted by centrifugation at 12000 g for one minute in an eppendorf tube and the supernatant discarded. The pellet was completely resuspended in 100 µl of solution A and incubated at room temperature for 5 minutes. To this, 200 µl Solution B was added, mixed gently and incubated on ice for 5 minutes followed by addition of 150 µl Solution C and incubation on ice for at least 5 minutes. After centrifugation at 12000 g for 5 minutes the supernatant was extracted by adding an equal volume of phenol/chloroform/isoamyl alcohol (25:24:1), vortex-mixing and centrifugation for 3 minutes at 12000 g. The top aqueous layer was transferred to a fresh eppendorf tube and the DNA precipitated with 0.1 volumes 3 M sodium acetate pH 5.2 and 2.5 volumes 100 % ethanol incubated on ice for at least 5 minutes. After centrifugation at 12000 g for 10 minutes, the pellets were washed by addition of 500 µl 70 % ethanol and centrifugation at 12000 g for 5 minutes. The resulting

pellet was dried under vacuum and resuspended in 50 μl T.E buffer.

2.1.3 Alkaline Lysis/PEG Precipitation 'Mini-prep.' Method for Preparation of Plasmid DNA Suitable for ABI Sequencing

(Sambrook *et al.* 1989)

Approximately 1.5 - 4.5 ml of an overnight culture was centrifuged for one minute and the supernatant removed. The pellet was completely resuspended in 200 μl of solution A. This was mixed with 300 μl solution B and incubated on ice for 5 minutes followed by addition of 300 μl of solution C and incubation on ice for at least 5 minutes. After centrifugation at 12000 g for 10 minutes the supernatant was transferred to a new eppendorf tube and treated with 1.6 μl - 2 μl of 10 mg ml^{-1} RNase for 20 minutes at 37 °C. DNA was purified by the addition of 400 μl chloroform, mixing by inversion for 30 seconds followed by centrifugation at 12000 g for 1 minute. The top layer was transferred to a fresh eppendorf tube and the chloroform extraction repeated. An equal volume of 100 % isopropanol was added and centrifuged at room temperature for 10 minutes. The pellet was washed by the addition of 500 μl 70 % ethanol, centrifugation for 5 minutes and then dried under vacuum. The pellet was dissolved in 32 μl of water and to this 8 μl 4 M NaCl and 40 μl 13 % PEG were added, mixed and incubated on ice for 20 minutes. After centrifugation at 12000 g for 15 minutes at 4 °C, the pellet was washed with 500 μl 70 % ethanol and centrifugation at 12000 g for 5 – 10 minutes. The pellet was dried under vacuum and resuspended in 20 - 25 μl T.E buffer.

2.1.4 Alkaline Lysis 'Maxi-prep' Procedure for Isolation of Plasmid DNA

(Sambrook *et al.* 1989)

A single colony was picked from an L-agar plate containing appropriate antibiotics for selection of plasmid DNA and cultured overnight in 100 ml L-broth also containing antibiotics for selection. The culture was centrifuged at 4000 g for 10 minutes and the supernatant discarded. The pellet was completely resuspended in 2 ml of solution A containing 5 mg ml^{-1} lysozyme (dissolved just prior to use and kept on ice) and incubated at room temperature for 10 - 15 minutes. To this, 4 ml of Solution B was added, mixed gently and thoroughly, and incubated on ice for 10 minutes. Next, 3 ml of ice cold Solution C was added and incubated on ice for at least 10 minutes. After centrifugation at 47000 g for 20 minutes at 4 °C, the supernatant was transferred to a fresh centrifuge tube and DNA precipitated by addition of 0.6 volumes of 100 % isopropanol, mixing and incubation at room temperature for 20 – 30 minutes. After centrifugation at 47000 g for 20 minutes at room temperature, the pellet was washed by addition of 10 ml cold 70 % ethanol, which

was immediately discarded, and the pellet briefly air-dried. The pellet was gently resuspended in 0.5 – 1 ml T.E buffer and transferred to an eppendorf tube. RNase was added to a final concentration of 10 μg ml^{-1} and incubated at 37 °C for 1 hour. Proteins were removed from the sample by extraction with an equal volume of phenol/chloroform/isoamyl alcohol (25:24:1); after vortex mixing and centrifugation for 3 minutes at 12000 g, the top aqueous layer was transferred to a fresh eppendorf tube. Extraction with phenol/chloroform was repeated, until the top layer was clear. The sample was then extracted with chloroform in the same way and then with water-saturated ether; this time the top layer was discarded and excess ether evaporated by incubation at 65 °C for approximately 10 minutes. DNA was precipitated with 0.1 volumes 3 M sodium acetate pH 5.2 and 2.5 volumes ethanol incubated on ice for 30 minutes followed by centrifugation at 12000 g at 4 °C for 30 minutes. Pellets were washed with 500 μl 70 % ethanol and centrifugation at 12000 g at 4 °C. The 70 % ethanol was discarded, the pellet dried under vacuum and resuspended in 200 μl T.E buffer.

2.1.5 Agarose Gel Electrophoresis

(Sambrook *et al.* 1989)

A suspension of agarose in either TAE or TBE buffers (typically 0.8 % w/v) was melted using a microwave oven (buffer components: Appendix A, section A5). Ethidium bromide was added to a concentration of 1 μg ml^{-1}. The agarose was poured into a casting tray and allowed to set. Once set, the gel was immersed in a buffer tank containing TAE or TBE buffer. Samples to be loaded were mixed with 0.2 volumes loading buffer (50 % v/v glycerol, 0.025 M EDTA pH 8, 0.01 % w/v bromophenol blue powder). Maximum sample volume depended on the well size. Samples were loaded and a constant voltage (100 V) applied across the gel. At neutral pH nucleic acids have a negative charge and so migrate towards the anode. The DNA loading buffer contains bromophenol blue dye so the migration of the DNA could be followed. Separation by agarose gel electrophoresis could be used to size DNA fragments by comparing their migration with that of fragments of known size. The ethidium bromide in the gel intercalates into nucleic acids causing it to fluoresce under UV irradiation so that band positions could be visualised.

2.1.6 Spectrophotometric Determination of Nucleic Acid Concentration and Purity

Both DNA and RNA absorb at wavelengths of 260 and 280 nm and their concentrations can be calculated by measuring absorbance at 260 nm (Sambrook *et al.* 1989). An OD_{260} of 1 corresponds to a concentration of 50 μg ml^{-1} for double stranded DNA, 40 μg ml^{-1} for RNA, and 33 μg ml^{-1} for single stranded DNA. The ratio of absorbance at 260 and 280 nm

(OD_{260}/OD_{280}) gives a guide to the purity of the sample. Pure preparations of DNA and RNA have OD_{260}/OD_{280} values of 1.8 and 2.0 respectively. If there is contamination with protein or phenol this ratio will be less and accurate quantification is not possible.

2.1.7 Preparation of 'Competent' *E. coli* Cells

The preparation of competent *E. coli* cells was based on the method of Inoue *et al.* 1990. A single colony of the *E. coli* host strain of choice was picked from an L-Agar plate and used to inoculate 10 ml L-broth containing antibiotics to maintain F′ plasmids (tetracycline for SURE cells and chloramphenicol for CJ236 cells) and grown at 37 °C overnight. The overnight culture (1 ml) was used to inoculate 100 ml of SOB containing appropriate antibiotics, in a 250 ml flask. The cells were grown at 30 °C with good aeration to an OD_{600} of 0.6. The cells were cooled on ice for 10 minutes and then pelleted by centrifugation at 2500 g at 4 °C for 10 minutes. The supernatant was discarded and the pellets gently resuspended in 40 ml of ice-cold TB (Transformation Buffer: 10 mM PIPES, 55 mM $MnCl_2^*$, 15 mM $CaCl_2$, 250 mM KCl, pH 6.7). After incubation on ice for 10 minutes the cells were pelleted by centrifugation at 2500 g for 10 minutes at 4 °C. The pellet was resuspended in 8 ml of ice-cold TB, dimethyl suphoxide (DMSO) was added to a final concentration of 7 % and incubated on ice for 10 minutes. The cells were aliquoted into pre-chilled eppendorf tubes, flash frozen in liquid nitrogen and then stored at – 70 °C.

*$MnCl_2$ was added after adjustment of pH to 6.7

2.1.8 Transformation of Competent *E. coli* Cells

(Sambrook *et al.* 1989)

Competent cells were thawed on ice. 100 µl thawed competent cells were added to 10 ng - 100 ng of plasmid DNA in a maximum volume of 10 µl and incubated on ice for 30 min. The cells were heat shocked for 45 sec at 42 °C, incubated on ice for 2 minutes, followed by the addition of 350 µl of L-Broth (containing antibiotics for plasmid or F′ selection) that had been pre-warmed to 42 °C. The cells were incubated at 37 °C for one hour with gentle agitation and then 50 - 100 µl aliquots were spread onto L-Agar plates (containing required antibiotics) inverted and incubated overnight at 37 °C. For blue/white screening, plates also contained Xgal and IPTG.

2.1.8.1 Blue/white screening

The multiple cloning site (MCS) of the pBluescript plasmid is flanked by DNA coding for the N-terminus of β-galactosidase. This α-peptide can complement a truncated form of the enzyme produced by a bacterial host that has the ΔM15 deletion mutation of the β-galactosidase gene (*lacZ*), to form a functional enzyme. IPTG is necessary for specific

induction of *lacZ* transcription. When functional β-galactosidase is produced it converts colourless Xgal into a blue product. Therefore blue colonies are obtained when the pBluescript plasmid without any insert at the MCS is transformed into an *E. coli* strain with the *lacZ* ΔM15 mutation (e.g. SURE). When the multiple cloning site is disrupted, the α-peptide is no longer produced and colonies containing recombinant molecules are white in colour.

2.1.9 Gel Purification of DNA Fragments

DNA fragments from digestion with restriction enzymes were separated by agarose gel electrophoresis on a 1 % low-melting-point agarose gel prepared in TAE buffer containing 1 μg ml^{-1} ethidium bromide. A gel slice containing the fragment of interest was cut out using a scalpel, placed into an eppendorf tube and freeze-thawed two times. A small plug of repel-coated glass wool was pushed to the bottom of a 0.5 ml eppendorf tube into which a hole had been pierced with a needle. This was placed inside a 1.5 ml microfuge tube with no lid. The thawed gel slice was placed on top of the glass wool and centrifuged at 12000 g for one minute. The filtrate (in the microfuge tube) was briefly vortex-mixed with an equal volume of water-saturated butanol, centrifuged for 1 minute, the top layer discarded and the remaining aqueous layer extracted using water-saturated ether in the same way. Excess ether was evaporated by incubation at 65 °C for 10 minutes. DNA was precipitated with 0.1 volumes of 3 M sodium acetate pH 5.2 and 2.5 volumes of ethanol incubated on ice for 30 minutes. After centrifugation at 12000 g for 30 minutes the pellet was washed by addition of 500 μl 70 % ethanol and centrifugation at 12000 g for 5 – 10 minutes. The resulting pellet was dried under vacuum and resuspended in 20 - 25 μl T.E buffer.

2.1.10 Restriction Digest of DNA

Digestion of DNA by restriction enzymes was carried out using conditions recommended by the enzyme supplier (Life Technologies Inc.). Typically, digestions were performed at the appropriate temperature in a total volume of 10 – 50 μl with approximately 1 - 2 units of enzyme for 0.2 – 1 μg DNA and the appropriate restriction buffer (usually 10 X concentration: see Appendix A: A6) supplied by Life Technologies Inc. Unless otherwise stated, all restriction digests were carried out at 37 °C for 2 hours. If the DNA preparation being digested contained RNA, such as 'mini-prep.' DNA, 1 μg RNase per μl total reaction mixture was also included in the digest.

2.1.11 Treatment with Calf intestinal phosphatase

Calf intestinal alkaline phosphatase (CIP) removes 5′-phosphate groups to generate a hydroxyl terminus. The enzyme is used to prevent unwanted ligation of DNA fragments

during cloning, such as recircularisation of vector. The conditions for treatment were those recommended by the supplier, Life Technologies Inc.

Vector DNA was restriction digested. To the restriction digest reaction was added 1 unit of CIP diluted in Dilution Buffer (25 mM Tris-HCl, pH 7.6, 1 mM $MgCl_2$, 0.1 mM $ZnCl_2$, 50 % glycerol) and 0.1 volumes of 10 X CIP Dephosphorylation Buffer (500 mM Tris-HCl, pH 8.5, 1 mM EDTA). CIP requires Zn^+ for activity (contributed from storage buffer and dilution buffer) at a concentration of approximately 0.01 mM. It was therefore necessary to dilute CIP to a concentration so that it would contribute at least 1/10 of the final volume. Reactions were incubated at 37 °C for 5 minutes for DNA with a 5' overhang, or at 50 °C for 5 minutes for 5'-recessed and blunt-ended DNA. The CIP was then inactivated by incubation at 65 °C for 15 minutes.

2.1.12 Ligation Reaction

T4 DNA Ligase was used to join DNA strands between 5'-phosphate and 3'-hydroxyl groups of adjacent nucleotides with cohesive or blunt ends. Generally a molar ratio of insert to vector of 3:1 was used when cloning a fragment into a plasmid vector. T4 DNA Ligase and Ligase 5 X Buffer from Gibco BRL, Life Technologies Inc. were added and reactions were set up as recommended by the supplier. To the vector and insert DNA (total DNA 0.01 - 1 μg), 2 μl of T4 DNA Ligase (1 unit μl^{-1}) and 4 μl Ligase 5 X Buffer (250 mM Tris-HCl, pH 7.6, 50 mM $MgCl_2$, 15 mM DTT, 5 mM ATP and 25 % (w/v) PEG-8000) were added. The total volume was made up to 20 μl with sterile water. The reaction was incubated at room temperature for 3 hours, 4 °C overnight or 15 °C for 4 – 18 hours. The optimal temperature for a ligation reaction is a balance between the optimal temperature for T4 DNA Ligase enzyme activity (25 °C) and the temperature necessary to ensure annealing of fragment ends. Blunt-end ligations are generally efficient at temperatures between 15 - 20 °C for 16 – 24 hours, while cohesive ends are ligated effectively at room temperature (22 °C) for 3 hours or 4 – 8 °C overnight.

2.1.13 DNA Sequencing

DNA samples were sequenced by fluorescent cycle sequencing with dye-labeled terminators using an ABI 373A DNA Sequencer with 48-cm well-to-read gel plates. The ABI PRISM™ Dye Terminator Cycle Sequencing Ready Reaction kits contain AmpliTaq® DNA Polymerase FS. Sequencing reactions were carried out according to the protocol (P/N 402078) supplied with the kit from Perkin-Elmer.

Specific chain termination is achieved using dideoxy derivatives of the triphosphates (Sanger *et al.* 1977). These do not have hydroxyl groups at the 3′-position of the deoxyribose ring preventing condensation with the 5′-terminal triphosphate group of another residue. Synthesis of the new DNA chain is by AmpliTaq DNA Polymerase FS (Fluorescent Sequencing), a mutant form of *Taq* DNA polymerase developed specifically for fluorescent cycle sequencing, having reduced 5'-3' nuclease activity and allowing more efficient incorporation of dideoxynucleotides (ddNTPs). A set of prematurely foreshortened transcripts are generated which, when resolved by polyacrylamide gel electrophoresis, give a ladder of bands allowing determination of the DNA sequence from the positions of the dye-labeled terminators. A laser that scans across the bottom end of the gel as electrophoresis occurs induces fluorescence of the dye-labels, which can then be detected by the Sequencer.

The concentrations of dye-labeled ddNTPs and normal deoxynucleotides (dNTPs) in the Ready Reaction Premix are optimised to give a balanced distribution of signal between base 10 and base 700 +. Using this optimised Premix, up to 650 bases at 98% accuracy can be read on 48-cm well-to-read gels on the ABI PRISM 373.

Components of the ABI PRISM™ Dye Terminator Ready Reaction Premix

A-Dye Terminator, C-Dye Terminator, G-Dye Terminator, T-Dye Terminator, dITP, dATP, cDTP, dTTP, Tris-HCl, pH 9, MCl_2, thermal stable pyrophosphatase, and AmpliTaq DNA Polymerase, FS.

2.1.13.2 Cycle Sequencing

The modified 'mini' alkaline-lysis/PEG precipitation procedure (section 2.1.3) provided DNA of suitable quality for sequencing and was used for the preparation of double-stranded DNA templates. The reagents for cycle sequencing were mixed in a 0.5 ml tube. To 50 – 100 ng single-stranded or 250 – 500 ng double-stranded template DNA were added 20 ng (3.2 pmole) primer and 8 µl Ready Reaction Mix in a total volume of 20 µl made up with sterile water. Each reaction was overlayed with a drop of light mineral oil and cycle sequencing carried out using a Perkin-Elmer Thermal Cycler by the following steps: -
96 °C held for 30 seconds,
50 °C held for 15 seconds,
60 °C held for 4 minutes,
repeated for 25 cycles and then held at 4 °C until ready to purify the extension products.

2.1.13.3 Purification of extension products

To purify the extension products after cycle sequencing, reaction mixes were transferred into eppendorf tubes containing 2 µl of 3 M sodium acetate pH 5.2 and 50 µl of 95 % ethanol. Tubes were vortex mixed and placed on ice for 10 minutes. After centrifugation at 12000 g for 15 – 30 minutes the ethanol mix was carefully aspirated. Pellets were washed with 500 µl 70 % ethanol by centrifugation at 12000 g for 10 minutes followed by thorough aspiration. The remaining pellets were dried under vacuum. Before loading onto the sequencing gel the pellets were resuspended in 3 µl of loading buffer (5:1 ratio of deionized formamide and 50 mg ml^{-1} blue dextran in 25 mM EDTA, pH 8), heated to 90 °C for 2 minutes, pulse span and placed on ice.

2.1.13.4 Electrophoresis of extension products

The gel was prepared by stirring 50 g urea into 10 ml 40 % 10:1 acrylamide and 43 ml pure water until dissolved. The mix was deionised by adding 1 g amberlite resin and mixing for 5 minutes, then vacuum filtered into 10 ml 10 X TBE buffer and degassed for 5 minutes. A pair of clean gel plates, held 0.3 mm apart by spacers along each side, was clamped together. To the gel mix, 500 µl 10 % APS and 500 µl TEMED were added, mixed carefully and injected between the gel plates using a 60 ml syringe. A well-former was pushed into the top of the gel, which was left to set for 2 hours. The plates containing the set gel were placed into the ABI 373 Sequencer and locked into place. Default settings on the 373 keypad were checked (volts = 2500, watts = 40, mAmps = 40, 16-18 hours). After ensuring that the plates were clean in the region scanned by the laser, the well former was removed and a comb inserted at the top of the gel to separate lanes for loading samples. Upper and lower buffer chambers were filled with TBE buffer, and the wells rinsed out using a pipette. After a short gel pre-run to ensure a steady base line, the wells were washed out again and the samples loaded into them. Data was sent to an attached computer as electrophoreses occurred. When the gel had finished running, data was processed and the 'gel file' created by the ABI PRISM 373 sequencing software was viewed to check the tracking of lanes. If necessary, tracking could be altered manually and new sample files were generated from the modified lanes. The sequence data could then be viewed within the Perkin-Elmer program SeqEd.

2.2 Generation of Lipase Mutants

2.2.1 RNA Extraction

RNA was extracted from *Aspergillus niger* mycelia expressing Lipase 3 using the method

described by Sokolofsky *et al.* (1990). All buffers used were treated by the addition of 0.1 % DEPC (diethylpyrocarbonate), left overnight and then autoclaved. Exceptions were 1 M Tris-HCl pH 8 buffer which was made with DEPC treated water and then autoclaved, and 10 % SDS which was made using DEPC treated water. All glassware, spatulas and pestle and mortar were DEPC treated by soaking them overnight in 0.1 % DEPC in water and then autoclaving.

Mycelial mats (1.231 g) obtained from Danisco were ground to a powder under liquid nitrogen and transferred straight into microfuge tubes (divided between 10 tubes) containing equal volumes (0.65 ml) of lysis buffer (0.6 M NaCl, 10 mM EDTA, 100 mM Tris-HCl pH 8 and 4 % SDS), and phenol (saturated with 0.1 M Tris-HCl, pH 8). The tubes were mixed on a windmill rotator for 20 minutes and then centrifuged at 12000 g for 10 minutes. Supernatants were transferred to microfuge tubes containing equal volumes of phenol (pH 8) and mixed for 20 seconds using a vortex mixer. Centrifugation was repeated and the upper phases transferred to equal volumes of 8 M LiCl. After overnight storage at 4 °C the tubes were mixed on a vortex mixer, centrifuged and the pellets resuspended in 0.3 ml DEPC treated water. The RNA was precipitated by addition of 30 µl 3 M sodium acetate pH 5.2 and 0.75 ml ethanol, mixing by inversion and incubation at -70 °C for 1 hour. The RNA was pelleted by centrifugation at 12000 g for 10 minutes. The pellets were washed by addition of 500 µl 70 % ethanol, centrifugation at 12000 g for 10 minutes, drying under vacuum and each pellet resuspended in 20 µl DEPC treated water. Spectrophotometric measurements at 260nm and 280nm were used to calculate the concentration of the RNA (approximately 1 µg μl^{-1}) and the OD_{260}/OD_{280} to indicate the quality of the RNA. This ratio was 1.74, indicating contamination from protein or phenol. The RNA was also analysed by electrophoresis on a 0.8 % agarose gel.

2.2.2 Preparation of cDNA

2.2.2.1 DNase treatment of RNA

To remove contaminating genomic DNA, the RNA sample was treated with RNase-free DNase I (10 units μl^{-1}) supplied by Boehringer Mannheim. DNase I was diluted 1:20 in dilution buffer (25 mM Tris-HCl, 50 % glycerol, pH7.6) and 0.5 units (1 µl) used to treat 1 µl of the RNA preparation (approximately 1 µg). The total reaction volume was 20 µl and the conditions for treatment, as recommended by the supplier, were 0.1 M sodium acetate, pH 5.2 and 5 mM $MgSO_4$. The reaction was incubated at room temperature (25 °C) for one hour, followed by inactivation of the enzyme by incubation at 65 °C for 15 minutes.

The treated RNA was immediately submitted to RT-PCR (Reverse Transcriptase-Polymerase Chain Reaction). This was performed using the Titan™ One Tube RT-PCR System from Boehringer Mannheim with gene-specific primers.

2.2.2.2 Reverse Transcriptase-PCR

The advantage of one step RT-PCR is that the cDNA synthesis reaction and the PCR are performed with an optimised buffer and enzyme system without requiring the addition of reagents between cDNA synthesis and PCR. The Titan™ One Tube RT-PCR System uses AMV reverse transcriptase for first strand synthesis and the Expand™ High Fidelity enzyme blend, consisting of *Taq* DNA polymerase and *Pwo* DNA polymerase, for amplification by PCR. The reaction was carried out following the instructions supplied by Boehringer Mannheim with the kit.

Table 2.1 Thermocycling profile for RT-PCR

1 x	denaturation at 94 °C for 2 min.
10 x	denaturation at 94 °C for 30 s annealing at 50 °C for 30 s elongation at 68 °C for 46 s
25 x	denaturation at 94 °C for 30 s annealing at 50 °C for 30 s elongation at 68 °C for 46 s + cycle elongation of 5 s for each cycle.
1 x	prolonged elongation time of 7 min at 68 °C.

Two reaction mixes, each in a total volume of 25 µl, were set up in separate eppendorf tubes. One tube contained 0.2 mM of each dNTP (dATP, dCTP, dGTP, dTTP), 0.4 µM of upstream and downstream primers, 5 mM DTT and 0.5 µg of RNA template (DNase treated). The other tube contained 1.5 mM $MgCl_2$, and 1 µl 'enzyme mix' (containing AMV reverse transcriptase and Expand™ High Fidelity PCR-System). After mixing in a 0.5 ml eppendorf tube kept on ice, the reaction was placed in a Thermo-Cycler equilibrated at 50 °C and incubated for 30 minutes (the reverse transcription step). The sample was then immediately subjected to thermal cycling as described in the Boehringer Mannheim protocol, using an annealing temperature of 50 °C, and described in Table 2.1. Samples were analysed on a 0.8 % agarose gel (in TBE).

2.2.2.3 PCR (of genomic clone)

The reaction mix for PCR consisted of: 0.1 mM of each dNTP, 1 μM each of upstream and downstream primers, 0.5 μl (2.5 units) Taq DNA polymerase (Gibco-BRL), 5 μl 10X Taq Reaction buffer (200 mM Tris pH 8.4, 500 mM KCl), 2 μl 50 mM $MgCl_2$, 20 ng *Sac* I digested pBSLip and sterile water in a total volume of 50 μl. This was subjected to the following incubation conditions using a thermal-cycler:
94 °C held for 30 seconds,
52 °C held for 30 seconds,
and 72 °C held for 1 minute,
repeated for 25 cycles and then held at 4 °C.
Samples were then analysed on a 0.8 % agarose gel (in TBE).

2.2.2.4 TOPO TA Cloning® of cDNA

The RT-PCR cDNA fragment was cloned into the pCR®-TOPO vector using the TOPO TA Cloning® kit from Invitrogen for the TA cloning of *Taq* polymerase-generated PCR products. *Taq* polymerase adds a single deoxyadenosine (A) to the 3' ends of PCR products. The pCR-TOPO vector (Figure 2.1) was supplied linearised with single 3'-deoxythymidine (T) overhangs and covalently bound to the enzyme Topoisomerase I. The system exploits the ligation reaction of the topoisomerase enzyme by providing an 'activated' linearised TA vector. The ligation occurs within 5 minutes at room temperature.

The RT-PCR product was mixed with the pCR-TOPO vector as described by the kit protocol (2 μl PCR product, 2 μl water and 1 μl pCR TOPO vector), incubated for 5 minutes at room temperature (25 °C) and then placed on ice. A 2 μl aliquot of the reaction was used to transform TOP10 One Shot™ *E. coli* competent cells, which were plated onto L-agar plates containing ampicillin and Xgal. Blue/white screening was used to pick transformants containing insert (the TOP10 strain allows blue/white screening without the addition of IPTG). Plasmid DNA was isolated by the 'mini-prep.' method and the presence of cDNA inserts were confirmed by restriction digest with *Eco* R1 and separation on a 0.8 % agarose gel (in TBE) followed by complete sequencing using M13 Forward and Reverse primers from Invitrogen (Table 2.2). When the complete cDNA sequence had been confirmed, the original bacterial clone was streaked onto an L-agar plate containing ampicillin, and plasmid DNA isolated by the 'maxi-prep.' method from overnight cultures of single colonies picked from this plate.

Table 2.2 M13 Forward (-20) and M13 Reverse Primers: Universal primers for sequencing from any vector containing the N-terminus of β-galactosidase such as the pCR-TOPO vector. Primer sites for this vector are described.

Primer name	Nucleotide Sequence	Primer Site
Universal M13 Forward (-20)	5'GTAAAACGACGGCCAG 3'	Bases 391-406
Universal M13 Reverse	5'CAGGAAACAGCTATGAC 3'	Bases 205-221

Figure 2.1 The pCR –TOPO vector The cDNA of the Lipase 3 gene was cloned into the *Eco* RI site by direct TOPO TA Cloning of the RT-PCR product generated from *A. niger* RNA using specific primers.

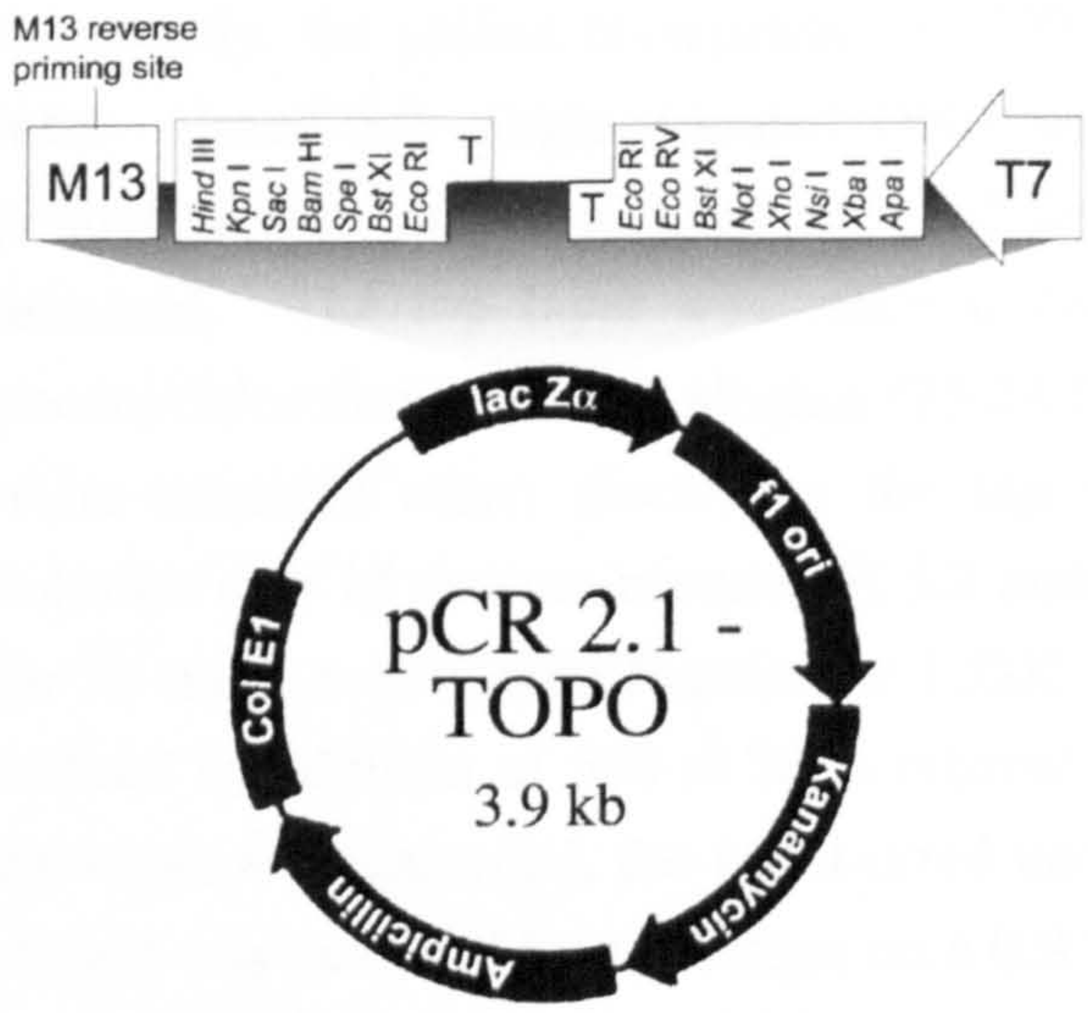

pCR®2.1-TOPO (3908 nucleotides)

LacZα fragment: bases 1-571
M13 reverse priming site: bases 205-221
Multiple cloning site: bases 234-357
T7 promoter/priming site: bases 364-383
M13 Forward (-20) priming site: bases 391-406
F1 origin: bases 548-962
Kanamycin resistance ORF: bases 1296-2090
Ampicillin resistance ORF: bases 2108-2968
ColE1 origin: bases 3113-3786

2.2.3 Site-Directed Mutagenesis

Site-directed mutagenesis was carried out by the method of Kunkel *et al.* (1987) and based on methodology described in the BIO-RAD Mutagene® M13 In Vitro Mutagenesis Kit manual. After annealing of mutagenic primers to a uracil-rich single-stranded template, a complementary DNA strand is synthesised. The SURE *E. coli* strain transformed by the mutagenesis reactions results in a high percentage of mutant progeny being replicated as the functional uracil N-glycosylase enzyme of this strain inactivates the uracil-rich parent strand.

2.2.3.1 Production of single-stranded DNA

Double-stranded plasmid DNA (pBSLip or pHILcLip) was transformed into the *dut⁻ ung⁻ E. coli* strain CJ236 and plated onto L-Agar plates containing chloramphenicol (necessary to

maintain F') and ampicillin (for plasmid selection). An overnight culture grown from a single colony was used to inoculate 100 ml of L-Broth containing chloramphenicol and ampicillin, diluting 1:50. The inoculated culture was grown to an OD_{600} of 0.3 in a shaking incubator at 37 °C. R408 helper phage was then added with a multiplicity of infection (m.o.i) of 0.2 phage/cell. After further incubation for 6 hours, the culture was centrifuged at 17000 g for 15 minutes at 4 °C. Approximately 5/6 of the supernatant was carefully transferred to a fresh centrifuge tube and centrifuged again at 17000 g at 4 °C for 10 minutes. The supernatant was treated with 300 μg RNase at room temperature for 30 minutes. Phage were precipitated from the culture supernatant with 0.25 volumes of 20 % PEG, 2.5 M NaCl solution incubating at room temperature for 30 minutes followed by centrifugation at 47000 g at 4 °C for 20 minutes. The PEG/NaCl solution was drained off thoroughly, the pellets resuspended in 500 μl T.E buffer and transferred to an eppendorf tube. Uracil-rich single-stranded DNA was extracted with an equal volume of neutral phenol (vortex-mixed, allowed to stand for 1 minute, re-vortexed and centrifuged for 5 minutes). The top layer was retained and extracted again, with an equal volume of phenol/chloroform/isoamyl alcohol (25:24:1), then with chloroform and finally with 1 ml water-saturated ether, discarding the top layer. The DNA was precipitated with 0.1 volumes of 3 M sodium acetate pH 5.2 and 2.5 volumes of ethanol, incubation at - 70 °C for 30 minutes and centrifugation at 12000 g for 30 minutes at 4 °C. The precipitate was washed by addition of 500 μl 70 % ethanol, centrifugation at 12000 g for 5 – 10 minutes, the wash was discarded, the pellet dried under vacuum and resuspended in 50 μl T.E. An aliquot was analysed by separation on a 0.8 % agarose gel prepared in TBE buffer. Single-stranded PBSLip DNA ran at approximately 2 kb and pHILcLip at approximately 3.5 kb relative to double-stranded standards. Concentrations determined from OD_{260} measurements were 0.17 μg μl^{-1} for single-stranded (ss) pBSLip and 0.67 μg μl^{-1} for ss pHILcLip.

2.2.3.2 Phosphorylation of primers

To 200 pmol of oligonucleotide, 3 μl 1 M Tris, pH 8.0, 1.5 μl 0.2 M $MgCl_2$, 1.5 μl 0.1 DTT and 1.3 μl 10 mM ATP were added in a total volume of 30 μl and mixed. (The final reaction concentrations for phosphorylating 200 pmol of oligonucleotide were 100mM Tris pH 8.0, 10 mM $MgCl_2$, 5 mM DTT and 0.4 mM ATP). T4 Polynucleotide Kinase (5 units) was then added (= 0.5 μl T4 Kinase from Gibco BRL), the reaction mixed and incubated at 37 °C for 45 minutes. The reaction was stopped by heating at 65 °C for 10 minutes and then diluted to an oligonucleotide concentration of 6 pmol μl^{-1} with T.E.buffer.

2.2.3.3 Annealing conditions

pBSLip single-stranded DNA template

Phosphorylated primers were annealed to the pBSLip single-stranded DNA template in a 30:1 molar ratio of primer to template. Phosphorylated primers (3 pmol of a single primer and 1.8 pmol each, if two primers used) were mixed with 0.1 pmol (200 ng) of pBSLip uracil rich single-stranded DNA and 1 µl 10 X annealing buffer (Appendix A: A7) in a total volume of 10 µl. Final reaction concentrations of the annealing buffer components were 20 mM Tris-HCl, pH 7.4, 2 mM $MgCl_2$ and 50 mM NaCl. A control reaction with no primers was also set up. Reaction mixes were incubated at 90 °C and cooled to 30 °C over approximately 1.5 hours then transferred to an ice-water bath.

pHILcLip single-stranded DNA template

Phosphorylated primers were annealed to pHILcLip single-stranded DNA template in a 18:1 molar ratio of primer to template. Phosphorylated primers (3 pmol of a single primer and 1.8 pmol each, if two primers used) were mixed with 0.165 pmol (500 ng) of pHILcLip uracil rich single-stranded DNA with 1 µl 10 X annealing buffer in a total volume of 10 µl. A control reaction containing no primers was also set up. Reaction mixes were incubated at 90 °C and cooled to 30 °C over approximately 1 hour then transferred to an ice-water bath.

2.2.3.4 Synthesis of the complementary DNA Strand

As 0.5 units of T7 DNA polymerase was required for this reaction, the unmodified T7 DNA Polymerase from New England BioLabs (10 units μl^{-1}), was diluted 1:20 in Dilution Buffer just prior to use and stored at – 20 °C. To the annealing reactions on ice-water, 1 µl 10 X synthesis buffer (Appendix A: A7), 1 µl (5 units) T4 DNA Ligase HC (Gibco BRL) and 1 µl (0.5 units) of unmodified T7 DNA Polymerase were added. The final reaction conditions provided by the synthesis buffer were: 23 mM Tris, pH 7.4, 5 mM $MgCl_2$, 35 mM NaCl, 1.5 mM DTT, 0.4 mM dATP, dCTP, dGTP and dTTP, 0.75 mM ATP. The reactions were incubated on ice for 5 minutes, at 25 °C for 5 minutes, at 37 °C for 30 minutes and then stopped by the addition of 90 µl stop buffer (10 mM Tris pH 8, 10 mM EDTA) and frozen.

Reactions were analysed on 1 % agarose gels (prepared in TAE buffer) containing 0.5 µg ml^{-1} ethidium bromide. The second strand synthesis reaction results in the formation of relaxed covalently closed circular (ccc) DNA (RF-IV DNA). Ethidium bromide binds to

this form of DNA resulting in condensation to positive supercoils, which causes the DNA to migrate more rapidly through the gel. Since this form binds less ethidium bromide than the negatively supercoiled RF-I DNA, it often migrates slightly faster than the RF-I form, but very close together. Therefore a band migrating with or slightly ahead of RF-1 plasmid DNA indicates successful conversion to the covalently closed circular RF-IV. A band in this position from the control reaction is an indication of endogenous priming occurring from a contaminated template.

Successful reactions, as indicated by gel analysis, were used to transform competent SURE *E. coli* cells. The number of colonies obtained in the no-primer reaction should be less than 20 % of that obtained with primer. Transformants were analysed by DNA sequencing.

2.3 Expression of Lipases

Transformation of the pHIL-D2 expression vector containing cDNA coding for Lipase3 (pHILcLip) into *Pichia pastoris* yeast by the spheroplast method, followed by the expression of Lipase 3 were carried out following instructions in the manual supplied with the *Pichia* Expression Kit (Version 1.5) from Invitrogen. For transformation into *Pichia* competent cells, the *Pichia* EasyComp™ Kit was used following instructions in the manual supplied (Version A).

The *Pichia pastoris* strain GS115 possesses a mutation in the gene for histidinol dehydrogenase (*his4*) that prevents synthesis of histidine, which must therefore be added to growth media. The *HIS 4* gene is present in *Pichia* expression vectors and allows the selection of transformants (phenotype His^+) by their ability to grow on histidine-deficient medium. Induction of expression is driven specifically by methanol, acting at the *AOX1* promoter (P_{AOX1}) present in *Pichia* expression vectors.

The components of media used in the methods described below are listed in Appendix A, sections A3.2 (stock solutions for preparing yeast media) and A3.3 (yeast media).

2.3.1 Transformation into *Pichia Pastoris* GS115

2.3.1.1 Preparation of DNA

For transformation into *Pichia pastoris* strain GS115, 2 - 5 μg pHILcLip DNA was digested with *Not* 1 in a total volume of 20 μl using Life Technologies (Gibco) restriction enzyme and React 2 buffer. Digestion was confirmed by separation of an aliquot by agarose gel

electrophoresis (0.8 % in TBE buffer). This was adequate for transformation by the spheroplast method. For transformation into competent GS115 cells (using the *Pichia* EasyComp. kit™ from Invitrogen) the digest was extracted using phenol/chloroform/isoamyl alcohol (25:24:1) to remove proteins (by vortex-mixing with an equal volume, centrifugation at 12000 g followed by extraction of the top aqueous layer using water-saturated ether). The digest was then precipitated with 0.1 volumes 3 M sodium acetate pH 5.2 and 2.5 volumes ethanol, incubation on ice for 30 minutes and centrifugation at 12000 g for 30 minutes. The pellet was washed using 500 µl 70 % ethanol, dried and resuspended in 5 µl T.E buffer.

2.3.1.2 Spheroplast Transformation Method

Cell Growth

From a frozen stock, GS115 was streaked onto a YPD plate and single colonies allowed to grow at 30 °C. A single colony was picked, grown in 10 ml YPD overnight and 20 µl of this stock culture used to inoculate 200 ml YPD, which was grown to OD_{600} 0.2 - 0.3 at 30 °C taking approximately 20 hours. Cells were harvested by centrifugation at 1500 g for 5 minutes at room temperature.

Preparation of Spheroplasts

The cells were washed by resuspension in 20 ml sterile water and centrifugation at 1500 g for 5 minutes at room temperature and then in SED buffer (1ml 1 M DTT mixed with 19 ml of SE: 1 M sorbitol, 25 mM EDTA, pH 8) in the same way. The cells were then resuspended in 20 ml SCE buffer (1 M sorbitol, 1 mM EDTA and 10 mM sodium citrate buffer, pH 5.8).

Half of the cell suspension in SCE (10 ml) was used to calculate the incubation time with the spheroplasting enzyme, Zymolyase to give 70 % spheroplasts. 7.5 µl of Zymolyase solution (3 mg ml^{-1}) kept on ice, was added to the sample and incubated at 30 °C. Over the next 40 minutes 200 µl aliquots were taken at time intervals (2, 4, 5, 6, 7, 8, 9, 10, 15, 20, 30 and 40 minutes), added to 800 µl aliquots of 5 % SDS solution and mixed. OD_{800} readings of these samples were taken (sample at t = 0 was taken before the addition of enzyme) using 800 µl 5 % SDS and 200 µl SCE as a reference (blank). The formula % Spheroplasting = 100 - (OD_{800} time t/OD_{800} time 0) x 100 was used to determine the percentage of spheroplasting at each time point, allowing the time of incubation resulting in 70 % spheroplasting to be determined (usually about 15 minutes).

The remaining cells were treated with 7.5 µl Zymolyase (3 mg ml^{-1}) to give 70 % spheroplasts and then harvested by centrifugation at 750 g for 10 minutes at room temperature. They were washed by resuspension in 10 ml 1 M sorbitol and centrifugation at 750 g as before, then in 10 ml CaS buffer (1 M sorbitol, 10 mM Tris-Cl, pH 7.5, 10 mM $CaCl_2$), and finally resuspended in 0.6 ml of CaS.

Transformation

Not 1 digested DNA (2 – 5 µg) was added to 100 µl of the spheroplast suspension in an eppendorf tube and incubated for 10 minutes at room temperature. To this, 1 ml of PEG/CaT solution (1:1 mixture of 40 % PEG and CaT: 10 mM Tris, pH 7.5 and 10 mM $CaCl_2$) was added, incubated for 10 minutes at room temperature and then centrifuged at 750 g for 10 minutes. The pellet was resuspended in 150 µl SOS (1 M sorbitol, 0.3 X YPD, 10 mM $CaCl_2$) and incubated for 20 minutes at room temperature. Finally, 850 µl 1 M sorbitol was added.

Plating

Aliquots of the transformed cell solution (100 - 300 µl) were added to 10 ml molten RD top agar (pre-incubated at 45 °C) and poured onto RDB base plates. Alternatively, aliquots were added to 10 ml molten RD + 1 mM 3-AT top agar and poured onto RDB + 1 mM 3-AT plates (to select for His^+ transformants in which multiple-integration of the transforming DNA has occurred). These were incubated at 30 °C until transformants appeared (4 - 6 days). Transformation efficiencies were typically 10^2 - 10^4 transformants μg^{-1} DNA. To test the viability of spheroplasts a 100 µl aliquot of the spheroplast solution in CaS was added to 900 µl 1 M sorbitol, of this 100 µl was mixed with molten RDH top agar and poured onto a RDHB base plate.

2.3.1.3 EasyComp transformation method into Pichia pastoris

Using solutions supplied with the *Pichia* EasyComp™ Kit from Invitrogen.

Preparation of competent cells

A single GS115 colony was picked from a YPD plate and grown in 10 ml YPD broth overnight. The culture was diluted to an OD_{600} of 0.1 - 0.2 in 10 ml YPD and grown to OD_{600} 0.6 - 1.0 at 30 °C taking approximately 5 hours. Cells were harvested by centrifugation at 500 g for 5 minutes at room temperature and resuspended in 10 ml of Solution I (a sorbitol solution containing ethylene glycol and DMSO). They were then pelleted by centrifugation at 500 g for 5 minutes at room temperature and resuspended in 1

ml of Solution I. The competent cells were frozen in 50 µl aliquots in a Styrofoam box placed in a – 80 °C freezer to freeze the cells down slowly.

Transformation

Using either freshly prepared competent cells or thawed out frozen aliquots, 3 µg of *Not* I linearised DNA was added to 50 µl of competent cells. To the DNA/cell mixture 1 ml of Solution II (PEG solution) was added and mixed by vortexing. The transformation reactions were incubated for 1 hour at 30 °C and vortex-mixed every 15 minutes. The cells were heat-shocked at 42 °C for 10 minutes and then pelleted at 3000 g for 5 minutes at room temperature. The cells were washed by resuspension in 1 ml of Solution III (salt solution) and were pelleted by centrifugation at 3000 g for 5 minutes at room temperature. The cell pellet was resuspended in 100 to 150 µl of Solution III and the entire transformation plated onto selection plates (RDB) and incubated for 2 to 4 days at 30 °C.

2.3.2 Screening Transformants

Transformation of linearised plasmid into GS115 involves recombination with the *Pichia pastoris* genome at regions of homology (at the *his4* or *AOX1* loci) by replacement or insertion. Two different phenotypic classes of His^+ recombinant strains can be generated from transformation into GS115: Mut^+ and Mut^S. Mut^+ (Methanol utilisation plus) refers to the wild type ability of strains to metabolise methanol as the sole carbon source. Mut^S refers to slow growth on methanol due to the loss of alcohol oxidase activity (required for methanol metabolism) that occurs on gene replacement at the *AOX1* locus of the GS115 strain.

2.3.2.1 Screening for AOX1*-disrupted transformants*

To assess the His^+ transformants for Methanol utilisation phenotype (Mut), colonies were picked using a sterile toothpick and "patched" onto an MM (minimal methanol) plate and then an MD (minimal dextrose) plate in a regular pattern (50 colonies were 'patched' onto each plate with the aid of a scoring template). For each transformation 100 transformants were patched and the plates incubated at 30 °C for at least 2 days (usually left for 5 days for a clear result). Normal growth on dextrose and slow growth on methanol is indicative of the Mut^S phenotype of GS115.

2.3.2.2 Screening for lipase expression on Rhodamine B plates

After screening for *AOX1* disrupted transformants (see above), the His^+ transformants were patched using sterile toothpicks from the MD plates onto minimal methanol plates containing rhodamine B and olive oil in a regular pattern, and incubated at 30 °C overnight.

The hydrolysis of olive oil by expressed lipase (from induction by methanol) releases fatty acids, which react with rhodamine B causing it to fluoresce. Lipase positive transformants could be visualised under UV light as fluorescing patches.

2.3.3 Small Scale Expression of Lipase

A small amount of cells taken from colonies (or patches) on the MD plate were used to inoculate 10 ml BMGY (buffered glycerol - complex medium). Covered by loose caps, the cultures were incubated at 30 °C with vigorous shaking until grown to saturation (2 days), with OD_{600} in the range 10 - 20. Cells were harvested by centrifugation at 4000 g for 10 minutes at room temperature and resuspended in 2 ml BMMY (buffered methanol - complex medium). These cultures were covered with 2 layers of sterile gauze and incubated at 30 °C with shaking for 3 days. Cells were then pelleted by centrifugation at 4000 g as before and supernatants analysed for expressed product.

2.3.4 Large Scale Expression of Lipase

2.3.4.1 Expression of Mut$^+$ *transformants.*

BMGY cultures (25 ml) were grown from single colonies of GS115 transformants streaked onto MD plates, or from frozen stocks, at 30 °C with shaking in 250 ml conical flasks to OD_{600} = 2 - 6 (taking 16 - 18 hours). Cells were harvested by centrifugation at 4000 g for 10 minutes at room temperature and resuspended to an OD_{600} of 1 in BMMY media in 1 l baffled flasks, which were covered with 2 layers of sterile gauze and further incubated with vigorous shaking at 30 °C for 4 days. Methanol was added to a final concentration of 0.5 % methanol every 24 hours to maintain induction. Cultures were centrifuged at 4000 g as before and the supernatants retained.

2.3.4.2 Expression of Mut^s *transformants*

BMGY cultures (10 ml) were grown from single colonies of GS115 transformants streaked onto MD plates, or from frozen stocks, and grown overnight at 30 °C with shaking. From these, 5 ml aliquots were used to inoculate 500 ml BMGY media and grown in 2 l conical flasks at 30 °C with vigorous shaking to saturation (OD_{600} 10 - 20). Cultures were harvested by centrifugation at 4000 g for 10 minutes at room temperature and resuspended 100 ml BMMY media in 1 l flasks, which were covered with 2 layers of sterile gauze and further incubated with vigorous shaking at 30 °C for 4 days. Methanol was added to a final concentration of 0.5 % methanol every 24 hours to maintain induction. Cultures were centrifuged at 4000 g as before and the supernatants retained.

2.3.5 Preparation of Frozen stocks

Single colonies of His^+ transformants were cultured overnight in YPD media (10 ml) at 30 °C. The cells were harvested by centrifugation at 500 g and resuspended in YPD containing 15 % glycerol at a final OD_{600} of 50 - 100 (approximately 2.5 - 5 x 10^9 cells ml^{-1}) followed by flash freezing in liquid nitrogen and storage at – 70 °C.

2.4 Purification of Lipases

2.4.1 Anion-Exchange Chromatography

Supernatants from the culture media were dialysed overnight at 4 °C against 20 mM triethanolamine, pH 7.3 using dialysis tubing. A 10 ml sample of dialysed supernatant was applied to a 1 ml Hi-trap™ Q column from Pharmacia Biotech (charged group: Quaternary ammonium strong anion exchanger) using an FPLC system (Pharmacia Biotech). The pumps were first equilibrated and the column washed with 20 mM triethanolamine, pH 7.3 buffer that had been filter sterilised through a 0.22 μm filter (Millipore). Lipase activity was eluted with a 60 ml linear NaCl gradient from 0 to 0.6 M NaCl in 20 mM triethanolamine, pH 7.3 buffer for mutant enzymes and a 70 ml gradient up to 0.35 M NaCl for the wild type. Flow rate was 2 ml min^{-1} and 1 ml fractions were collected. Lipase activity, as detected by resorufin-ester assay of fractions (section 2.5.1), eluted between 0.15 and 0.2 M. Pooled fractions were dialysed overnight at 4 °C against 20 mM triethanolamine, pH 7.3 buffer using dialysis tubing.

2.4.2 SDS-Polyacrylamide Gel Electrophoresis (PAGE)

2.4.2.1 Sample Preparation

Supernatants (20 μl) and anion exchange fractions (10 μl) were resuspended in 0.2 volumes Loading Buffer (0.0625 M Tris pH 6.8, 20 % v/v glycerol, 0.2 % w/v SDS, 20 % v/v β-mercaptoethanol, 0.00125 % bromophenol blue), heated at 100 °C for 2 minutes and centrifuged for 5 minutes if the samples contained particulate material. Samples were kept on ice until they were applied to the gel. All samples were separated on a 12 % separating gel with a 5 % stacking gel.

2.4.2.2 Gel Electrophoresis

The Bio-Rad Mini Gel System was used. A pair of clean plates, separated by spacers, were assembled in a casting stand. A 12 % separating gel was prepared by mixing 1.5 M Tris-HCl, pH 8.8, 0.4 % SDS solution with 30 % acylamide, TEMED, 10 % APS and water so that final concentrations were 0.375 M Tris-HCl, pH 8.8, 0.1 % SDS, 12 % acrylamide,

0.05 % TEMED and 0.05 % APS. The TEMED and APS were added just before the gel was poured between the gel plates using a 1 ml Gilson pipette to the required height (taking into account the shrinkage that occurs on polymerisation and the stacking gel to be poured on top). Approximately 5 ml of separating gel was made for each gel to be poured. Before the separating gel had polymerised it was overlaid with 50 µl water-saturated Butanol. When the gel had set the butanol was rinsed out thoroughly with dH_2O and the top of the gel blotted dry using filter paper. A 5 % stacking gel was prepared by mixing 0.25 M Tris-HCl, pH 6.8, 0.2 % SDS solution with 30 % acrylamide, TEMED, 10 % APS and water so that the final concentrations were 0.125 M Tris-HCl, pH 6.8, 0.1 % SDS, 3 % acrylamide, 0.1 % TEMED and 0.1 % APS. Again, the APS and TEMED were added to the gel mix just prior to pouring on top of the separating gel, using a 1 ml pipette. Approximately 1 ml of stacking gel mix was required per gel. The relevant combs were positioned in the stacking gel as soon as possible after pouring. When this had polymerised, gels were arranged in pairs in a gel tank for electrophoresis. The tank was filled with SDS running gel buffer (Appendix A: A8). The combs were carefully removed and the wells rinsed out with buffer. Samples were loaded into the wells, a cover was placed over the gel chamber and 200 V were applied. When the samples had run a sufficient distance down the gel, electrophoresis was stopped and the plates were prised apart. The separating gel was cut away from the stacking gel, rinsed in water and either stained for direct visualisation or prepared for Western Transfer. Gels were stained in Coomassie Blue Gel Stain (0.25 % Coomassie Brilliant Blue R, 10 % glacial acetic acid, 25 % isopropanol) for at least 2 hours. The gel was then soaked in Destain (10 % glacial acetic acid, 30 % propan-2-ol and water) for about 1 hour, and in water for about 1 hour.

2.4.2.3 Western Blotting

After SDS-PAGE, the gel was transferred into electroblotting buffer (25 mM Tris, 192 mM glycine, 20 % methanol) for 30 - 60 minutes. Two pieces of Whatman 3MM paper and 1 piece of Immobilon-P PVDF (polyvinylidene difluoride) membrane cut to the size of the gel, were soaked in electroblotting buffer. Two fibre pads supplied with the Bio-Rad Transblot apparatus were also soaked in electroblotting buffer. A "sandwich" was then constructed between the fibre pads starting with a piece of Whatman paper on the anode plate, followed by the membrane that had been pre-soaked in methanol, the gel and then a second sheet of Whatman paper. This was placed into the Transblot apparatus, which was filled with electroblotting buffer. Proteins were transferred to the membrane at 4 °C by applying a constant current of 100 mA for 14 hours. The sandwich was disassembled and the membrane rinsed in PBST (Appendix A: A8) for 15 - 30 minutes followed by blocking

of non-specific protein binding sites by soaking in PBST + 3 % BSA for 1 hour and then 4 x 5 minute washes with shaking in PBST. The primary antibody (a polyclonal rabbit antibody, supplied by Danisco, and raised against a deglycosylated form of Lipase 3) was added at a 1:1000 dilution in PBST 1 % BSA and left for 1 hour with gentle shaking. The antibody solution was removed and the filter washed thoroughly with PBST as before. Second antibody (goat anti-rabbit IgG alkaline phosphatase conjugate) diluted 1:30000 in PBST 1 % BSA was added and left for 1 hour with gentle shaking. The filter was washed thoroughly with PBS and colour developed using Sigma fast BCIP/NBT buffered substrate tablet. One tablet dissolved in 10 ml water contains 0.15 mg ml^{-1} BCIP (5-bromo-4-chloro-3-indolyl phosphate), 0.3 mg ml^{-1} NBT (Nitroblue tetrazolium), 100 mM Tris and 5 mM $MgCl_2$. When colour had developed after 20 minutes the filter was rinsed with water.

2.4.2.4 Electro-blot for N-terminal sequencing

After SDS-PAGE, proteins were electro-blotted onto Immobilon-P PVDF (polyvinylidene difluoride) membrane as for Western Blotting. The membrane was removed form the transblotting sandwich, rinsed with distilled water and then saturated with methanol for a few seconds. The blot was stained with 0.1 % Coomassie Blue R-250 in 40 % methanol, 1 % acetic acid for 1 minute. The blot was destained with 50 % methanol, rinsed well with water and bands to be sequenced cut out using scissors. Immobilised proteins were sequenced using automated Edman degradation (Matsudaira, 1987).

2.4.3 Protein Quantitation

Spectrophotometrically, protein concentrations were measured from OD readings taken at 320, 280 and 260 nm. Concentrations were either calculated automatically by the ProEst. software or by the Warburg Christian method (Warburg and Christian, 1941) from the equation: protein (mg ml^{-1}) = 1.45 OD_{280} - 0.74 OD_{260}.

The Bio-Rad protein assay reagent was used for the Bradford assay (Bradford, 1976), with a BSA (bovine serum albumin) standard curve from 2 - 20 μg ml^{-1} in buffer (e.g. 0.1 M potassium phosphate buffer, pH 6 or 10 mM MOPS-KOH, pH 7.3). The Bio-Rad Protein Assay Dye Reagent Concentrate contains Coomassie Brilliant Blue G-250. Dye Reagent (30 μl) was mixed with 120 μl samples (diluted with buffer to be within the range of the standard curve) in wells of a microtitre plate and after a period of 5 minutes to 1 hour the OD at 595nm recorded against a blank (buffer plus reagent). By comparison with the OD_{595} values of the BSA standards, protein concentrations could be calculated.

2.5 Lipase Activity Assays

2.5.1 Resorufin Ester Assay

To 120 µl buffer (0.1 M KH_2PO_4 pH 5.4) and 15 µl resorufin ester substrate (1 mg ml^{-1} 1,2-O-Dilauryl-rac-glycero-3-glutaric acid-resorufin ester in isopropanol), 7.5 µl enzyme (*Pichia* supernatant or dialysed anion exchange fraction) was added and mixed in a microtitre plate well. After 190 seconds the reaction was stopped by addition of 7.5 µl 1 M KOH and the absorbance read at 572 nm (A_2) using a microtitre plate reader. The absorbance at 572 nm of 1 M KOH added to buffer and substrate only provided a reference value, A_1. Lipase activity was calculated using the formula: -

$$U\,l^{-1} = \frac{V \times 1000}{v \times \varepsilon \times d} \times \Delta A\,min^{-1}$$

Where V: final volume (150 µl), v: sample volume (7.5 µl), ε: Absorption coefficient of resorufin at 572nm = 60 (l x $mmol^{-1}$ x cm^{-1}), pH 6.8, d: light path (0.4 cm), $\Delta A\,min^{-1} = (A_2 - A_1) / 3$ and U: mmol min^{-1} resorufin released.

2.5.2 *para*-Nitrophenyl Acetate (*p*-NPA) Assay

p-Nitrophenyl acetate substrate solution (10 mM) was prepared in ethanol. This was diluted 1:10 in assay buffer (10 mM 3-[N-Morpholino] propanesulfonic acid (MOPS)-KOH pH 7.3, 1 mM $CaCl_2$) and 140 µl added immediately to the enzyme sample (supernatant or anion exchange fraction) in a volume of 10 µl in a microtitre plate well and mixed. The OD_{405} was monitored every 20 seconds for 10 minutes.

p-Nitrophenol Standard Curve. A series of concentrations from 0.2 - 1 mM of *p*-nitrophenol were prepared from a stock solution (10 mM) in ethanol and 140 µl added to 10 µl assay buffer in a microtitre plate well and the OD_{405} recorded.

2.5.3 Olive Oil Emulsion Assay

Olive oil (0.5 ml) was added to 10 ml emulsification buffer (0.2 M $CaCl_2$, 5 % gum arabic (w/v)) (Hult and Holmquist 1997) and sonicated for 1 minute using an MSE Soniprep 150 sonicator set at 20 µm (full power). The emulsion (1 ml) was added to 3 ml 10 mM MOPS-KOH buffer, pH 7.3 in a thermostatted reaction vessel and stirred. Reactions were carried out at 37 °C and a set point pH of 7.3. The reaction temperature was monitored using a glass temperature sensor (T201) attached to a pHM-290 pH-stat controller (both from Radiometer). The starting pH was adjusted to the set point by titration with 20 mM NaOH.

The pH was measured and adjusted automatically by the pHM-290 pH-stat controller using 'Red Rod' glass pH (pHG200-8) and reference (Ref. 200) microelectrodes, plus an ABU901 (1 ml) autoburette for the addition of NaOH (all from Radiometer). The reaction was started by the addition of purified enzyme. The pH of the reaction was monitored by the pH-stat controller, which automatically titrated 20 mM NaOH to maintain the reaction pH at the set point. Reactions were run for 5 minutes and enzyme activity was calculated from the maximal rate of base addition to maintain a steady set point pH, usually between 2 and 5 minutes from addition of enzyme.

The temperature of the thermostatted reaction vessel was adjusted in experiments investigating temperature optima of the enzymes. For reactions investigating pH effects, the pH of 10 mM MOPS-KOH buffer was varied between 6.5 - 8. The pH-stat controller and autoburette were used to titrate 20 mM NaOH to adjust the substrate mixture to a fixed set point pH before addition of the enzyme. In experiments where the effect of substrate concentration was investigated, the ratios of olive oil and 10 mM MOPS-KOH pH 7.3 buffer in a total volume of 0.5 ml were varied and added to 10 ml emulsification buffer before sonication. The highest substrate concentration used was 0.5 ml olive oil, added to 10 ml emulsification buffer. The volume of olive oil was varied between 0.025 – 0.5 ml in the total emulsion volume of 10.5 ml. Around 10 emulsions were usually prepared over this range (= 2.38 – 47.62 g l^{-1}, before dilution in the reaction mix).

2.5.4 Measurement of Emulsion Surface Area

The distribution of particle sizes in the substrate emulsions was measured by laser diffraction using a Mastersizer *S* and a Malvern MS1 small sample presentation unit (Malvern Instruments Ltd.). The Optical Unit of the Mastersizer consists of a transmitter, sample area and receiver, and collects information from scattered light when a laser is passed through a sample. Data collected is then sent to an attached computer for analysis using Mastersizer software.

A 300RF lens was used (for particle measurement in the range 0.05 - 900 μm) and a fixed beam length of 2.4 μm for Malvern sample cells. Density was entered as 1 g ml^{-1} (for olive oil) and this was used in the calculation of specific surface area (S.A.), expressed in m^2 g^{-1}. The presentation used for particle analysis was set to that for olive oil emulsion in water (using the pre-determined code 3NAD where olive oil has a refractive index of 1.4504, an imaginary relative refractive index (absorption) of 0 and the dispersant (water) has a refractive index of 1.330).

A few drops of emulsified sample were pipetted into the sample presentation unit containing approximately 100 ml reverse osmosis water. The unit pumps the diluted sample through the optical unit and disperses it across the laser. The sample concentration is measured from the obscuration (the extent to which the light transmitted is attenuated by the sample). A blank reading is taking before the addition of sample to obtain a base line, which is then subtracted from the sample reading. The sample was added to obtain an obscuration of 10 – 30 %, which is the ideal range for accurate analysis. The angular distribution of the scattered light from the particles is characteristic of the size of the particles. As well as the particle size analysis, in which the frequency distribution of size classes is expressed, a range of derived parameters including mean diameters and specific surface areas were also calculated from the data collated by the Mastersizer software.

Specific surface area was calculated from the equation:

$$\text{Specific S.A.} = \frac{\text{total area}}{\text{total volume}}$$

$$= \frac{6\,V/D}{V}$$

$$= \frac{6}{D}$$

Where V is the volume of the oil phase in the emulsion and D the mean diameter of oil droplet. Specific S.A. was given in units of $m^2\ g^{-1}$.

2.6 Data Analysis

For the determination of enzyme activity, protein concentration and emulsion particle size, measurements were made in duplicate unless otherwise stated. The average (arithmetic mean) of these measurements have been presented or used in analysis (for example, in the plotting of rates against substrate concentration to determine kinetic constants). The standard deviations from average values were calculated using Microsoft Excel software, in which the 'STDEVP' function calculates standard deviation based on a population of numbers using the "biased" or "n" method. STDEVP uses the following formula :

$$\sqrt{\frac{n\Sigma x^2 - (\Sigma x)^2}{n^2}}$$

Where x = the number 'arguments' in a population, and n = the number of arguments in a population.

Standard deviations are presented either as error bars, where data is analysed in graphical form, or in tables under the column heading 'stdevp'.

CHAPTER 3 Molecular Modelling and Design of Mutants of Danisco's Lipase 3

3.1 Introduction

A model of the three-dimensional structure of Danisco's Lipase 3 was constructed, based on available crystallographic data of lipases with which it shares a high sequence homology. This structure provided a reasonable model for the rational design of mutants. The model allows the study of structure-function relationships and of charge interactions within Lipase 3, and enables the effects of specific residue alteration to be predicted. Mutations were designed from the model to improve lipase activity and to prevent N-linked glycosylation of Lipase 3. The need to prevent N-linked glycosylation was driven by industrial interest from Danisco since Lipase 3 appears to be subject to additional glycosylation upon over-expression which then leads to a drop in its specific activity.

3.1.1 Homology Modelling

Structural information is fundamental to the understanding of protein function. X-ray crystallography and NMR spectroscopy have experimentally determined approximately 9000 structures, a fraction of the known protein sequences. Data on the structures of proteins determined to atomic resolution are usually deposited in the Protein Data Bank (PDB) at Brookhaven National Laboratory, New York, from which the parameters needed to describe a protein structure can be obtained (Bernstein *et al.* 1997). The development of computer software now allows extensive analysis of protein structures from their co-ordinates in the Brookhaven Protein Data Bank, such as three-dimensional modelling and dynamic simulations of structures, and the study of charge-charge interactions using electrostatics calculations. Also, recent advances in automated protein design algorithms have provided a useful tool for structure-based design of protein variants (Hellinga, 1998).

For protein sequences without a known structure, comparative-modelling methodology can be used to build structural models. Comparative modelling uses experimentally determined protein structures to predict conformations of other proteins with similar amino acid sequences (Sali and Blundell, 1993). The accuracy of a model depends on the degree of similarity between the primary structures, especially the number of insertions and deletions of residues. Automated homology modelling software, such as the MODELER component of QUANTA (an extensive library of crystallographic software programs), can generate a refined homology model of a protein from alignment of a target sequence with homologous templates of known structure. The MODELER program creates a three-dimensional (3D) model of a protein by optimally satisfying both spatial restraints derived from the alignment and local molecular geometry (Sali and Blundell, 1993). The spatial restraints are expressed as probability

functions for features such as Cα-Cα distances, main-chain N-O distances and main-chain and side-chain dihedral angles. Loop construction is also optimised by searching structural fragments among homologues in the Protein Data Bank to fill gaps in the alignment and energy calculations are used to anneal the structure around deletions.

With 40 % sequence homology or more, three-dimensional models can be produced that are equivalent to a medium resolution X-ray structure. Even with lower homology, useful working models can be developed, as limited homology information can be augmented with spatial restraints determined from experimental techniques, allowing structural models to be generated with as little as 30 % homology to known structures. The ability to construct homology models correctly is improving, as the general rules of protein structure become understood and as more structures are experimentally determined. In fact, enough similar conformations are being discovered to suggest that only a limited number of folded conformations are used by all proteins (Creighton, 1993). Indeed, the CATH database (Orengo *et al.* 1997) attempts to cluster proteins according to their fold structures, using global structure comparison algorithms. Such databases are useful as they increase and improve our understanding of sequence/structure relationships within fold families and improves the prospect of the *ab initio* prediction of protein structure.

3.1.2 Modelling Electrostatic Interactions

Electrostatic interactions in proteins can be divided into contributions from interactions between pairs of fully or partially charged atoms and interactions of individual charges with the dielectric and counterions of the environment (the solvent). Charged residues can generate electrical potentials that may extend several Ångströms into solution, depending on solvent and temperature conditions. These potentials play an important role in catalysis as they can enhance substrate binding, stabilise transition states, and assist in efficient product release. In biological macromolecular systems electrostatic interactions appear to contribute to folding, conformational stability, enzyme activity and binding energies as well as to protein-protein interactions (Petersen *et al.* 1997).

To understand the properties of aqueous solutions requires models of the solute, the solvent, and the interactions between them. One approach is the continuum or macroscopic model, in which properties are described in terms of average values. Recent computational advances have made it possible to describe solute molecules in atomic detail while treating the solvent as a continuum, providing a more realistic representation of the protein-solvent interface in macroscopic models. The classical treatment of electrostatic interactions of proteins in

solution is based on the Poisson-Boltzmann equation (PBE)(Honig and Nicholls, 1995). The PBE relates the charges present on the atoms in the system to the electrostatic potential at all points in space, taking into account the effects of the solvent. The PBE is considered to be a good model for describing protein molecules in aqueous solutions as it accounts for the effects of both dielectrics and ionic strength. The dielectric constant (ε) reflects the reorientation of dipoles under the local electric field. The interior of a protein has a low dielectric constant because dipolar groups are fixed in a hydrogen-bonded lattice and cannot reorient in an external electrostatic field. Water, however, has a very high dielectric constant because its dipoles re-orientate more freely. A protein molecule in aqueous solution therefore creates a system with two very different dielectric media.

The dielectric regions are seen as a low-ε cavity (the protein) embedded in a continuous medium with a different value of ε. The PBE can be analytically solved only for systems with simple geometric shapes, such as spheres or planar surfaces. However most molecules have complex shapes, and their conformations may have a significant effect on electrostatic properties. The alternative to analytical solutions is to use numerical techniques to find an approximate solution. Due to recent advances in computational and algorithmic techniques, numerical solutions to the PBE can now be used to describe solute molecules with complex shapes and charge distributions in atomic detail, whilst maintaining a continuum description of the solvent (Petersen *et al.* 1997, Honig and Nicholls, 1995).

3.1.2.1 Calculating Electrical Potentials

Finite Difference Poisson-Boltzmann Method

The molecular surface is defined as the contact surface formed between the van der Waals envelope of the molecule and a probe solvent molecule. All regions inside the surface are assigned a low value of dielectric constant, ε (-2 to 4) and exterior regions are assigned the ε of water (approximately 80). The charge distribution of the molecule is usually represented in the form of point charges located at atomic nuclei. Numerical procedures to solve the PBE for the electrostatic potential first require discretisation of some sort, such as finite difference methods that map the molecule onto a three-dimensional cubic grid. The second step usually involves an iterative procedure, where an initial guess to a solution is refined successively. Warwicker and Watson (1982) reported the first numerical (finite difference) solution to the Poisson equation for a protein.

The Electrostatic Model

Electrostatic calculations in macromolecular systems using the method of finite differences also allow graphical representation of the electrostatic potential field around a macromolecule. Proteins generate unique patterns of electrostatic potentials, which can point to residues or regions with specific functions, for example in thermal stability, substrate specificity, activity, or pH optimum. More detailed finite difference calculations may be employed to estimate the interactions between ionisable groups and their surroundings, such as in determination of interaction energies, pK_as and solvation energies. This second application of finite difference electrostatic modelling requires greater numerical accuracy and normally involves more extensive calculations.

Software packages such as DelPhi and QUANTA can be used to calculate the electrostatic potential in and around macromolecules using the finite difference solution to the Poisson-Boltzmann equation. The calculation of electrostatic potentials by solvation of the PBE is dependent on the parameters assigned to describe the protein-solvent system. As well as a co-ordinate file (in PDB format), input files include an atomic radii file and an atomic charge file. Also, the location of the protein-solvent interface, the ionic strength and dielectric constants for protein and solvent must be assigned (Petersen *et al.* 1997). Software such as GRASP, or QUANTA can also be used to visualise electrostatic potentials by producing a solid surface colour coded with the local electrostatic potential. The molecular surface can thus be viewed simultaneously with the electrostatic potential features.

3.2 Design of Mutants of Lipase 3

3.2.1 The Homology Model of Lipase 3

An homology model of the 'closed' Lipase 3 was derived from crystallographic data of *Humicola lanuginosa* fungal lipase, with which it shares 49.6% sequence homology (Figure 3.1). The α-carbon co-ordinates of the *Humicola lanuginosa* lipase (*Hl*L) were obtained from the Brookhaven Protein Data Base (code 1TIB) (Derewenda *et al.* 1994b) and the homology model was created using the program QUANTA (Molecular Simulations Inc., 200 Fifth Avenue, Waltham, MA, USA) running on a Silicon Graphics Indigo workstation. The lipase primary sequence was fitted to the co-ordinates of the *Hl*L structure. This left 2 extra residues and a gap relative to *Hl*L. Regularisation within the QUANTA program tidied up the model conformation apart from the extra C-terminal residue, which was moved manually and its local structure energy minimised. The final model was then subjected to extensive energy

minimisations within QUANTA. The resulting homology model was of the 'closed' enzyme. Residue numbering began at residue 28, eliminating the 27-residue signal sequence of the proenzyme.

A model of the 'open' enzyme was constructed from the 'closed' homology model using the co-ordinates of the lid domain from the structure of the inhibited fungal lipase of *Rhizomucor miehei* (bound to diethyl *p*-nitrophenylphosphate, PDB code 4TGL) (Derewenda *et al.* 1992). The co-ordinates of the lid fragment were transferred to the lipase model in place of the 'closed' lid co-ordinates (residues 109-121). The fragment had the same number of residues and shared high sequence homology, 9 out of 13 residues being identical. The loop co-ordinates were inserted into the model, which was then regularised. This left a gap between residues 121 and 122 that required annealing, this was regularised again and then energy minimised. Extensive energy minimisation of the whole structure resulted in a homology model of the 'open' enzyme. Representations of the homology models of Danisco Lipase 3 in the 'open' and 'closed' conformations are shown in Figure 3.2.

QUANTA allowed graphic representation and manipulation of the three-dimensional model. Electrostatics calculations could also be made for interactions between charges using continuum electrostatics by the method of finite differences, which solves the Poisson-Boltzmann equation for the irregular geometry of the protein/solvent system. Overall electrostatic potential fields were calculated at neutral pH and 0.15 M ionic strength for display with QUANTA.

3.2.2 Design of 'Glycosylation' Mutants

The homology model was firstly used to design mutants to prevent hyper-glycosylation on over-expression of the recombinant *Aspergillus niger* lipase by Danisco. Aberrant glycosylation was occurring during over-expression resulting in a drastic reduction in the specific activity. N-type glycosylation occurs on the nitrogen atom of asparagine (Asn) side chains that are part of the sequence –Asn-Xaa-Ser/Thr/Cys- (Xaa can be any residue except proline). Two potential solvent-exposed glycosylation sites could be observed on the homology model at asparagine (Asn) 59 and Asn 269 (Figure 3.3). Mutagenic primers were designed in which these residues were changed to either threonine or glutamine (N59T, N269T and N269Q), in order to prevent glycosylation occurring at these sites and restore the specific activity of the lipase. Mutation to threonine eliminates the amide group through which asparagine is glycosylated whilst the side-chain length remains the same and polarity is retained. Glutamine possesses an amide group, as does asparagine, however has a longer side

chain by one extra carbon. Asparagine at position 59 was not changed to glutamine as the model structure indicated that steric clashes would occur between this longer residue and the surrounding protein. The mutants proposed were N59T, N269T, N269Q, N59T N269T and N59T N269Q.

3.2.3 Design of 'Activity Mutants'

The homology model was also used to design mutants of Danisco Lipase 3 with improved specific activity. To be able to design mutants with increased activity in dough systems, lipase substrates that are present in wheat-flour dough should be considered.

3.2.3.1 Lipase substrates in dough

The lipid fraction in wheat flour (1.5 – 2.5 %) consists of glycolipids (5 %), phospholipids (89 %) and neutral lipids (6 %), which include tri-, di- and mono-acylglycerols. About 25 % of the lipids in wheat flour are bound to starch (most of these are phospholipids). It is non-starch-bound lipids that affect the rheological properties of dough and the major constituents of these are triacylglycerols (47 %) and digalactosyl-diacylglycerols (DGDG, 20 %). When flour is kneaded into dough, the glyco-lipids (such as DGDG) become completely bound to gluten. The other lipids are bound to gluten to a less extent, and the extent of binding triacylglycerols depends on dough handling. The increase in binding of lipids to gluten when flour is made into dough can be explained by considering the lipid phases in dough. In flour, neutral lipids are present as spherosomes with phospholipid membranes, while the remaining phospholipids and the glycolipids form inverse hexagonal phases, which are converted to a laminar phase on the addition of water during dough making and in turn are able to stabilise a microemulsion of the neutral lipids. These microemulsion vesicles are themselves enclosed by the network of gluten proteins (Belitz and Grosch, 1999). As lipase substrates (tri- and di-acylglycerols) are therefore present in dough as microemulsion vesicles, enzyme activity on emulsified substrate should be considered, in the design of Lipase 3 mutants. (As discussed in Chapter 1 Section 1.61, the effect of lipases in bread making is believed to be due to hydrolysis of triacylglycerols resulting in an *in situ* production of di- and mono- acylglycerols, which are effective emulsifiers for the stabilisation of gas cells in dough).

3.2.3.2 Stabilisation of the Active Enzyme

To design mutants of Danisco's Lipase 3 with improved activity in dough, the residues of the lid domain were observed in the homology models. In particular, interactions with the surrounding protein were examined in order to identify residues involved in stabilising the two conformational extremes adopted by the lipase lid domain, i.e. 'closed' and 'open'. It was thought that by pushing the equilibrium between these two conformational states in favour of

the 'open' form, lipase activity would increase as the enzyme would be effectively 'fixed' in its active state. This could be achieved by introducing interactions to stabilise the 'open' enzyme, or alternatively to destabilise the 'closed' form. The lid opening of lipases in the presence of a lipid-water interface appears to be an efficient process; however, this conformational change could be a rate-limiting step in lipase action (Verger, 1980). By fixing the lipase lid in the 'open' conformation, adsorption to the interface should be more efficient and less likely to limit the overall reaction rate. Activity on monomeric substrate should also be improved, as the lipase, which is usually stabilised in the 'closed' conformation in an aqueous environment, will have a more accessible active site.

So, by making the 'open' (active) enzyme energetically more favourable, or the 'closed' enzyme energetically less favourable, reaction equilibrium could be pushed towards the active enzyme state to increase overall activity. The mutants that were designed on this basis were:

The T112D E114Q double mutant

In the 'open' homology model it can be seen that the threonine lid-residue at position 112 is close to arginine 108 (Figure 3.4). T112D E114Q was designed to stabilise the 'open' enzyme conformation by replacement of the threonine 112 with an aspartate residue (T112D). The negative side-chain of aspartate was predicted to interact favourably with the positive side-chain of arginine 108 in the 'open' enzyme. The interaction between these two oppositely charged groups should be stronger than between the polar hydroxyl group of the threonine residue side-chain and arginine. However, the close proximity of another negative lid-residue (glutamate, E114) to aspartate 112 could result in repulsive interactions between the two, destabilising the local structure (Figure 3.4). The mutant was therefore designed with a neutral glutamine residue in place of the negative glutamate at position 114 (E114Q). Glutamine is the amide form of glutamate; they have the same length side-chains, however glutamine possesses an amide group in place of the acidic carboxyl group of glutamate.

The W116A single mutant and W116A I113W double mutant

From the homology model, the tryptophan 116 lid-residue is seen to lie over the catalytic triad when the lipase is 'closed' and is exposed to solvent when 'open' (Figure 3.4). The hydrophobicity and position of this residue imply that it could be involved in maintaining the 'closed' enzyme conformation via hydrophobic interactions. The loss of the large hydrophobic side chain of tryptophan by replacement with the much smaller methyl group of alanine was predicted to result in destabilisation of the 'closed' lid in the W116A single

mutant. Sequence alignments show that this tryptophan residue is conserved in many fungal lipases. In the *Humicola lanuginosa* lipase a tryptophan residue exists in the equivalent position (Trp 89). Site-directed mutagenesis of this residue has been used to demonstrate a role for this residue in formation of the Michaelis-Menten complex, in particular binding and positioning the scissile acyl chain at the active site (Holmquist *et al*, 1994, Martinelle *et al*, 1996). The binding affinity for the interface was unaffected for all the mutants generated, implying that it plays a role after adsorption to the interface has taken place. In the lipase of *Rhizopus oryzae* an alanine residue is present in the equivalent position (Ala 89) where it is thought to provide a more favourable geometry for the formation of the tetrahedral intermediate than tryptophan, based on site-directed mutagenesis studies by Beer *et al* (1996).

Isoleucine 113 is a hydrophobic lid residue that is exposed to the solvent in the 'open' structure and was changed to tryptophan in the design of a double mutant. This was to compensate for the lack of hydrophobic interactions that may have occurred with the Trp 116 residue on binding to the interface (Figure 3.4), or in light of the results of mutagenesis studies carried out on this residue (Holmquist *et al*, 1994, Martinelle *et al*, 1996), with the substrate molecule itself.

3.2.3.3 Stabilisation of Transition State

Another method for improving enzyme activity is by stabilisation of the transition state by long-range electrostatic interactions, to increase the value of k_{cat}. A charge separation develops in the transition state complex of the lipase reaction mechanism as a result of the protonated histidine of the catalytic triad (His 285) and the negative oxyanion of the substrate bound to catalytic serine, as the reaction proceeds via an acylenzyme mechanism (Fersht, 1985). The dipolar field of this charge separation can be calculated by the method of finite differences (Warwicker and Watson, 1982) and represented on the homology model. Experimental and theoretical evidence has suggested that long range electrostatic interactions play a role in the stabilisation of catalytic transition states (Jackson and Fersht, 1993). Calculation of electrostatic interactions with surface charges can be used to predict mutations that by increasing transition state stabilisation lead to an increase in k_{cat} without causing structural changes at the active site (Sheffield *et al*, 1995). One mutant of Danisco Lipase 3 was designed to increase lipase activity by this method: -

H225D mutant

The H225D single mutant was designed to increase the activity of Danisco Lipase 3 by stabilisation of the transition-state to increase k_{cat}. The model was used to view the charge

separation that would develop in the lipase transition state complex (Figure 3.5). Replacement of the positive Histidine 225 residue with a negative aspartate residue was predicted to interact favourably with the positive lobe of the transition state dipole.

Figure 3.1 Sequence alignment of Danisco Lipase 3 (Lip3) & *Humicola lanuginosa* lipase (*Hl*L). Active site triad residues are marked with an asterisk (Ser 173, Asp 238 and His 285 of Lipase 3) and the lid regions are underlined. The 27-residue signal sequence of Lipase 3 is included.

```
                    10        20        30        40        50
                    |         |         |         |         |
Lip3  MFSGRFGVLLTALAALGAAAPAPLAVRSVSTSTLDELQLFAQWSAAAYCSNNIDSK-
                                      ..        ....  ......   . .
HlL   ------------------------------EVSQDLFNQFNLFAQYSAAAYCGKNNDAPA
                                      |         |         |
                                      10        20        30

                    60        70        80        90        100       110
                    |         |         |         |         |         |
Lip3  DSNLTCTANACPSVEEASTTMLLEFDLTNDFGGTAGFLAADNTNKRLVVAFRGSSTI
       . ... .... .. .  .  .  .       .  .... .....  .  .... .  .
HlL   GTNITCTGNACPEVEKADATFLYSFE-DSGVGDVTGFLALDNTNKLIVLSFRGSRSI
                    |         |         |         |         |
                    40        50        60        70        80

                    120       130       140       150       160       170
                    |         |         |         |         |         |
Lip3  ENWIANLDFILEDNDDLCTGCKVHTGFWKAWESAADELTSKIKSAMSTYSGYTLYFT
      .... .. .  .  .  .. .  .. .  .  .. .  .  .  .  .  .  .. .
HlL   ENWIGNLNFDLKEINDICSGCRGHDGFTSSWRSVADTLRQKVEDAVREHPDYRVVFT
                    |         |         |         |         |         |
                    90        100       110       120       130       140

                        180       190       200       210       220
                    *   |         |         |         |         |
Lip3  GHSLGGALATLGATVLRNDGYSVELYTYGCPRIGNYALAEHITSQGSGANFRVTHLN
      .........     ..  ..       .. .. .. . ..  . .  .  .  . .. .
HlL   GHSLGGALATVAGADLRGNGYDIDVFSYGAPRVGNRAFAEFLTVQTGGTLYRITHTN
                    |         |         |         |         |
                    150       160       170       180       190       200

                  230       240       250       260       270       280
                *  |         |         |         |         |         |
Lip3  DIVPRVPPMDFGFSQPSPEYWITSGNGASVTASDIEVIEGINSTAGNAGEATVSVVA
      ..... ..  ..  .  ...... ..     ..  ..  .... . ..           .
HlL   DIVPRLPPREFGYSHSSPEYWIKSGTLVPVTRNDIVKIEGIDATGGNNQPNIPDIPA
                    |         |         |         |         |
                  210       220       230       240       250

                    290
                *   |
Lip3  HLWYFFAISECLL
      .....   .   ..
HlL   HLWYFGLIGTCL-
                  |
                  260
```

Figure 3.2 Homology modelling of Danisco Lipase 3. (a) The 'closed' form of Lipase 3 (white) was modelled to the 'closed' form of *Humicola lanuginosa* lipase (PDB 1TIB), shown in blue. (b) The 'open' form of Lipase 3 (red) was modelled from the 'closed' model (white) and the lid domain of the 'open' form of *Rhizomucor miehei* lipase (yellow - PDB 4TGL). The atoms of the active site residues are marked in both diagrams, as van der Waals spheres in (a) and with side chains in (b).

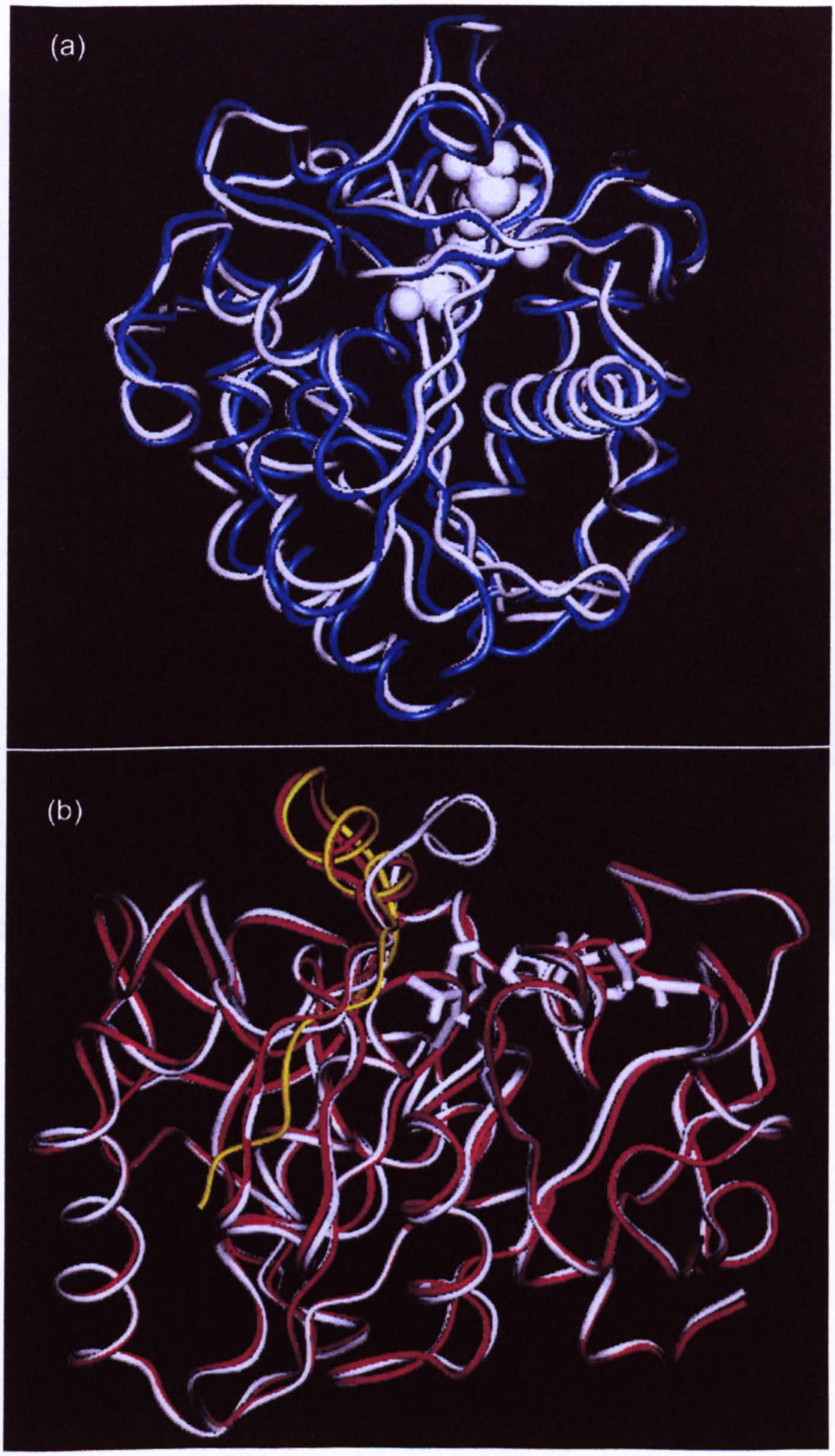

Figure 3.3 The α-carbon backbone of the Danisco Lipase 3 homology model and potential sites for N-glycosylation. Mutants were designed to prevent glycosylation occurring at asparagine 59 and asparagine 269 (shown with side-chains) on Danisco Lipase 3.

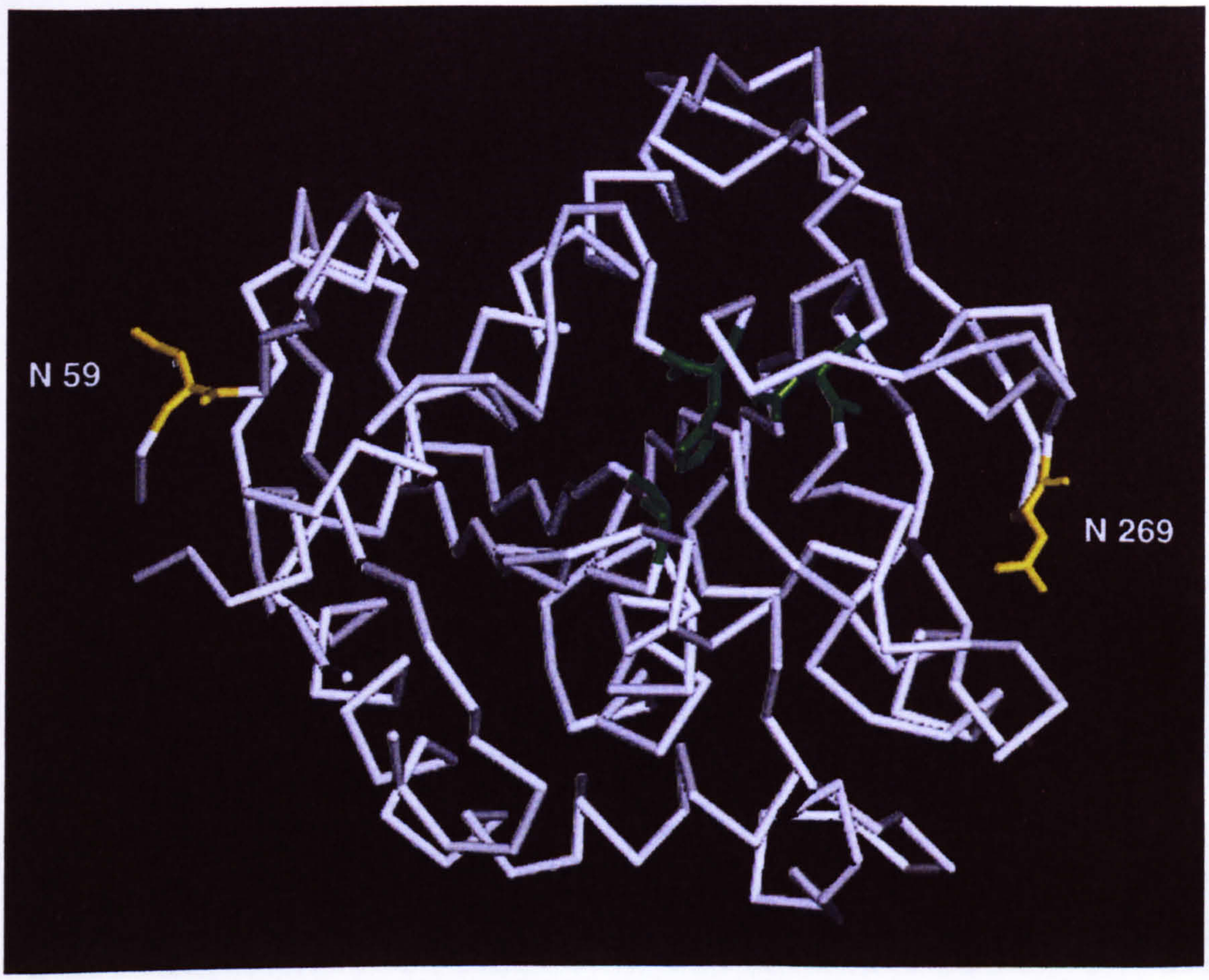

Figure 3.4 Mutants of Danisco Lipase 3 designed to improve activity by pushing equilibrium towards an 'open' lid. Altered residues are shown in relation to the α-carbon backbone of the lid domain and the catalytic triad residues of Lipase 3 in 'open' and 'closed' conformations. (a) The W116A single mutant and the W116A I113W double mutant were designed to destabilise the 'closed' enzyme conformation. (b) The T112D E114Q double mutant was designed to stabilise the lid in its 'open' conformation.

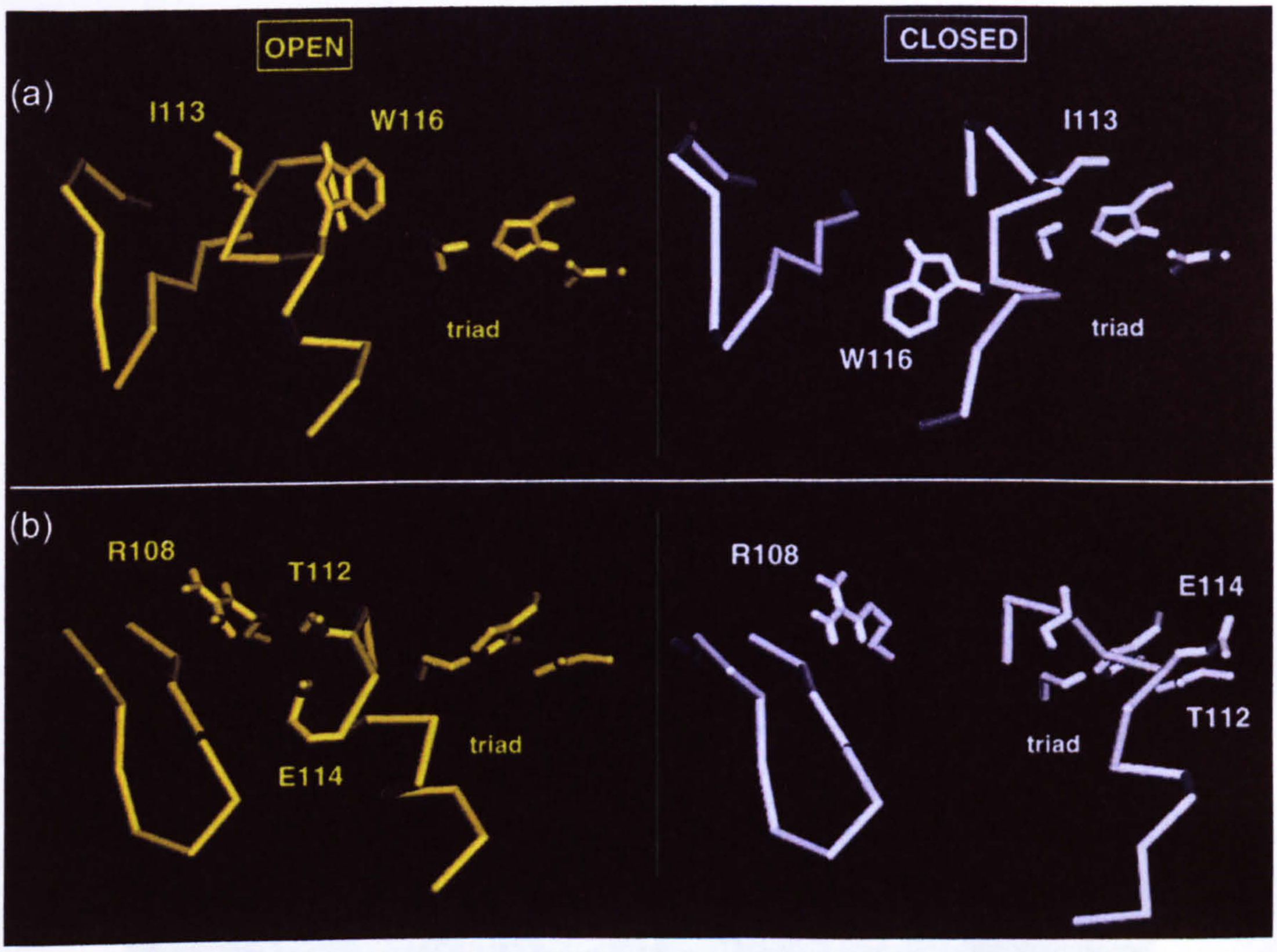

Figure 3.5 A diagram of the Danisco Lipase 3 homology model showing the potential field of a simple transition state model. The electrostatic potential field from the transition-state charge separation is displayed at – 25 mV (red) and + 25 mV (blue). An 'activity' mutant (H225D) was designed to stabilise the transition-state by introducing a negative residue (aspartate) to interact favourably with the positive lobe of the transition state dipole. The atoms of the active site triad and His 225 residue are shown with van der Waals radii.

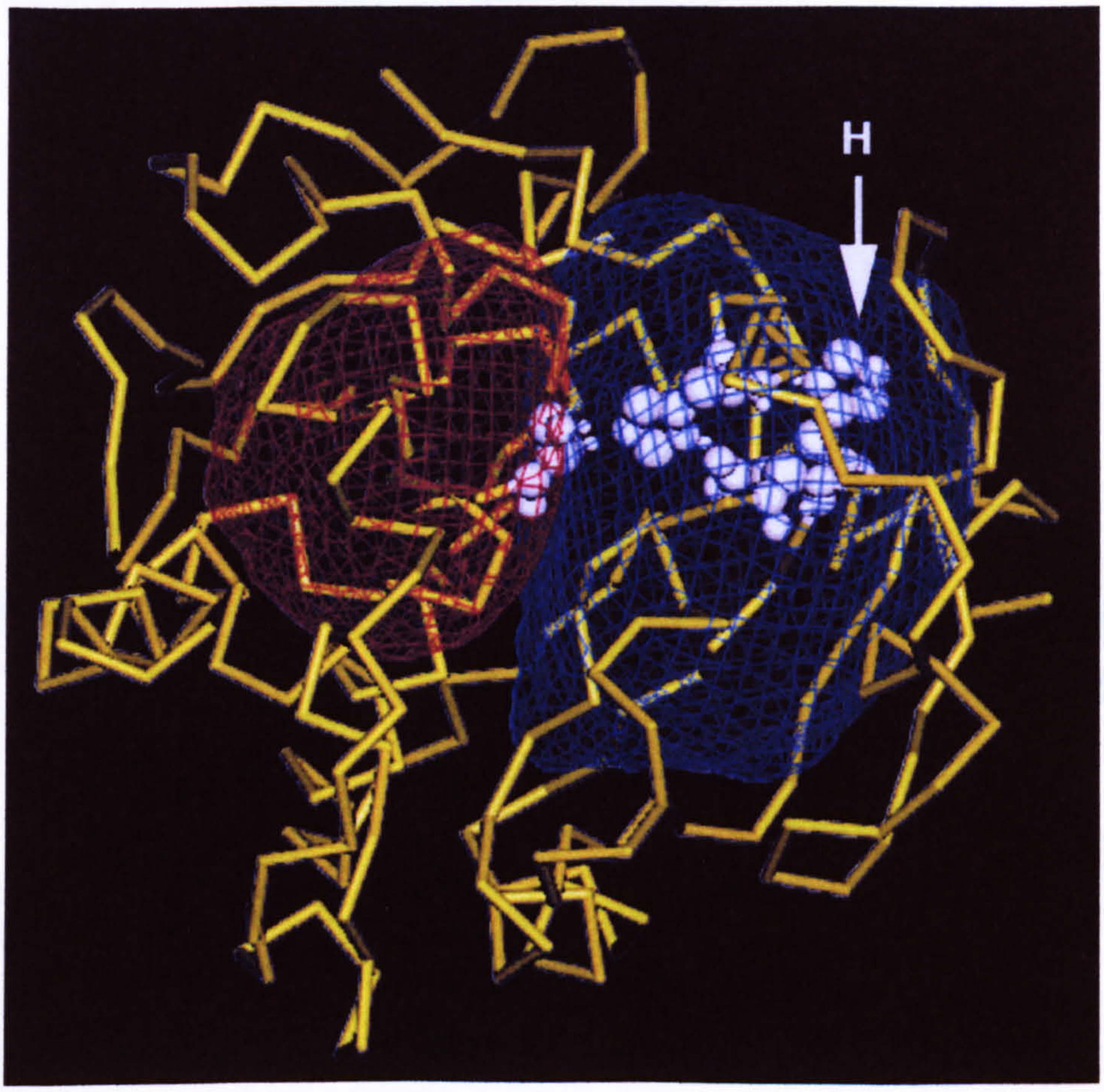

CHAPTER 4 Production of Genes Coding for Variants of Danisco's Lipase 3 by Site-Directed-Mutagenesis

4.1 Introduction

Mutants of Danisco's Lipase 3 were designed from a homology model of the enzyme's three-dimensional structure, in order to improve activity ('activity' mutants) and to prevent N-linked glycosylation occurring on expression ('glycosylation' mutants). The mutant genes were generated by the *dut⁻ ung⁻* method (Kunkel *et al.* 1987) of site-directed-mutagenesis. Using this method, mutagenic primers are annealed to a uracil-rich single-stranded DNA template. After synthesis of a complementary strand, the double-stranded construct is transformed into an *E. coli* host strain that selects against the uracil-rich parent strand, providing a very strong selection in favour of the mutagenised strand.

The Lipase 3 gene (*lipA*) was obtained from Danisco in the pBluescript vector, and the cDNA coding for Lipase 3 was prepared using RNA extracted from *Aspergillus niger* that expresses the enzyme. The cDNA coding for Danisco's Lipase 3 was cloned into the *Pichia pastoris* expression vector pHIL-D2, as lipase variants were to be expressed using this system. Both the full gene and the cDNA coding for Lipase 3 were used as templates in mutagenesis.

4.1.1 Site-Directed *in vitro* Mutagenesis Using Uracil-Containing Single-Stranded DNA

4.1.1.1 Isolation of Single-Stranded DNA

It was shown by Dotto *et al.* (1981) that plasmids containing the intergenic region (IG) of filamentous phage f1 could enter the f1 replication mode resulting in production of single-stranded (ss) DNA. In an F^+ *E. coli* strain, the plasmid DNA replicates in double-stranded RF (replicative form) until infection with f1 helper phage. Phage require pili for entry into the bacterial cell and the functions to manufacture pili are coded for on F' plasmids present in the host strain (these tend to be lost if selective pressure is not maintained). After entry into the cell, proteins coded by the helper phage act at the f1 origin causing single-stranded DNA to be produced and packaged into phage-like particles that are then extruded from the cells (Figure 4.1). Single-stranded DNA can be isolated from these particles, which can be used as a template in site-specific oligonucleotide-directed mutagenesis.

Figure 4.1 Synthesis of phagemid single-stranded DNA. Single-stranded DNA of plasmids containing the bacteriophage f1 origin of replication can be produced and packaged into phage-like particles within *E. coli* on infection with helper phage via the F pili. Both packaged phagemid and helper phage are secreted into the medium.

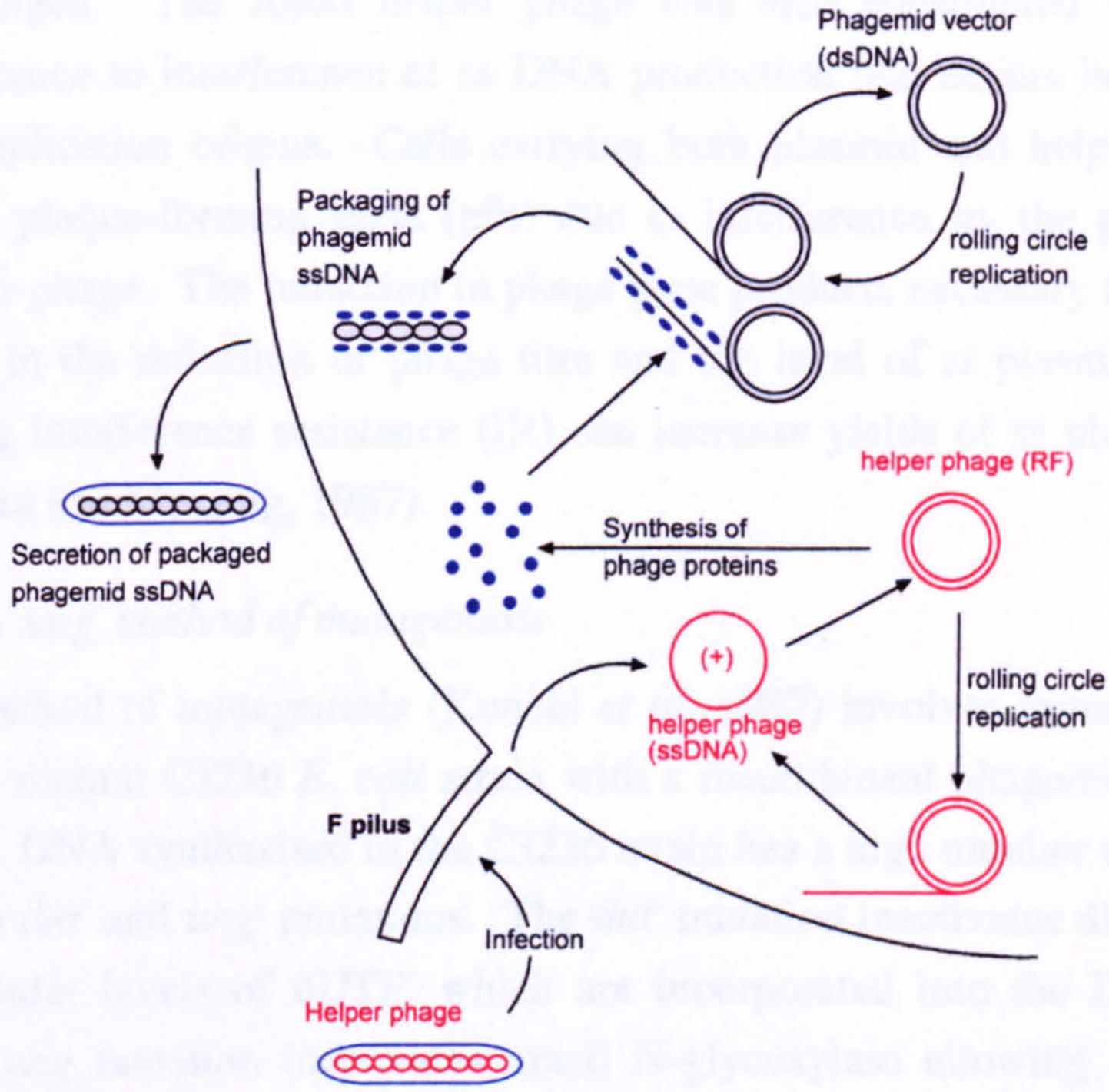

This discovery led to the development of a number of cloning vectors containing a filamentous phage IG such as pEMBL (Dente *et al.* 1983) and pBluescript (Stratagene, San Diego, CA). These vectors, termed phagemids, combine the advantages of plasmids (high-copy number and stability of cloned inserts) with the features of phage (the ability to produce single-stranded DNA). The secreted phage-like particles contain either the single-stranded plasmid DNA or f1 single-stranded DNA, in about equal frequency. The presence of helper phage DNA in recombinant plasmid single-stranded DNA preparations should not interfere with applications such as DNA sequencing or site-directed-mutagenesis where specific primers are used (that cannot hybridise with the helper phage DNA). However, it did lead to ambiguities in sequencing reactions and also resulted in low yields of packaged ss plasmid DNA, which was found to be the main technical problem in using this type of vector.

Helper phages have been constructed to overcome these problems (Vieira and Messing, 1987), for example, the R408 helper phage (Russel *et al.* 1986). Using R408, single-stranded plasmid DNA is packaged and exported preferentially over phage single-stranded

DNA. This is due to a deletion in its Packaging Signal (PS), a region of the f1 origin that enables efficient packaging of single-stranded plasmid DNA. Whilst providing the proteins required for packaging single-stranded plasmid DNA, the helper phage itself is not efficiently packaged. The R408 helper phage was also constructed with a mutation conferring resistance to interference of ss DNA production that occurs in the presence of competing f1 replication origins. Cells carrying both plasmid and helper phage have a reduced titre of plaque-forming units (pfu) due to interference by the plasmid with the replication of the phage. The reduction in phage gene products necessary for production of ss DNA results in the reduction of phage titre and the level of ss plasmid DNA. Phage mutants showing interference resistance (IR) can increase yields of ss plasmid and phage by 10-fold (Vieira and Messing, 1987).

4.1.1.2 The dut⁻ ung⁻ *method of mutagenesis*

The *dut⁻ ung⁻* method of mutagenesis (Kunkel *et al.* 1987) involves transformation of the *dut⁻ ung⁻* double mutant CJ236 *E. coli* strain with a recombinant phagemid containing the gene of interest. DNA synthesised in the CJ236 strain has a high number of uracil residues as a result of the *dut⁻* and *ung⁻* mutations. The *dut⁻* mutation inactivates dUTPase resulting in high intracellular levels of dUTP, which are incorporated into the DNA in thymine positions. The *ung* mutation inactivates uracil N-glycosylase allowing the incorporated uracil to remain in the DNA. On infection with helper phage, the transformed CJ236 cells produce and package into phage particles single-stranded plasmid DNA that is rich in uracil residues. The F' in CJ236 *E. coli* (for manufacture of pili) carry genes for chloramphenicol resistance and so this strain must be grown in the presence of chloramphenicol to maintain the F'. The uracil-rich single-stranded (Uss) DNA can be isolated and used as a template for site-directed-mutagenesis.

Oligonucleotides containing the desired mutations are annealed to the Uss DNA template and used as primers in the synthesis of a complementary DNA strand by T7 Polymerase. The new strand is ligated to the 5' end of the primer using T4 Ligase. T7 DNA Polymerase is effective in *in-vitro* mutagenesis reactions as it is a highly processive enzyme and does not carry out strand displacement, which could remove the hybridised primer. When an *E. coli* strain with functional uracil N-glycosylase (such as SURE) is transformed with the double-stranded DNA, the uracil-rich parent strand is inactivated at high efficiency, leaving the non-uracil-containing strand to replicate. Typical mutagenesis frequencies obtained with this method are greater than 50 %, allowing screening for mutants directly by DNA sequencing.

4.2 Mutagenesis

4.2.1 Cloning the Lipase Gene into pBS-KS

The primary genomic clone of the *lipA* gene coding for Danisco's Lipase 3 had been excised in the pBluescript SK plasmid (pLIP4) from a ZAPII library by Danisco. The 9396 bp pLIP4 plasmid (Figure 4.2) was obtained from Danisco in the SOLR *E. coli* strain as ampicillin-resistant colonies on an L-agar plate.

Figure 4.2 Restriction map of Danisco's primary *lipA* clone (pLIP4). The plasmid was made by *in vivo* excision of a lambda ZAP II clone. The coding region for Lipase 3 is indicated (Lip3).

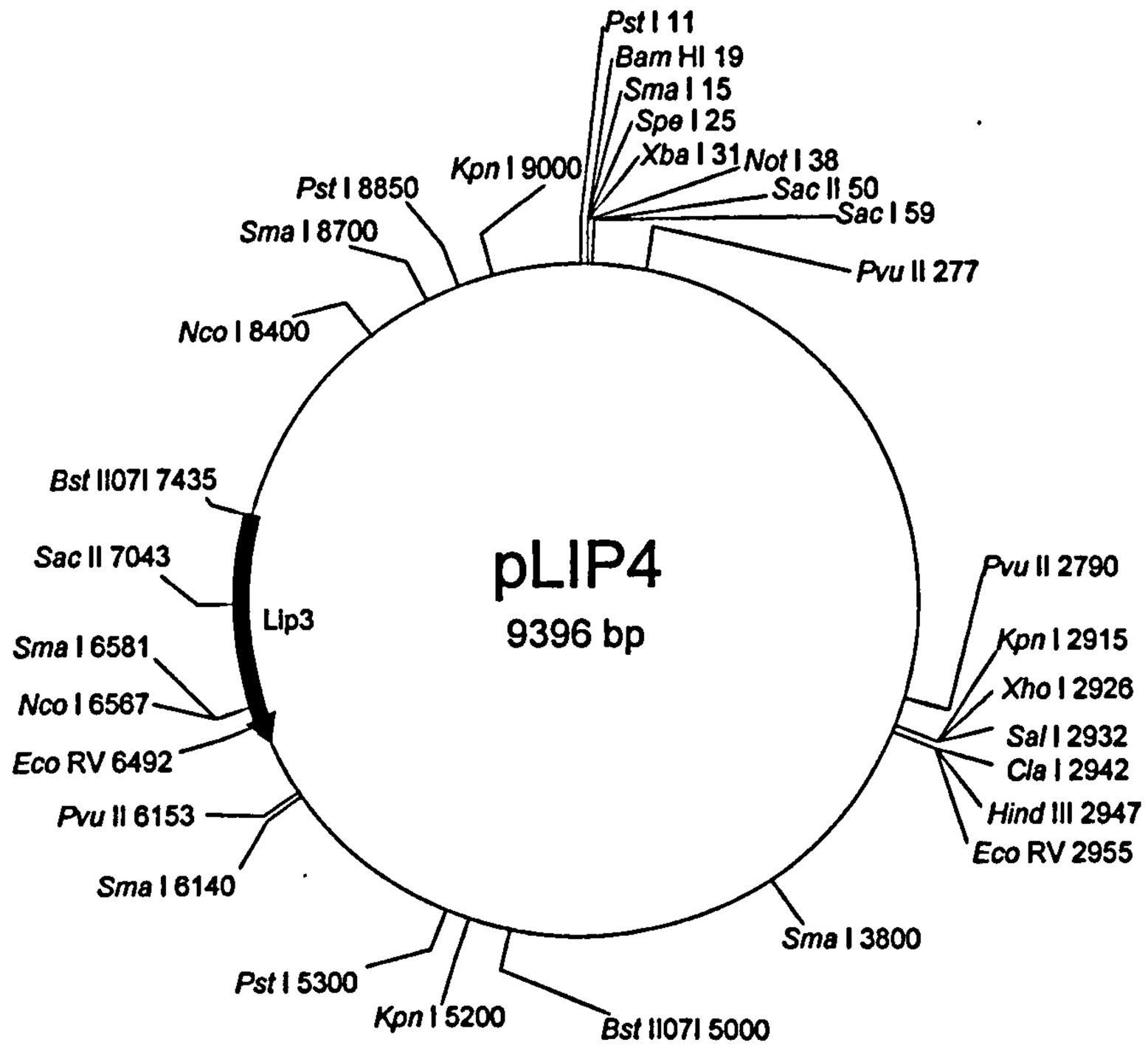

A single SOLR *E. coli* colony containing pLIP4 was picked and streaked out onto a fresh L-agar plate containing ampicillin. A single colony was picked from this plate and grown in culture, from which 'mini-prep' DNA of the pLIP4 plasmid was prepared. The Lipase 3 gene (*lipA*) was excised from pLIP4 as a 3550bp fragment by digestion with the restriction enzyme *Pst* I (at sites 8850 and 5300 in pLIP4) using the Life Technologies (Gibco) React 2 buffer. The digest was electrophoresed on a 1 % low-melting-point agarose gel (in TAE), from which a gel slice containing the *lipA* gene was excised and the DNA fragment purified. This fragment was cloned into the *Pst* I site of pBluescript KS (-) vector (Figure

4.3). The vector was digested with *Pst* I and treated with CIP (calf intestinal phosphatase). The *lipA* DNA fragment was ligated into the cut vector with T4 DNA Ligase using a 3:1 insert to vector molar ratio. The ligation reactions were used to transform competent SURE *E. coli* cells to ampicillin resistance, as the gene for resistance to ampicillin is present in the pBluescript vector (Figure 4.3). IPTG and Xgal included in the plates allowed blue/white screening to detect transformants containing insert. Plasmid DNA was isolated by the 'mini prep.' method from overnight cultures of single colonies and the presence of insert confirmed by restriction digest with *Pst* I. The resulting 6511 bp construct was referred to as pBSLip. This smaller plasmid (pBSLip) was used for mutagenesis of the Lipase 3 gene.

Figure 4.3 The pBluescript vector from Stratagene. The Lipase 3 gene was cloned into the single *Pst* I site of pBluescript II KS (-) at position 705 (within the Multiple Cloning Site, MCS).

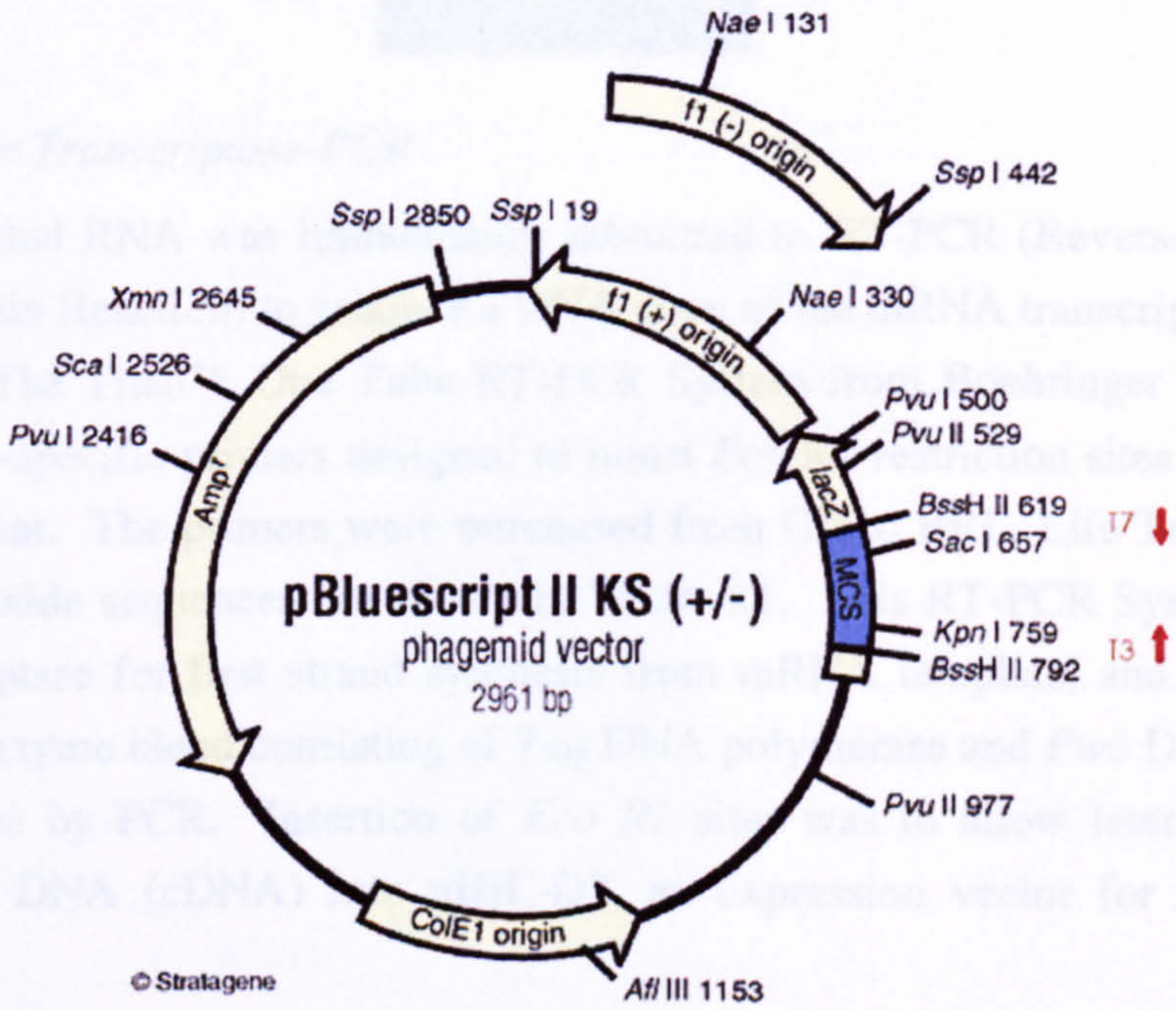

4.2.2 Isolation of cDNA Coding for Danisco Lipase 3

4.2.2.1 RNA extraction

RNA was extracted from mycelia of *Aspergillus niger* that over-express Danisco's Lipase 3 by the method of Sokolofsky *et al.* (1990). The RNA was analysed by electrophoresis on a 0.8 % agarose gel which revealed three bands present in a smear down the gel (Figure 4.4). A faint band was also present at the top of the gel indicating contamination by genomic

DNA. The RNA was treated with RNase-free DNase to remove genomic DNA from the preparation.

Figure 4.4 Agarose gel electrophoresis of RNA extracted from *Aspergillus niger* mycelia that over-expresses Danisco's Baking Lipase 3. In lanes labelled a and b are aliquots (1 μl) of total RNA prepared in parallel from the same original mycelial mat.

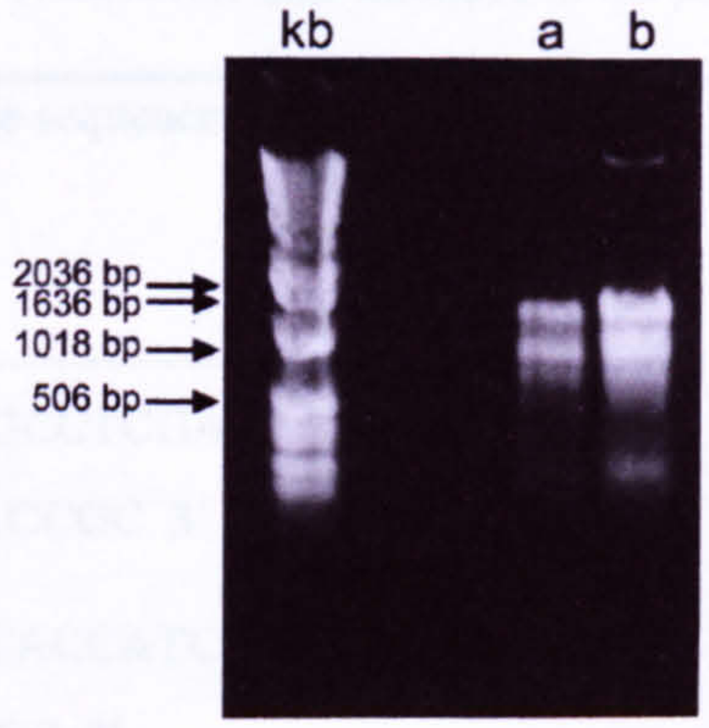

4.2.2.2 Reverse Transcriptase-PCR

The DNase-treated RNA was immediately submitted to RT-PCR (Reverse Transcriptase-Polymerase Chain Reaction) to produce a DNA copy of the mRNA transcript from the gene for Lipase 3. The Titan™ One Tube RT-PCR System from Boehringer Mannheim was used, with gene-specific primers designed to insert *Eco* R1 restriction sites at either end of the PCR fragment. The primers were purchased from Gibco BRL, Life Technologies Inc. and their nucleotide sequences are shown in Table 4.1. This RT-PCR System uses AMV reverse transcriptase for first strand synthesis from mRNA template, and then Expand™ High Fidelity enzyme blend consisting of *Taq* DNA polymerase and *Pwo* DNA polymerase for amplification by PCR. Insertion of *Eco R1* sites was to allow later cloning of the complementary DNA (cDNA) into pHIL-D2, an expression vector for *Pichia pastoris* yeast.

4.2.2.3 PCR of genomic clone

The primers used for the preparation of cDNA by RT-PCR (Table 4.1) were also used in a PCR reaction using the *lipA* genomic clone as template, for comparison of the sizes of the two products. The pBSLip plasmid was first linearised using the *Sac* I restriction enzyme (from Promega): 'mini-prep' DNA of pBSLip was digested using *Sac* I and Promega buffer C. There is one *Sac* I restriction site in this plasmid, occurring within the pBluescript vector (Figure 4.3). The linearised plasmid was subjected to PCR using Taq Polymerase. Samples of the reaction were then analysed on a 0.8 % agarose gel (in TBE) and compared to the RT-PCR reaction product (Figure 4.5). Analysis of the RT-PCR product revealed a 1

kb band as would be expected for a *bona fide* cDNA fragment (1011 bp, see Appendix B), migrating ahead of the genomic PCR fragment obtained using the same primers (a band of approximately 1.2 kb).

Table 4.1 RT-PCR Primers. For the isolation of cDNA coding for Lipase 3 using RNA extracted from *A. niger* that expresses the lipase. Restriction sites included in the primers are underlined.

Primer name	Primer nucleotide sequence	Tm °C (PCR)	Binds to strand (+ / –)	Nucleotide sequence alteration	Restriction site inserted[a]
*Eco*R1 F	5′GTTGAATTCGCCTCGA TTGTTTGTATACCGC 3′	57	–	TTGGTC→GAATTC	*Eco* R1 at position 1
*Eco*R1 R	5′TTCGAATTCCACCATC ACCACCACTGGC 3′	58	+	GTGAAA→GAATTC	*Eco* R1 at position 1163

[a] The position numbers are relative to each other and refer to genomic DNA.

Figure 4.5 Agarose gel electrophoresis of RT-PCR reactions showing the isolation of lipase cDNA. (a) RT-PCR reaction using DNAse treated RNA; (b) RT-PCR reaction using RNA that had not been treated with DNAse; (c) RT-PCR reaction using lipase genomic DNA. The size difference between bands implies that the RT-PCR product from DNAse-treated RNA is the cDNA that codes for Lipase 3.

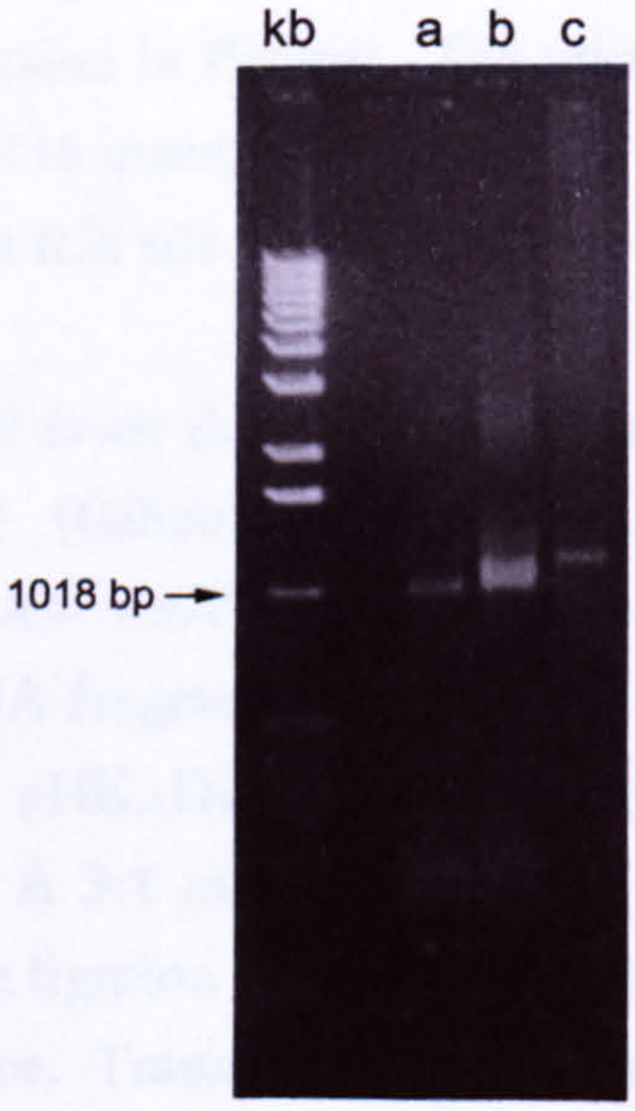

The RT-PCR product was immediately ligated into the pCR-TOPO vector by T/A cloning, taking advantage of the A-base overhang of Taq polymerase PCR products. Ligation reactions were transformed into the TOP10 strain of *E. coli*, which allowed the identification of transformants containing inserts by blue/white screening. DNA plasmid

preparations of transformants were made, and the presence of the complete cDNA confirmed by DNA sequencing.

4.2.2.4 Cloning Lipase cDNA into the Pichia pastoris *expression vector pHIL-D2*

Industrial scale production of Lipase 3 by Danisco is in *Aspergillus niger*. However, for characterisation of proteins prior to the commitment of resources for industrial scale production, the quicker and more convenient *Pichia pastoris* yeast expression system was selected.

The pHIL-D2 *Pichia* expression vector (Figure 4.6) was selected for expression of Lipase 3 from cDNA isolated by RT-PCR. This vector is effectively a phagemid as it contains an f1 origin of replication permitting generation of single-stranded DNA for mutagenesis, as well as the normal ColE1 origin and ampicillin selection. It also does not have a region coding for an N-terminal protein secretion signal. This is present in some *Pichia* expression vectors for targeting the expressed protein to the secretory pathway. The cDNA isolated for expression of Lipase 3 includes the DNA sequence that codes for its native signal sequence. It was intended that Lipase 3 would be expressed in *Pichia pastoris* by secretion using its native secretion signal sequence. The pHIL-D2 vector has a unique *Eco* R1 site after the *5'AOX1* region (Figure 4.6), which contains the *AOX1* promoter (for methanol-inducible high level expression in *Pichia*). The primers used to prepare the Lipase 3 cDNA by RT-PCR were designed to insert *Eco* R1 sites at each end of the product so that it could be cloned into the vector at this site.

Lipase cDNA was excised from the pCR-TOPO vector by restriction digest with *Eco* R1 using Life Technologies (Gibco) React 3 buffer. The digest was subjected to electrophoresis on a 1 % low melting point agarose gel (in TAE), from which a gel slice containing the *Eco* R1 DNA fragment was cut. The fragment was purified and then ligated into the *Eco* R1 site of the pHIL-D2 vector (Figure 4.6). The vector was digested with *Eco* RI and treated with CIP. A 3:1 ratio of insert to vector was used in the ligation reaction with T4 DNA Ligase. The ligation reaction was used to transform competent SURE *E. coli* cells to ampicillin resistance. Transformed cells were selected by plating onto L-agar plates containing ampicillin. DNA was isolated by the 'mini-prep' method from overnight cultures of single colonies. The presence of inserts were detected by restriction digest with *Eco* RI and DNA sequencing using the Invitrogen *Pichia* 5' AOX1 and 3' AOX1 primers (Table 4.2) which also revealed the orientation of the fragment in the vector. A clone was selected in which the cDNA had inserted in the correct orientation in relation to the AOX1

promoter of pHIL-D2 for expression of lipase to occur in *Pichia pastoris*. The original bacterial clone was then streaked out onto an L-agar plate containing ampicillin. The plasmid DNA was isolated by the 'maxi-prep.' method from overnight cultures of single colonies picked from this plate. The pHIL-D2 vector containing lipase cDNA was referred to as pHILcLip (plasmid size: 9172 bp).

Table 4.2 *Pichia* 5' and 3' AOX1 Primers: The 5' and 3' AOX1 Sequencing Primers from Invitrogen are designed to allow a gene of interest that has been inserted into any of the *Pichia* expression vectors to be sequenced. The primer sites of the pHIL-D2 vector are described.

Primer name	Nucleotide Sequence	Primer Site
5' AOX1	5' GACTGGTTCCAATTGACAAGC 3'	Bases 868-888
3' AOX1	5' GCAAATGGCATTCTGACATCC 3'	Bases 1036-1056

Figure 4.6 The pHIL-D2 *Pichia pastoris* expression vector. Lipase cDNA was ligated into the single *Eco* RI site of pHIL-D2. (The actual orientation of the f1 origin is opposite to that shown).

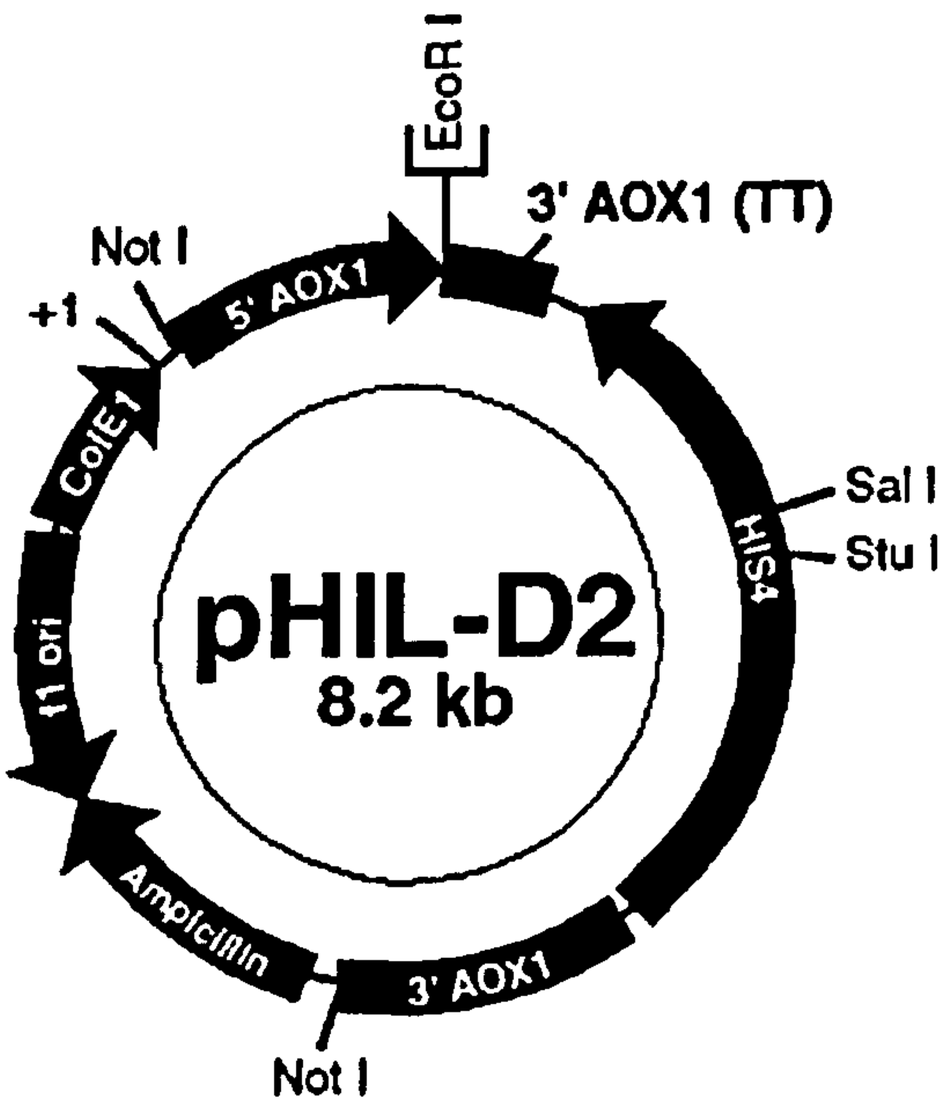

pHIL-D2 (8209 nucleotides)

5' AOX1 promoter fragment: bases 12-941
5' AOX1 primer site: bases 868-888
Eco R1 SIte: bases 956-961
3' AOX1 primer site: bases 1036-1056
3' AOX1 transcription termination (TT)
fragment: bases 963-1295
HIS4 ORF: bases 4223-1689
3' AOX 1 fragment: bases 4578-5334
Ampicillin resistance gene: bases 5686-6546
f1 origin of replication: bases 7043-6588
ColE1 origin: bases 7138-7757

4.2.3 Site-Directed-Mutagenesis

4.2.3.1 Preparation of Uss pHILcLip and pBSLip DNA

Both the pBluescript and pHIL-D2 plasmids contain an f1 bacteriophage origin of replication that permits the generation of single-stranded DNA suitable for use as a

template in oligonucleotide-directed site-specific mutagenesis. Transformation of CJ236 *E. coli* with the double-stranded pBSLip and pHILcLip plasmids (containing the *lipA* gene and cDNA coding for Lipase 3 respectively), followed by co-infection with R408 helper phage allowed isolation of uracil-rich single-stranded plasmid DNA from phage-like particles secreted into the culture media (Figure 4.7).

Figure 4.7 Agarose gel of uracil-rich single-stranded DNA preparations of (a) pHILcLip and (b) pBSLip. 1 µl of each preparation was loaded onto the gel. The sizes of pHILcLip and pBSLip are 9200 bases and 6500 bases respectively. The extra band in lane a (pHILcLip) may be R408 helper phage Uss DNA, which is 6387 bases in size (see text). A kilobase-pair ladder has been run on the same gel.

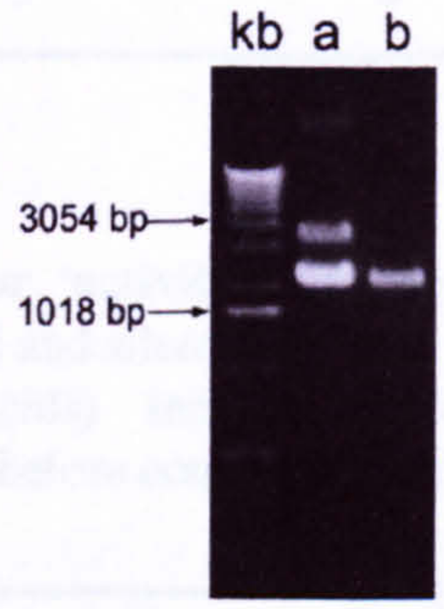

The Uss DNA preparation of pHILcLip gave two bands on agarose gel electrophoresis (Figure 4.7). The extraction was repeated several times and each preparation gave the same two bands. Comparison with the single band obtained from electrophoresis of pBSLip Uss DNA implies that the higher band of the two is pHILcLip Uss DNA, as the sizes of these phagemids are 6500 and 9200 bases respectively. The band at the lower position on the gel from pHILcLip Uss DNA runs at approximately the same position on the gel as the pBSLip Uss DNA. It is possible that this is R408 helper phage Uss DNA, which is 6387 bases in size, even though this phage was developed to prevent packaging of its own single-stranded form. It was interesting that a Uss DNA preparation of the pHIL-D2 vector alone using the R408 helper phage also gave a band in this position, as well as a band of larger size (again, presumably the pHIL-D2 Uss DNA). The presence of this extra band did not effect DNA sequencing of the single-stranded pHILcLip DNA or the success of site-directed-mutagenesis, although it was necessary to increase the amount of template used in the reactions for these applications.

4.2.3.2 Synthesis of the mutagenic strand

The orientation of the f1 origin in both the pBluescript and pHIL-D2 vectors resulted in the isolation of the sense strands of the *lipA* gene and cDNA. Reverse mutagenic primers were therefore designed and were obtained from Life Technologies Inc. The primers used for

mutagenesis are shown in Table 4.3 and Table 4.4.

Table 4.3 Mutagenic Primers for 'glycosylation' mutants (N59T, N269T, N269Q). The site of alteration is underlined.

Primer nucleotide sequence	Binds to strand (+/-)	Codon alteration	Amino acid change introduced
5'GTCAAGGTGGAGTCTTTCG 3'	+	AAT → ACT	Asn 59 → Thr
5'CCGTTGAAGTGATTCCCTCG 3'	+	AAT → ACT	Asn 269 → Thr
5'CCGTTGACTGGATTCCCTCG 3'	+	AAT → CAG	Asn 269 → Gln

Table 4.4 Mutagenic Primers for 'activity' mutants (H225D, W116A, W116A I113W and T112D E114Q). Altered codons are in bold and silent restriction sites are underlined. A 'silent' restriction site (that did not alter the encoded amino acids) included in the primer allowed initial screening for successful mutagenesis by restriction digestion before confirmation by sequencing.

Primer nucleotide sequence	Binds to strand (+/-)	Codon alteration	Amino acid change introduced	Silent restriction site
5'CGATATCGTTCAAGTCTGTAACA CGGAAGTTGGCCCC 3'	+	CAC → GAC	His 225 → Asp	*Eco* RV
5'GCAATCGCGTTCTCGATCGTGCT GCTTCCCCGGAAGGCG 3'	+	TGG → GCG	Trp 116 → Ala	*Pvu* 1
5'GCAATCGCGTTCTCCCACGTGCT GGATCCCCGGAAGGCGACCACG 3'	+	TGG → GCG ATT → TGG	Trp 116 → Ala Ile 113 → Trp	*Bam* H1
5'GCAATCCAGTTCTGAATGTCGCT GGATCCCCGGAAGGCGACCACG 3'	+	ACG → GAC GAG → CAG	Thr 112 → Asp Glu 114 → Gln	*Bam* H1

Mutagenic primers were annealed to the template Uss DNA by mixing together in molar ratios of 18:1 for pHILcLip template and 30:1 for pBSLip template, followed by incubation at a temperature above the melting temperature of the primer (90 °C) and gradual cooling to 30 °C. After the synthesis and ligation of a complementary DNA strand using T7 Polymerase and T4 Ligase respectively, the reactions were used to transform the SURE *E. coli* strain.

Analysis of reaction products

Successful mutagenesis, where priming had occurred and a second strand synthesised, resulted in formation of covalently closed circular (ccc) relaxed DNA (RF-IV). Migration of reaction products with or slightly ahead of the RF-I (negatively supercoiled) plasmid DNA on a 1 % agarose gel containing 0.5 μg ml^{-1} ethidium bromide, indicated conversion to RF-IV. Under these conditions, it is possible to distinguish ccc DNA from incomplete circular DNA or nicked circular DNA (oc DNA) (Figure 4.8). A no-primer control reaction was also run on the gel, to test for non-specific endogenous priming caused by contaminating nucleic acids in the template preparation, as this could result in lowered mutation efficiency. Production of RF-IV in the absence of mutagenic primer would be indicative of contaminated DNA template. The control reactions with pBSLip and pHILcLip templates gave only single bands migrating in the positions of ss DNA implying that no endogenous priming had occurred.

Figure 4.8 Agarose gel electrophoresis of mutagenesis reactions using pBSLip single-stranded DNA and 'glycosylation' mutant primers. Control (C; no primer added) and mutagenesis reactions (lanes 1-5) were analysed by agarose gel electrophoesis. The primers used in these reactions were as follows: - 1; N269T, 2; N269Q, 3; N59T, 4; N59T and N269T and 5; N59T and N269Q. pBSLip RF DNA (ds) and uracil-rich single-stranded DNA (Uss) were also loaded onto the gel. The percentages of mutants obtained from transformation of the corresponding reactions into SURE *E. coli* cells are indicated below the gel. Only a few colonies were obtained from transformation of the N269Q reaction, indicating that this mutagenesis reaction had not worked.
(oc: open circles; ccc: covalently closed circular DNA)

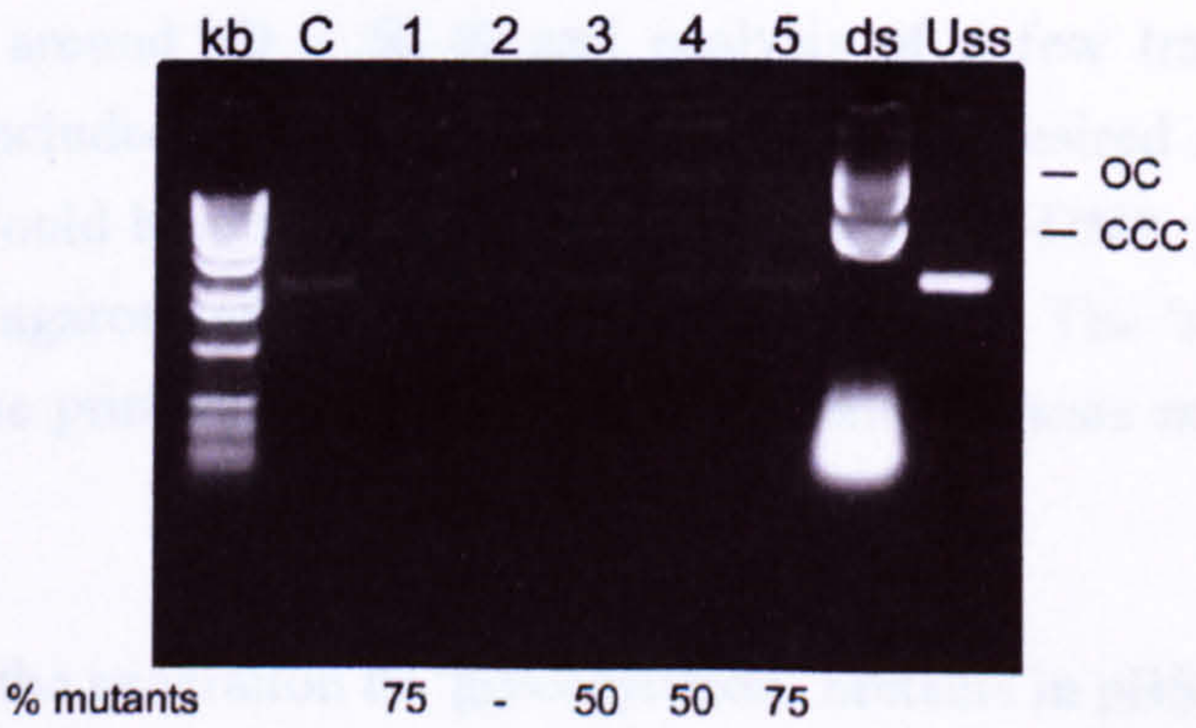

Transformation of SURE *E. coli* cells with the mutagenesis reactions gave from 10 to 500 colonies (depending on competency of cells and success of synthesis and ligation of a second DNA strand). From the transformation of no-primer control reactions using pBSLip or pHILcLip templates, just a few or no colonies at all were obtained again indicating that endogenous priming was not occurring. When the results of transformation into SURE *E.*

coli indicated that mutagenesis had been successful, colonies were picked from these plates and plasmid DNA prepared for sequencing. DNA sequencing was used to identify the plasmids containing mutants.

pBSLip mutagenesis

The 'glycosylation' mutants (N59T, N269T, N269Q, N59T N269T and N59T N269T) were generated from the genomic *lipA* clone (pBSLip) and sent to Danisco for expression in *Aspergillus niger* as this was an immediate problem. The results of this mutagenesis are indicated in Figure 4.8. Generally mutagenesis rates were at least 50 % (on average about 70 % successful priming with mutagenic primers occurred).

pHILcLip mutagenesis

Uss DNA template of the Lipase 3 cDNA in pHIL-D2 (pHILcLip) was prepared for generation of mutants to be expressed in *Pichia pastoris*. The 'activity' mutants (H225D, T112D E114Q, W116A and W116A I113W) and 'glycosylation' mutants (N59T, N269T, N269Q, N59T N269T and N59T N269T) were generated using the pHILcLip template.

Although 'silent' restriction sites were included in the 'activity' mutagenic primers, the insertion of the site into the cDNA clone did not necessarily coincide with the presence of the mutation and so failed to provide an adequate method for initial screening of mutants. This can only be attributed to errors in the synthesis of the oligonucleotides supplied to undertake the mutagenesis. Despite the mutagenesis rate being lower than usual for this method, it was still around 40 – 50 % and analysis of a few transformants by DNA sequencing usually included at least one that contained the desired mutation. The lower rate of mutagenesis could be due to contamination of the Uss DNA preparation, indicated by the extra band on agarose gel electrophoresis (Figure 4.7). The 'silent' restriction sites were included in these primers in anticipation of low mutagenesis rates as a result of this extra band.

The primers used for the generation of 'glycosylation' mutants in pBSLip were also used to generate these mutants in pHILcLip and the rate of successful mutagenesis with these primers was 55 %.

CHAPTER 5 Expression and Purification of Danisco Lipase 3 Variants from *Pichia pastoris*

5.1 Introduction

The industrial production of Lipase 3 by Danisco is in *Aspergillus niger*. However, for characterisation of proteins prior to the commitment of resources to industrial scale production, a quicker and more convenient expression system using *Pichia pastoris* yeast was selected. While possessing the properties of a eukaryotic expression system, such as protein processing, protein folding, and post-translational modification, the *Pichia pastoris* yeast expression system is easy to use and the low-level expression of its native secreted proteins facilitates the purification of secreted heterologous protein. *Pichia pastoris* has the potential to express high levels of heterologous proteins using the native alcohol oxidase promoter, which displays strong transcriptional induction in response to methanol as the sole carbon source.

The genes coding for mutants of Lipase 3 to improve specific activity ('activity' mutants) and to prevent N-linked glycosylation ('glycosylation' mutants) and for the wild type enzyme were present in the pHIL-D2 vector for expression in *Pichia pastoris* (pHILcLip). Once the expression of wild-type Lipase 3 had been successfully established using this system, the mutants were also transformed into the *Pichia pastoris* where they were expressed. The lipase variants were secreted into cell supernatants, from which they were purified by anion-exchange chromatography. Lipase activity levels were measured using a chromogenic resorufin ester substrate and proteins were analysed by SDS-PAGE at the stages of expression and purification. The purified 'glycosylation' mutants were also analysed by mass spectrometry.

5.1.1 The *Pichia pastoris* Expression System

The GS115 strain of *Pichia pastoris* has a mutation in the histidinol dehydrogenase gene (*his4*) preventing synthesis of histidine. The *HIS4* gene is present in *Pichia pastoris* expression vectors, allowing selection of GS115 transformants by their ability to grow on histidine-deficient medium (phenotype His^+).

Pichia pastoris expression vectors also contain the *AOX1* gene promoter (P_{AOX1}) to induce expression of the inserted gene. The *AOX1* gene in *Pichia pastoris* codes for alcohol oxidase. *Pichia pastoris* is a methylotrophic yeast and can metabolise methanol as its sole carbon source. The enzyme alcohol oxidase is responsible for the oxidation of methanol to formaldehyde using molecular oxygen, the first step in its metabolism. As alcohol oxidase

has a poor affinity for O_2, *Pichia pastoris* compensates for this by generating large amounts of the enzyme. Expression of this gene is tightly regulated and specifically induced by methanol when no other carbon sources are available, to very high levels (typically 30 % of the total soluble protein).

There is a second gene in *Pichia pastoris* that codes for alcohol oxidase, *AOX2*, however the *AOX1* gene is responsible for the vast majority of alcohol oxidase activity in the cell, and growth on methanol is much slower when only *AOX2* is available. Transformation of the linearised expression vector containing the gene of interest into GS115 involves recombination with the *Pichia pastoris* genome at regions of homology (i.e. at *his4* or *AOX1*), by replacement or insertion. When integration occurs by gene replacement at *AOX1*, the transformed strain (*aox1*) can be isolated by its slow growth on methanol (phenotype Mut^S: Methanol utilisation slow). Although alcohol oxidase activity encoded by the *AOX1* gene is lost, slow growth can occur due to the presence of the *AOX2* gene. Mut^+ refers to the wild type ability of strains to metabolise methanol as the sole carbon source. These two phenotypes are used to evaluate *Pichia* transformants for the type of integration of the introduced gene. It is useful to screen both integration types for expression if possible, as one phenotype may express the recombinant protein to higher levels than the other. Mut^S recombinant strains often demonstrate more efficient expression of heterologous protein, as competition for transcription factors of the *AOX1* promoter is eliminated.

5.1.1.1 Recombination events with GS115

Once the gene of interest has been cloned into the expression vector behind the *AOX1* promoter, the construct is linearised to stimulate homologous recombination events with the *Pichia pastoris* genome. Linearisation helps recombination, which usually starts by the DNA strands being 'nicked', and is used to target integration of the vector to a genomic locus. The *Pichia* expression vectors are designed with restriction sites to stimulate integration at the *his4* or *AOX1* loci of the GS115 strain when linearised by cleavage at these sites. Integration by insertion at the *his4* locus is favoured when the vector is cleaved at the *Sal* I or *Stu* I unique sites within the *HIS4* gene (Figure 5.1). Insertion at *AOX1* is favoured when the vector is cleaved at the unique *Sac* I site within the *5'AOX1* region (Figure 5.1). Digestion of the vector at the two *Not* I sites, occurring just outside of the *5'AOX1* and 3'*AOX1* regions, generates a DNA fragment with *AOX1* terminal sequences. Transformation of GS115 with this fragment favours gene replacement at the *AOX1* loci. How these events occur is explained in more detail below.

Figure 5.1 The generic structure of a *Pichia* expression vector. *Pichia* expression vectors share the features shown in black. The *Not* I, *Bgl* II, *Sac* I, *Sal* I and *Stu* I unique restriction sites permit linearisation of the vector for efficient integration into the *Pichia* genome. The 5'*AOX1* fragment contains the *AOX1* promoter (P_{AOX1}), and the 3'*AOX1* region consists of sequences from the *AOX1* gene that are further 3' to the *AOX1* transcription termination signal sequence. These regions (5'*AOX1* and 3'*AOX1*) target plasmid integration at the *Pichia AOX1* locus. The native transcription termination signal sequence (TT) and a multiple cloning site (MCS, for insertion of the gene of interest) are also present in *Pichia* vectors.

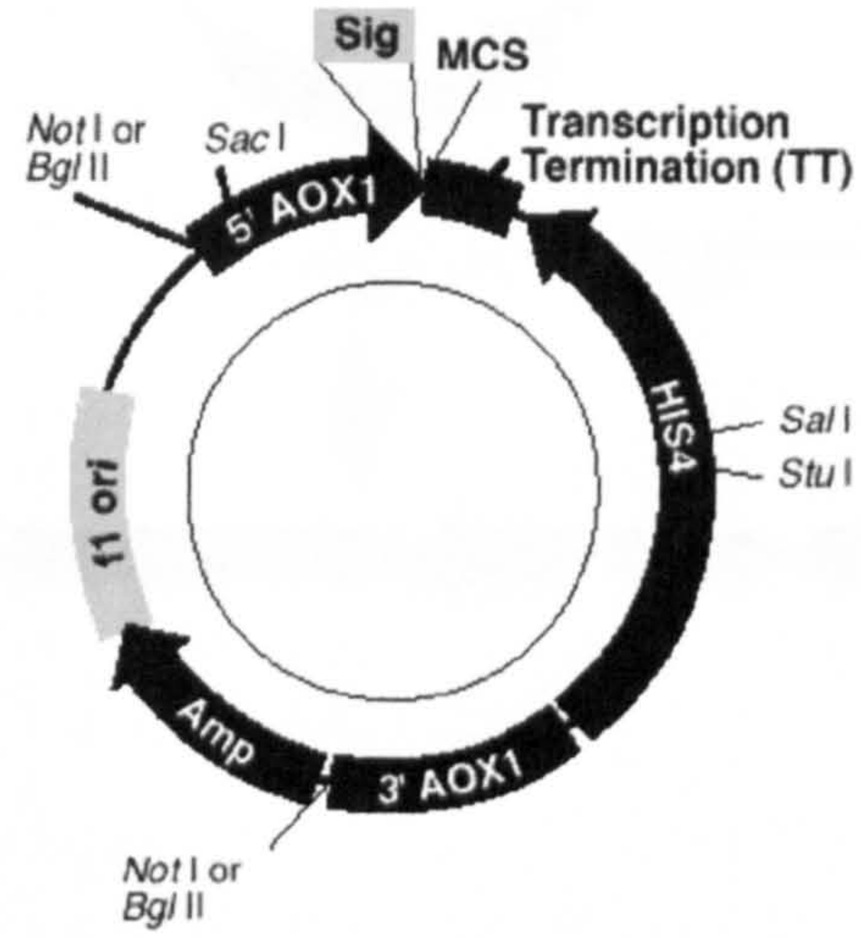

Integration by gene insertion

Insertion occurs by single crossover recombination of linearised (or circularised) plasmid, and can occur at the *AOX1* or *his4* loci of the GS115 *Pichia* genome (Figure 5.2). Repetition of this event can result in multiple-integration of the transforming DNA. Gene insertion at the *AOX1* locus occurs when the vector has been linearised at restriction sites within the *AOX1* regions of the vector (e.g. *Sac* I). Gene insertion at the *his4* locus occurs on linearisation of the vector at restriction sites within the *HIS4* region of the vector (e.g. *Sal* I or *Stu* I). Gene insertion events result in a Mut^+ phenotype of GS115, as the *AOX1* gene remains intact.

Gene insertion events can also occur between regions of homology with non-linearised plasmid or re-ligated plasmid and the *his4* and *AOX1* loci of the *Pichia* genome. However, these occur less frequently than insertion events with linearised plasmid.

Figure 5.2 Gene insertion at *his4*. Gene insertion arises from a single crossover event, in this case between the *his4* locus in the chromosome and the *HIS4* gene on the vector. By linearising the vector at a restriction site located in the *HIS4* gene one or more copies of the vector can be inserted at the *his4* locus. The resulting phenotype will be His^+ Mut^+.

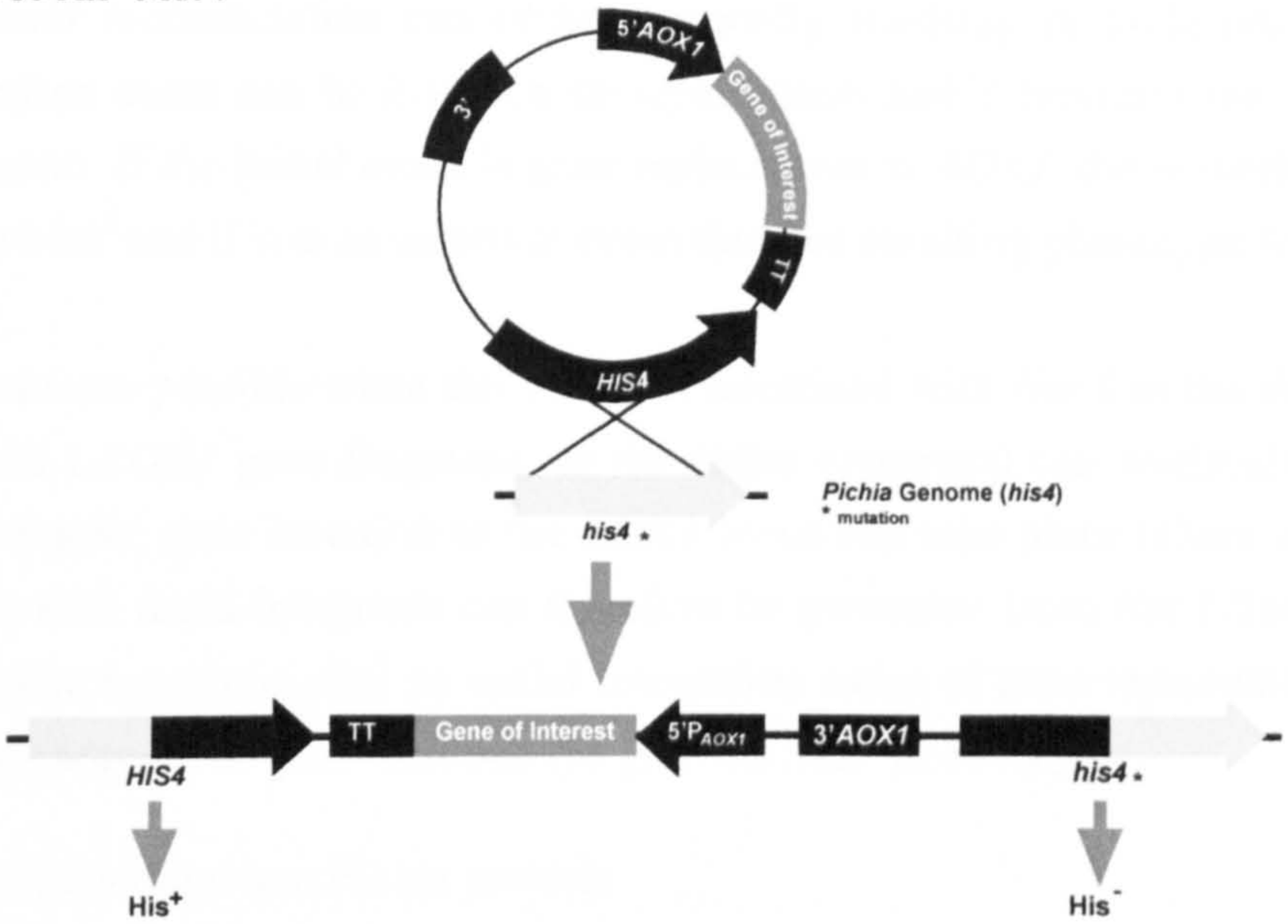

Integration by gene replacement

Gene replacement occurs by double crossover transplacement of the *Pichia AOX1* gene by the linearised plasmid (Figure 5.3). When the *Pichia* vector is linearised by digestion with *Not* I, crossover events can occur between the 5'*AOX1* and 3'*AOX1* regions of the vector and the corresponding regions of the *AOX1* locus in the *Pichia* genome. This results in replacement of the *AOX1* gene with the *Not* I-linearised 'expression cassette' (containing P_{AOX1}, the gene to be expressed and *HIS4*). The resulting phenotypic strain is Mut^S due to the loss of alcohol oxidase activity encoded by *AOX1* gene.

Figure 5.3 Gene replacement at *AOX1* in GS115. A double crossover event between the *AOX1* promoter and 3'*AOX1* regions of the vector and genome results in replacement of the *AOX1* coding region by the expression cassette (containing P_{AOX1}, the gene of interest and *HIS4*). The resulting phenotype is His^+ Mut^S.

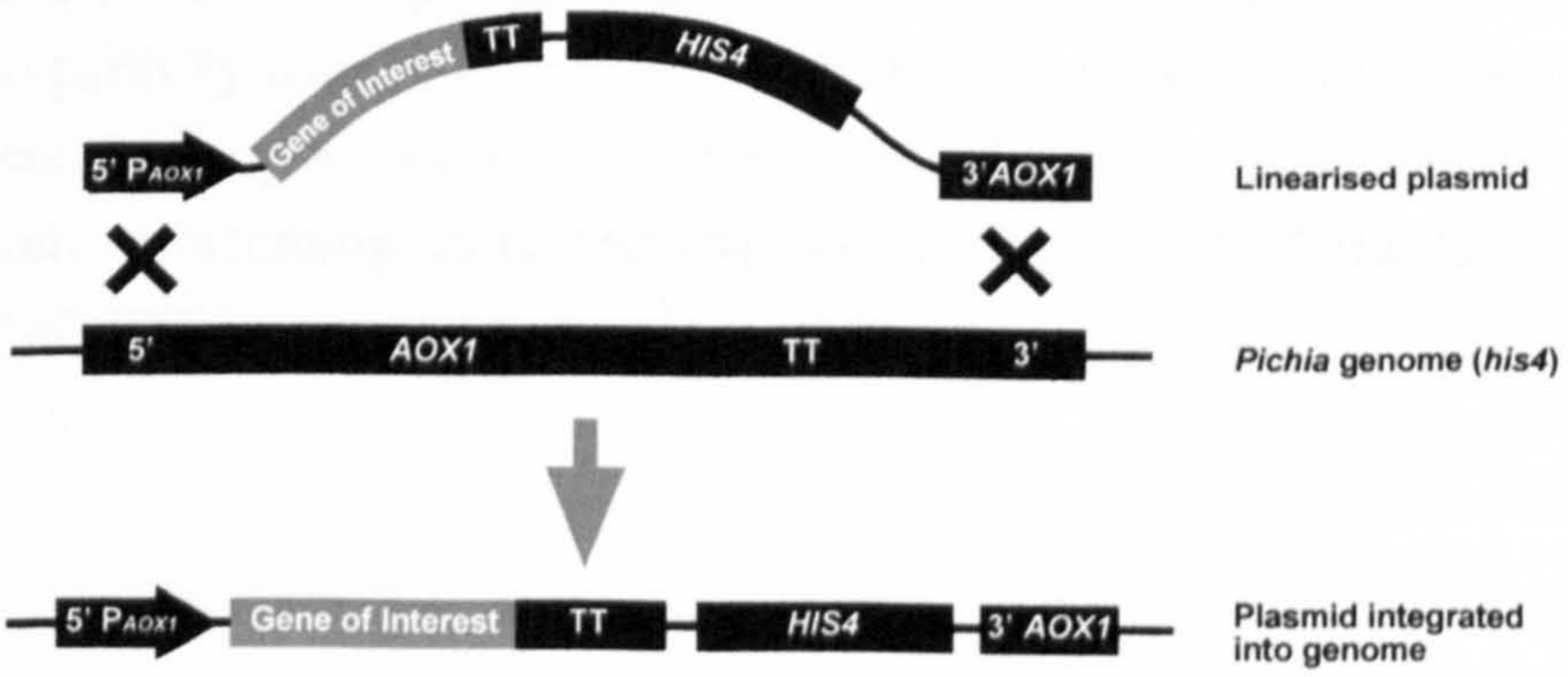

Multiple gene insertion events

On top of the initial integration event at the *AOX1* or *his4* loci of GS115, gene insertion by single crossover recombination can occur repeatedly resulting in multi-integrants. The initial integration event can be insertion or replacement and determines the phenotype of the transformant. If the initial event is gene replacement at *AOX1*, the recombinant GS115 strain will be Mut^S and if it is an insertion event then the resulting phenotype will be Mut^+.

Gene insertions are possible when the vector is linearised with *Not* I as the digested DNA (either the *Not* I *AOX1* gene fragment, or the entire construct) can re-circularise *in vivo*. When this happens, gene insertion at the *AOX1* locus can take place (Clare *et al.* 1991a). Transfomants with multi-integrants can therefore be generated from *Not* I-linearised DNA by repeated gene insertions after an initial integration event of gene replacement (resulting in the Mut^S phenotype) or gene insertion (to give the Mut^+ phenotype).

5.1.1.2 Transformation into Pichia pastoris

Linear DNA can generate stable transformants of *Pichia pastoris* via homologous recombination between transforming DNA and regions of homology with the genome. Such integrants show extreme stability in the absence of selective pressure even when present as multiple copies. Gene insertion is more likely to occur than gene replacement as the recombination event. Replacement of the *AOX1* gene by *Not* I-linearised plasmid occurs at a frequency of 5-35 %. Multiple gene insertion events at a single locus occur at a low frequency, usually between 1 and 10 % of all selected His^+ transformants.

Transformation of the linearised vector into spheroplasts of *Pichia pastoris* appears to favour multi-copy integration of transforming DNA. The Invitrogen Kit manual recommends using this method if multi-copy inserts are desired, rather than other methods such as electroporation or use of chemically competent cells. The efficiency of the spheroplast transformation method is high and the expected number of His^+ transformants by this method is $10^3 - 10^4$ per μg DNA. Spheroplasts are generated by treatment with Zymolyase to partially remove the cell wall, which enables the yeast to take up DNA. The insertion of multiple copies of the gene to be expressed into the *Pichia* genome can result in increased levels of heterologous protein expression (Clare *et al.* 1991a, Clare *et al.* 1991b and Cregg *et al.* 1993).

5.1.2 MALDI-TOF mass spectrometry

Recent developments in mass spectrometric techniques now allow mass determination of intact proteins with accuracy far superior to that permitted by more traditional methods such as SDS-PAGE, gel filtration or analytical ultracentrifugation. One such technique is matrix-assisted laser desorption/ionisation combined with time-of-flight mass analysis (MALDI-TOF MS).

In MALDI mass spectrometric analysis, the critical step in generating gas phase molecular ions is sample preparation where analyte and a UV absorbing matrix compound are mixed and dried to produce protein-doped matrix crystallites on the sample probe (Jensen *et al.* 1996). These are introduced into the mass spectrometer and irradiated by a pulsed UV laser. Rapid sublimation of the analyte/matrix crystallites leads to the formation of gas phase protonated molecular ions from the solid crystalline matrix/analyte substrate. The mass analyser separates molecular ions based on their mass-to-charge ratio (*m/z*). Ions are accelerated to a constant kinetic energy, then allowed to fly through a high vacuum field-free region of 0.5 – 1.5 m in length (a hollow tube). They are then recorded by the electric signal generated upon impact at a detector. The time-of-flight in the field-free region is related to the *m/z* of a given ion. Having identical kinetic energy, small molecular ions move faster than large molecular ions and so arrive earlier at the detector. The *m/z* for an ion can be determined from its time-of-flight by comparison to the time-of-flight of known standards. The practical mass range for MALDI TOF MS is between 0.5 kD and 150 kD.

5.2 Expression of Lipases

A cDNA encoding Danisco's Lipase 3 had been cloned into the pHIL-D2 *Pichia* expression vector (described in Chapter 3, Section 3.3.2). Before carrying out site-directed-mutagenesis of the Lipase 3 cDNA in the pHIL-D2 vector (pHILcLip), transformation into *Pichia pastoris* strain GS115 was carried out to ensure that expression of wild type Lipase 3 was possible. The spheroplast method was chosen for transformation into the GS115 (*his4*) strain of *Pichia pastoris*.

5.2.1 Transformation and Expression of Wild-Type Lipase in *Pichia pastoris*

5.2.1.1 Spheroplast transformation of wild type pHILcLip and screening of His⁺ recombinants

Not 1-linearized pHILcLip (wild type) DNA was transformed into GS115 by the spheroplast method and plated onto RDB (Regeneration Dextrose Base) plates lacking

histidine, to select for His^+ transformants. The efficiency of this transformation was 10^2 transformants per μg of DNA.

Linearisation with *Not* 1 targets integration of the fragment (containing P_{AOX1}, Lipase 3 cDNA, and *HIS4*) into the *Pichi*a genome by gene replacement at the *AOX1* locus of GS115. Displacement of the GS115 *AOX1* gene results in the Mut^S phenotype, which can be assessed on minimal dextrose (MD) and minimal methanol (MM) plates. Transformants that grow normally on MD media but slowly on MM media (Mut^S) cannot efficiently metabolise methanol, indicating replacement of the *AOX1* gene. The methanol utilisation phenotype (Mut^+ or Mut^S) of 100 His^+ transformants selected from RDB transformation plates were determined before screening for expression of lipase. Determination of the Mut phenotype is useful in optimising expression of the recombinant clone (His^+ Mut^S transformants cannot metabolise methanol as the sole carbon source and so are grown to a high cell-density in glycerol-containing media before inducing expression). Also, one phenotype may be found to express the protein better than the other, which could facilitate future selection of transformants for expression. Of 100 His^+ transformants screened for replacement of the *AOX1* gene from this transformation, 8 were of the Mut^S phenotype.

The rhodamine B plate assay provided a direct means of selecting His^+ transformants that expressed and secreted lipase. In this assay, transformants are "patched" onto minimal methanol plates that also contain rhodamine B and olive oil. Lipase expressed as a result of methanol induction hydrolyses the olive oil, releasing fatty acids that cause rhodamine B to fluoresce under UV light. The 100 His^+ transformants that were screened for Mut^S phenotype were also screened for lipase expression by patching onto rhodamine B plates. Of these, 39 appeared to express lipase. A number of transformants that demonstrated lipase activity in this assay were selected for small-scale expression using culture volumes of a few millilitres, in order to identify the recombinant strain which could be induced to the highest level of expression, for large-scale expression of this lipase.

5.2.1.2 Expression of wild type lipase and screening of expression levels from His^+ recombinant strains

From results of the rhodamine B plate assay, 12 His^+ transformants that demonstrated expression were selected for expression on a small-scale, to select the recombinant strain that expressed to the highest level. These were grown to a high cell density in 10 ml glycerol media and then expression induced by resuspension of the cells in 2 ml of methanol containing media. As the lipase cDNA also encodes for the native signal

sequence necessary for secretion, the supernatants of these cultures were analysed for presence of protein, firstly by SDS-polyacrylamide gel electrophoresis (PAGE) and Coomassie Blue staining (Figure 5.4a). In seven of the supernatants, two bands were observed migrating at approximately 36 kD compared to adjacent molecular weight markers. Western blotting after SDS-PAGE and immuno-detection using rabbit anti-lipase antibody (obtained from Danisco) confirmed that these were the correct gene products (Figure 5.4b). The presence of Lipase 3 on the immunoblot was detected using alkaline phosphatase conjugated to goat anti-rabbit Fc secondary antibody on addition of the BCIP/NBT (5-bromo-4-chloro-3-indolyl phosphate/nitroblue tetrazolium) chromogenic substrate. Transformation of *Not* 1-linearised pHIL-D2 vector alone provided control transformants that, when induced in the same way, gave supernatants with no obvious bands following separation by SDS-PAGE.

The protein bands from SDS-PAGE of *Pichia* supernatants were electro-blotted onto Immobilon-P PVDF (polyvinylidene difluoride) membrane for N-terminal sequencing (carried out at Danisco). The protein extracted in this way gave identical sequence results, implying that the differences in molecular weight were not due to incomplete processing of the enzyme on expression and that *Pichia pastoris* is capable of processing the proteins to the mature N-termini as observed for the native enzyme from *Aspergillus niger*. The two bands could represent different glycosylated forms of the enzyme. Later purification of lipases by anion exchange chromatography resulted in separation of these bands.

Lipase activity in the cell supernatants was detected using resorufin ester chromogenic substrate. The release of resorufin by the reaction of lipase with resorufin ester substrate (1,2-O-Dilauryl-rac-glycero-3-glutaric acid-resorufin ester) can be monitored by absorbance at 572 nm, and is used as a measure for the detection of lipase activity. Lipase activity was measured in four of the cell supernatants (that gave the strongest bands on SDS-PAGE) and ranged from 122 to 644 U l^{-1} (U: mmol min^{-1} resorufin released). No lipase activity was detected in the supernatants of control transformants. Of these four His^+ transformants, only one was of Mut^S phenotype. This also happened to demonstrate the highest level of lipase activity on expression, as detected by the resorufin ester assay, and gave the strongest band on SDS-PAGE (lane 1 in Figure 5.4). Apart from this, the variation in band intensity and activity levels could be due to multiple integration of the transforming DNA resulting in different numbers of copies of the Lipase 3 gene in these recombinant strains.

Figure 5.4 SDS-PAGE of supernatants from small-scale expression of wild-type lipase *in Pichia pastoris* GS115: (a) Coomassie Blue stained gel; (b) Western blot of gel and detection using rabbit antibody against Danisco Lipase 3, detected using secondary antibody-alkaline phosphatase conjugate and 5-bromo-4-chloro-3-indolyl phosphate / nitroblue tetrazolium substrate The results are shown for seven different His^+ transformants, selected for small-scale expression from the results of screening His^+ transformants on Rhodamine B plates (for detection of lipase expression).

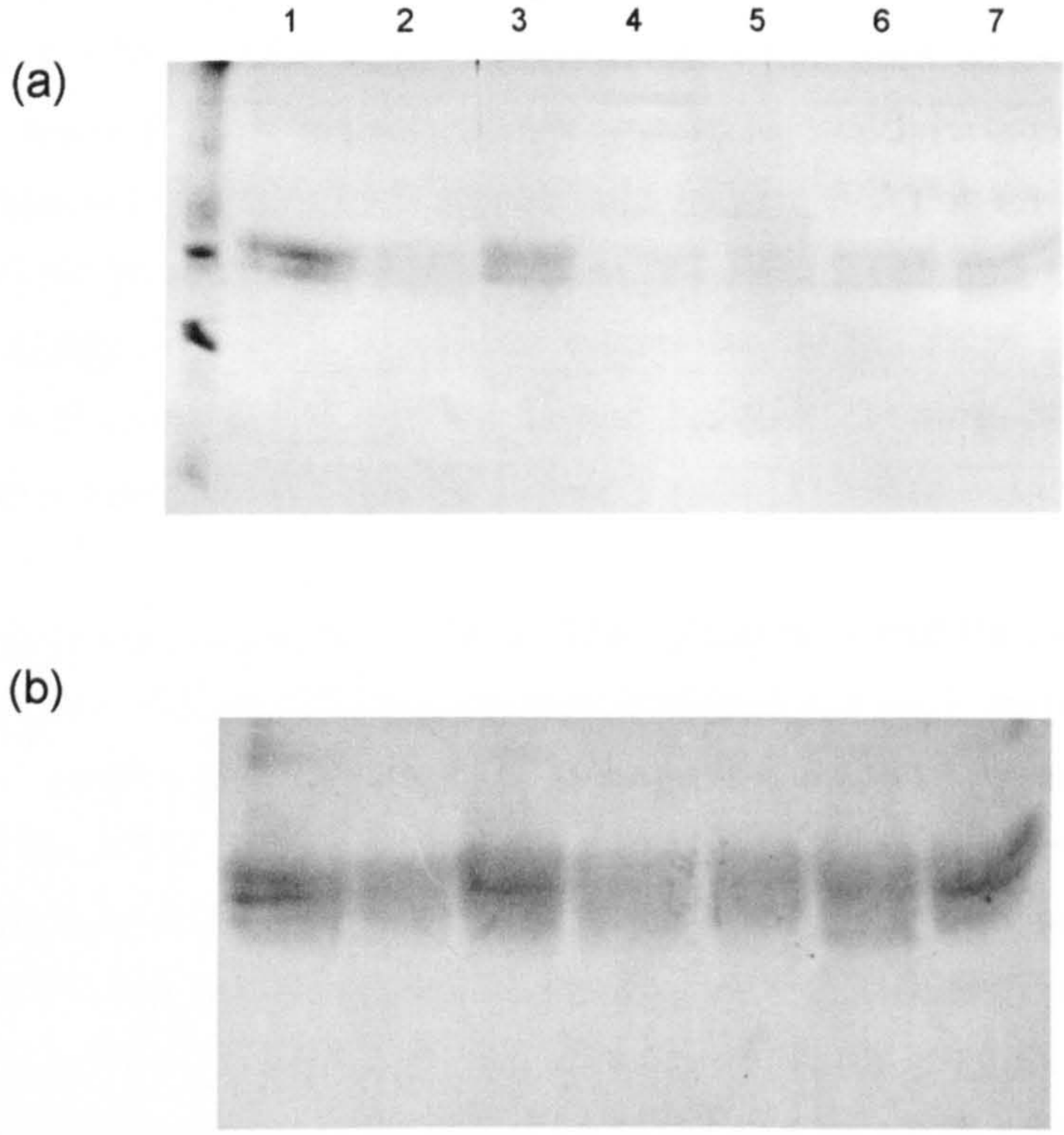

5.2.2 Transformation and Expression of Mutant Lipases in *Pichia pastoris*

When successful expression of wild-type Lipase 3 in *Pichia pastoris* had been established, site-directed-mutagenesis of the pHILcLip construct was carried out (Chapter 3, Section 3.3.3). Then, the pHILcLip plasmids containing cDNA coding for 'activity' mutants of Lipase 3 (H225D, T112D E114Q, W116A I113W and W116A) were used to transform the *Pichia pastoris* strain GS115, for expression of these enzymes. Following this, the genes coding for the 'glycosylation' mutants (N59T, N269T, N269Q and N59T N269T and N59T N269Q) present in the pHIL-D2 vector (pHILcLip) were used to transform *Pichia* strain GS115 for the expression of these mutants.

5.2.2.1 Spheroplast transformation of 'activity' mutant pHILcLip DNA and selection for multiple-integrants using 3-AT

The pHIL-D2 expression vector containing the cDNA encoding Lipase 3 'activity' mutants (pHILcLip) were digested with *Not* 1 and transformed into the GS115 *Pichia* strain by the spheroplast method. The transformation efficiencies were 10^3 His^+ transformants per μg DNA on RDB plates. Approximately 10-fold fewer transformants were obtained on RDB plates to which 1 mM 3-amino-1,2,4-triazole (3-AT) had been added. This was added to RDB plates to select for His^+ transformants containing multiple copies of the 'expression cassette' (containing P_{AOX1}, Lipase 3 cDNA, and *HIS4*). 3-AT is an inhibitor of histidinol dehydrogenase, the product of the *HIS4* gene. Therefore, colonies that grow under these conditions are likely to exhibit significant expression of the *HIS4* gene to overcome the inhibitor. Since this gene is linked to the Lipase 3 cDNA, isolation of hyper-resistant 3-AT transformants may also indicate that the Lipase 3 gene is present in multiple copies.

His^+ transformants were screened for Mut^+/Mut^S phenotype and for expression of lipase on rhodamine B plates. Of the 100 transformants picked for each mutant, 25 were selected from the RDB + 3-AT plates. Overall, the average frequency of recombination resulting in replacement of the *AOX1* gene, and therefore displaying the Mut^S phenotype, was 8.5 % (± 4 %). The rhodamine B plate assay was used to screen for transformants that could express lipase (Figure 5.5). The percentages of fluorescing patches (indicating expression of lipase) were 22 % for T112D E114Q, 18 % for H225D, 13 % for W116A I113W and 5 % for W116A (cf. 39 % for wild type). It should be noted that levels of activity and therefore the degree of fluorescence might be influenced by the introduced mutations.

Although a large number of transformants picked from the RDB + 3-AT plates did show lipase expression, the highest levels of expression (as indicated by large fluorescent halos on the rhodamine B plates) were from transformants selected from RDB plates. Using 3-AT as a method for selecting recombinant strains with multiple-integrants did appear to work as a higher proportion of the transformants picked from these plates demonstrated lipase expression on rhodamine B plates, when compared to those picked from the plates without 3-AT. However, the highest expressing colonies were from the RDB transformation plates.

Figure 5.5 Rhodamine B plate assay for detection of His$^+$ GS115 transformants expressing lipase. The plates shown are for the screening of His$^+$ transformants picked from RDB plates using (a) the pHIL-D2 vector (control) and (b) pHILcLip T112D E114Q 'activity' mutant DNA transformed into GS115 by the spheroplast method. Fluorescence under UV indicates expression of lipase from recombinant GS115.

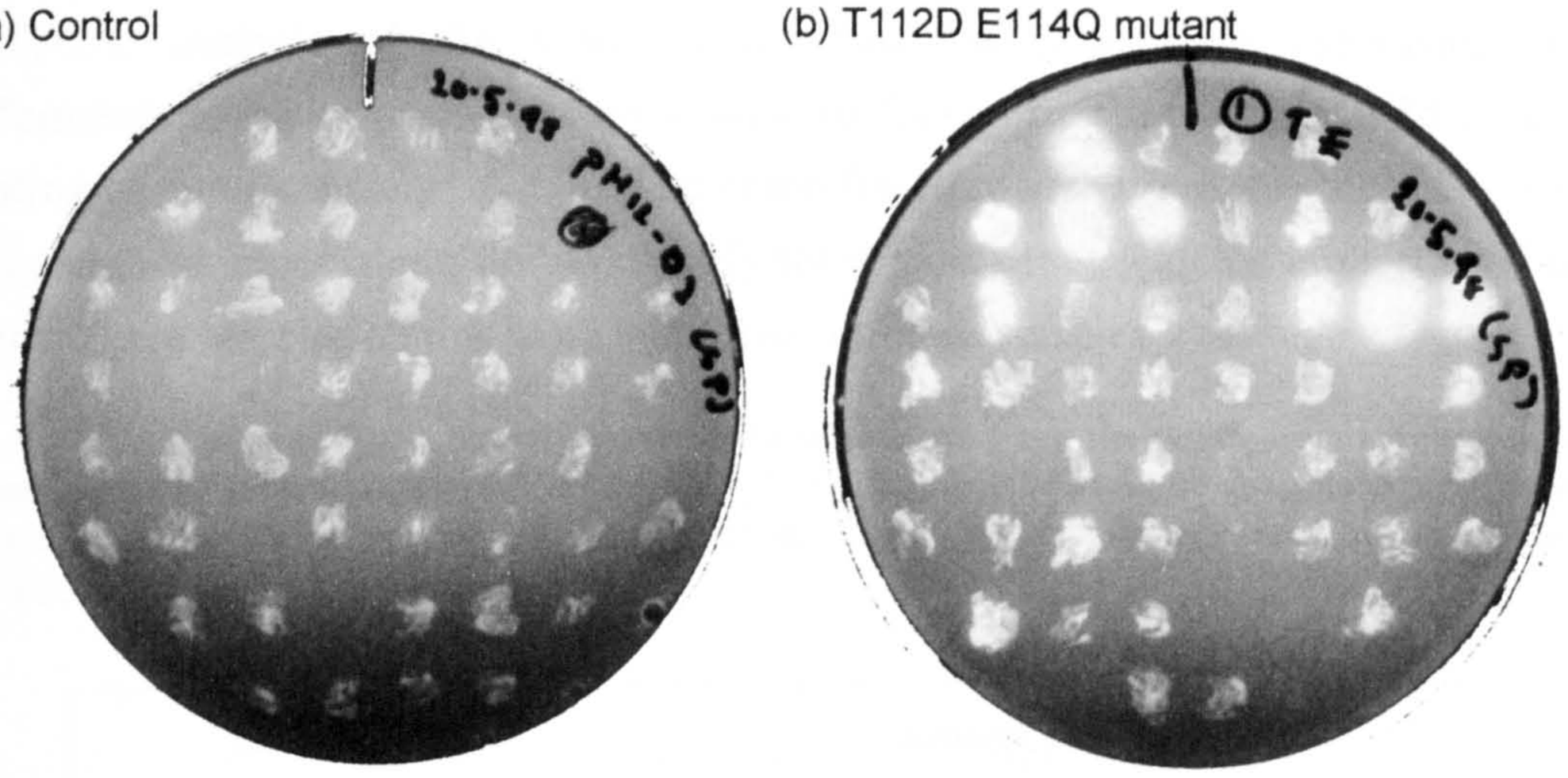

5.2.2.2 Expression of 'activity' mutants, and comparison of transformants from EasyComp™ and spheroplast methods of transformation

After initial attempts to transform the 'activity' mutant constructs into *Pichia pastoris* using the spheroplast method had failed, an alternative method was sought. The *Pichia* EasyComp. Transformation kit is available from Invitrogen, in which competent GS115 cells can be prepared and stored in frozen form, ready for transformation. Recombinant strains from the transformation of 'activity' mutant pHILcLip DNA by the EasyComp. method were picked for screening of expression levels on a small scale. Three transformants were picked for each mutant, selecting those that displayed fluorescence on the rhodamine B plates (with this method of transformation only a few colonies showed any fluorescence on rhodamine B). Although this method proved to be considerably quicker and easier to perform, and reliably yielded at least 50 transformants per plate, the levels of expression of lipase from these transformants were extremely low.

Once the spheroplast transformation method was functioning again the expression levels of the strains arising from the two transformation protocols were compared following selection of lipase active strains on rhodamine B plates. Four transformants were picked for each mutant from the spheroplast transformation and expression induced on a small-scale. As shown in Table 5.1 the expression levels from the EasyComp-generated strains were poor in comparison. The higher levels of lipase activity from His$^+$ recombinants using the spheroplast method could be due to multiple-copy integration, which would also

explain the very wide range of expression levels observed. To obtain the higher levels of expression, as originally seen with the wild type lipase, it was necessary to transform the DNA by the spheroplast method.

SDS-PAGE analysis of the supernatants from the small-scale expression of His^+ transformants revealed protein bands similar to those observed for the wild type lipase, migrating at approximately 36 kD. The resorufin-ester assay was used to measure lipase activity in these supernatants and to identify the strains expressing the highest level of each mutant. These selected strains were later used for large-scale expression.

Table 5.1 The range of lipase activity levels in supernatants from the small-scale expression of wild-type and 'activity' mutant lipases. The His^+ GS115 transformants used for small-scale expression are from spheroplast and EasyComp. methods of transformation. Lipase activity was measured by the resorufin ester assay. (U: mmol min^{-1} resorufin released)

Lipase	Activity U l^{-1}			
	EasyComp. method[a].		Spheroplast method[b].	
	Average	*Range*	*Average*	*Range*
H225D	16	14 - 18	545	307 - 742
T112D E114Q	18	0 - 27	585	545 - 600
W116A	11	10 - 12	137	70 - 235
W116A I113W	12	12 - 13	233	208 - 247
wild type	33	26 - 46	393	122 – 644

[a]Results from the assay of 3 independent transformants expressing the lipases.
[b]Results from the assay of 4 independent transformants expressing the lipases.

5.2.2.3 Spheroplast transformation and expression of 'glycosylation' mutants

The 'glycosylation' mutants of the pHILcLip construct were digested with *Not* 1 and transformed into the GS115 *Pichia* strain by the spheroplast method. The transformation efficiencies were 10^3 His^+ transformants per μg DNA on RDB plates for each mutant. Again, approximately 10-fold fewer transformants were obtained on RDB plates to which 1 mM 3-AT had been added. His^+ transformants were screened for Mut^+/Mut^S phenotype and also for expression of lipase on rhodamine B plates. Of 100 transformants picked for each mutant, half were selected from the RDB + 3-AT plates. For these mutants, selection on RDB + 3-AT plates for high-expressers of lipase appeared to work more effectively than for the 'activity' mutants. Not only did a higher percentage of His^+ transformants picked from the 3-AT plates fluoresce on rhodamine B plates (56 % as opposed to 42 % from the

RDB plates) but they generally fluoresced with a greater intensity than the transformants picked from RDB plates (Figure 5.5).

Of the 100 His^+ transformants picked for screening, 6.4 % were found to be of the Mut^S phenotype. Although nearly all of these showed some level of expression on Rhodamine B plates, the transformants exhibiting the highest levels of lipase (and those that were consequently selected for screening by small-scale expression) were of the Mut^+ phenotype. All these were originally picked from the RDB + 3-AT transformation plates. Four or five transformants were selected for screening of expression levels on a small scale. Expression levels were determined by the resorufin ester assay and by SDS-PAGE with Coomassie Blue staining. The strain expressing the highest level for each mutant was selected for large-scale expression.

5.2.3 Large Scale Expression of Lipases.

Two methods have been described for the expression of GS115 transformants depending on their methanol utilisation phenotype. Transformants able to metabolise methanol (Mut^+) were grown to log phase in glycerol containing media before inducing expression by resuspension and dilution in a greater volume of methanol containing media. For Mut^S transformants, that are unable to metabolise methanol, cells were grown to high density before inducing expression by resuspension in a smaller volume of methanol containing media.

Nearly all the lipase transformants selected for large-scale expression were Mut^+. Supernatants from the expression of the Mut^+ transformants using the method suggested by the manufacturer (Invitrogen) for this phenotype, yielded lower levels of lipase activity (142 - 634 U l^{-1} as measured by the resorufin ester assay) than those obtained using the method described for Mut^S transformants (317 - 1408 U l^{-1}). Therefore, all transformants, irrespective of methanol utilisation phenotype, were expressed in this way (grown to a high cell density before induction of expression) to gain the maximum levels of lipase in the growth supernatants.

Selected transformants were grown to high cell density in glycerol containing media (500 ml BMGY) before inducing expression by concentration of cells in methanol containing media (100 ml BMMY). Protein levels were found to be maximal after 4 days of induction and so supernatants were harvested after this time. The analysis of cell supernatants from the large-scale expression of mutant and wild type lipases by SDS-PAGE is shown in

Figure 5.5 Rhodamine B plates for screening of 'glycosylation' mutant lipase expression from His$^+$ GS115 transformants. The spheroplast method was used to transform 'glycosylation' mutant DNA (pHILcLip). His$^+$ transformants for each mutant were picked from RDB + 3-AT plates and patched onto rhodamine B plates: (a) N59T; (b) N269T; (c) N269Q; (d) N59T N269T and (e) N59T N269Q. Fluorescence of patches under UV indicates expression of lipase from recombinant GS115.

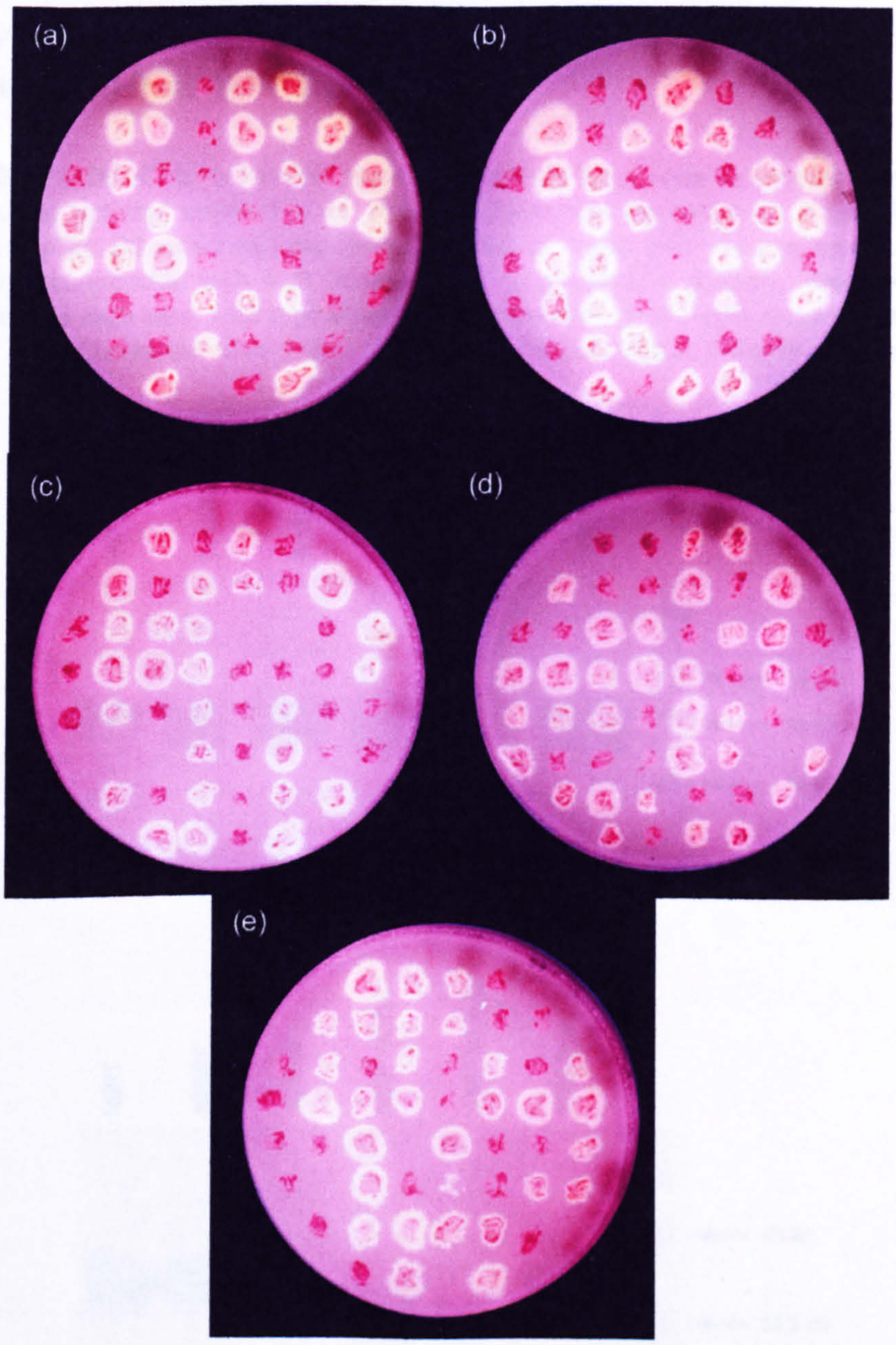

Figure 5.6. SDS-PAGE and Coomassie Blue staining reveals bands at approximately 36 kD, migrating at a similar position to that of wild type enzyme. The 'activity' mutants and the wild type enzyme produced two bands as observed by SDS-PAGE. However, the 'glycosylation' mutants, with the exception of N59T, appeared as single bands (Figure

5.6b) that migrated at slightly lower molecular weights than either the 'activity' mutant or wild type lipases. The N59T lipase however, yielded two bands, one intense band plus a lighter band migrating at a slightly lower molecular weight. The levels of lipase activity in these supernatants as measured by the resorufin ester assay, and protein concentrations measured by the Bradford assay, are shown in Table 5.2 and Table 5.3, along with specific activities determined from these measurements.

Figure 5.6 SDS-PAGE of *Pichia pastoris* supernatants from large-scale expression of mutant and wild-type Lipase 3. (a) 'activity' mutant lipases, wild-type lipase, and supernatant of a control culture from the transformation of pHIL-D2 vector only and (b) 'glycosylation' mutant and wild type lipases. Wild type lipase was expressed in conjunction with both 'activity' and 'glycosylation' mutants, which were expressed in separate batches. In each case, wild type lipase was expressed from the same recombinant strain. Proteins were detected with Coomassie Blue stain. Sizes of molecular weight markers also run on the gel are indicated.

(a)

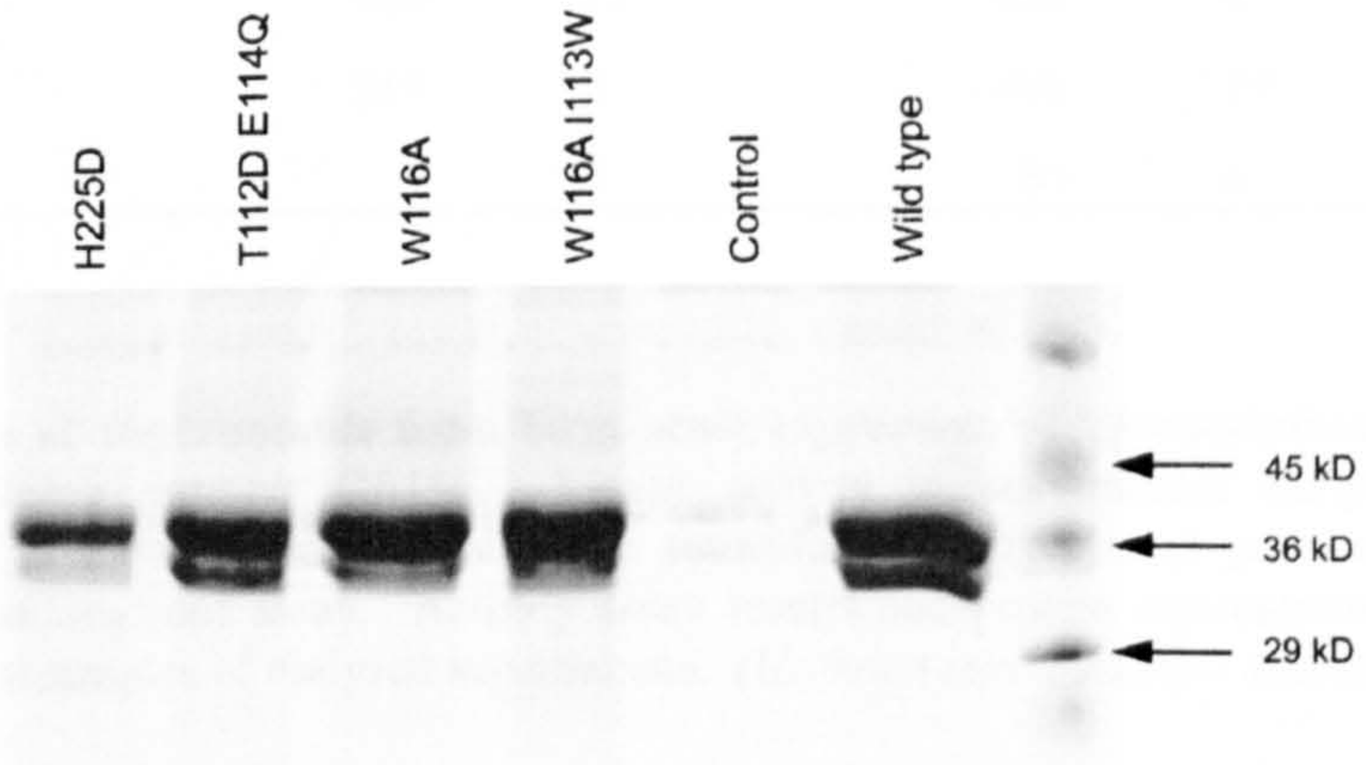

(b)

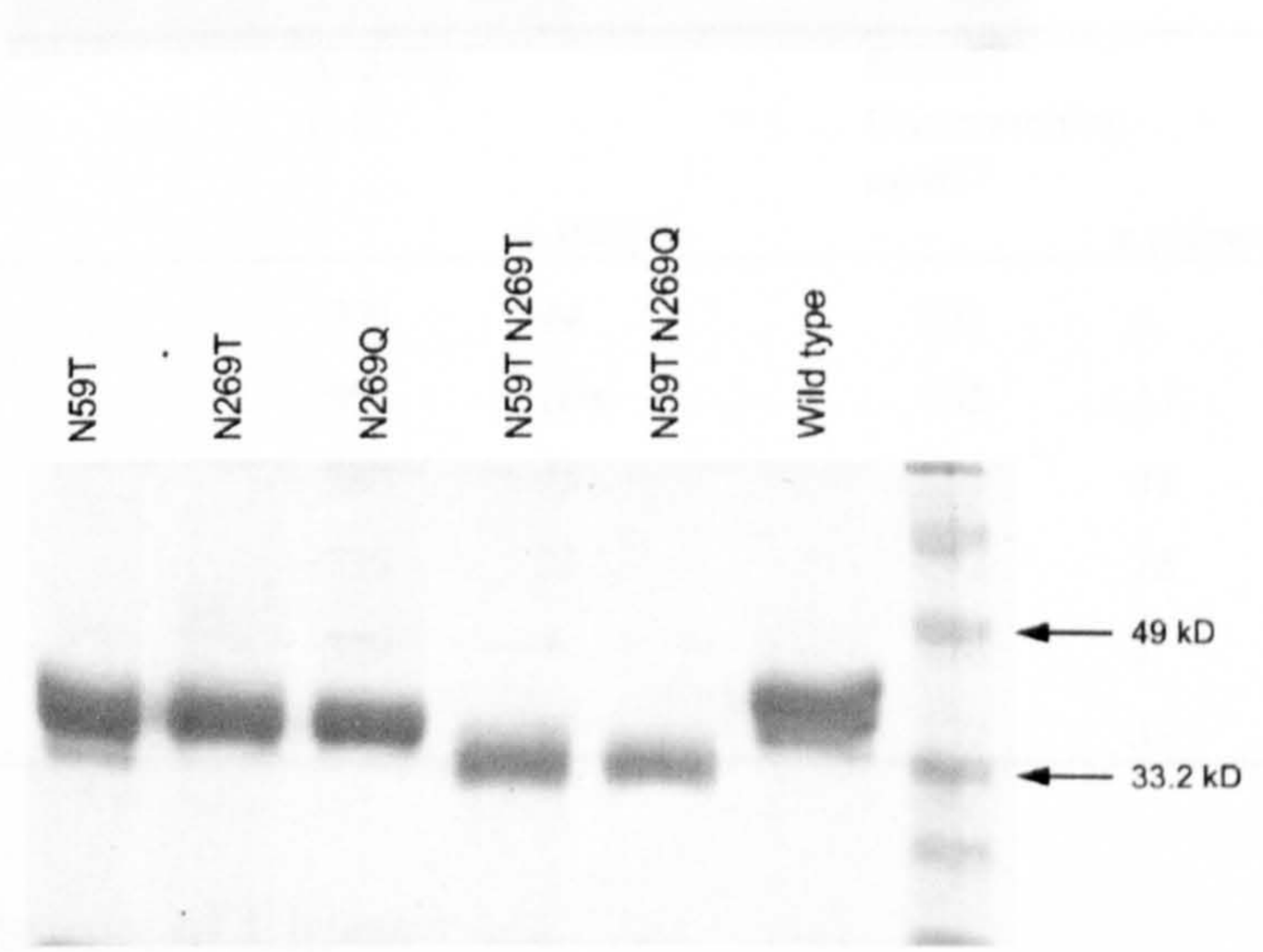

Table 5.2 Analysis of supernatants from large-scale expression of wild-type and 'activity' mutant lipases in *Pichia pastoris* GS115. Lipase activity in supernatants dialysed against 20 mM triethanolamine, pH 7.3 was measured using the resorufin ester assay and protein concentrations were determined using the Bradford assay. Activity assay results and protein concentrations represent average values from duplicate samples of dialysed supernatants. *(U: mmol min^{-1}; stdevp.: standard deviation).*

Lipase	Activity $U\ l^{-1}$	± *stdevp.*	Protein Concentration $\mu g\ ml^{-1}$	± *stdevp.*	Specific Activity, $U\ g^{-1}$
wild type	1408	*83*	334	*7*	4216
T112DE114Q	1248	*50*	290	*16*	4303
H225D	842	*61*	316	*18*	2665
W116AI113W	408	*75*	420	*4*	971
W116A	317	*6*	400	*19*	793
control	0	*0*	80	*8*	0

Table 5.3 Analysis of supernatants from large-scale expression of 'glycosylation' mutants and wild-type lipases in *Pichia pastoris* GS115. Lipase activity in supernatants dialysed against 20 mM triethanolamine, pH 7.3 was measured using the resorufin ester assay and protein concentrations were determined using the Bradford assay. Activity assay results and protein concentrations represent average values from duplicate samples of dialysed supernatants. *(U: mmol min^{-1}; stdevp.: standard deviation).*

Lipase	Activity $U\ l^{-1}$	± *stdevp.*	Protein Concentration $\mu g\ ml^{-1}$	± *stdevp.*	Specific activity, $U\ g^{-1}$
wild type	703	*44*	231	*8*	3043
N59T	550	*108*	262	*13*	2100
N269T	580	*55*	359	*31*	1615
N269Q	739	*21*	292	*18*	2536
N59T N269T	329	*7*	278	*3*	1187
N59T N269Q	491	*62*	239	*32*	2051

5.3 Purification of Lipases

Wild type and mutant lipases were purified by anion exchange chromatography at pH 7.3. Supernatants were dialysed against 20 mM triethanolamine pH7.3 buffer, and applied to Pharmacia HiTrap Q anion exchange columns by FPLC. Lipase activities eluted with a 60 ml linear NaCl gradient from 0 to 0.6 M NaCl in 20 mM triethanolamine pH 7.3 buffer for

mutant enzymes and a 70 ml gradient from 0 to 0.35 M NaCl for the wild type. Lipase activities in each fraction were determined using the resorufin ester assay. In general the lipases eluted as a single absorbance (A_{280}) peak at approximately 0.2 M NaCl (Figure 5.9). For the wild type enzyme a shallower NaCl gradient was used, and this enzyme eluted in a single peak at approximately 0.15 M to 0.2 M (Figure 5.8).

SDS-PAGE of anion-exchange fractions indicated that no contaminating proteins were present. For the wild type and 'activity' mutant lipases, separation of the double bands observed previously on SDS-PAGE of cell supernatants could be achieved (Figure 5.7 and Figure 5.10). As indicated earlier, N-terminal sequencing of these two bands gave identical results implying that the differences in molecular weight were not due to incomplete processing of the enzyme on expression. They could instead represent different glyco-forms of the enzyme. The molecular weights of the wild type iso-forms were determined by MALDI TOF mass spectrometry (results in following section). The molecular masses were 32,606 and 30,544 (Figure 5.12). SDS-PAGE of anion exchange fractions from the purification of 'glycosylation' mutants (Figure 5.11) showed separation of two protein bands for the N59T lipase. Gels for the remaining 'glycosylation' mutants showed purification of a single band.

Fractions containing lipase were combined and dialysed. The specific activities of the purified lipases from activity measurements using the resorufin ester assay and spectrophotometric determination of protein concentrations are shown in Table 5.4 and Table 5.5.

Figure 5.7 SDS-PAGE of anion-exchange chromatography fractions 31-45 from the purification of wild type Lipase 3. Proteins were detected using Coomassie brilliant blue stain. The sizes of the molecular weight markers are indicated.

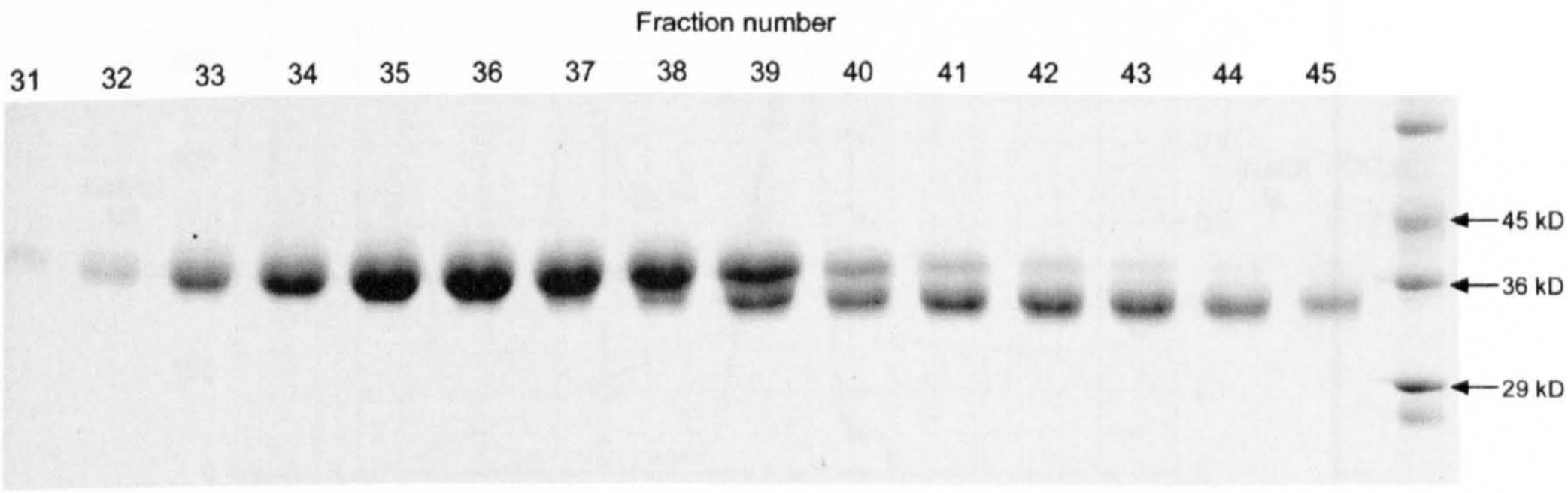

Figure 5.8 FPLC HiTrap Q anion-exchange separation of wild type lipase from *Pichia pastoris* culture supernatant. The graph shows activity in fractions measured by the resorufin ester assay (green line). The second y-axis shows the concentration of sodium chloride in the applied gradient (straight red line on FPLC trace) and the third y-axis shows the absorbance at 280 nm (blue FPLC trace).

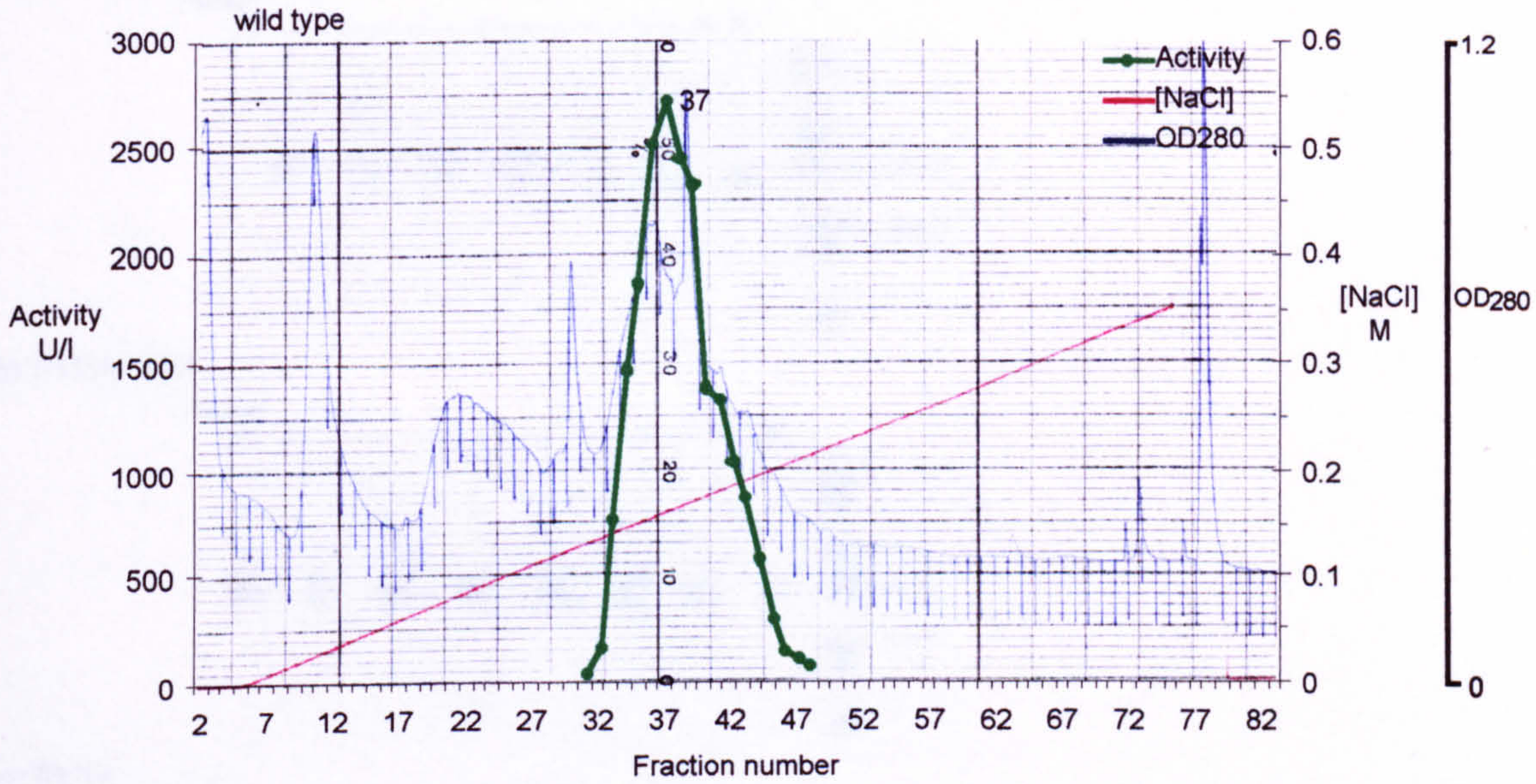

Figure 5.9 FPLC HiTrap Q anion-exchange separation of a 'glycosylation' mutant of Lipase 3 from *Pichia pastoris* culture supernatant. The graph shows activity in fractions measured by the resorufin ester assay (green line). The second y-axis shows the concentration of sodium chloride in the applied gradient (red line on FPLC trace) and the third y-axis shows the absorbance at 280 nm (FPLC trace). The results shown are from purification of the N59T N269T mutant of Lipase 3.

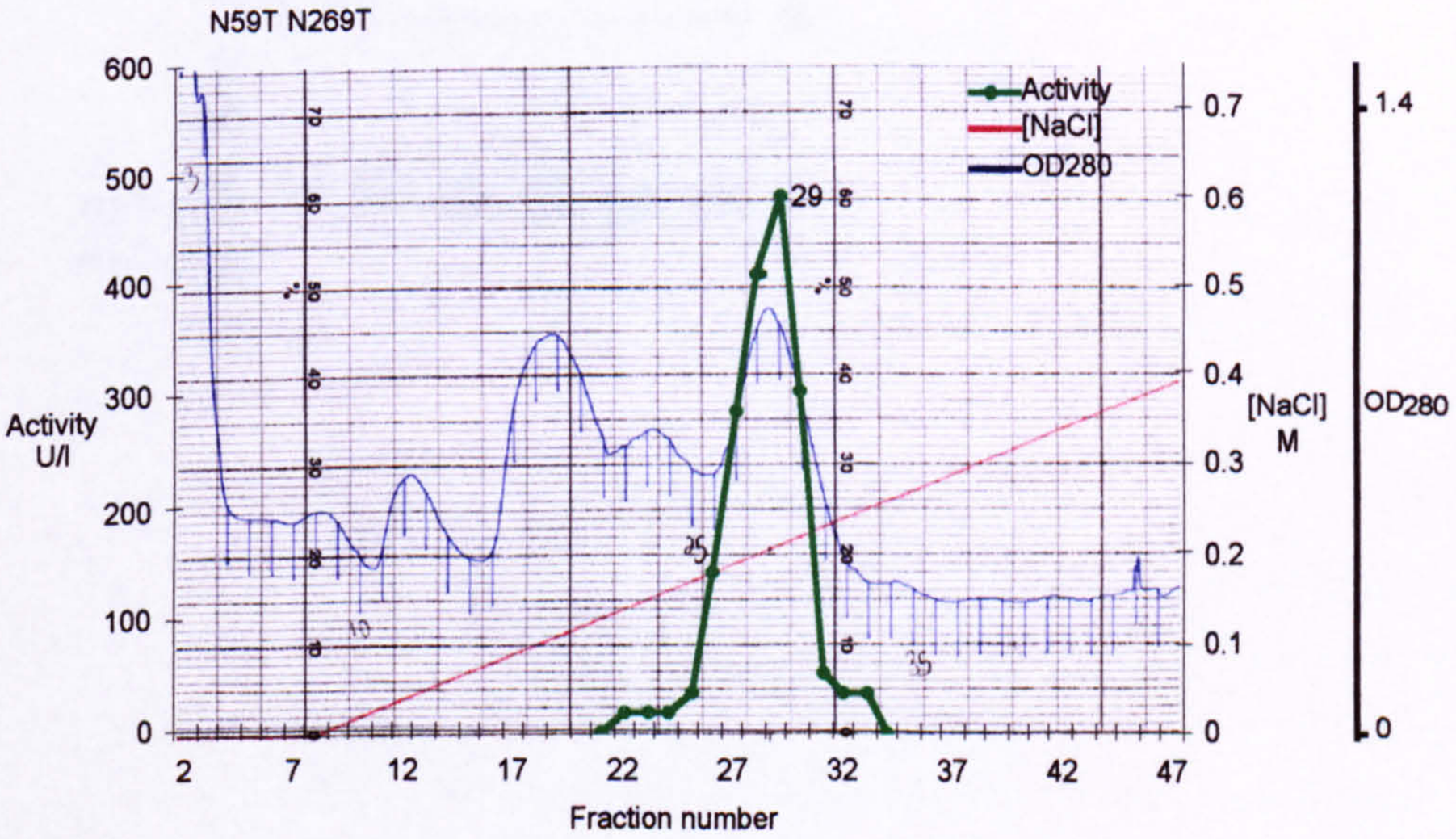

Figure 5.10 SDS-PAGE of anion-exchange chromatography fractions from purification of 'activity' mutants of Lipase 3. Proteins were detected using Coomassie brilliant blue stain. The sizes of the molecular weight markers are indicated.

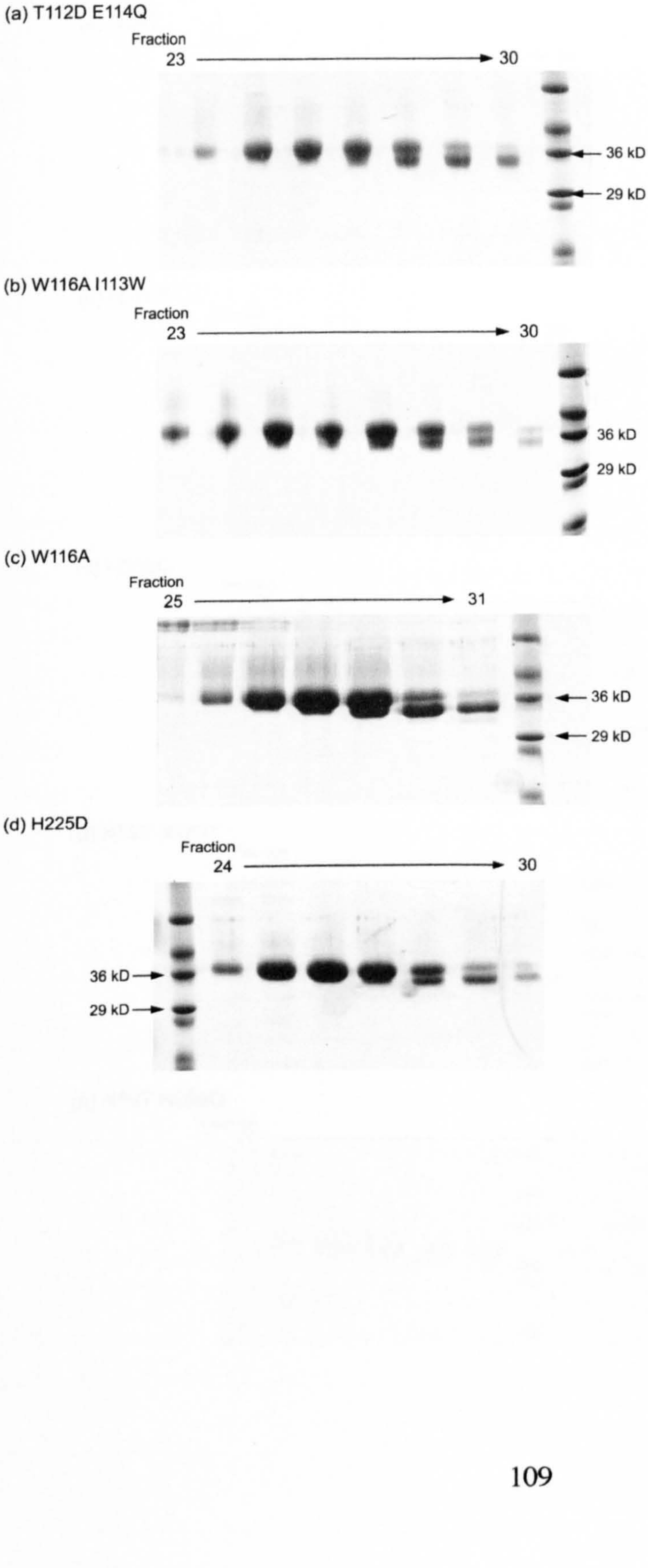

Figure 5.11 SDS-PAGE of anion-exchange chromatography fractions from purification of 'glycosylation' mutants of Lipase 3. Proteins were detected with Coomassie brilliant blue stain. The sizes of the molecular weight markers are indicated.

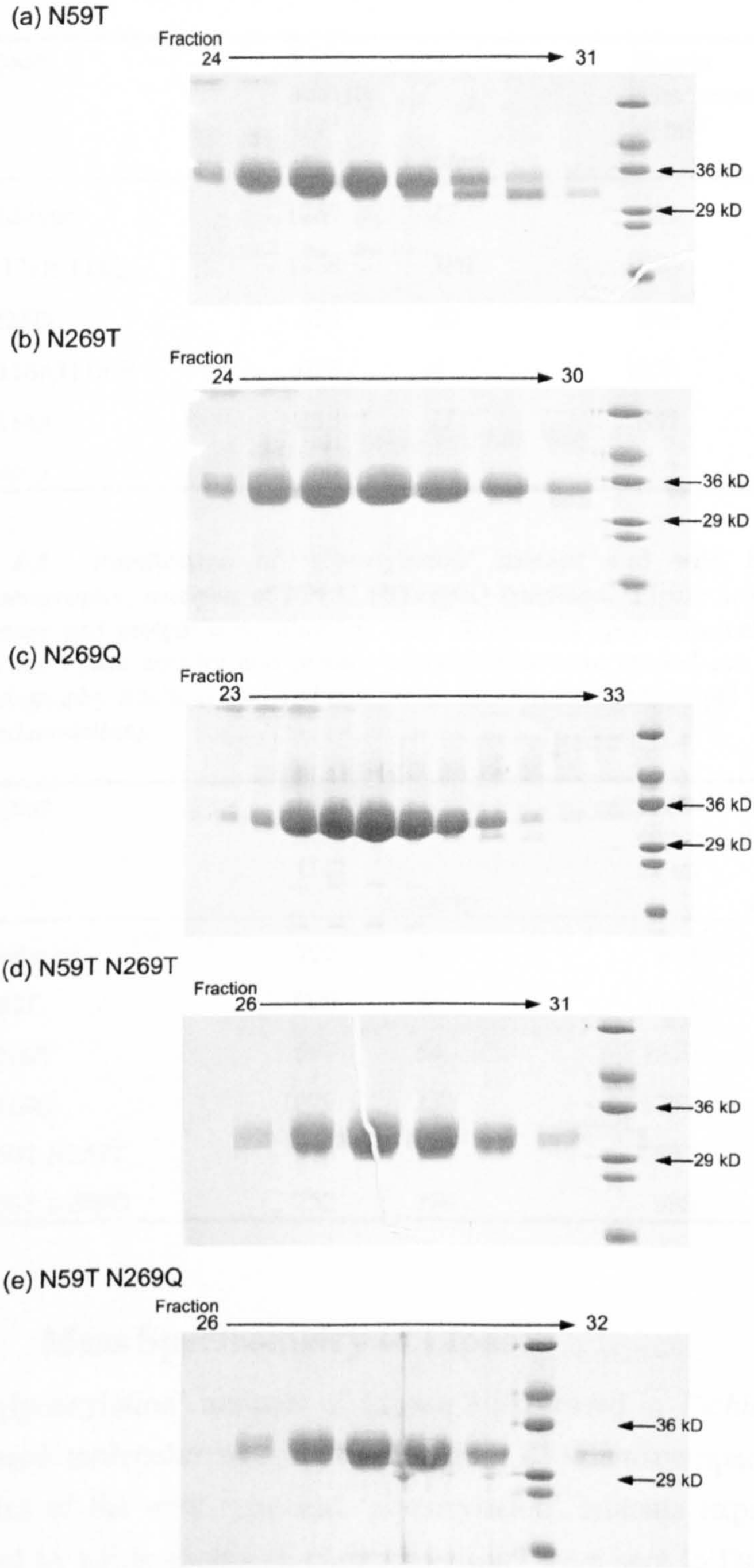

Table 5.4 Purification of wild type and 'activity' mutant lipases by anion exchange chromatography; analysis of FPLC HiTrap Q fractions. Lipase activity was measured by the resorufin ester assay and protein concentrations were determined spectrophotometrically at 320, 280 and 260 nm. Assays for lipase activity and protein concentration were carried out on duplicate samples of combined chromatography fractions dialysed against 20 mM triethanolamine pH 7.3 buffer. *(U: mmol min^{-1}).*

Lipase	Lipase activity U l^{-1}	± *stdevp.*	Protein concentration µg ml^{-1}	± *stdevp.*	Specific activity U g^{-1}
wild type	1259	*17*	892	*49*	1412
T112DE114Q	1358	*380*	1096	*56*	1239
H225D	522	*10*	366	*21*	1429
W116AI113W	625	*6*	1054	*60*	593
W116A	335	*11*	657	*33*	509
control	*0*		*7*		*0*

Table 5.5 Purification of 'glycosylation' mutant and wild type lipases by anion exchange chromatography; analysis of FPLC HiTrap Q fractions. Lipase activity was measured by the resorufin ester assay and protein concentrations were determined spectrophotometrically at 320, 280 and 260 nm. Assays for lipase activity and protein concentration were carried out on duplicate samples of combined chromatography fractions dialysed against 20 mM triethanolamine pH 7.3 buffer. *(U: mmol min^{-1}; stdevp: standard deviation).*

Lipase	Lipase activity U l^{-1}	± *stdevp.*	Protein concentration µg ml^{-1}	± *stdevp.*	Specific activity U g^{-1}
wild type	702	*45*	903	*32*	778
N59T	800	*24*	1123	*7*	713
N269T	597	*64*	1630	*40*	367
N269Q	1079	*130*	1753	*136*	615
N59T N269T	610	*195*	933	*7*	655
N59T N269Q	752	*190*	988	*47*	762

5.4 Mass Spectrometry of Lipases

The 'glycosylation' mutants of Lipase 3 expressed in *Pichia pastoris* yeast demonstrated decreased molecular weights on SDS-PAGE when compared to the wild type enzyme. Samples of the wild type and 'glycosylation' mutants expressed in *Pichia pastoris* and purified by anion-exchange chromatography were sent to Danisco for analysis by MALDI TOF mass spectrometry. The results are shown in Figure 5.12.

Figure 5.12 MALDI-TOF Mass Spectrometry of wild type and 'glycosylation' mutants of Danisco's Lipase 3. Lipase variants were expressed in *Pichia pastoris* and purified from cell supernatants by anion-exchange chromatography.

(a) Wild Type Lipase: Low molecular weight iso-form (30.5 kD)

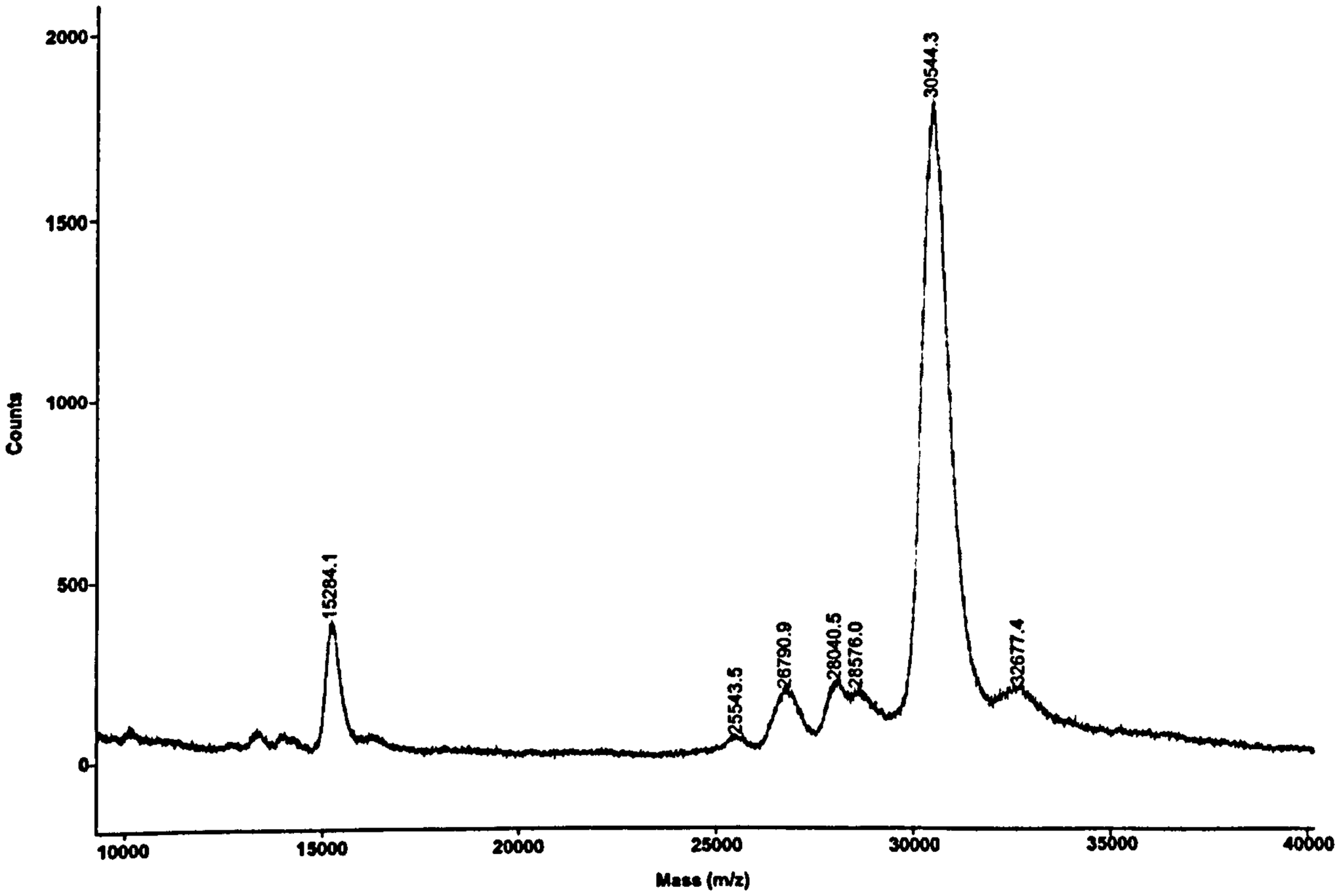

(b) Wild Type Lipase: High molecular weight iso-form (33 kD)

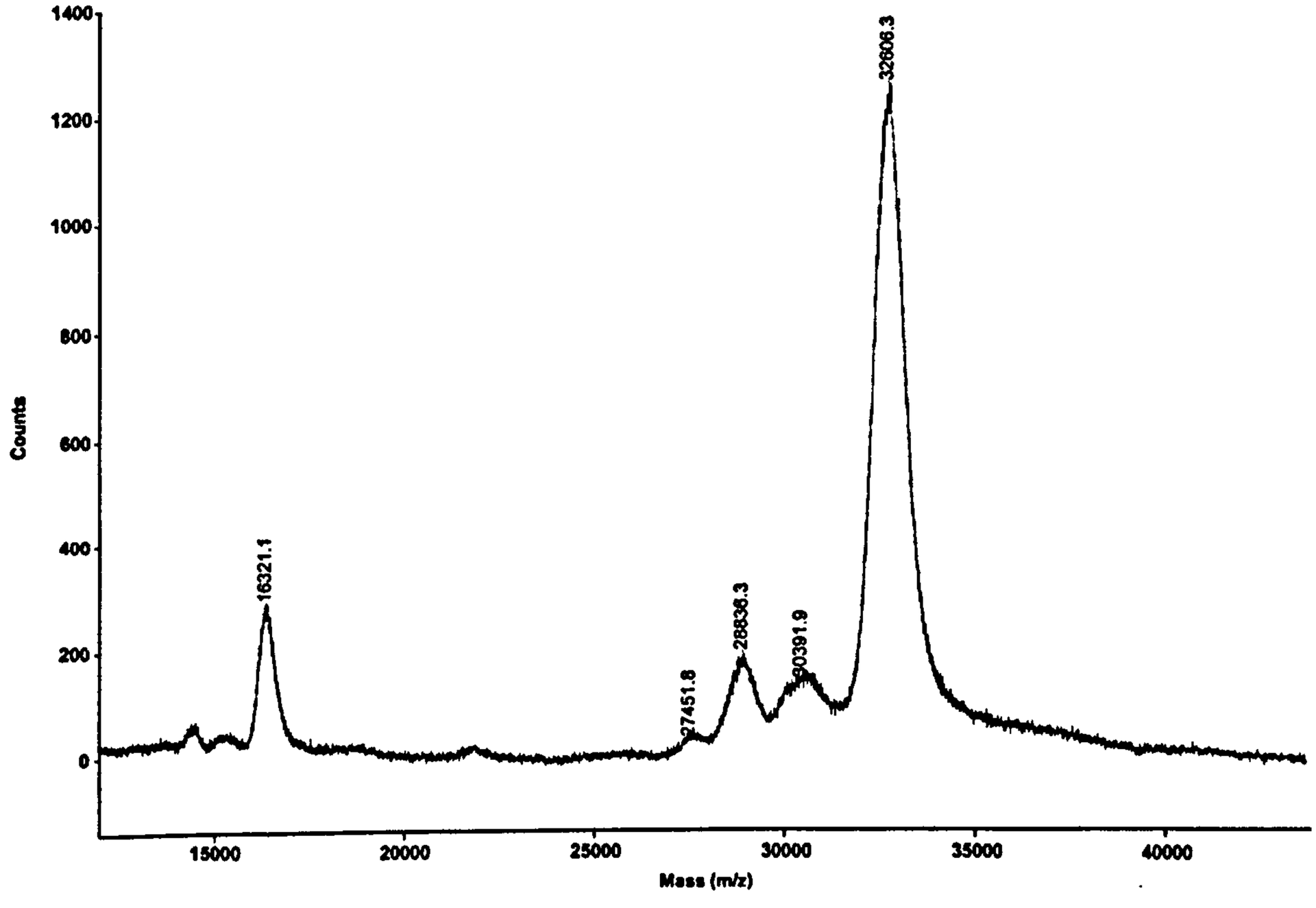

(c) 'Glycosylation' Mutant Lipase: N59T

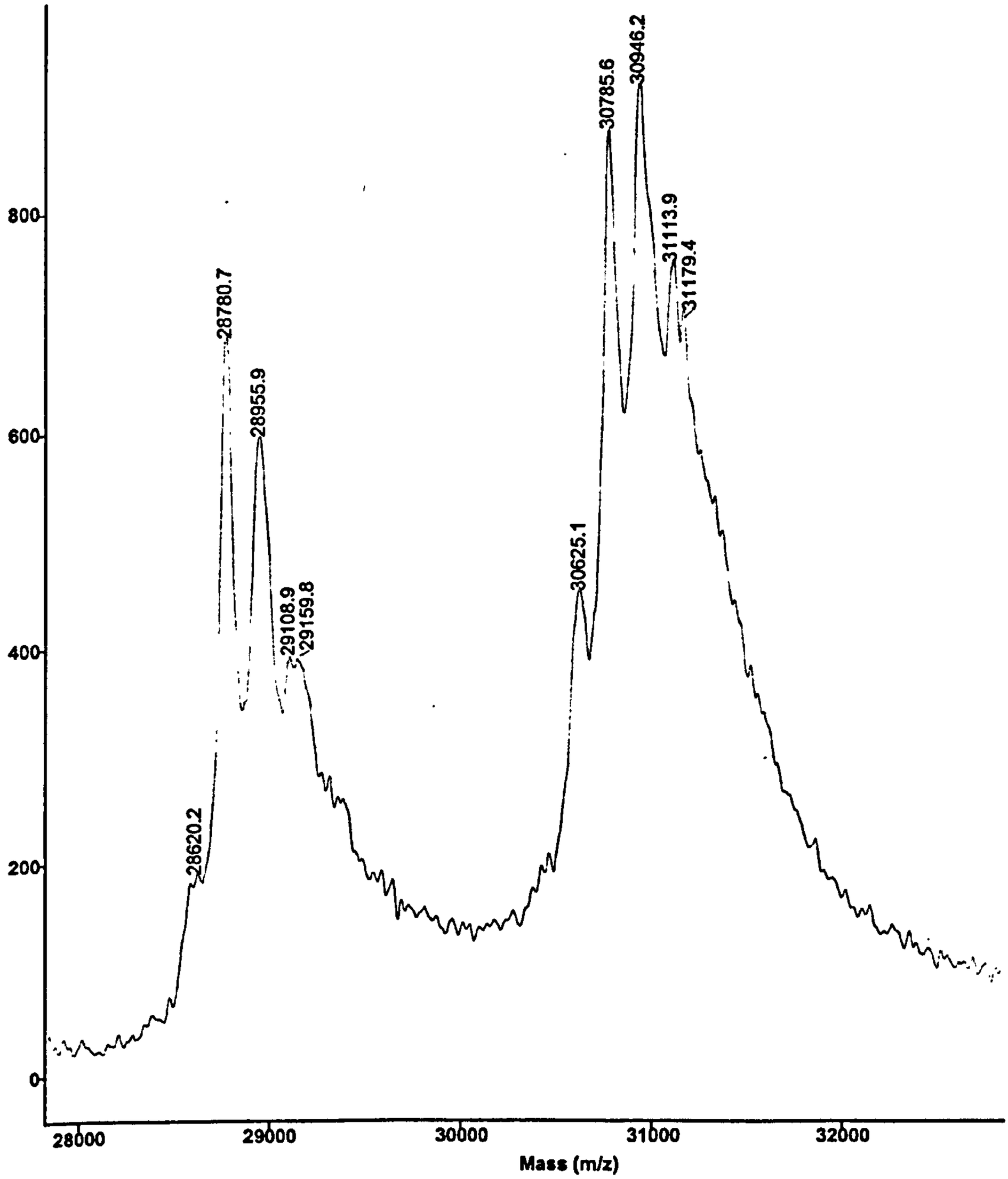

(d) 'Glycosylation' Mutant Lipase: N269T

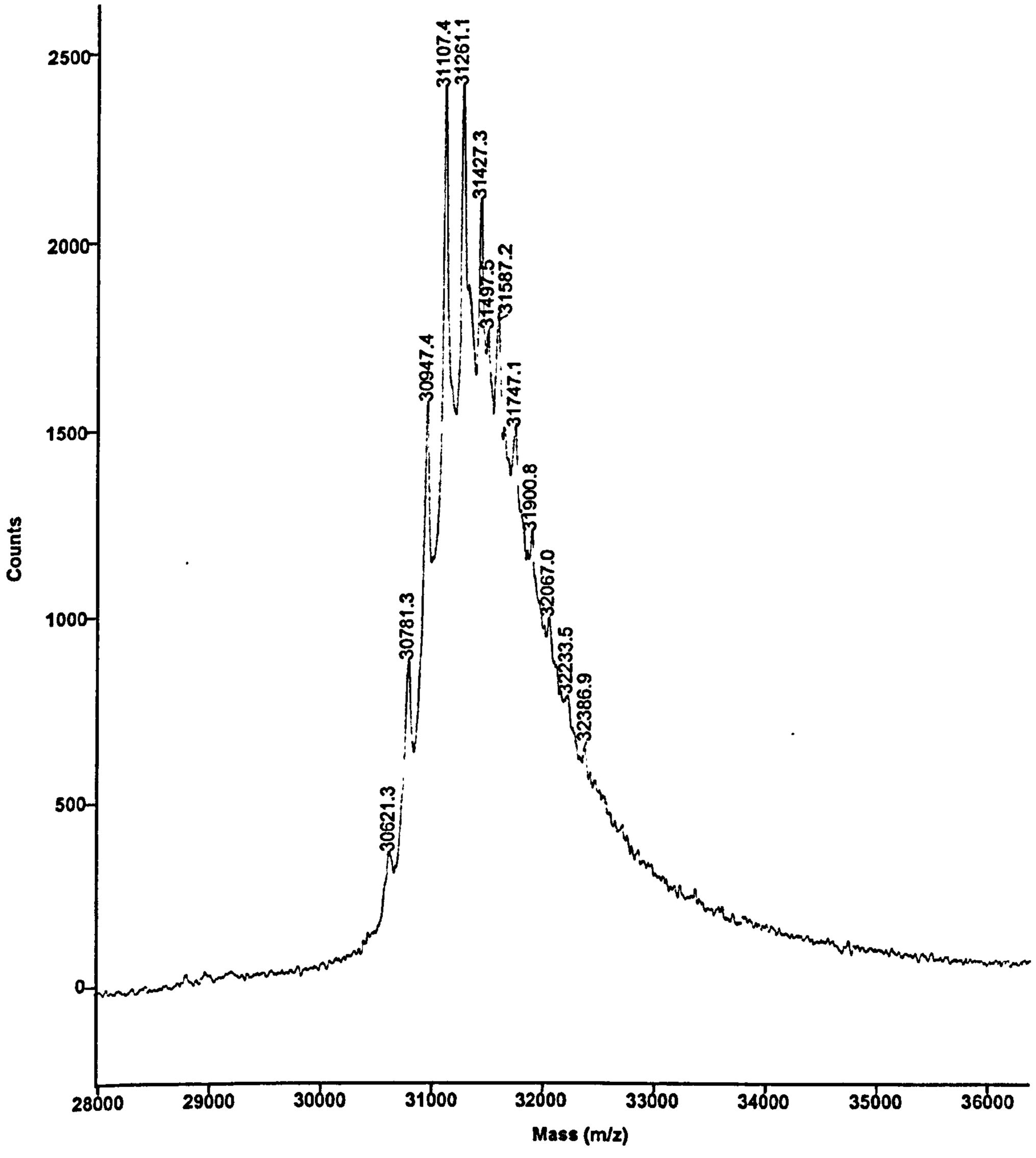

(c) 'Glycosylation' Mutant Lipase: N269Q

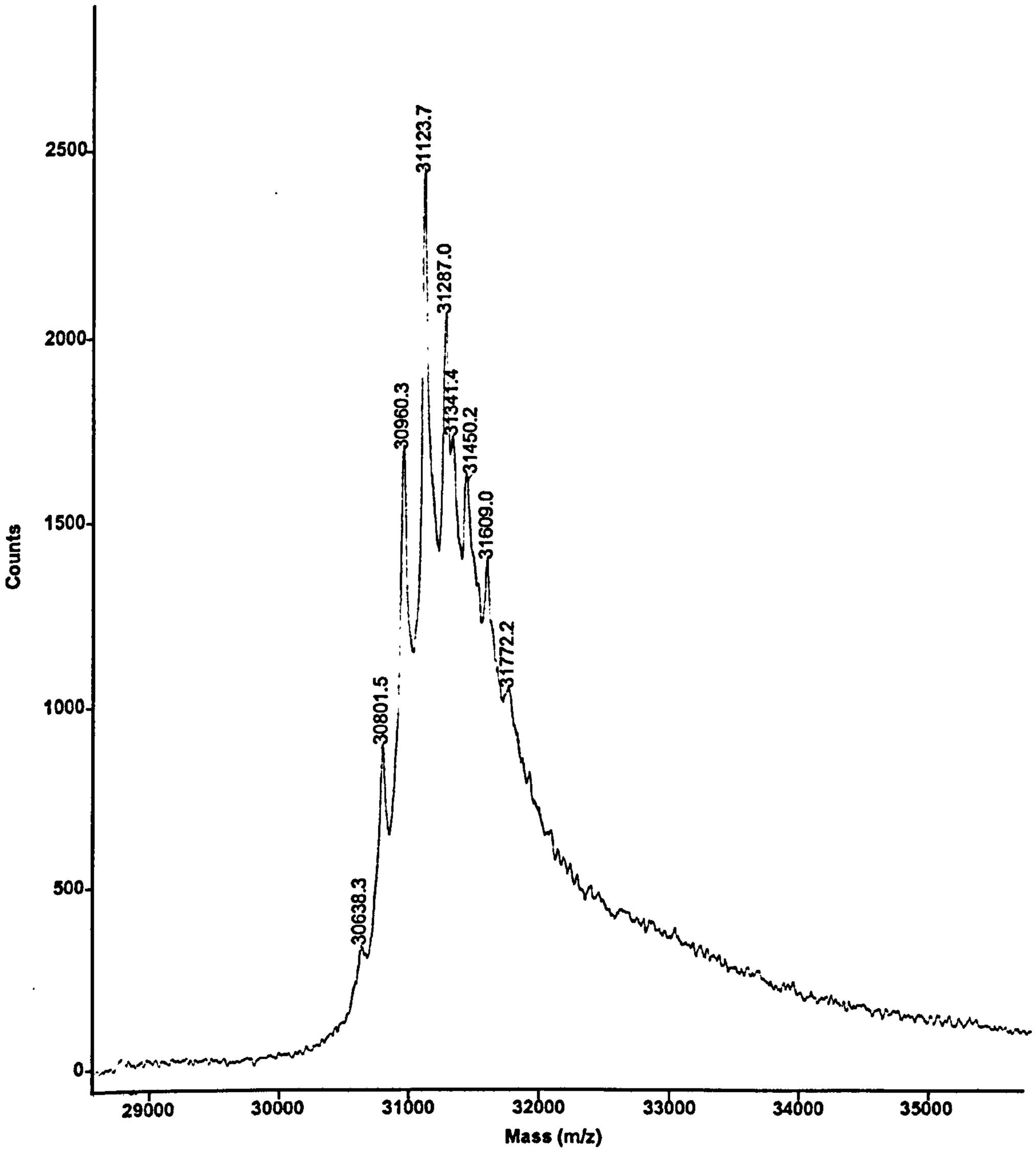

(d) 'Glycosylation' Mutant Lipase: N59T N269T

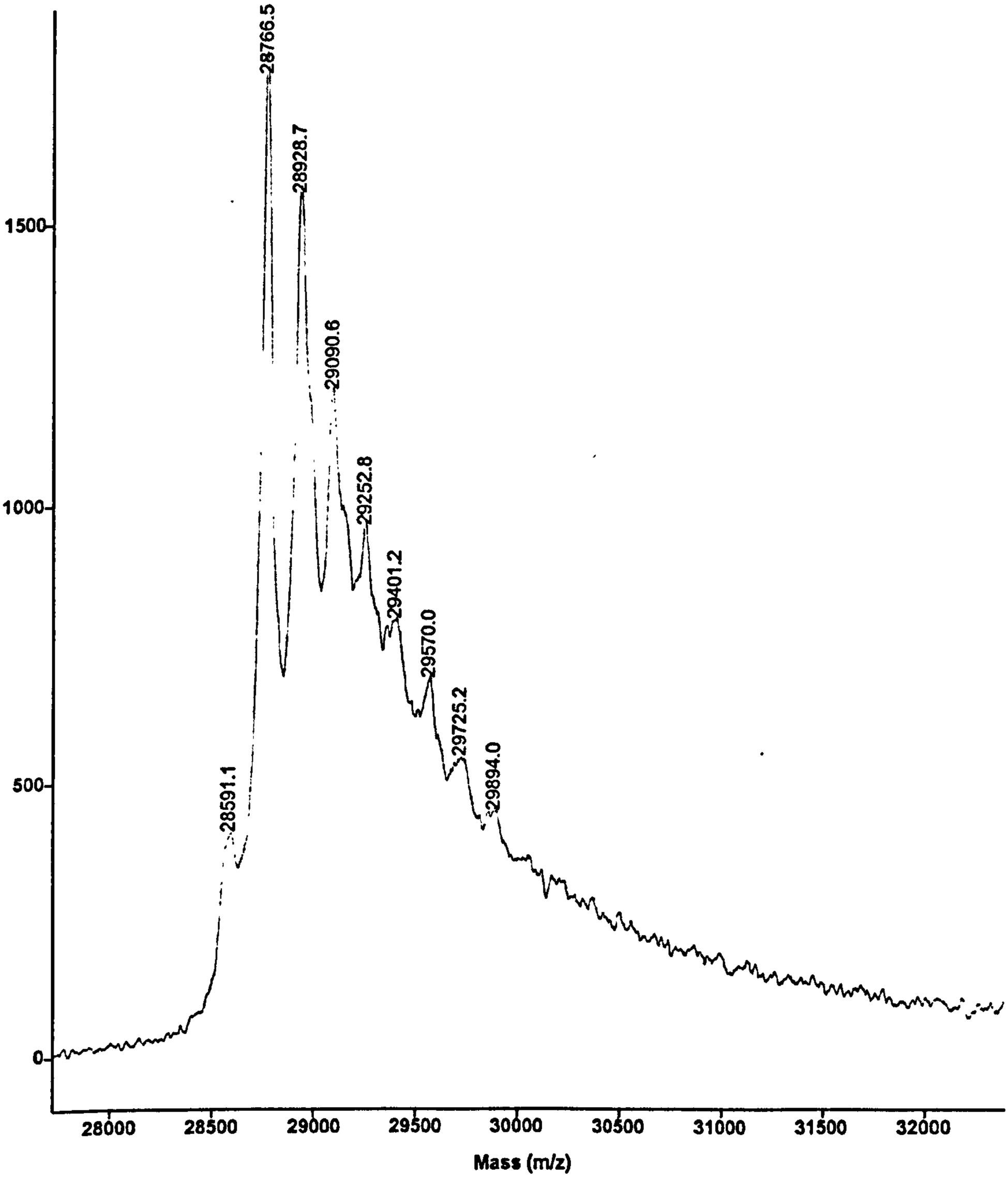

(c) 'Glycosylation' Mutant Lipase: N59T N269Q

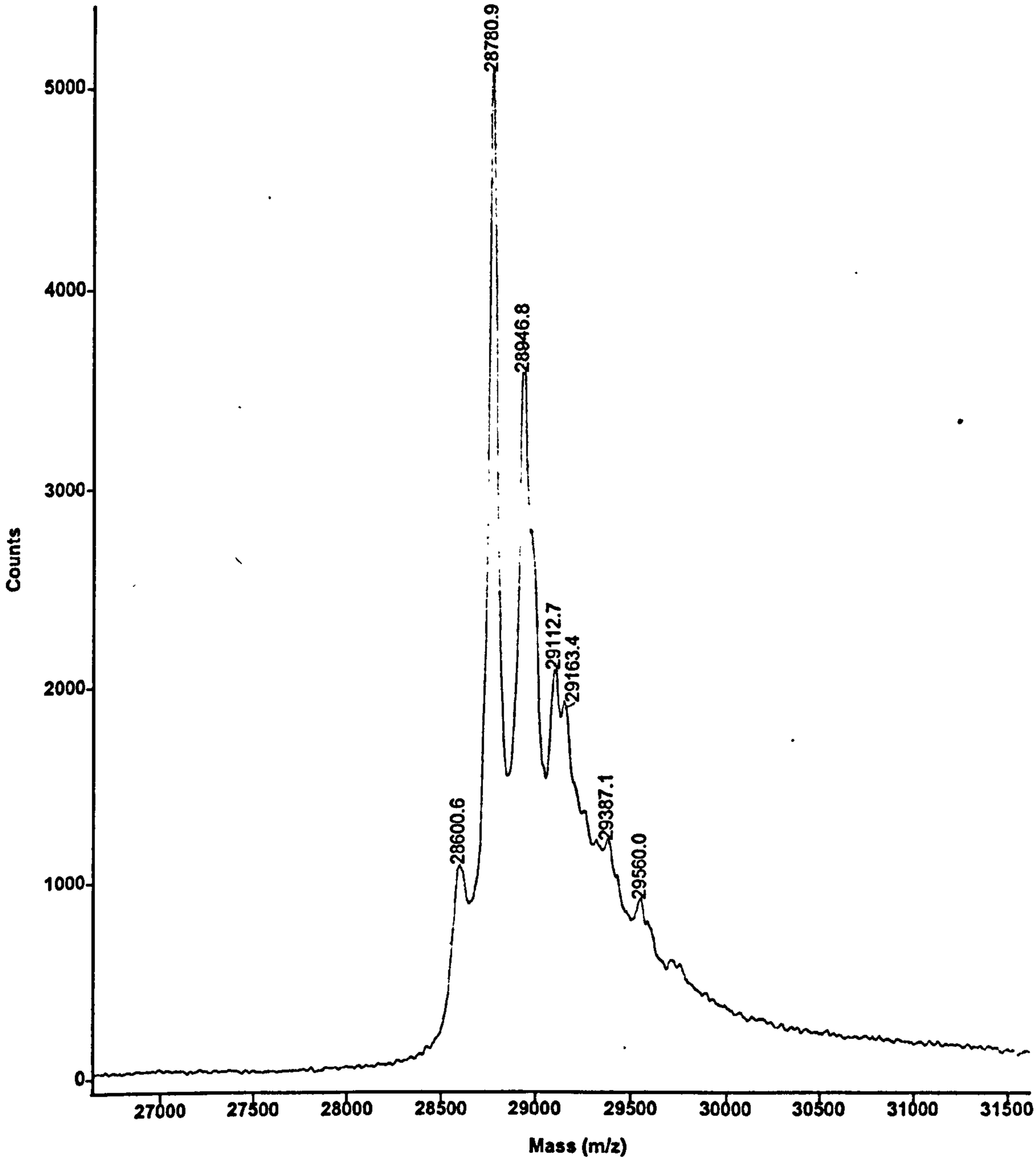

5.5 Discussion

The expression and secretion of the wild type and all the mutant forms of Danisco Lipase 3 was successfully achieved by secretion using the native enzyme signal sequence in *Pichia pastoris*. Transformation by the spheroplast method resulted in recombinant GS115 strains that showed wide variation in levels of lipase expressed. The expressing strains could be detected directly by the rhodamine B plate assay and were picked for screening by small-scale expression. Plating of the transformed cells onto regeneration plates containing 3-AT was found to provide an effective method for selecting transformants that were able to express lipase to high levels on methanol induction. The differences in expression levels could be due to multi-integration of the transforming DNA into the *Pichia* genome, with highest expressers containing several copies of the lipase gene.

The methanol utilisation phenotypes (Mut) of 100 His^+ transformants from each transformation carried out were determined before testing for expression of lipase on rhodamine B plates. Most recombinant strains chosen for large-scale expression of protein were Mut^+. Only two of these strains were Mut^S, indicating that gene replacement of the *AOX1* gene had occurred. The Invitrogen protocol advised testing both types of phenotype for expression as one might be found to express heterologous protein better than the other. The two Mut^S phenotypic strains selected arose from the constructs directing the expression of wild type and N59T N269T 'glycosylation' mutant lipases. The resorufin ester assay and SDS-PAGE results from expression of these lipases revealed that expression was no more efficient than the mutant lipases from Mut^+ phenotypic strains. It seems that multiple-integration of the transforming DNA is the most important factor when attempting to produce high expression levels of lipase, as opposed to the type of integration event in the *Pichia pastoris* genome (replacement or insertion).

The scaling up of expression resulted in the production of high concentrations of protein in cell supernatants (up to 0.42 g l^{-1} measured with the Bradford assay). Efficient expression was achieved by growth of recombinant GS115 strains to a high cell density in glycerol containing media, followed by resuspension in methanol containing media for induction of expression from the P_{AOX1} promoter.

SDS-PAGE of cell supernatants showed that two iso-forms of the wild type and 'activity' mutant enzymes were being secreted. These migrate at approximately 36 kD as compared to the molecular weight markers. The molecular weights of these enzyme forms, as

determined by MALDI TOF mass spectrometry, are 32,606 and 30,544 (Figure 5.12). N-terminal sequencing showed that processing was complete and both N-termini were of the mature enzyme. The mass differences may represent different glyco-forms of the enzymes. Separation of the bands could be achieved on purification by anion-exchange chromatography. Fractions containing lipase activity, detected by the resorufin ester assay, were combined and dialysed against 20 mM triethanolamine pH 7.3 buffer. SDS-PAGE indicated that no contaminating proteins were present after purification.

5.5.1 Purification of 'Glycosylation' Mutant Lipases

Comparison of wild type and 'glycosylation' mutants by SDS-PAGE analysis (Figure 5.6) revealed a drop in molecular weight of the enzyme upon mutation of N-linked glycosylation sites (N59 and N269). The greatest drop in weight was observed for the double mutants, where both glycosylation sites had been altered. These differences could be explained by the prevention of enzyme glycosylation occurring on expression in *Pichia pastoris*, due to elimination of the N-linked glycosylation sites. It was also noted that all lipase mutants in which the asparagine at position 269 had been changed were expressed as a single enzyme form. The N59T mutant appeared to have two bands, similar to those observed for the wild-type enzyme. On purification of the N59T mutant by anion-exchange chromatography, separation of these bands was possible (Figure 5.11), as also observed for both the wild type and 'activity' mutant lipases. N-linked glycosylation at asparagine 269 may therefore be responsible for the heterogeneity of wild type (and 'activity' mutant) lipases expressed in *Pichia pastoris*, as the two iso-forms are no longer observed when this site is altered.

5.5.2 Mass Spectrometry Analysis of Wild Type and 'Glycosylation' Mutants

The results of the MALDI TOF mass spectral analysis of wild type and 'glycosylation' mutants of Lipase 3, from expression in *Pichia pastoris*, carried out by Danisco are presented in Figure 5.12.

5.5.2.1 Glycosylation of secreted proteins

Most secreted proteins are glycoproteins. Glycosylation is a stepwise process that proceeds as the nascent secretory protein moves through the endoplasmic reticulum (ER) and Golgi body, before being packaged into secretory vesicles. There are two types of glycosylation, N-type or O-type depending on the atom of the protein to which the carbohydrate is attached (Creighton, 1993). N-type occurs on the nitrogen atom of asparagine (Asn) side chains, and O-type on the oxygen atoms of hydroxyl groups, particularly of serine and threonine residues. N-glycosylation occurs co-translationally soon after the Asn residue

emerges into the endoplasmic reticulum, whereas O-type glycosylation occurs primarily in the Golgi as a post-translational modification.

N-Glycosylation

N-type glycosylation occurs on the nitrogen atom of asparagine (Asn) side chains that are part of the sequence –Asn-Xaa-Ser/Thr/Cys- (Xaa can be any residue except proline) (Kornfeld and Kornfeld, 1985, Creighton, 1993). However, the presence of this sequence is not the only determinant for glycosylation as not all such Asn residues of proteins entering the ER are modified. After attachment of a core glycan to the Asn residue of a protein in the ER, the glycan is extensively modified during passage of the protein through the ER and Golgi.

N-linked oligosaccharides can be divided into three main categories: high mannose, hybrid and complex (Figure 5.13a). They all share a common pentasaccharide core structure of $Man_3(GlcNAc)_2$ (where Man is the sugar residue mannose and GlcNAc is N-acetylglucosamine) but differ in their outer branches. The high mannose-type oligosaccharides typically have two to six additional mannose residues linked to the common pentasaccharide core. The complex-type structure may be modified by the addition of extra branches on the α mannose residues or by the addition of extra sugar residues that elongate the outer chains and typically have two to five outer branches. The hybrid molecules have features of both high-mannose and complex type oligosaccharides (i.e. mixed branches of the two types).

Proteins secreted by *Pichia pastoris* have a majority of N-linked glycosylation of the high-mannose type. On average, the length of oligosaccharide chains added post-transitionally is 8-14 mannose residues, with no terminal α1,3 glycan linkages (Invitrogen *Pichia* Expression Kit manual Version F).

O-Glycosylation

The attachment of carbohydrates to the oxygen atoms of amino acid side chains occurs primarily in the Golgi apparatus (Creigton, 1993). N-acetylgalactosamine (GalNAc) groups are added to the O-atoms of serine and threonine residues (Figure 5.13b). The signals that determine which serine and threonine residues are glycosylated are not apparent from the amino acid residues surrounding them. O-glycosylation occurs in proteins that are already folded and where the three-dimensional structure is probably important. In some

proteins, the amino acid residues that are glycosylated are clustered in the primary structure and the carbohydrate content of these proteins can be as high as 65 – 85 % by weight.

Figure 5.13 The structures of typical glycosylation groups attached to proteins. (a) The major types of N-linked oligosaccharides. The boxed area encloses the pentasaccharide core common to all asparagine–linked structures. (b) A typical O-linked structure, added to a serine residue. The abbreviations of the sugar residues are Man, mannose; Gal, galactose; GlcNAc, N-acetylglucosamine; GalNAc, N-acetylgalactosamine; and S.A., sialic acid. (Reproduced from Kornfeld and Kornfeld, 1985 (a) and Creighton, 1993 (b)).

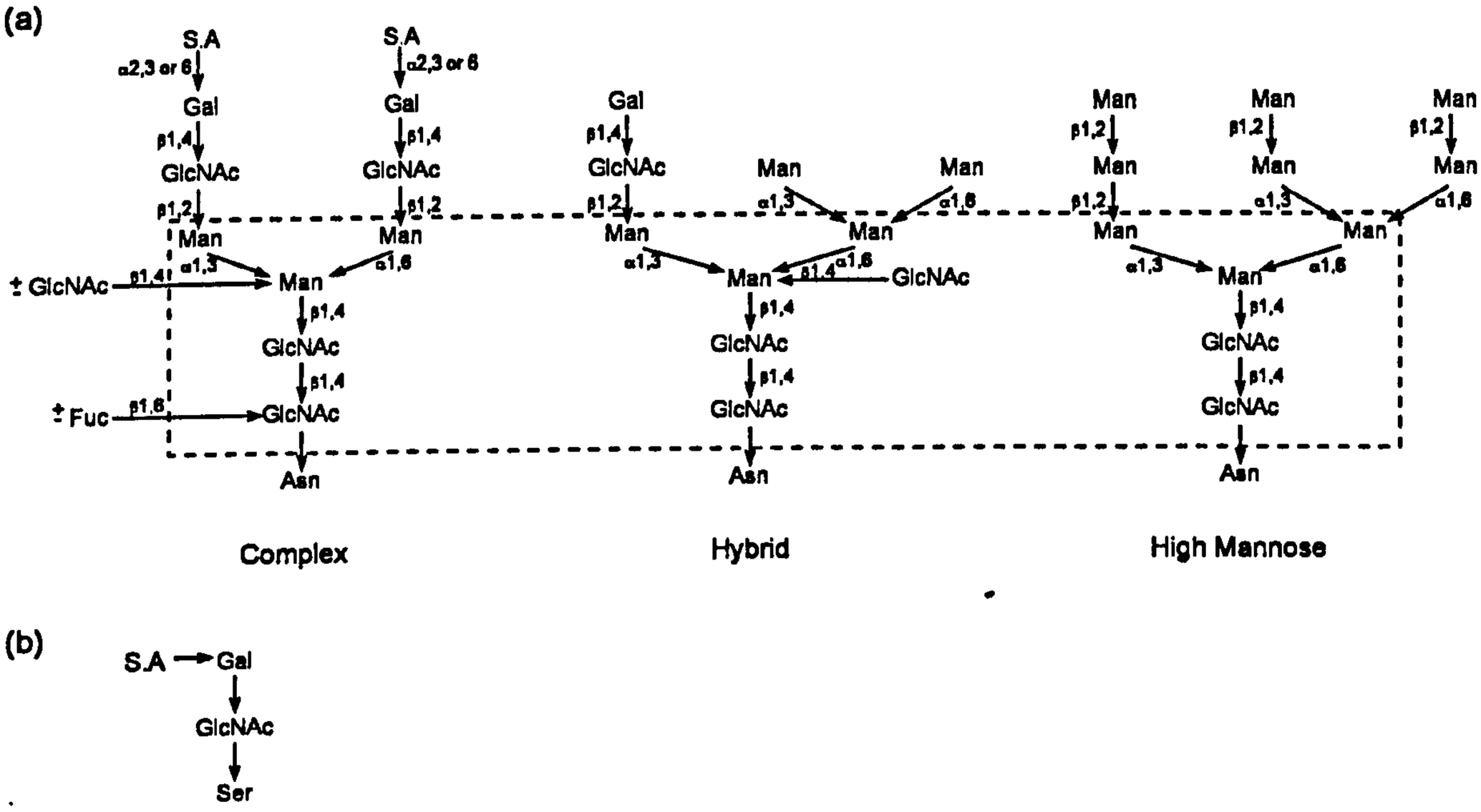

5.5.2.2 Mass spectrometry of wild-type Lipase 3

The MALDI TOF mass spectrometry results of the two wild type isoforms separated and purified by anion-exchange chromatography are shown in Figure 5.12a and b. The mass spectrum of the high-molecular weight iso-form has a major peak with a *m/z* value of 32606.3. The spectrum of the lower molecular weight iso-form gives a peak with a *m/z* value of 30544.3.

The difference in mass between the low molecular weight iso-form (seen on SDS-PAGE of the wild type enzyme) and the predicted molecular weight of the mature, unmodified enzyme from its amino acid sequence (28942.05) equals 1602.25 which is close to the mass difference for the $Man_7GlcNAc_2$ group (1541.4).

The difference in mass of the two wild type iso-forms equals 2062, which is close to that for the N-linked oligosaccharide group $Man_{10}GlcNAc_2$ (2027.8). The $Man_{10}GlcNAc_2$ group could therefore be responsible for the higher molecular weight iso-form of this enzyme. Alternatively this mass difference may be due to more extensive modification of the oligosaccharide present in the low molecular weight form. The mass difference shown by twelve mannose units would be 1944. The $Man_{10}glcNAc_2$ group corresponds more closely to the mass difference seen and so it seems more likely that this group is present at one of the glycosylation sites of Lipase 3 and the $Man_7GlcnAc_2$ is attached to the other site.

5.5.2.3 Mass spectrometry of 'glycosylation' mutants of Lipase 3

The mass spectrometry results for the N269T and N269Q single mutants indicate that the main oligosaccharide group attached to the remaining site (N59) could be $Man_{11}GlcNAc_2$. The mass change for this group is 2190. The predominant forms in the mass spectra of these enzymes have *m/z* values of 31107 for N269T and 31124 for N269Q. These are close to the calculated masses for these lipases plus the $Man_{11}GlcNAc_2$ oligosaccharide (equal to 31119 and 31146 respectively).

Two main peaks are seen in the mass spectrum generated for the N59T mutant. These have *m/z* values of 28955.9 and 30946.2. The former iso-form could be the non-glycosylated enzyme as it is close to the predicted mass of the unmodified mature form of this mutant (28929.05). The latter iso-form is closest to the predicted mass of the $Man_{10}GlcNAc_2$ glycosylated enzyme (30957), which would be present at the remaining glycosylation site, Asn 269.

The double mutants, where both sites have been altered, show predominant mass peaks with *m/z* values of 28766.5 for N59T N269T and 28780.9 for N59T N269Q. These values are 162 and 166 below the calculated masses of the non-glycosylated forms for N59T N269T and N59T N269Q (28916 and 28943.1 respectively). This cannot be due to incorrect processing of the N-terminal signal sequence as N-terminal sequencing carried out by Danisco has shown these to be of the mature enzyme. Peaks are also present with *m/z* values of 28928.7 for N59T N269T and 28946.8 for N59T N269Q, which are close to the masses calculated for the non-glycosylated forms of these mutant lipases.

For all of the mutants analysed, a number of peaks were observed, separated by mass differences of approximately 160 (the average mass difference between the peaks equals 161.8), which corresponds to the mass difference (162) of one hexose group (fructose,

galactose, glucose or mannose). The number of these peaks ranges from 5 for each of the isoforms of N59T to 12 for N269T and 7-9 for the other mutants occurring around each main iso-form. It could be that a number of N-linked oligosaccharide species differing in the number of mannose units attached to the core $Man_3GlcNAc_2$ group are assembled at each glycosylation site on secretion by *Pichia pastoris*. However, these peaks were also observed for the double mutants where both N-linked glycosylation sites had been mutated (preventing N-linked glycosylation from occurring). It is possible that the protein is also modified by O-linked glycosylation, although this has not been reported for proteins expressed in *Pichia*. This can occur at serine or threonine residues and post-translational modification of this type would result in a mass change of 162 (corresponding to an O-Glycosyl- group).

Overall, the results of MALDI TOF mass spectrometry imply that the main N-linked oligosaccharide added to lipases on secretion by *Pichia pastoris* is $Man_{7\text{-}11}GlcNAc_2$. The results for the wild type enzyme indicate that a $Man_7GlcNAc_2$ and a $Man_{10}GlcNAc_2$ group could be attached to the N-glycosylation sites of Lipase 3. The main peaks in the mass spectra for the wild type can be accounted for if, in one isoform of the enzyme, both these groups are linked to the enzyme and in a second isoform of lower molecular weight, a single $Man_7GlcNAc_2$ group is attached. The results for the single 'glycosylation' mutants (N59T, N269T and N269Q) imply that the remaining glycosylation site of each of these has a $Man_{10\text{-}11}GlcNAc_2$ group attached. The N59T mutant also has a major peak with a *m/z* value that could represent an un-glycosylated form. As mutation of N59 gives two dominant mass peaks for the expressed enzyme (one apparently representing the non-glycosylated form) and mutation of Asn 269 gives just one major peak, it would appear that differences in glycosylation at Asn 269 results in two isoforms of Lipase 3 being secreted by *Pichia*. Two lipase isoforms are observed for the wild type, the N59T 'glycosylation' mutant, and also for the 'activity' mutants on SDS-PAGE.

These results are consistent with reported sizes of N-linked oligosaccharide groups characterised for proteins expressed in *Pichia pastoris* (Montesino *et al.* 1998) where the average number of side chain mannose units is 8 - 14. A number of iso-forms of each mutant appears to be expressed, which could be due to varying numbers of mannose units attached to N-linked oligosaccharides or possibly due to O-linked glycosylation, either being consistent with the results of mass spectrometry. As the iso-forms are also observed when both N-linked sites are mutated to prevent this form of glycosylation, they could arise from O-linked glycosylation.

CHAPTER 6 Characterisation of Wild type and Mutant Lipases Expressed in *Pichia pastoris*

6.1 Introduction

During the purification of variants of Danisco's Lipase 3 from the culture medium of *Pichia pastoris*, lipase activity was monitored using the resorufin ester assay. The results of these assays can only be compared when obtained from the same batch of substrate (prepared in isopropanol for each assay) as activity levels were found to vary widely between preparations and also with the age of the substrate itself. While this assay provided a quick and simple method for detecting and comparing the levels of lipase activity in cell supernatants, it is not suitable for more accurate measurements of activity to determine specific activities and for kinetic analysis. Also, although the resorufin ester is a derivative of a triacylglycerol molecule, it is not a natural lipase substrate. A more suitable substrate to study the potential effects of the lipase variants in a dough system would be a long-chain triacylglycerol.

Specific activities were determined using lipases that had been purified by anion-exchange chromatography, with a soluble esterase substrate (*para*-nitrophenyl acetate) and insoluble emulsified substrate (olive oil). First of all, the optimal conditions for assaying lipase activity with *para*-nitrophenyl acetate (*p*-NPA) and olive oil substrates were determined, by measuring the effect of pH and temperature on lipase activity with these substrates. Analysis of the wild type Lipase 3 produced by Danisco from expression in *Aspergillus niger* was also carried out. The properties of the wild type lipase expressed in *Pichia pastoris* could then be compared to the industrial enzyme itself.

6.1.1 Lipase assays

The usual site of action of lipases is at lipid/water interfaces. As lipase activity seems to depend on an equilibrium between two conformational states; predominantly closed (inactive) in solution and open (active) at the hydrophobic surface of the interface, lipase activity occurring at the interface and in solution were both investigated. The substrates selected to determine lipase activity in solution and at the lipid-water interface were *para*-nitrophenyl acetate (*p*-NPA) and olive oil, respectively.

6.1.1.1 Activity in solution (p-*NPA assay)*

To investigate lipase activity in solution, the water soluble esterase substrate *para*-nitrophenyl acetate (*p*-NPA) was used. The release of *p*-nitrophenol from the hydrolysis of *p*-NPA can be measured due to its optical absorption at 405 nm. Although resorufin ester is a soluble substrate, it is a triacylglycerol derivative and so could easily form micellar

structures resulting in activity levels that would not accurately represent activity occurring solely with monomeric substrate. Optimum pH conditions and specific activities were determined with this substrate before evaluating the lipases with emulsified substrate as this assay could be performed quickly and easily in microtitre plate wells. These results therefore provided a starting point to estimate the quantities of enzyme required for the assays with emulsified substrate and the pH and temperature conditions employed.

6.1.1.2 Activity at the lipid-water interface

For determination of enzyme activity at an interface, emulsified olive oil was used as a substrate. Olive oil is predominantly composed of triolein (glycerol esterified to oleic acid, which has an acyl chain of eighteen carbon atoms with a *cis* double bond at position 9, i.e. C18:1, cis-9). It also contains small percentages of triacylglycerols esterified with linoleic (C18:2, cis-9,12), palmitic (C16:0) and stearic acids (C18:0). The predominant fatty acids of acyl lipids in wheat are linoleic acid (55 %), palmitic acid (20 %) and oleic acid (14 %), with the remaining percentage composed of C18:3, C18:1 and C16:1 acyl chains (Belitz and Grosch, 1999). Whilst the basic structure of the predominant fatty acid in olive oil (oleic acid) is the same as that in wheat (linoleic acid), the degree of unsaturation is different (C18:1 as opposed to C18:2 of linoleic acid). However, this should not unduly effect the structure of the emulsion and as such olive oil was considered a suitable model substrate to study the effects of lipase in a dough system.

Olive oil is an ideal substrate for investigating lipase activity as it is composed of long-chain triacylglycerols, which are the usual substrates of lipases. They are insoluble in water and will aggregate to form monolayers, or can be converted to a stable emulsion if energy is applied, for example by mechanical dispersion. Emulsions are characterised by a "core" or bulk lipid phase surrounded by a surface monolayer of amphiphilic molecules. The surface components can include other amphiphilic compounds such as gum arabic, a polysaccharide that can sterically stabilise the dispersed lipid particles. In the absence of such an emulsifier, lipid particles will tend to coalesce in order to minimise the amount of apolar surface exposed to water. For emulsions with liquid or liquid crystalline cores, rapid equilibrium probably exists between bulk lipid and the surface layer, making core lipids available to lipases at the interface (Brockman, 1984).

With no monomeric substrate in solution, all lipase activity will originate from interfacial catalysis, allowing lipase activity at the interface to be investigated. The release of fatty acids from emulsified olive oil can be monitored by titration with sodium hydroxide to

maintain the reaction at a set pH. This is carried out automatically using a pH-stat controller, in which pH and temperature electrodes monitor reaction pH and temperature and the addition of sodium hydroxide to the reaction vessel from an 'autoburette' is controlled so that a steady pH is maintained. The rates of hydrolysis can then be calculated from the rates of addition of sodium hydroxide (of known concentration).

6.2 Assay Conditions

6.2.1 Stability of Olive Oil Emulsions

Olive oil suitable for use as a lipase substrate was purchased from Sigma. Sonication of olive oil in emulsification buffer containing 5 % (w/v) gum arabic and 0.2 M calcium chloride (Hult and Holmquist, 1997) provided a stable emulsion that was used to determine lipase activity at an interface. Prepared emulsions were found to be stable for at least the course of the experiments in which they were used (8 – 12 hours). Hydrolysis rates were comparable over this time and particle sizes, as measured by laser diffraction using the Mastersizer χ (Malvern Instruments), remained constant.

6.2.2 Effect of Calcium Chloride

In assays described for lipase acitivity with triacylglycerol substrate, calcium chloride is often a component in the reaction buffer (Hult and Holmquist, 1997, Desnuelle, 1972, Brockerhoff and Jensen, 1974). It has been found that the presence of calcium ions (Ca^{2+}) increases the activity of many lipases (Iwai and Tsujisaka, 1984, Wang *et al.* 1987), and in the case of pancreatic lipase, is necessary for activity (Verger, 1984). It was thought that calcium ions may accelerate adsortion of lipase at the substrate-water interface by removing released reaction products (free fatty acids or partial glycerides) covering the emulsion surface. Another suggestion made, from a study of Ca^{2+} activation of *Aspergillus niger* lipase (Iwai *et al.* 1964), was that the formation of the Ca^{2+}-soap of the fatty acid product may improve the emulsified state of the oil in the reaction mixture, by creating a finer emulsion with increased interfacial area. Alternatively, the soap may accelerate the formation of the enzyme-substrate complex by removing reaction products accumulated on the substrate dispersion. However, the role of these ions in the activity of lipases remains unclear.

Very low activity levels were first observed when the Lipase 3 variants were tested with the *p*-NPA assay. In optimising conditions for the *p*-NPA assay, the effect of adding calcium chloride to the reaction buffer was tested (even though the effect of calcium ions on the

activity of lipases had only previously been reported with lipid emulsion substrate). The presence of calcium chloride in the assay buffer was found to improve the measured activities on this substrate (Table 6.1) and so was included in further assays. However, the mechanism of this apparent activation is unknown.

With olive oil emulsion substrate, an established protocol for testing lipase activity with olive oil substrate was used (that of Hult and Holmquist, 1997), which included 0.2 M calcium chloride in the reaction buffer. When this was omitted, only a slight drop in activity was observed, most likely because there is sufficient calcium chloride already present in the gum arabic (used to stabilise the emulsion).

Table 6.1 Effect of calcium chloride on lipase activity using *p*-NPA substrate. The activities of wild type and 'activity' mutant lipases were measured using assay buffer with (+) or without (-) 1 mM $CaCl_2$.

Lipase	Activity U g^{-1}	
	- $CaCl_2$	+ $CaCl_2$
wild type	0.28	2.82
T112D W114Q	0.06	0.83
H225D	0	0.23
W116A	0	0.26
W116A I113W	0.08	0.65

6.2.3 Determination of pH Optima

6.2.3.1 Soluble substrate

The optimum pH values for measuring lipase activity with soluble *p*-NPA substrate were determined for wild type and mutant lipases, using the supernatants from large-scale expression in *Pichia pastoris* yeast. The assay buffer (10 mM MOPS-KOH, 1 mM $CaCl_2$) was adjusted to pH values between 6.5 and 8 in order to determine the optimum for activity.

Bell-shaped curves were observed for each of the lipase variants (Figure 6.1). Although precise optimum pH values could not be determined from these graphs, especially for H225D and the tryptophan mutants (W116A, W116A I113W) which had very low activities, maximum activities for all the lipases appeared to lie in the range pH 7.1 to pH 7.4. It was decided to measure lipase activity with *p*-NPA substrate at pH7.3.

Figure 6.1 Effect of pH on hydrolytic activity of (a) wild type and 'activity' mutant lipases and (b) 'glycosylation' mutant lipases with soluble substrate. Activity was measured by the *para*-nitrophenyl acetate assay. Lipases were produced extracellularly in *Pichia pastoris* and cell supernatants of these cultures were used in activity measurements. Protein concentrations for the calculation of specific activities were measured using the Bradford assay. *(U: mmol min^{-1}).*

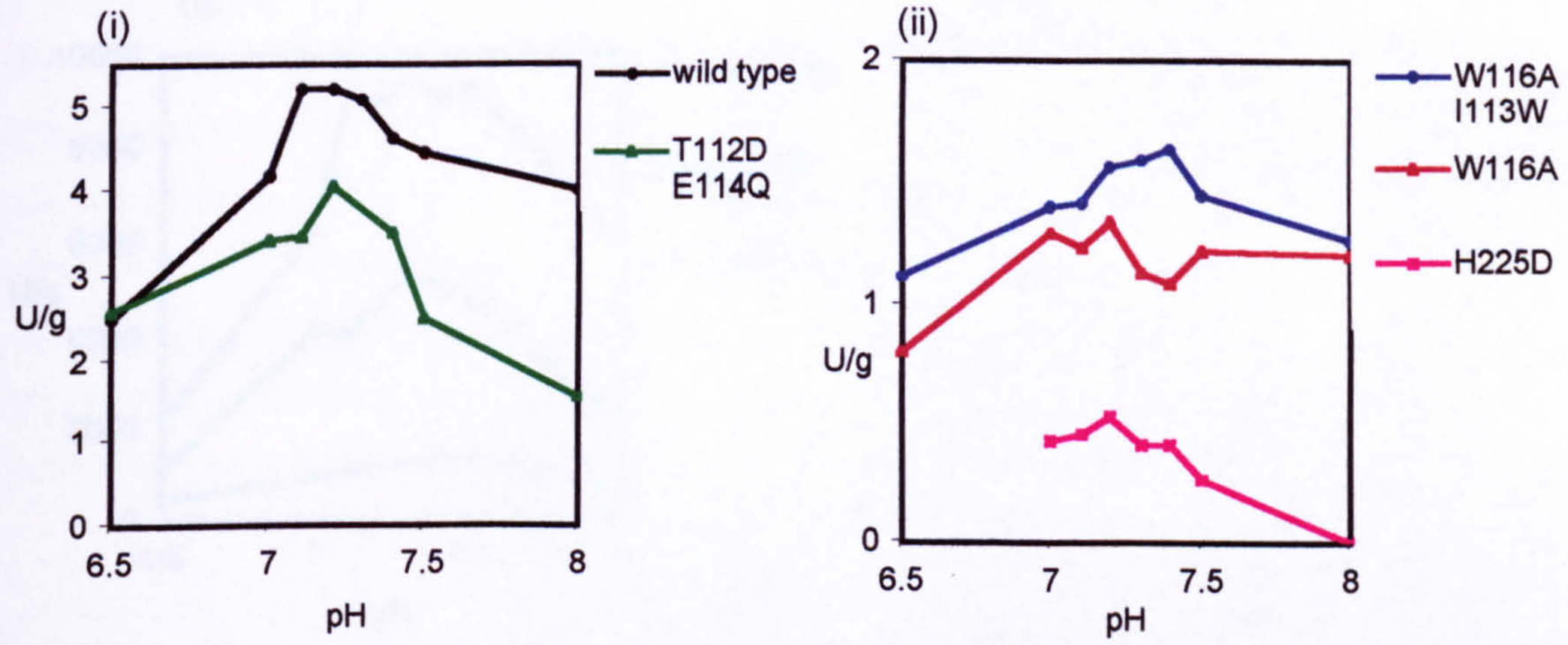

6.2.3.2 Insoluble substrate

The optimum pH values for measurement of lipase activity with emulsified olive oil substrate were determined for wild type and mutant lipases, using the supernatants from large-scale expression in *Pichia pastoris* yeast. The pH of the assay buffer (10 mM MOPS-KOH) used for activity measurement was varied between 6.5 and 8. The pH-stat controller could be used to automatically adjust the pH of the reaction mixture to a pre-set value by controlling the addition of sodium hydroxide solution (20 mM NaOH), before adding the enzyme.

Figure 6.2 Effect of pH on hydrolytic activity of (a) wild type and 'activity' mutant lipases and (b) 'glycosylation' mutant lipases with insoluble, emulsified substrate. Activity was measured using emulsified olive oil substrate with a pH-stat titrator. Lipases were produced extracellularly in *Pichia pastoris* and cell supernatants of these cultures were used in activity measurements. Protein concentrations for the calculation of specific activities were measured using the Bradford assay. *(U: mmol min^{-1}).*

(a) Wild type and 'activity' mutants

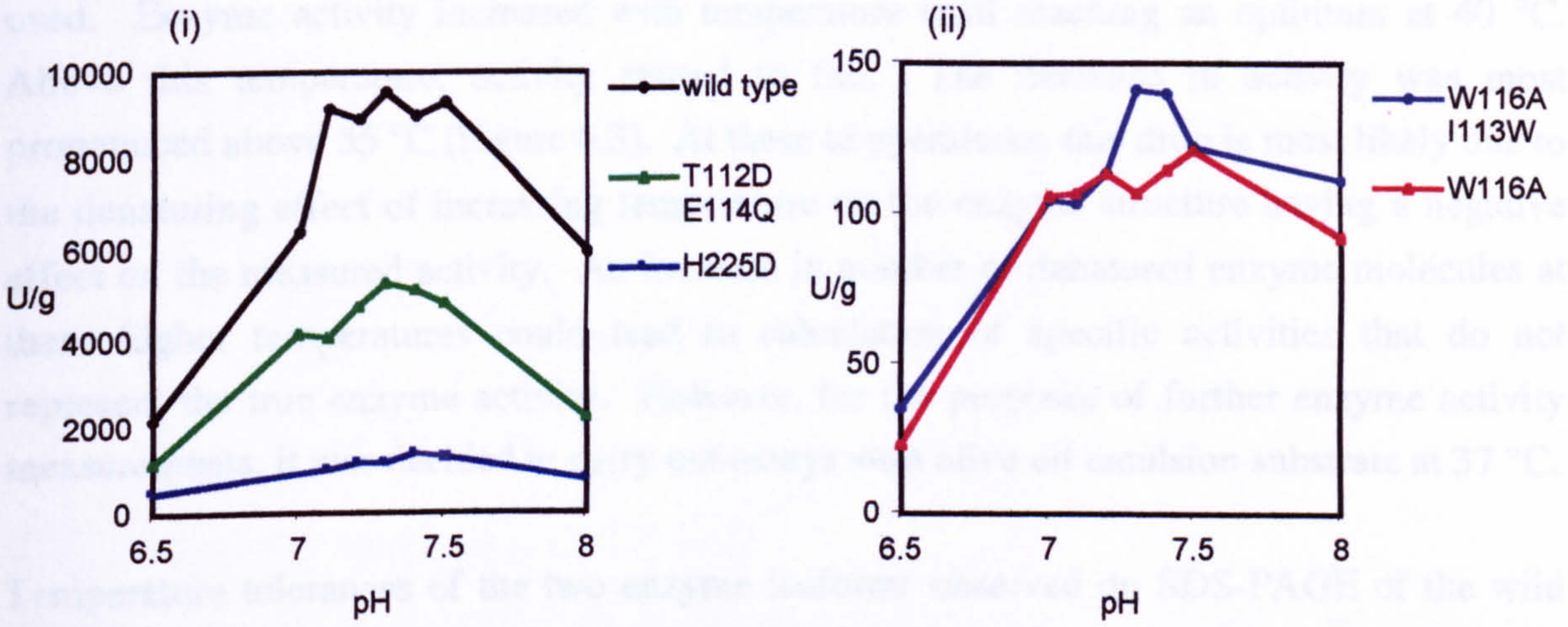

(b) 'Glycosylation' mutants

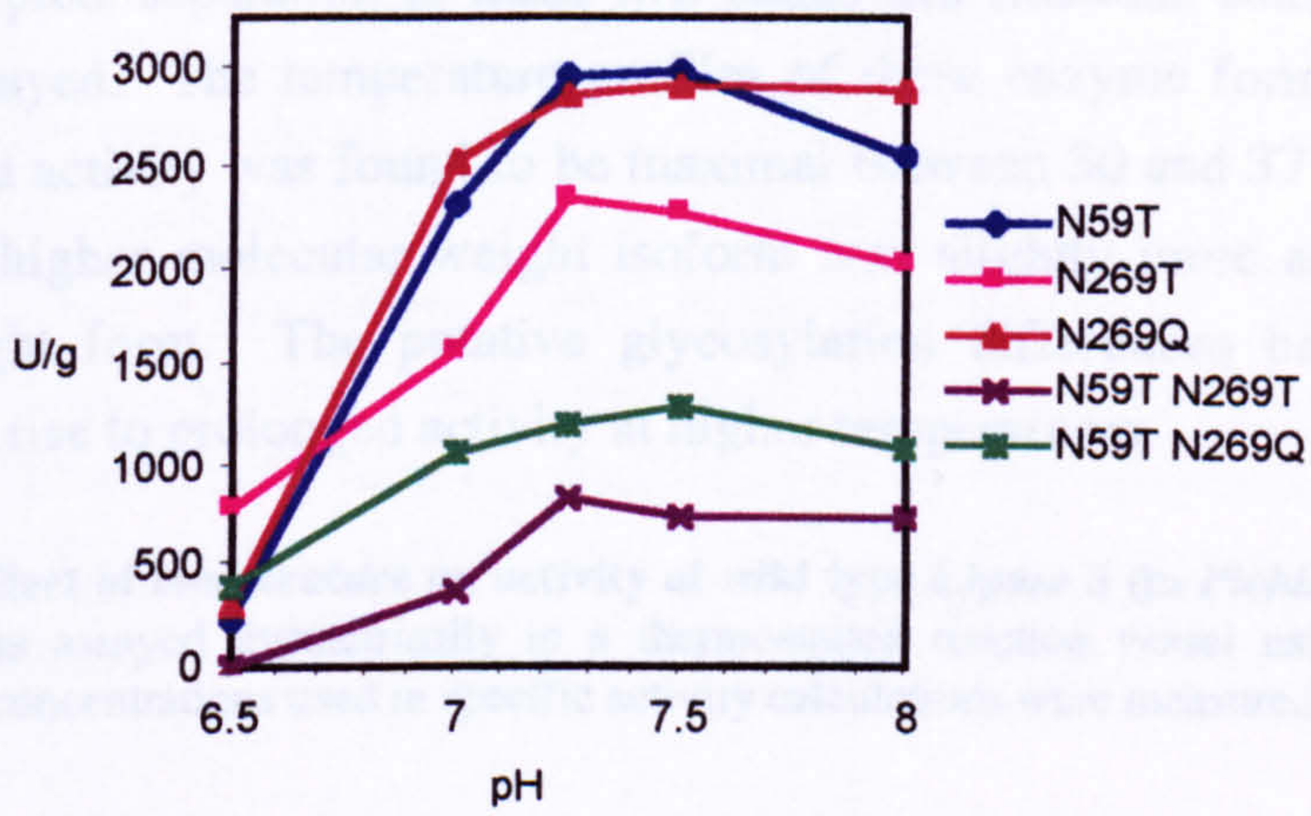

As with soluble substrate, precise values for pH optima could not be determined from these graphs (Figure 6.2). The pH range over which maximal activity appeared to occur was between pH 7.1 and 7.5 for the wild type and 'activity' mutant lipases. Although the highest rates of activity for the 'glycosylation' mutants were measured between pH 7.2 and 7.5, activities remained high at pH 8, particularly for the N269Q mutant. This effect was not seen for the wild type and 'activity' mutant lipases (Figure 6.2), for which activities dropped at alkaline pH. It is not clear how reducing the glycosylation of Lipase 3 would

result in improved activity at alkaline pH. Further lipase activity measurements with olive oil emulsion substrate were made at pH 7.3.

6.2.4 The Effect of Temperature on Lipase Activity

The effect of temperature on lipase activity was investigated using olive oil emulsion as substrate. Supernatants of *Pichia pastoris* cultures expressing the wild type lipase were used. Enzyme activity increased with temperature until reaching an optimum at 40 °C. Above this temperature, activity started to fall. The decrease in activity was most pronounced above 55 °C (Figure 6.3). At these temperatures, this drop is most likely due to the denaturing effect of increasing temperature on the enzyme structure having a negative effect on the measured activity. An increase in number of denatured enzyme molecules at these higher temperatures could lead to calculation of specific activities that do not represent the true enzyme activity. However, for the purposes of further enzyme activity measurements, it was decided to carry out assays with olive oil emulsion substrate at 37 °C.

Temperature tolerances of the two enzyme isoforms observed on SDS-PAGE of the wild type lipase were also investigated. Purification by anion exchange chromatography resulted in complete separation of these two bands and fractions containing the separated bands were assayed. The temperature profiles of these enzyme forms were very similar (Figure 6.4) and activity was found to be maximal between 30 and 37 °C. Between 35 °C and 50 °C the higher molecular weight isoform was slightly more active than the lower molecular weight form. The putative glycosylation differences between the isoforms apparently give rise to prolonged activity at higher temperatures.

Figure 6.3 The effect of temperature on activity of wild type Lipase 3 (in *Pichia pastoris* supernatant). Lipase activity was assayed titrimetrically in a thermostatted reaction vessel using emulsified olive oil substrate. Protein concentrations used in specific activity calculations were measured by the Bradford assay.

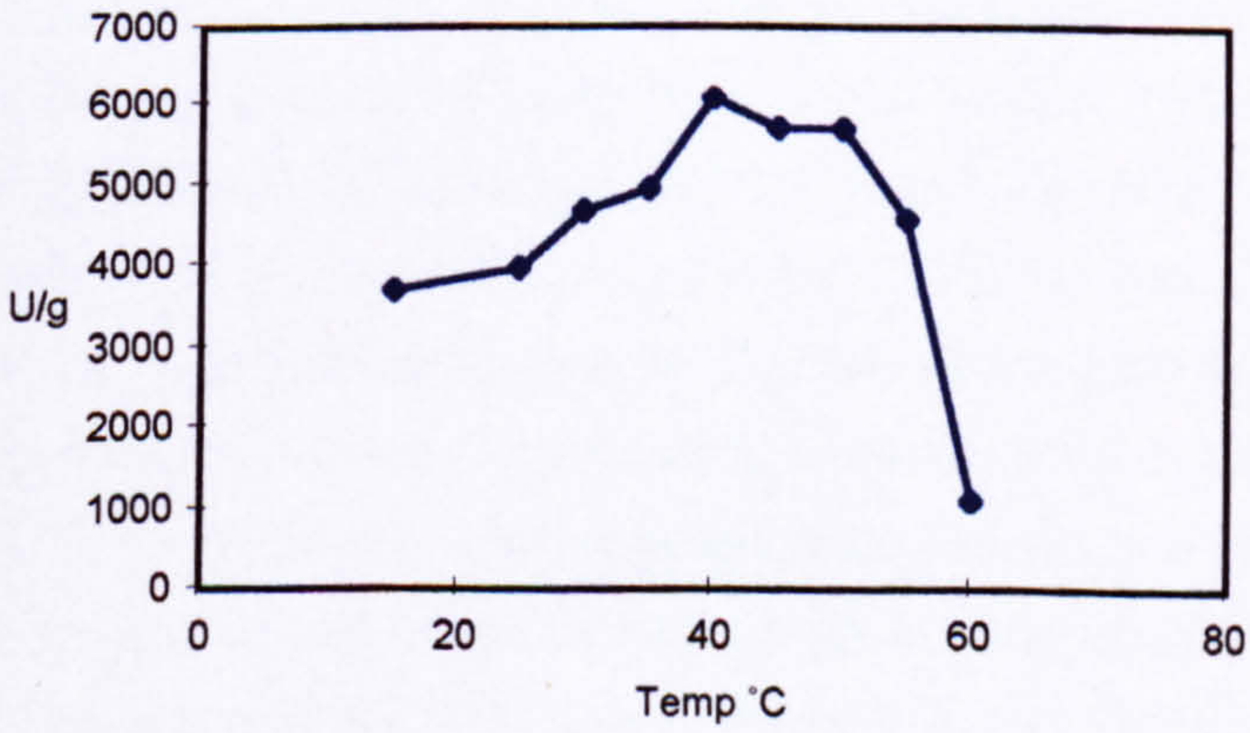

Figure 6.4 The effect of temperature on activity of wild type Lipase 3 iso-forms separated by anion exchange chromatography. Activity was assayed titrimetrically in a thermostatted reaction vessel using emulsified olive oil substrate. Protein concentrations used in specific activity calculations were determined spectrophotometrically at 320, 280 and 260 nm.

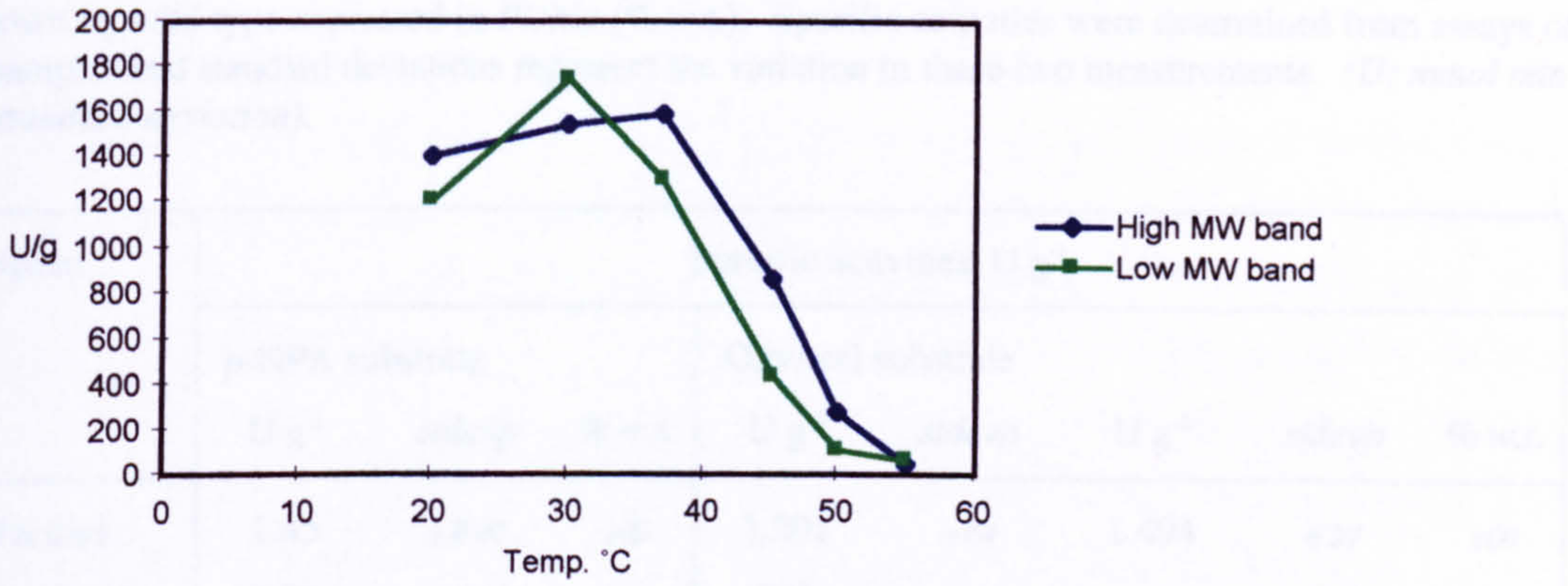

6.3 Specific Activities of Lipases

Specific activities of the wild type and mutant lipases were determined with *p*-NPA and olive oil substrates using lipases purified by anion exchange chromatography. Excess substrate concentrations (or surface areas) were used such that any increase had no further effect on measured rates. Also, increasing enzyme concentration resulted in a proportional increase in enzyme activity. When these conditions are satisfied, substrate is in excess and catalysis is occurring at the maximal rate. In the case of olive oil emulsion substrate, it is presumed that all enzyme would be in the interfacially adsorbed state and so the observed reaction rates will reflect maximal enzyme activity. Specific activities were measured with *p*-NPA and olive oil emulsion substrates at pH 7.3 and with olive oil at 37 °C. The results are shown in Table 6.2.

Table 6.2 Specific activities of purified mutant and wild type lipases with *p*-NPA and olive oil emulsion substrates. Lipases were purified by anion exchange chromatography and dialysis against 10 mM triethanolamine buffer pH 7.3. The specific activities of Danisco's industrial Lipase 3 from expression in *Aspergillus niger* are also shown. Protein concentrations for the calculation of specific activities were determined spectrophotometrically at 320, 280 and 260 nm. Activities are also shown as percentages of the activity shown by wild type expressed in *Pichia* (% w.t.). Specific activities were determined from assays of duplicate samples and standard deviations represent the variation in these two measurements. *(U: mmol min^{-1}; stdevp: standard deviation).*

Lipase	Specific activities, U g^{-1}							
	p-NPA substrate			Olive oil substrate				
	U g^{-1}	*stdevp*	*% w.t.*	U g^{-1}	*stdevp*	U g^{-1}	*stdevp*	*% w.t.*
w.t. (*Pichia*)	1.45	*± 0.00*	*100*	1,201	*± 64*	1,494	*± 27*	*100*
w.t. (*A. niger*)	0.96	*± 0.05*	*66*	797	*± 8*			*66*
N59T	1.57	*± 0.08*	*108*	781	*± 2*			*65*
N59T N269Q	1.49	*± 0.22*	*103*	590	*± 20*			*49*
N59T N269T	1.19	*± 0.00*	*82*	564	*± 2*			*47*
N269T	1.13	*± 0.01*	*78*	915	*± 26*			*76*
N269Q	0.96	*± 0.06*	*66*	991	*± 44*			*83*
T112D E114Q	1.20	*± 0.05*	*83*			1,044	*± 131*	*70*
W116A I113W	0.85	*± 0.01*	*59*			35	*± 0*	*2*
W116A	0.61	*± 0.03*	*42*			34	*± 1*	*2*
H225D	0.04	*± 0.01*	*3*			451	*± 18*	*30*

6.3.1 'Activity' Mutants

None of the 'activity' mutants had specific activities above that of the wild type enzyme with *p*-NPA or olive oil (Table 6.2). The T112D E114Q mutant showed the highest specific activities of the 'activity' mutants with both substrate types; this mutant showed 70 % the activity of wild type lipase toward olive oil substrate and 83 % activity with *p*-NPA. The remaining mutants designed to improve lipase activity (W116A, W116A I113W and H225D) all had specific activities much lower than wild type with both substrate types, but especially with olive oil. The tryptophan mutants (W116A and W116A I113W) had only 2% the activity of wild type enzyme with emulsified olive oil substrate, however, with soluble substrate the W116A mutant had 42 % and W116A I113W mutant had 59 % the

level of activity shown by wild type. The H225D mutant demonstrated the lowest specific activities of all the 'activity' mutants, particularly with soluble *p*-NPA substrate: activity levels were 30 % of that shown by the wild type with olive oil and just 3 % of wild type activity with *p*-NPA for this mutant.

6.3.2 'Glycosylation' Mutants

On both soluble and insoluble substrates, all of the glycosylation mutants except for the N59T N269T double mutant had high activities (from 66 to 108 % of the activity shown by wild type lipase on soluble *p*-NPA substrate and between 47 and 83 % on emulsified olive oil substrate, Table 6.2). With insoluble substrate, the N59T N269T and N59T N269Q double mutants had the lowest specific activities (47 % and 49 % activity of wild type enzyme respectively). However, these enzymes demonstrated much higher activity with the *p*-NPA substrate (82 % and 103 % of activity shown by the wild type enzyme).

6.3.3 Wild type *A. niger*

The *Aspergillus niger* wild type lipase produced by Danisco was also analysed allowing a comparison with the properties of the lipase expressed in *Pichia pastoris*. The *A. niger* lipase showed 66 % the activity of wild type lipase that had been expressed in *Pichia* with both soluble and insoluble substrates. These differences may reflect variation in the glycosylation patterns of these proteins.

6.4 Discussion

Initial characterisation studies were carried out on mutant and wild type Lipase 3 variants expressed in *Pichia pastoris* yeast. Optimum assay conditions were determined using soluble (*para*-nitrophenyl acetate) and insoluble (olive oil emulsion) substrates. The condtions chosen for measuring lipase activity with both these substrates were a pH of 7.3 and temperature of 37 °C, as all the lipases tested showed high activties under these conditions. The specific activities of the wild type and mutants of Lipase 3 were determined using the soluble and emulsified substrates. Activities were much higher with emulsified substrate than with soluble substrate (by 800-fold for the wild type forms). On binding to a lipid-water interface an 'active' enzyme conformation is induced. For lipases with lids, such as Danisco's Lipase 3, structures of the inhibited enzyme reveal that the lid is 'open' and oxyanion hole residues are aligned. In aqueous solution, the 'closed' conformation is stabilised and so the proportion of activated enzyme is likely to be lower than in the presence of an interface, explaining the decreased activities with monomeric substrate.

The wild type lipase expressed in *Pichia pastoris* was found to be the most active on both substrate types. None of the 'activity' mutants displayed improved activities with the soluble or interfacial substrates as compared to the wild type lipase. Of these the T112D E114Q mutant showed the highest activity levels of these mutants with both substrate types (70 – 80 % of wild type activity). The activities of the tryptophan mutants (W116A and W116A I113W) were effected to a much greater degree with the olive oil substrate than with soluble *p*-NPA substrate, indicating an important role of Trp 116 for the action of Lipase 3 with emulsified triacylglycerol substrate. None of the 'glycosylation' mutants showed significantly increased activity over wild type. The double mutants, N59T N269Q and N59T N269T, had low activities with the olive oil emulsion substrate (approximately 50 % of the activity shown by the wild type enzyme). Apart from these, the specific activities of the 'glycosylation' mutants were in the same order as the wild type.

To further investigate the effects of the introduced mutations on the catalytic mechanism of Lipase 3, a kinetic analysis of the purified enzymes with interfacial (emulsified olive oil) substrate was carried out, and is discussed in the following chapter.

CHAPTER 7 Kinetic Analysis of Lipase 3 Variants Expressed in *Pichia pastoris*

7.1 Introduction

A kinetic analysis of Lipase 3 variants was carried out in order to investigate the effects of mutations on catalytic activity and interfacial behaviour. A study of steady state kinetics was used to obtain V_{max}, k_{cat} and Km constants of the purified enzymes. Activities were measured using the olive oil titration assay. The kinetic constants for wild type and mutant lipases with olive oil substrate were calculated from plots of initial rates against substrate concentration.

The *p*-NPA spectrophotometric assay that had been used to determine specific activities with soluble substrate (Chapter 6) did not provide results that were consistent enough to use for accurate determination of kinetic constants. The comparison of lipase activities with soluble and insoluble substrates (Chapter 6) could not therefore be augmented by a similar comparison of kinetic constants with these substrates. However, as lipase substrates tend to exist in emulsified form in physiological systems and, as in this case, in industrial applications (i.e. in dough), a kinetic study using only emulsified lipid substrate was considered adequate. The preference of Lipase 3 variants for this substrate was illustrated in Chapter 6. When specific activities with soluble *p*-NPA and insoluble olive oil substrates were compared, all lipases tested demonstrated considerably higher activities with emulsified olive oil substrate.

7.1.1 Steady-State Kinetics

In enzyme catalysed reactions the concentrations of enzyme bound intermediates are in a 'steady state' when they are being produced as rapidly as they are degraded. When an enzyme is mixed with an excess of substrate, the concentrations of these intermediates build up to their steady state levels during an initial 'pre-steady state' period and once reached the reaction rate changes relatively slowly with time. 'Initial rate' measurements are made during this steady state period over a short time interval so that products have not significantly accumulated and substrates have not been appreciably depleted (Fersht, 1985).

The initial rates of most enzyme reactions follow saturation kinetics with respect to the concentration of substrate. At sufficiently low levels of substrate the rate of catalysis is proportional to substrate concentration ([S]). As [S] increases the rate tends towards a limiting value, V_{max}. Velocity is maximal and independent of substrate concentration when the enzyme is saturated with substrate and the concentration of free enzyme is negligible. Thus, at high substrate concentrations, the initial rate is directly proportional to the total

enzyme concentration, $[E]_o$. The mathematical relationship between the initial rate of an enzyme-catalysed reaction (v) as a function of substrate concentration and total enzyme concentration ($[E]_o$), is expressed by the Michaelis-Menten equation:

$$v = \frac{[E]_o[S]k_{cat}}{Km + [S]} \qquad (7.1)$$

where:

$$V_{max} = k_{cat}[E]_o \qquad (7.2)$$

The substrate concentration at which v is equal to half the value of V_{max} is termed Km, the Michaelis constant. At low substrate concentrations (where [S] << Km), the Michaelis-Menten equation becomes:

$$v = \frac{k_{cat}}{Km}[E]_o[S] \qquad (7.3)$$

or,

$$v = \frac{V_{max}[S]}{Km} \qquad (7.4)$$

Thus, when substrate concentration is very low, the initial rate is proportional to [S]. From equation 7.3 it can be seen that k_{cat}/Km is an apparent second-order rate constant. It is only a true rate constant in the extreme case in which the rate-determining step is the combination of enzyme and substrate. At low substrate concentration, the enzyme is largely unbound and the concentration of free enzyme approximately equals the total enzyme concentration ($[E] \approx [E]_o$), the reaction rate is given by:

$$v = \frac{k_{cat}}{Km}[E][S] \qquad (7.5)$$

This apparent constant relates the reaction rate to the concentration of free, rather than total, enzyme and expressed in terms of free enzyme this equation is valid for all substrate concentrations. It is also referred to as the specificity constant. The value of k_{cat}/Km cannot be greater than that of any second-order rate constant on the forward reaction pathway and so sets a lower limit on the rate constant for the association of enzyme and substrate. Because an enzyme and a substrate cannot combine more rapidly than diffusion permits, there is an upper limit on enzyme catalysis; that is the maximum rate of diffusion of substrate to the enzyme (approximately 10^9 M^{-1} s^{-1}). Enzymes with specificity constants of this order have evolved to maximum kinetic efficiency.

The basic scheme proposed by Michaelis and Menten for an enzyme-catalysed reaction is: -

$$E + S \underset{}{\overset{Ks}{\rightleftharpoons}} ES \xrightarrow{k_{cat}} E + P \qquad (7.6)$$

The formation of ES (the Michaelis complex), in which enzyme and substrate are held together by physical forces, is rapid and reversible with no chemical changes taking place. The chemical processes then follow, with a first-order rate constant k_{cat} (the turnover number). The Michaelis-Menten mechanism assumes that the enzyme-substrate complex is in equilibrium with the free enzyme and substrate. This is only true however, if in the following scheme, $k_2 << k_{-1}$:

$$E + S \underset{k_{-1}}{\overset{k_1}{\rightleftharpoons}} ES \xrightarrow{k_2} E + P \qquad (7.7)$$

When this is the case it can be shown that Km is equal to the dissociation constant of the Michaelis complex, Ks (Fersht, 1985). In general, k_2 is comparable to k_{-1} (the Briggs-Haldane mechanism) and:

$$Km = \frac{k_2 + k_{-1}}{k_1} \qquad (7.8)$$

The value of Km is therefore usually greater than or equal to Ks. It can be smaller than Ks however, if additional intermediates occur in significant amounts on the reaction pathway after formation of the initial Michaelis complex and with smaller dissociation constants. In all cases Km is the substrate concentration at which $v = V_{max}/2$. The Km is an apparent constant that may be treated as the overall dissociation constant of all enzyme-bound species. Similarly, k_{cat} is not necessarily the first-order rate constant for the chemical conversion of the ES complex to the EP complex. For reactions more complicated than the simple Michaelis-Menten mechanism, k_{cat} is a function of all the first-order rate constants. The k_{cat} (or turnover number) represents the maximum number of substrate molecules converted to products per active site per unit time.

7.1.2 Lipase Kinetics at the Interface

The interpretation of kinetic constants derived from steady state kinetics with interfacial substrate is not straightforward as the lipase reaction occurs on two-dimensional substrate and is preceded by adsorption of the enzyme to the hydrophobic surface, which may also involve a conformational change.

A simple model for lipolysis was proposed by Verger *et al* (1973) and consists of two successive equilibria (Figure 7.1). The first is the reversible penetration of the water-soluble enzyme (E) into an interface, where it has a different conformational state (E*) with

more efficient catalytic properties than the soluble enzyme. This is followed by a second equilibrium in which one molecule of penetrated enzyme (E*) binds a single substrate molecule (S) to give a Michaelis-Menten complex (E*S), characterised by the interfacial Michaelis-Menten constant Km* (defined as $(k_{-1} + k_{cat})/k_1$). The catalytic steps take place, regenerating the enzyme in the E* form and liberating the reaction products (P), according to the catalytic constant k_{cat}. In this model the lipase changes conformation concomitantly with, or after, adsorption to the lipid-water interface.

Figure 7.1 Proposed model for the action of a soluble enzyme at an interface. Key to symbols: - I: interfacial area, V: volume, E: enzyme, E*: penetrated enzyme, S: triacylglycerol substrate, P: product, k_p: penetration rate constant, k_d: desorption rate constant. (From Verger *et al.* 1973).

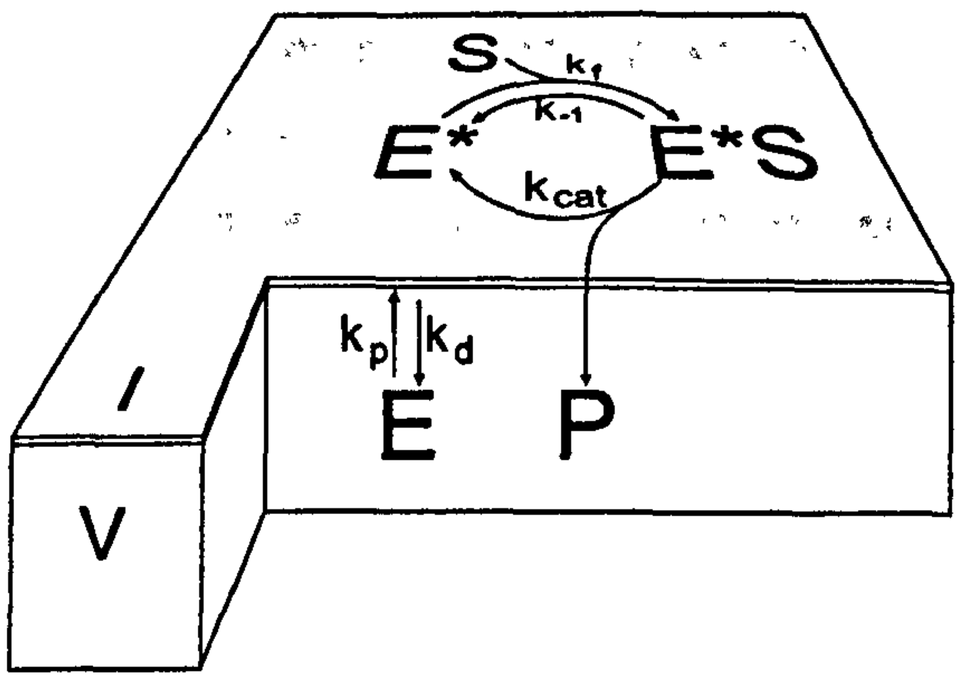

Recent models (described by Hult and Holmquist, 1997, Holmquist *et al.* 1994 and Martinelle and Hult, 1994) suggest that the two conformational states of lipases (open and closed) can exist in free equilibrium. In solution, the closed conformation is favoured. When an interface is introduced, the lipase adsorbs to the surface and the overall equilibrium changes to favour the open conformation as it is stabilised by the hydrophobic surrounding (low dielectric constant) at the interface (Figure 7.2).

Figure 7.2 A kinetic model for lipase catalysis. This model for lipolysis was proposed by Hult and Holmquist (1997). E, enzyme in bulk water (closed inactive form); E*, enzyme in bulk water (open active form); E_a enzyme adsorbed at the lipid interface (closed inactive form); E_a*, active enzyme adsorbed at the lipid interface (open active form); E_a*S, Michaelis-Menten complex, P;products.

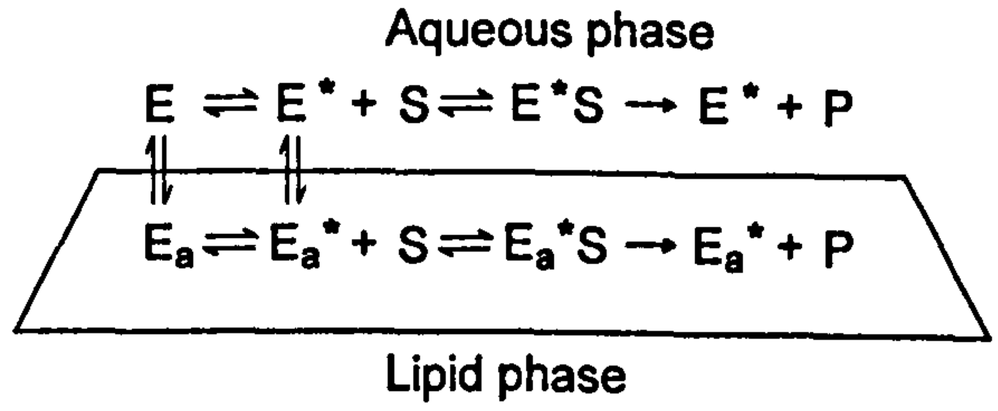

The implication made by the authors in this model is that lipase bound to the interface may have different conformations, with different specific activities that exist in equilibrium. In the model they describe, the lipase may adopt an active conformation once it has adsorbed to the interface (Hult and Holmquist, 1997, Holmquist *et al.* 1994).

7.1.2.1 Kinetic Constants

Overall V_{max} and Km values can be obtained from steady state kinetic measurements using emulsified substrate by measuring initial rates as a function of substrate concentration (Brockman, 1984, Verger *et al.* 1973). It is the amount of surface available to the enzyme that changes with bulk substrate concentration and saturation behaviour thus reflects the overall adsorption and catalytic processes. By increasing the amount of substrate (interfacial area) it is possible to reach a situation in which all the added enzyme is in the penetrated form (E* + E*S, in Figure 7.1) and catalytic rate is maximal (V_{max}). It should be noted however, that the effective substrate concentration (molecules per unit surface) of an emulsion cannot be changed. This means that an unknown fraction of E* is converted to E*S and so V_{max} and Km values measured under bulk conditions are only apparent values (Verger, 1973). For a more detailed kinetic analysis to determine the influence of individual rate constants involved in the mechanism of lipase catalysis, a study of transient kinetics from pre-steady state measurements should be carried out.

Km_{app}

For enzyme catalysed reactions occurring at an interface this constant is not necessarily equal to the interfacial Km*, as more than one equilibrium exists on the reaction pathway. The Km may primarily reflect the properties of enzyme adsorption to the interface and several Km_{app} values presented in the literature have been reported as interfacial affinity constants (Lookene *et al.* 1997, Hult and Holmquist, 1997, Holmquist *et al.* 1994, Brockman, 1984). It was demonstrated by Benzonana and Desnuelle (1965) that the quantity of interface as determined by the size of the emulsion droplets strongly influences the value of Km. When the rates of lipolysis using coarse and fine emulsions of a long-chain triacylglycerol were compared, the Michaelis constants were found to differ. However when substrate concentration was expressed as area/volume rather than as weight/volume, the Lineweaver-Burk plots coincided and a single Km value was obtained. They concluded that the Km_{app} defined the binding affinity between the enzyme and the interface.

7.1.2.2 Monolayer Conditions

An alternative method that has been used for kinetic analysis of lipases is the monolayer technique. By spreading lipid at an air-water interface, the kinetics of the surface reaction can be followed by continuously recording the decrease in area of the film with time. This method also allows the surface density of lipid (molecules per unit surface) to be changed continuously and it has been used to demonstrate a surface pressure (π) dependence of the enzymic reaction (Brockman, 1984). The monolayer and bulk conditions differ mainly by the respective values of I/V (where I is the total interfacial area and V the total volume). In the case of the monolayer method, this ratio is about 1 cm^{-1} while in bulk conditions it can be as high as 10^5 cm^{-1}, depending on the amount of substrate used. As a consequence, bulk conditions allow the adsorption of nearly all the enzyme at the interface, whereas with a monolayer the penetrated enzyme will represent only a small fraction of the total protein added (Verger, 1980).

The model for lipolysis described in Figure 7.1 was originally investigated using a monolayer technique where surface pressure was kept constant during hydrolysis (Verger *et al.* 1973). By this technique, it is possible to measure pre- steady-state kinetics. After injection of the enzyme, the velocity increases with time and approaches an asymptotic limit. Two parameters are used to describe these kinetics: the slope of the asymptote (velocity, v) and the lag time τ, which is the sum of two independent induction times, τ_1 and τ_2 reflecting the first and second equilibrium of the model described in Figure 7.1. τ_1 describes the establishment of the penetration-desorption equilibrium and τ_2 the establishment of the interfacial Michaelis-Menten equilibrium. From their results they concluded that the limiting step was in the penetration ($\tau_1 >> \tau_2$). In other words, the establishment of the equilibrium E ↔ E* was the rate-limiting step in the overall enzymatic process.

In fact, it has been established that the lipid/water 'interfacial quality', in terms of the tension at the interface, is a decisive parameter when working with lipolytic enzymes (Verger, 1980, Ferrato *et al.* 1997). As yet undefined, it is thought to contain contributions from molecular and charge density, molecular orientation and hydration forces. The determination of an interfacial Km value therefore requires that the 'quality' of the lipid-water interface remains constant during the experiment and valid comparisons can be made only between data obtained under strictly identical conditions, preferably in the same laboratory (Ferrato *et al.* 1997).

7.2 Results

7.2.1 Lipase Activity at the Interface

To compare the reactions of wild type and mutant lipases toward a lipid interface, the initial reaction rates of a fixed amount of lipase were measured over a range of interfacial areas using emulsified olive oil substrate. As the reaction of lipase occurs at the interface, substrate concentration was expressed in surface concentration units ($m^2\ l^{-1}$), (which is proportional to the molar concentration). Surface areas were calculated from the emulsion particle sizes, which were measured by laser diffraction using a Mastersizer for each emulsion. Particle sizes were determined from duplicate or triplicate samples taken from each prepared emulsion. The average mean particle diameter (from measurements taken for a total of 56 emulsions) was 0.90 μm ± 0.18. After re-location to the University of Nottingham a different sonicator was used, resulting in emulsions with a smaller particle size. The average particle diameter of emulsions prepared here was 0.43 μm ± 0.05 (from measurements taken for a total of 80 emulsions). However, it should be noted that all kinetic constants presented in this chapter (Chapter 7) were determined before re-location. The effect of differences in emulsion particle sizes on lipase kinetic behaviour is discussed in Chapter 8.

Typical graphs for initial rate measurements are shown in Figure 7.3. From the legends to these graphs it can be seen that substrate surface area is not directly proportional to olive oil concentration (in $g\ l^{-1}$). This is due to variation in particle size between emulsions, and is illustrated in Table 7.1, which shows the particle sizes and Specific Surface Areas (S.S.A.) for these emulsions. When substrate concentration increases from 6.7 and 11.2 $g\ l^{-1}$ (i.e. with a ratio of 3:5), the substrate surface area does not increase a proportional amount (the increase here is from 111.5 to 144.2 $m^2\ l^{-1}$; i.e. approximately with a ratio of 4:5). In this case, it is the smaller than average particle size of the 6.7 $g\ l^{-1}$ emulsion (compared to those of the remaining emulsions) that results in a relatively larger total surface area. These results emphasise the need to measure the average particle sizes of each emulsion, so that substrate surface areas can be accurately determined.

Specific activities were calculated from the rates of addition of 20 mM NaOH to the reaction mixture when a steady state had been reached (rates were usually measured between 2.5 and 5 minutes from the addition of enzyme). For the reaction progress curves shown in Figure 7.3 the approximate amounts of lipid hydrolysed over the course of these reactions, which were monitored for 5 minutes, were calculated and are noted in the legend.

(These calculations were made presuming a molecular weight for the lipid substrate to be that of pure triolein (885.4) and also taking into account that the release of 3 mmol of fatty acids is equivalent to the hydrolysis of 1 mmol of olive oil.) For starting substrate concentrations of (a) 1.7 g l^{-1} (b) 3.4 g l^{-1} (c) 6.7 g l^{-1} and (d) 11.2 g l^{-1}, the approximate amounts of lipid hydrolysed were (a) 0.06 g l^{-1} (b) 0.17 g l^{-1} (c) 0.66 g l^{-1} and (d) 0.8 g l^{-1}, respectively. As the amount of lipid hydrolysed in each of these reactions is less than ten percent of the starting amount of lipid used, substrate depletion should not significantly effect the rate measurements made over this time, which can therefore be taken to represent 'initial rates'. It was also noted that no visible changes to the prepared emulsions occurred over the course of the experiment. All the emulsions used were milky in appearance both before and after rate measurements were made. Although it is not certain that this 5-minute 'titration' assay of lipase activity does not result in changes to the lipid-interfacial structure of the substrate (which could effect rate measurements), no changes to the emulsion structure were indicated by the appearance of the emulsion in the reaction mixture itself.

Table 7.1 Determination of Substrate Surface Areas for Emulsions used in Lipase Activity Measurements shown in Figure 7.3. The olive oil concentrations used in the reaction rate measurements represented in Figure 7.3 are shown (column 1). A Mastersizer *S* was used to determine the average particle size in these emulsions (column 2). Duplicate samples were subjected to particle size measurement and average values plus the standard deviation are shown. The Mastersizer software also calculates Specific Surface Area (S.S.A) in $m^2 g^{-1}$. From this, substrate surface area in terms of volume ($m^2 l^{-1}$) could be derived by multiplying olive oil concentration (g l^{-1}) and S.S.A. ($m^2 g^{-1}$).

Olive oil concentration, g l^{-1}	Mean diameter, µm	± *stdevp*	Specific Surface Area, $m^2 g^{-1}$	± *stdevp*	Surface Area, $m^2 l^{-1}$	± *stdevp*
1.7	0.46	± *0.03*	13.03	± *0.81*	21.9	± *0.7*
3.4	0.43	± *0.005*	14.02	± *0.14*	47.2	± *0.2*
6.7	0.37	± *0.015*	16.59	± *0.78*	111.5	± *2.6*
11.2	0.47	± *0.015*	12.87	± *0.35*	144.2	± *1.9*

Figure 7.3 Typical graphs for measurement of lipase initial rates with emulsified olive oil using a pH-stat controller. Traces show the volume of 20 mM NaOH added over five minutes from the addition of purified wild type lipase (3.61×10^{-6} g) expressed in *Pichia pastoris* with (a) 22 $m^2 l^{-1}$ (1.7 g l^{-1}) (b) 47 $m^2 l^{-1}$ (3.4 g l^{-1}) (c) 112 $m^2 l^{-1}$ (6.7 g l^{-1}) and (d) 144 $m^2 l^{-1}$ (11.2 g l^{-1}) olive oil emulsion. Rates were taken when pH was steady at 7.3, usually between 2.5 and 5 minutes. The approximate amounts of lipid hydrolysed over the course of these reactions (5 minutes) are (a) 0.06 g l^{-1} (b) 0.17 g l^{-1} (c) 0.66 g l^{-1} and (d) 0.8 g l^{-1} respectively.

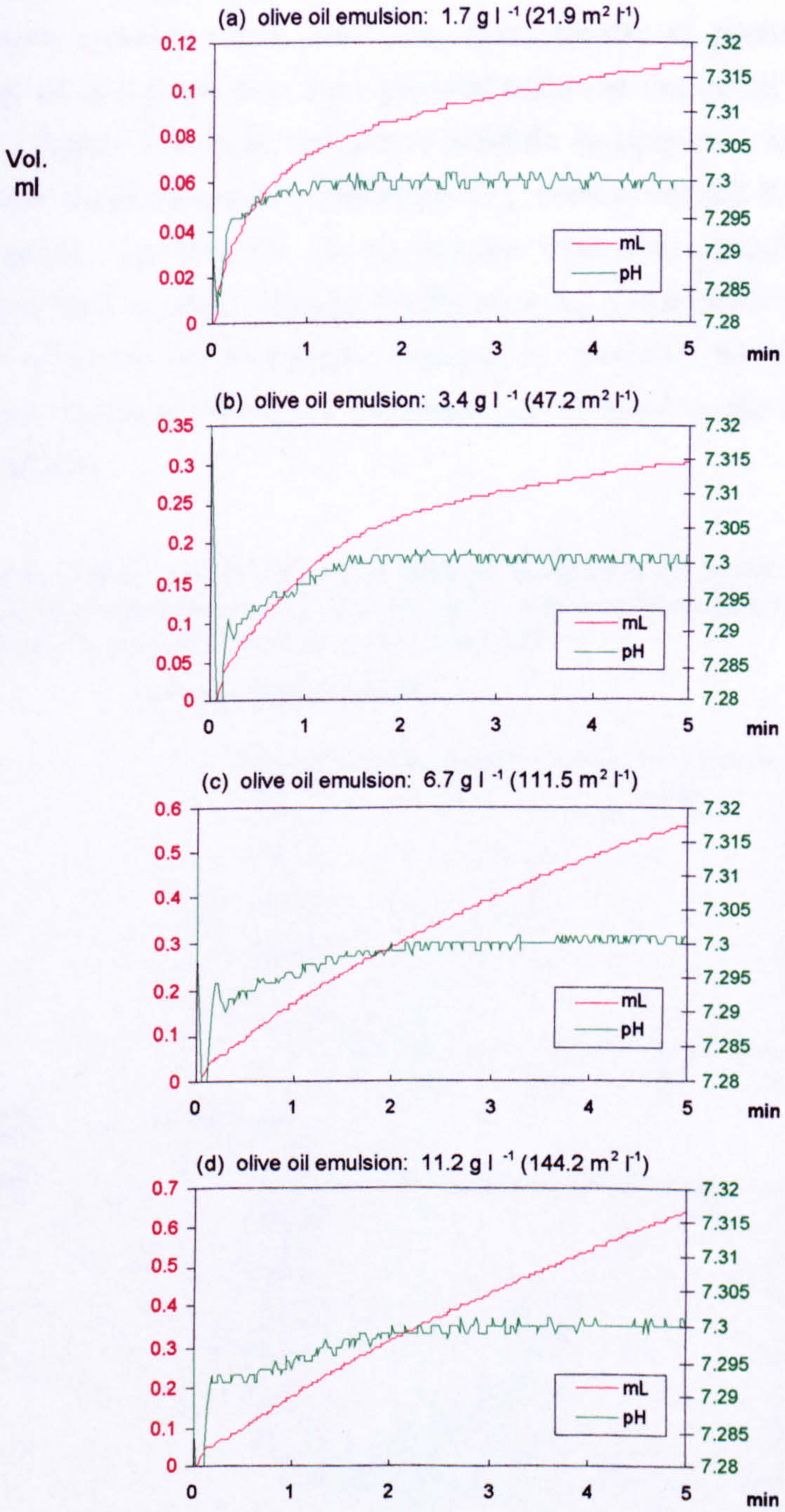

The effect of limiting substrate on the initial rates (v) of mutant and wild type lipases are illustrated in Figure 7.4, as plots of v against substrate concentration expressed in units of surface area. This data was also analysed using the Lineweaver-Burk plot, an example of which is shown in Figure 7.5 (for wild type lipase) and is typical of those seen for all the lipase variants. A plot of $1/v$ against 1/[S] usually gives a straight line with an intercept on the y-axis of $1/V_{max}$ and an intercept on the x-axis of –1/Km. However, for these enzymes, a concave upwards curve was seen, characteristic of positive co-operativity. The non-linearity of this graph plus the sigmoidal nature of the initial rate vs. substrate surface area graphs (Figure 7.4) both indicate a possible co-operative mechanism. The Lineweaver-Burk plot could be used to determine V_{max} values, but not Km values (as the x-axis is not intercepted). Incidentally, for an enzyme with a co-operative mechanism the Michaelis constant (Km) is often replaced by the term $S_{0.5}$. Just as for the classical Km, this is equal to the substrate concentration required to produce 50 % saturation of the enzyme. However, the term 'Km_{app}' is used here and is equal to the surface area when v is at half maximal rate.

Figure 7.4 Kinetic analysis of lipase variants using olive oil emulsion substrate. Initial rates (v) were measured using a pH-stat titrator. Surface areas were calculated from emulsion particle sizes measured by laser diffraction using a Mastersizer χ. *(U: mmol min^{-1}).*

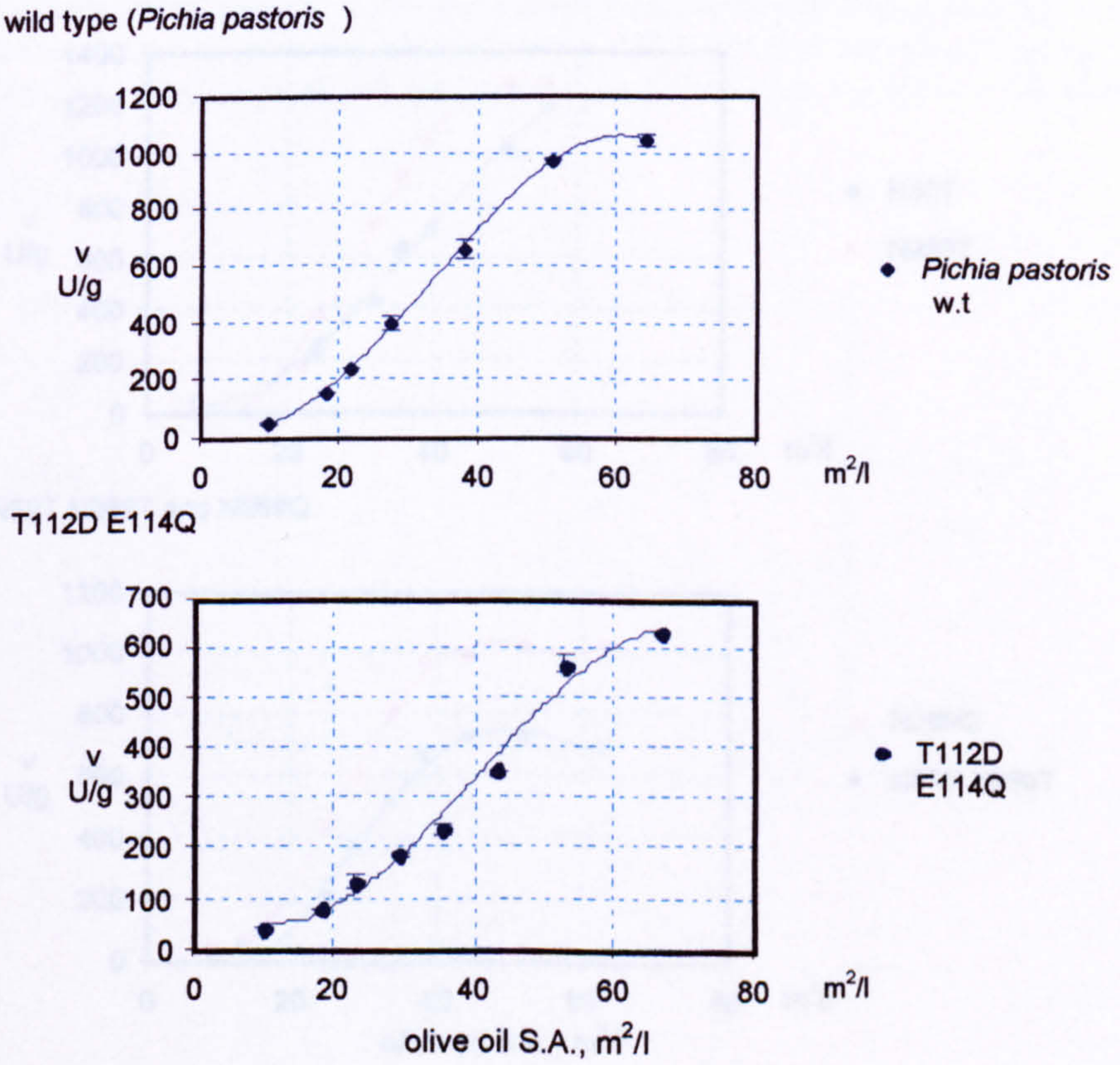

H225D

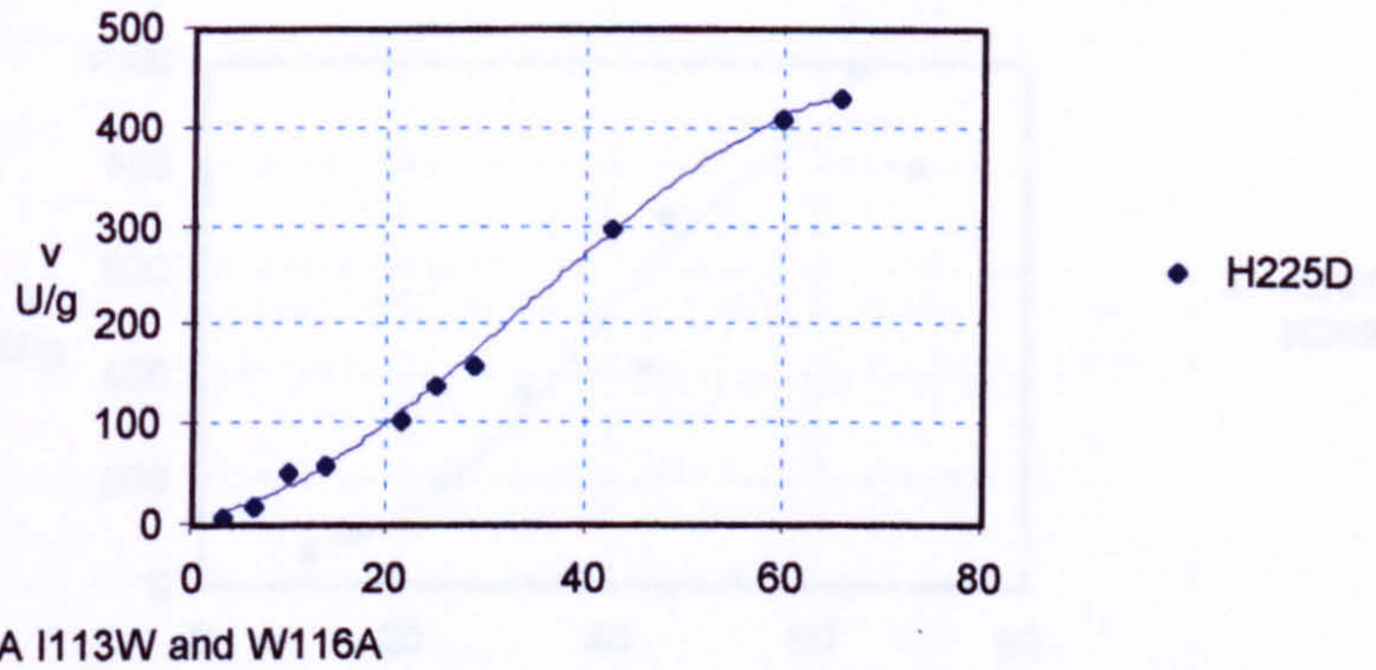

W116A I113W and W116A

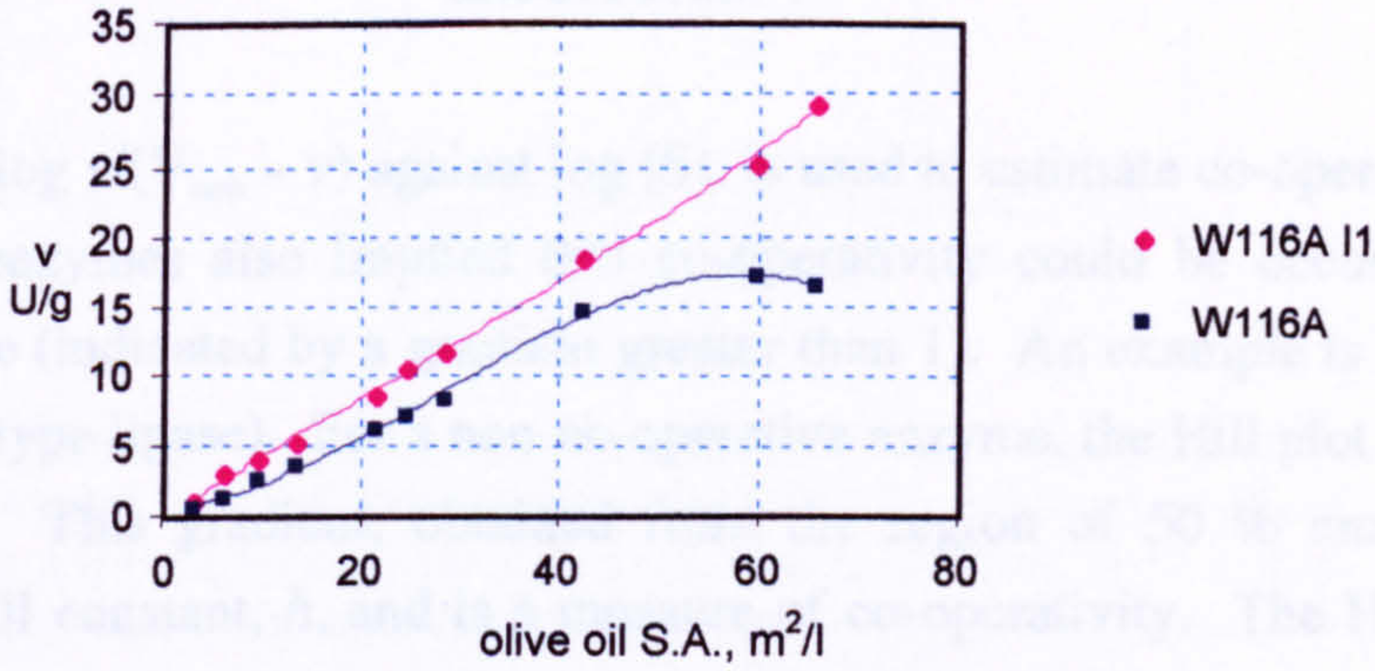

'Glycosylation'

mutants N59T and N269T

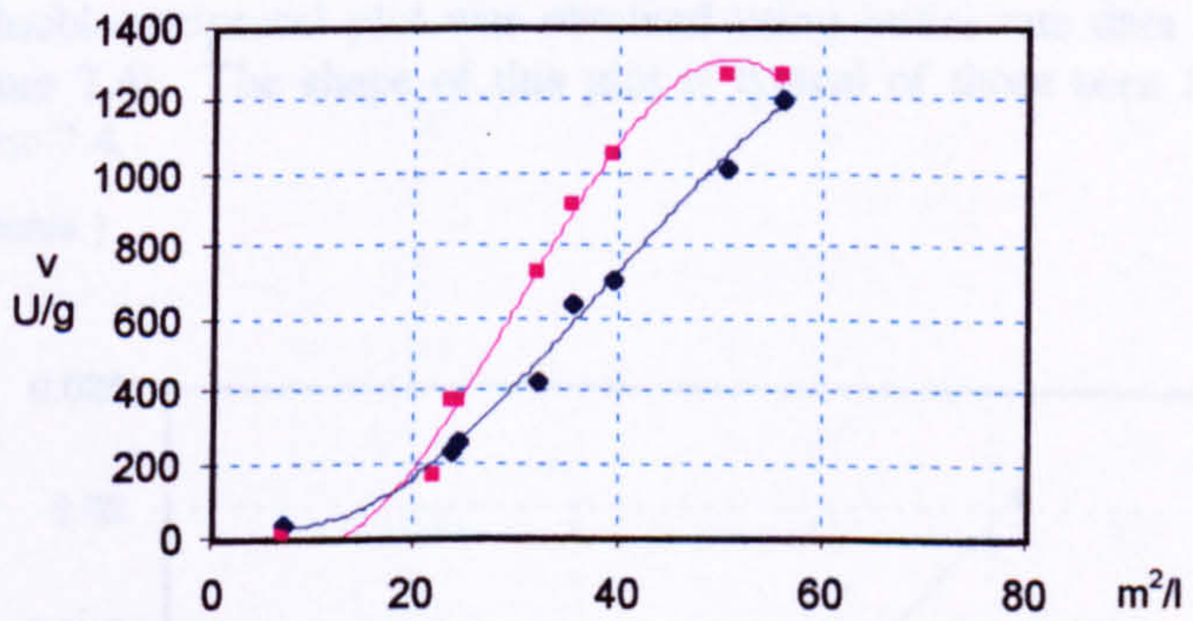

N59T N269T and N269Q

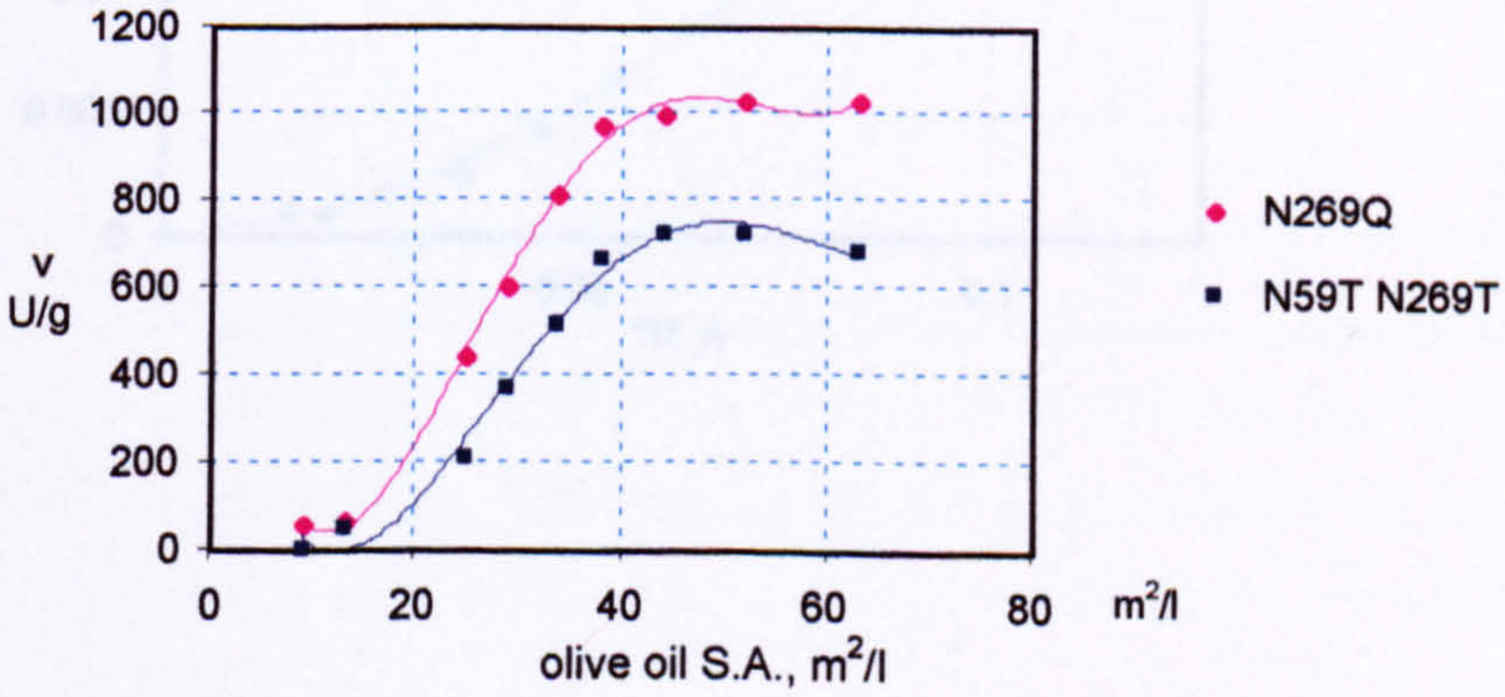

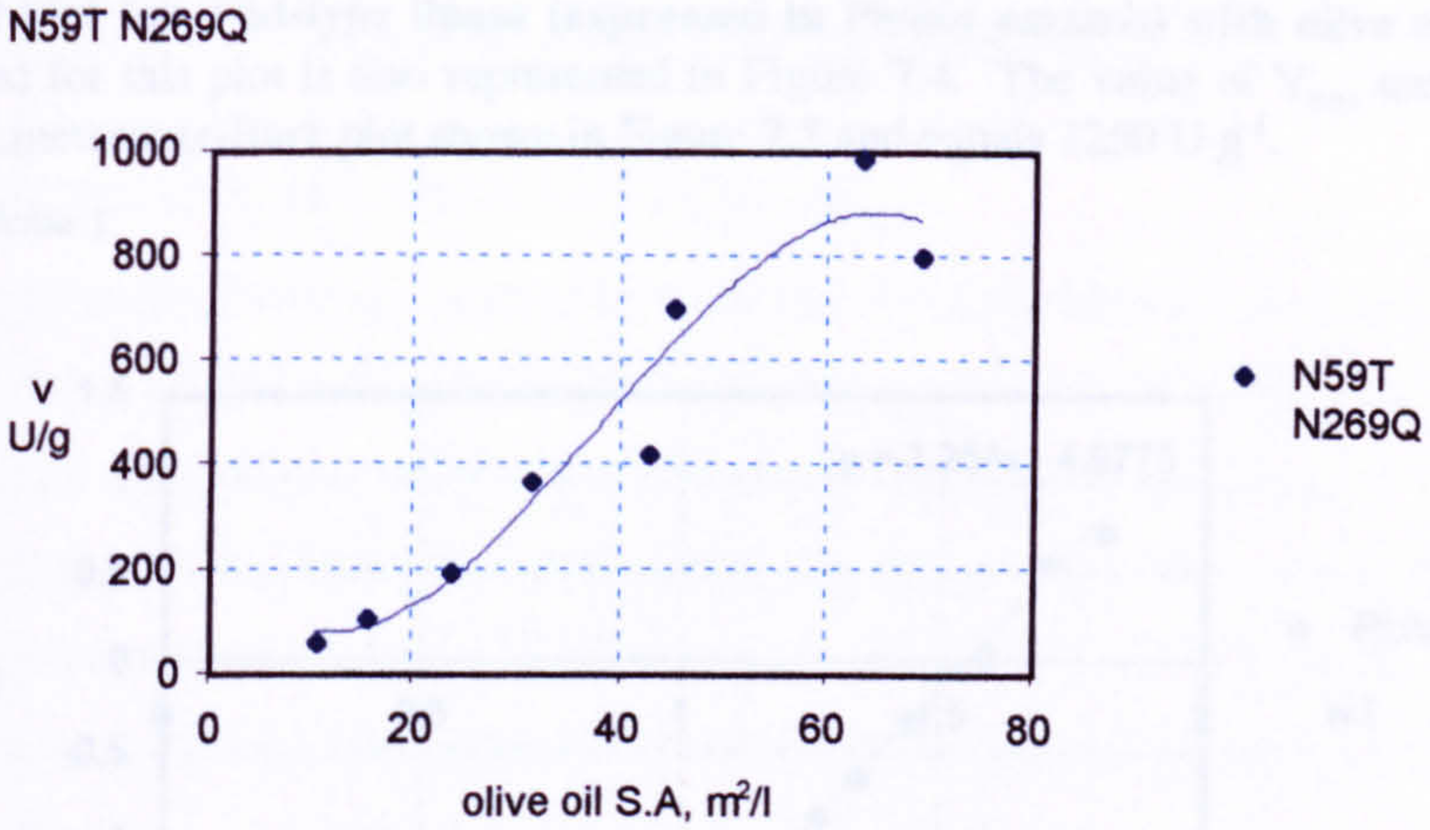

The Hill plot, of log $v/(V_{max} - v)$ against log [S], is used to estimate co-operativity. The Hill plots for these enzymes also implied that co-operativity could be occurring and that it would be positive (indicated by a gradient greater than 1). An example is shown in Figure 7.6 (for the wild type lipase). For a non-co-operative enzyme, the Hill plot is linear and has a gradient of 1. This gradient, obtained from the region of 50 % enzyme saturation, represents the Hill constant, *h*, and is a measure of co-operativity. The Hill constants for each of the lipase variants, obtained from these plots, are also presented in Table 7.2.

Figure 7.5 A Lineweaver–Burk plot for wild-type Lipase 3 (expressed in *Pichia pastoris*) with olive oil substrate. This double-reciprocal plot was obtained using initial rate data for the wild type lipase (also represented in Figure 7.4). The shape of this plot is typical of those seen for each of the lipase variants represented in Figure 7.4.

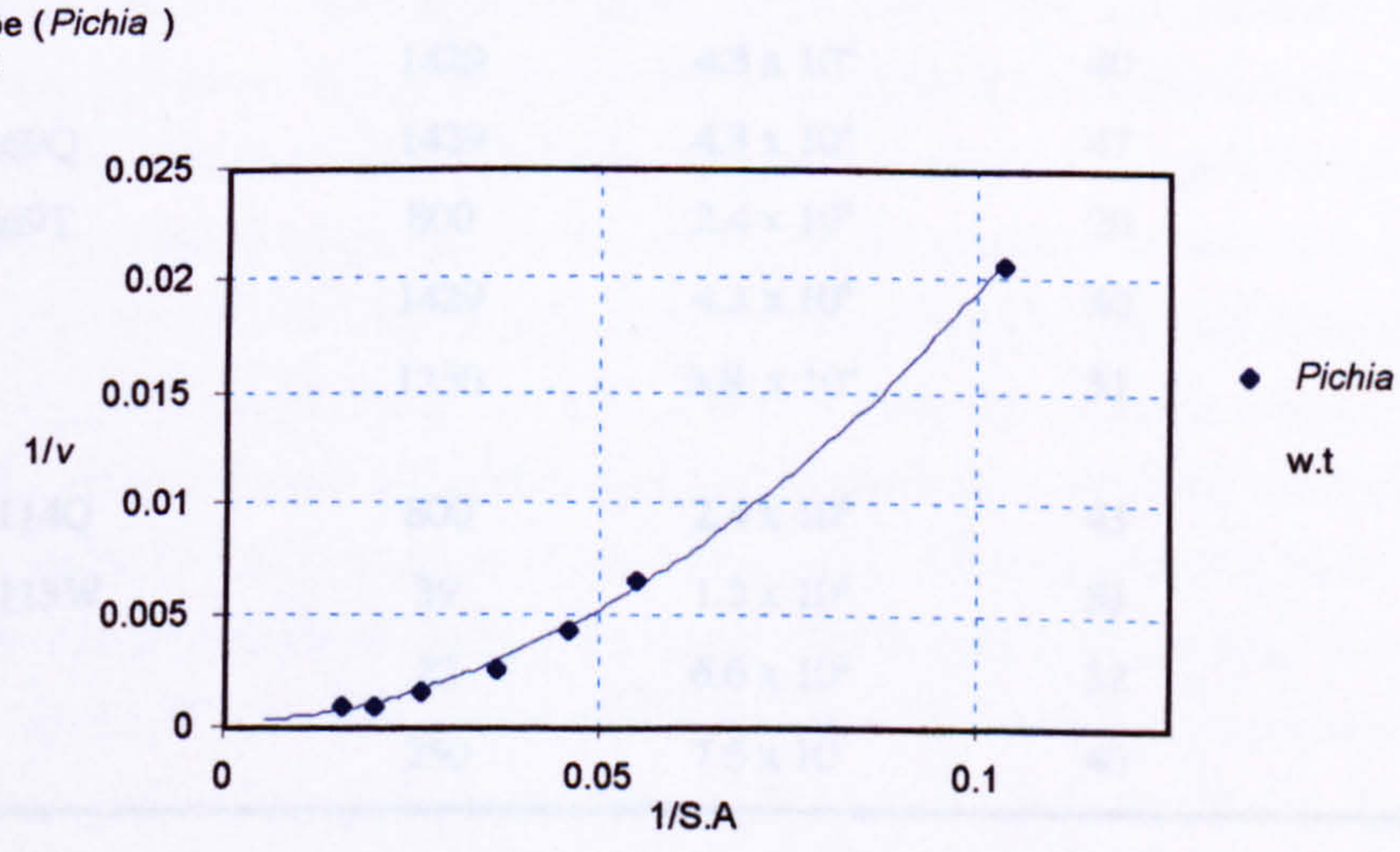

Figure 7.6 A Hill plot for wild-type lipase (expressed in *Pichia pastoris)* with olive oil substrate. The initial rate data used for this plot is also represented in Figure 7.4. The value of V_{max} used in this plot was obtained from the Lineweaver-Burk plot shown in Figure 7.5 and equals 1250 U g^{-1}.

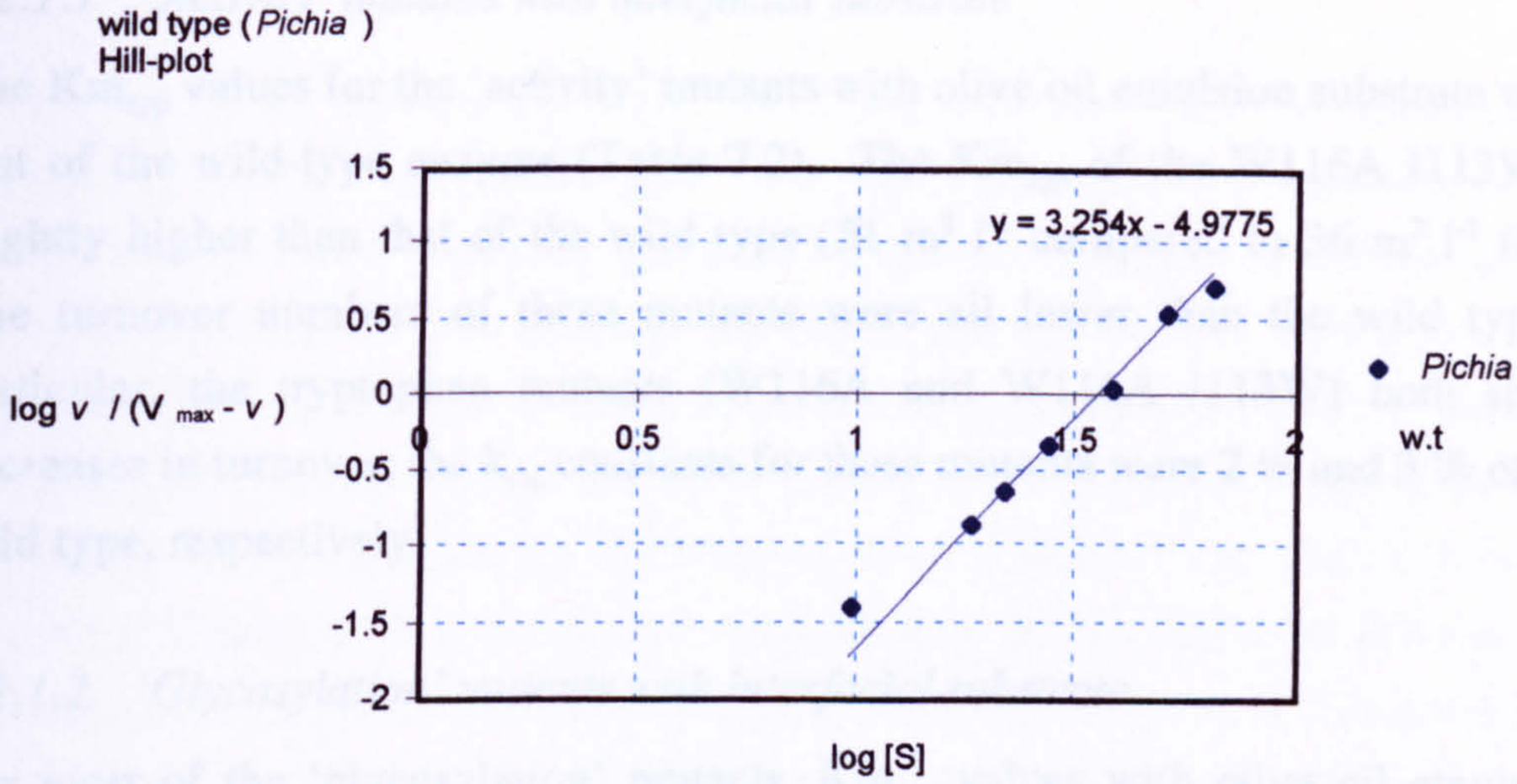

Table 7.2 Kinetic constants for wild type and mutant lipases with emulsified olive oil substrate. Constants were determined from data presented in Figure 7.4 using Lineweaver-Burk and Hill plots. Rates were measured using a pH-stat titrator over a range of limiting substrate surface areas (determined using a Mastersizer χ). The k_{cat} values were calculated from the equation $V_{max} = k_{cat}[E]_0$. *(U: mmol min^{-1}).*

Lipase	V_{max} U g^{-1}	k_{cat} min^{-1}	Km_{app} m^2 l^{-1}	Hill coefficient
Wild-type	1250	3.8×10^4	36	3
N59T	1429	4.3×10^4	40	3
N59T N269Q	1429	4.3×10^4	47	3
N59T N269T	800	2.4×10^4	28	4
N269T	1429	4.3×10^4	30	4
N269Q	1250	3.8×10^4	31	3
T112D E114Q	800	2.4×10^4	43	3
W116A I113W	39	1.2×10^3	51	2
W116A	22	6.6×10^2	32	2
H225D	250	7.5×10^3	40	2

To briefly summarise these results (with olive oil emulsion substrate): -

7.2.1.1 'Activity' mutants with interfacial substrate

The Km_{app} values for the 'activity' mutants with olive oil emulsion substrate were similar to that of the wild-type enzyme (Table 7.2). The Km_{app} of the W116A I113W mutant was slightly higher than that of the wild type (51 m^2 l^{-1} compared to 36 m^2 l^{-1} for wild type). The turnover numbers of these mutants were all lower than the wild type lipase. In particular, the tryptophan mutants (W116A and W116A I113W) both showed drastic decreases in turnover; the k_{cat} constants for these mutants were 2 % and 3 % of the value for wild type, respectively.

7.2.1.2 'Glycosylation' mutants with interfacial substrate

For most of the 'glycosylation' mutants, Km_{app} values with olive oil emulsion substrate were similar to the wild-type value (36 m^2 l^{-1}) (Table 7.2). The N59T N269Q mutant had a slightly higher Km_{app} value. For the N59T N269T this value was actually slightly lower than for the wild type enzyme (28 m^2 l^{-1}). This mutant (N59T N269T) however, also showed a lower rate of catalytic turnover (k_{cat}) than wild type. The other 'glycosylation' mutants had k_{cat} values that were equal to, or above that of the wild type (the values of V_{max} for N59T, N59T N269Q and N269T were 114 % the value of the wild type enzyme).

7.3 Discussion

A problem with the olive-oil-emulsion assay used here is that the different steps occurring at the substrate interface cannot be separately investigated, as the concentration of olive oil at the interface cannot be varied. Once the lipase has adopted an open active conformation, the efficiency of catalysis depends on the ability of the enzyme to extract substrate from the lipid phase into the active site (Km*) and to subsequently convert substrate to product (V_{max}). The V_{max} measured using this assay, whilst only an apparent constant, is thought to predominantly reflect the catalytic turnover, as the saturation kinetics observed imply that a situation is approached in which all of the enzyme is in the penetrated form. However, the apparent Km value measured using this assay technique may or may not represent the Michaelis constant, Km*. The absence of a lag phase in initial rate measurements (Figure 7.3) may be an indication that penetration of the interface is not a rate limiting step, in which case the Km_{app} could be taken to represent Km*. Alternatively, the Km_{app} could be a measure of enzyme affinity for the interface itself. The interpretation of this constant is further complicated by the observation of sigmoidal plots of initial rates against substrate

concentration (or interfacial surface area). These imply that some sort of co-operativity is occurring and is discussed later in this section.

Of all the lipase variants expressed in *Pichia pastoris*, none demonstrated significantly improved activity over wild type. For the 'glycosylation' mutants, activities were comparable to that of the wild type. As these were designed to prevent glycosylation of Lipase 3 occurring on over-expression, without altering the wild type activity level, protein engineering of Lipase 3 in this case appeared to be successful. For the 'activity' mutants, the mutations introduced did not have the effects on enzyme action predicted from the homology model of Lipase 3. For some of these mutants, large decreases in activity were observed, implying that the altered residues may have significant roles in the catalytic mechanism of Lipase 3. In these cases, the particular stages of the reaction mechanism in which they appear to be involved have been assigned, according to the values of the kinetic constants determined in this study and also from published results for other similar fungal lipases.

7.3.1 'Activity' mutants

7.3.1.1 T112D E114Q

The T112D E114Q mutant of Lipase 3 was designed to stabilise the 'open' conformation of Lipase 3 by replacing threonine 112 with an aspartate residue (T112D) predicted to interact favourably with the positive side-chain of arginine 108 in the 'open' enzyme. The mutant was also designed with a neutral glutamine residue in place of a nearby negative glutamate (E114Q) to avoid any repulsive interactions that may occur between these two lid residues.

By pushing the thermodynamic equilibrium between the two conformational states in favour of the 'open' state, the activity of Lipase 3 may be expected to improve by increasing the rate of enzyme adsorption to the interface. A decrease in the Km_{app} with olive oil emulsion substrate would be expected if this is the rate-limiting step. With the emulsified olive oil substrate a slight increase in Km_{app} over that of wild type was observed, and the value of V_{max} was 64 % that of the wild lipase and so was still fairly high.

Both mutated residues are in the lid of the enzyme. Although no specific role has been assigned to the Thr 112 (or equivalent) residue in related fungal lipases, a role has been postulated for Glu 114 (Glu 87 in the mature enzyme). Many investigations, involving molecular modelling and site-directed-mutagenesis have been carried out to establish the

role of this residue in lipase action (Martinelle *et al.* 1996, Holmquist *et al.* 1994, Peters *et al.* 1997). Glu 87 is present in the *Humicola lanuginosa* lipase (*Hl*L) where it stabilises the 'open' lid by electrostatic interactions with the cortex of the protein. In *Rhizomucor miehei* and *Rhizomucor delemar* fungal lipases an arginine residue is present in the equivalent position (Arg 86) and in the 'open' conformation is believed to interact with a surface aspartate residue (Asp 61). Mutation of *Hl*L Glu 87 to alanine resulted in approximately one-third the activity of the wild type enzyme toward triacylglycerol substrate (Martinelle *et al.* 1996). In the inhibited crystal structure, the side chain of Glu 87 points out into the solvent, however, when adsorbed at a lipid-water interface it encounters a hydrophobic environment and electrostatic interactions between the carboxyl group of Glu 87 and the surface of the protein would be more energetically favourable. The change of Glu to Ala may prevent this interaction and so alter the lid position. The lid conformation is important for activity as it interacts with the substrate and the complete oxyanion hole is created as it 'opens'.

The major effect of the T112D and E114Q mutations of Lipase 3 was to increase the value of Km_{app} indicating a possible decrease in affinity for aggregated substrate. Mutagenesis of Glu 87 in *Hl*L (which shares a high sequence homology with Lipase 3) demonstrated that this residue is important in attaining the 'open' conformation required for activity (Martinelle *et al.* 1996, Holmquist *et al.* 1994). This conformational change also results in the correct arrangement of residues that make up the oxyanion hole in the lipase reaction mechanism (Scheme 2 in Chapter 1). Therefore alteration to this conformation could adversely affect substrate binding and lipase activity. The decrease in activity and binding affinity seen for the T112D E114Q Lipase 3 mutant is therefore most likely due to the alteration of lid residues that are involved in maintaining the correct 'open' enzyme conformation for substrate binding and efficient catalysis. Mutation of the Glu 114 residue (or Glu 87 in the mature enzyme) in particular is likely to adversely effect catalysis in this way.

7.3.1.2 W116A and W116A I113W

The replacement of tryptophan 116 by the smaller alanine residue was to destabilise the 'closed' lid in the W116A single mutant. From the homology model of Lipase 3 this large hydrophobic residue appears to lie over the active site in the 'closed' conformation and is exposed to the solvent in the 'open' enzyme. Isoleucine 113 was changed to tryptophan in the design of a double mutant. This lid residue is also exposed to the solvent in the 'open' structure. The design of a double mutant was to compensate for the absence of

hydrophobic interactions that may have occurred between the Trp 116 residue and the interface, or, with the substrate molecule itself.

The activity of these mutants would be expected to improve by pushing the thermodynamic equilibrium between the two conformational states of Lipase 3 in favour of the 'open' state. The Km_{app} with emulsified substrate may be lowered by increasing the rate of adsorption to the interface.

The tryptophan mutants (W116A and W116A I113W) showed decreased activity with olive oil substrate, indicated by V_{max}, and k_{cat} values, and also demonstrated by specific activity measurements (Chapter 6). The drop in activity with olive oil was pronounced, and k_{cat} values were approximately 2 % of that for the wild type enzyme. The Km_{app} of Lipase 3 with emulsified substrate was not affected by mutation of tryptophan 116 alone. However, the Km_{app} of the W116A I113W mutant was slightly higher than that of the wild type.

In the *Humicola lanuginosa* lipase a tryptophan residue is present in the equivalent position (Trp 89). Site-directed mutagenesis of this residue has been used to demonstrate a role in forming the Michaelis complex, particularly in binding and positioning the scissile acyl chain at the active site (Holmquist *et al*, 1994, Martinelle *et al*, 1996). With emulsified tributyrin substrate the Km_{app} (interpreted as the binding affinity for the interface) for all the mutants generated, was unaffected. With a stock emulsion of 15.6 % tributyrin in Triton DF-16 (providing an excess of emulsion surface) the Km was increased only for a Trp 89 Glu (glutamate) mutant. Replacement with phenylalanine, leucine or glycine residues did not effect this Km, which was reported as representing the Km for catalysis at the interface, i.e. Km* (Holmquist *et al.* 1994). All of these mutants had much lower specific activities than the wild type. It was concluded that Trp 89 in *Hl*L plays a role in the catalytic steps after adsorption to the interface has occurred. The size and/or hydrophobicity of the residue in this position seemed to be important for high enzyme activity. When replaced by glutamate, a negative residue, activity dropped to 1 – 4 % of wild type. It was thought that the glutamate residue may effect electrostatic stabilisation of the lid position, resulting in an 'open' conformation that was not optimal for catalysis, or, that this charged residue may prevent penetration of the enzyme into the lipid phase.

In a separate study, the effect on activity was shown to be substrate dependent (Martinelle *et al.* 1996). The mutants generated had altered chain length specificity with higher relative activity towards triacetin (C_2 acyl chain) and trioctanoin (C_8) substrates compared with

tributyrin (C_4). With the short acetyl acyl chain, Trp 89 may not be able to sandwich the substrate into the active site crevice. As trioctanoin (C_8) binds such a large area, the interaction with tryptophan is less significant and activity is 4-fold less affected by a Trp 89 Gly mutant than toward C_4 substrate. Mutation of Trp 89 resulted in an exclusive effect on the acylation reaction rate, suggesting that Trp 89 is important in the process of binding the substrate acyl chain into the active site and positioning it for catalysis. As Km constants were generally unaffected, it was concluded that Trp 89 influences the binding of substrates into the active site in a qualitative, rather than a quantitative way.

In the lipase of *Rhizopus oryzae* an alanine residue is present in the equivalent position (Ala 89). Mutation of this residue to tryptophan resulted in a drop in activity to levels of 20 – 30 % that of wild type (Martinelle *et al.* 1996) implying that this enzyme has evolved to be efficient without the presence of the lid tryptophan. However, another study of this mutant (Beer *et al.* 1996) found that although the overall activity with triolein dropped to 56 % that of wild type, the Km (presumed to be Km*, as no lag phase was observed) for triolein was halved. Although the geometry for the formation of a tetrahedral intermediate is less favourable than for the wild type (resulting in a decreased k_{cat}), the introduction of a large hydrophobic group increased the affinity for triolein in formation of the Michaelis complexes.

The Km_{app} value of Lipase 3 was relatively unaffected by mutation of Trp 116. The most significant effect seen for the tryptophan mutants of Lipase 3 was on the catalytic turnover (V_{max} and k_{cat}) with emulsified olive oil substrate. This is in agreement with the role reported for this residue in related fungal lipases, where it appears to be involved in catalysis, particularly in the binding and positioning of the scissile acyl chain at the active site, rather than interfacial interactions. The specific activities of these enzymes with *p*-NPA and olive oil emulsion (Chapter 6) also support this suggested role. Lipase 3 activity was most negatively effected with olive oil substrate (the tryptophan mutants demonstrated approximately 2 % of the wild type activity with olive oil emulsion, compared to 40 - 60 % seen with *p*-NPA substrate).

7.3.1.3 H225D

The H225D single mutant was designed to increase the activity of Danisco Lipase 3 by stabilisation of the transition-state to increase k_{cat}. Replacement of the positive Histidine (His) 225 residue with a negative aspartate residue was predicted to interact favourably with the positive lobe of the transition state dipole.

The H225D mutant lipase had very low activity with the olive oil substrate, as indicated by a five-fold decrease in turnover compared to wild type. The Km_{app} of the H225D mutant lipase with olive oil emulsion was however, approximately equal to that of the wild type.

No studies on this particular residue have been reported in the literature. As it is not in the vicinity of the active site or lid region, it may not be expected to play a significant role in catalysis. The mutant was designed to introduce long-range electrostatic interactions, minimising disruption of the local structure at the active site. The drastic effect on lipase activity implies that the positive charge of His 225 is necessary in this position for effective catalysis. Although it may not be involved in transition state stabilisation it could be important in maintaining the conformational structure of the active enzyme.

7.3.2 'Glycosylation' mutants

The 'glycosylation' mutants were designed to prevent N-glycosylation of Lipase 3 at Asn 59 and Asn 269 by changing these residues to either threonine or glutamine; N59T, N269T and N269Q single mutants and N59T N269T and N59T N269Q double mutants were designed.

For most of the 'glycosylation' mutants, Km_{app} values towards the olive oil interface were similar to the wild-type value. Exceptions were the N59T N269Q, which had a slightly higher Km_{app} value and the N59T N269T, which had a slightly lower Km_{app}. The N59T N269T lipase also had a lower turnover number than wild type with olive oil. The other 'glycosylation' mutants (N59T N269Q, N59T, N269T and N269Q) had turnover numbers that were very similar to the wild type value.

The loss of either or both N-glycosylation sites on Danisco Lipase 3 did not seem to affect catalysis on emulsified olive oil substrate significantly. The most significant difference was for the N59T N269T mutant, having a V_{max} value 64 % that of wild type. From the homology model structure of Lipase 3, the asparagine residues of the glycosylation sites are seen to point into the solvent and do not appear to influence the active site region. In view of this, a significant effect on activity levels would not be expected. Glycosylation may affect the lipase Km through the adsorption efficiency of the enzyme, depending on the glycosylation groups presented to the solvent or lipid.

Proteins expressed by *Pichia pastoris* are not usually hyper-glycosylated (Montesino *et al.* 1998, Invitrogen *Pichia* Expression Kit manual Version 1.5). Therefore, the effect of over-glycosylation on lipase activity will not be seen for the variants expressed using this system. However, the results of kinetic analysis demonstrate that when N-linked glycosylation of Lipase 3 is prevented by mutagenesis of these sites (Asn 59 and Asn 269), the activity of Lipase 3 is not adversely affected. That the glycosylation of these mutants had been prevented was indicated by the results of SDS-PAGE and MALDI-TOF mass spectrometry. These results also implied that the glycosylation of Lipase 3 from expression in *Pichia pastoris* was of the high mannose type, with approximately 7 – 11 mannose units (or other hexose groups) attached.

7.3.3 The sigmoidal relationship between initial rates and interfacial surface area

For all the lipase variants analysed with emulsified olive oil substrate, plots of initial rates, v, against substrate concentration (in $m^2 l^{-1}$) were sigmoidal, indicating co-operative binding of substrate molecules to enzyme. The general models used to explain enzyme co-operativity are discussed below (Creighton, 1993, Fersht, 1985 and Neet, 1995).

7.3.3.1 Co-operativity

Co-operativity, in general, is any process in which the initial event (such as ligand binding) affects subsequent similar events via communication through intra- or intermolecular protein interactions (Neet, 1995). Co-operativity in enzyme systems usually begins with the observation of non-Michaelis-Menten (non-hyperbolic) curves when ligand binding or initial-rates are plotted against substrate concentration and later develops into a mechanistic explanation for the particular enzyme. Both equilibrium (e.g. site-site models, oligomer association) and kinetic (e.g. slow transition) mechanisms can give sigmoidal velocity vs. [S] plots. Generally, sigmoidal curves are characteristic of co-operative binding of ligands to proteins that have multiple binding sites. The increase (or decrease) in affinity with increasing saturation is due to the sites interacting, so that binding at one site causes an increase (or decrease) in affinity at another. Two ligand molecules that interact in this way may be identical (homotropic interactions) or may differ (heterotropic interactions).

The Hill Plot

The Hill Plot can be used to measure co-operativity. For positive co-operativity the slope in the middle of the curve, equal to the Hill coefficient, gives a quantitative measure of the degree of co-operativity. It corresponds to the hypothetical number of ligand molecules that would have to be bound fully co-operatively, in an all-or-none fashion, to give such a

slope. In this hypothetical case, only empty and fully occupied protein molecules are present and the Hill equation treats the data according to the following equilibrium:

$$E + nS \rightleftharpoons ES_n \tag{7.9}$$

For this system:

$$K_a = \frac{[ES_n]}{[E][S]^n} \tag{7.10}$$

and y is the degree of saturation:

$$y = \frac{[ES_n]}{[E]_o} \quad \text{and} \quad 1 - y = \frac{[E]}{[E]_o} \tag{7.11}$$

which gives:

$$\frac{y}{1 - y} = \frac{[ES_n]}{[E]} = K_a[S]^n \tag{7.12}$$

and:

$$\log\left(\frac{y}{1 - y}\right) = \log K_a + n\log[S] \tag{7.13}$$

The Hill equation may be extended to kinetic measurements by replacing y with v (the initial rate). By plotting log $v/(V_{max} - v)$ against log [S], the Hill coefficient, h, is obtained from the gradient and is a measure of the degree of departure from simple kinetics. K_a is an overall binding-constant related to the individual binding constants for n sites. The ends of the curves have slopes of unity as these linear segments correspond to the binding of the first and last ligand molecules to the enzyme. The Hill coefficient is therefore taken from the linear central portion of the plot. If $h = 1$, binding is non-co-operative, if $h > 1$, binding is positively co-operative and if $h < 1$, binding is negatively co-operative. Its value could be as large as the number of interacting binding sites, but only if there were complete co-operativity.

Two opposing models for allostery, or the interaction of different binding sites on a protein, have been proposed; these are the sequential model and the concerted model (Creighton, 1993, Fersht, 1985).

The Sequential Model

The binding of a ligand at one site can directly alter the protein conformation at another site, thereby affecting the affinity of the second site for its ligand (Creighton, 1993). In the sequential (or KNF) model proposed by Koshland, Nemethy, and Filmer the progress from

a low to a high affinity state is a sequential process. The conformation of each subunit changes in turn as it binds the ligand. The model assumes that in the absence of ligands, the protein exists in one conformation and on binding a ligand a conformational change of the subunit to which it has bound is induced, which in turn may be transmitted to neighbouring vacant subunits via the subunit interfaces. This model describes a series of tertiary structural changes, in contrast to the concerted model, which uses a series of quaternary structural changes.

The Concerted Model

In the scheme proposed by Monod, Wyman, and Changeux, the binding of a ligand at one site has no direct effect on the affinities of the other sites, but instead alters the conformational equilibrium between two alternative quaternary conformations of the protein. One conformation is the T (for *tense*) state, which has low affinity for ligand at all its sites. The other has high affinity for the ligand and is designated R (for *relaxed*). The two conformations coexist even in the absence of ligand, with an equilibrium constant L between the unbound T and R forms. The T_0 (unbound) form would normally be favoured ($L<1$), and the protein would have a relatively low affinity for the first ligand molecule. The R conformation has the higher affinity (by a factor c) and so ligand molecules bind to it preferentially, pulling the conformational equilibrium toward the R state. The conformational equilibrium between the forms with one ligand bound will be cL. The other vacant sites on all the R_1 (bound to one ligand) molecules will then be in the high-affinity form and the overall affinity of vacant sites in the entire population is increased. This occurs upon binding subsequent ligands, giving rise to positive co-operative homotropic interactions.

The model can also involve heterotropic interactions, in which another ligand (an allosteric effector) changes the enzyme affinity for a substrate by preferentially stabilising the R or T form and altering the ratio between the two. An 'activator' preferentially binds to the R state and increases its concentration. An 'inhibitor' binds preferentially to the T state causing transition to the R state to be more difficult. In extreme cases, a sufficiently high concentration of activator will displace the R-T equilibrium to such an extent that the R state predominates. Co-operativity is then abolished so that Michaelis-Menten kinetics will hold (Fersht, 1985).

Both models imply that ligand binding affects the protein conformation. In the sequential model, such effects extend directly to the other binding sites and affect their ligand

affinities. In the concerted model, the conformational effects need extend only to the interface between the subunits to alter the conformational equilibrium between the R and T quaternary states. Also, in the concerted model the two conformations are present even in the absence of ligand, whereas in the sequential model the R conformation is induced only upon ligand binding. The sequential model predicts that the conformational change upon ligand binding should parallel the extent of ligand binding. With the concerted model the conformational change should tend to occur at one particular stage of ligand binding of each molecule (when Lc^j becomes greater than unity) (Creighton, 1993).

Kinetic Co-operativity and Co-operativity in Monomeric Enzymes

Models have also been proposed for the generation of co-operativity by kinetic mechanisms, rather than by equilibrium effects of site-site interactions (Neet, 1995, Neet and Ainslie, 1980). The kinetic co-operativity observed in these cases has an appearance similar to that arising from other mechanisms and cannot be distinguished simply from the appearance of the steady-state velocity plots. Kinetic models of these types are dependent on catalytic turnover, therefore co-operativity will not be observed for the same substrate in equilibrium binding measurements. This marked distinction is the most diagnostic feature of these mechanisms.

Ligand-induced slow transitions and mnemonic mechanisms have been used to explain possible kinetic co-operativity in monomeric enzymes (Cornish-Bowden and Cardenas, 1987). The basic assumptions for either mechanism occurring in a monomeric enzyme are the existence of at least two kinetically distinct conformational forms of the enzyme and the ability for these forms to inter-convert through a relatively slow conformational change. In order to generate co-operativity by either mechanism, the relative populations of each form must be dependent upon the concentration of the co-operative substrate; i.e. they are not under equilibrium conditions. Kinetic mechanisms are maintained at non-equilibrium by the conversion of substrate to product (Neet, 1995).

Kinetic models involving slow conformational changes. The conditions for generation of kinetic co-operativity by the ligand-induced slow-transition (LIST) model (Ainslie *et al.* 1972) are; (1) the enzyme can exist in two or more different conformational states that are inter-convertible at slow rates compared with the rate of the catalytic reaction. (2) Each form of the enzyme is capable of accomplishing a complete catalytic cycle, but the rate constants are different. (3) The rate of inter-conversion and the proportions of the two states are influenced by the substrate concentration.

Conceptually, co-operativity occurs because the enzyme, E, can partition between formation of ES (and $v = k_1[S]$ in an equation of type 7.7) or isomerisation to the E* conformer (and $v = k_{t1}$, where k_{t1} is the forward rate constant in an equilibrium between E and E*). At low [S], the isomerisation will dominate, and the steady-state velocity (v_{ss}) will be mainly due to the cycle favoured by the E ↔ E* distribution. At high [S], E or E* will be trapped in the form from which product is released and that same cycle will predominate.

The steady-state rate for this mechanism is the sum of the rates for the catalytic cycles of the two enzyme states. Equilibration between conformational states is prevented by the rapid conversion to products (and so thermodynamic principles are not violated). As the substrate concentration is varied, the steady-state distribution of the enzyme between the two forms also varies and, provided that they have different kinetic constants, gives rise to co-operativity, which can be either positive or negative. One enzyme for which this model has been developed is glucokinase (Neet *et al.* 1990).

The mnemonic mechanism. The model for monomeric co-operativity depends on the existence of two forms of free enzyme that differ in stability and isomerise relatively slowly (Cornish-Bowden and Cardenas, 1987). The imbalance between the two states is the result of asymmetry in the catalytic reaction to products, such that the form of free enzyme released at the end of the reaction is the less stable of the two. These ideas imply the existence of "enzyme memory"; if substrate concentration is low, there is ample time for the isomerisation of free enzyme to occur, but if it is high the binding of substrate to the less stable form can occur before the enzyme "forgets" its earlier interaction with substrate.

The conditions for generation of kinetic co-operativity by the mnemonic model are: (1) the enzyme can exist in two inter-convertible conformational states, with an equilibrium constant that greatly favours one state in the absence of ligands. (2) The free enzyme liberated at the end of the catalytic cycle is the less stable form (and is thus different from the form that predominated initially). (3) The binding of the substrate to either form of free enzyme induces a new conformation necessary for catalysis (i.e. there is only one active enzyme-substrate complex). (4) The rate of the conformational change induced by the substrate is different for the two states of free enzyme.

A condition of the mnemonic mechanism is that substrate binding to the more stable enzyme form (E) leads directly to E*S (there is no ES). Co-operativity can arise provided the catalytic reaction from E*S to products is fast so preventing equilibration between the two forms of free enzyme and the substrate. Co-operativity is due to the lack of relaxation of the less stable form, E*, back to E at higher concentrations of S. At low substrate concentrations, the conformational transition (E ↔ E*) has time to occur and so the reaction process is primarily through the more stable form of free enzyme, E: (i.e. E + S → E*S → E*(S↔P)). At high concentrations, binding to the less stable form E* can occur before the conformational transition takes place and the pathway is predominantly through E* + S → E*S → E*(S↔P). The co-operativity can be considered to arise from a transition from one limiting behaviour at low substrate concentrations in which direct binding of S to E* is not possible, to a second limiting behaviour at high substrate concentrations, where the by-pass via E does not exist. The sign of co-operativity is determined by the ratio of the forward rate constants. If the rate constant for binding to E* divided by the rate constant for binding to E is greater than 1 then so is the Hill coefficient *h*, and co-operativity is positive. The mnemonical model has been used to explain co-operativity of hexokinase D from rat liver (Storer and Cornish-Bowden, 1977)

The main difference between the two kinetic mechanisms is that only one catalytic cycle occurs in the mnemonic mechanism whereas the LIST mechanism has two catalytic cycles (i.e. both E and E* are catalytic active).

7.3.3.2 Co-operativity of lipases?

Lineweaver-Burk and Hill plots have indicated a positive co-operative mechanism with olive oil emulsion substrate for the Lipase 3 variants generated in *Pichia pastoris*. An explanation for this effect is not obvious, as Lipase 3 is neither an oligomeric protein nor appears to possess more than one substrate binding-site. (The hydrophobic region via which adsorption to the interface occurs could be considered a separate site, although only one site exists for the binding of individual substrate molecules resulting in their hydrolysis).

Lipase activity depends on equilibrium between 'closed' and 'open' conformational states. The presence of an interface causes a shift in equilibrium to the 'open' state as it stabilises the enzyme in this form. The interface could possibly be considered a type of allosteric effector, binding to the hydrophobic region around the active site, stabilising the enzyme in the active conformation. If the amount of effector (interface) were increased over a

limiting range, the proportion of 'activated' enzyme (E*) would increase, with the plot of [E*] against [S] taking hyperbolic form (saturation behaviour). Alternatively, the lipase may undergo a second conformational change after binding to the interface, to form an 'active' enzyme (E_a* in Figure 7.2).

For an enzyme obeying Michaelis-Menten kinetics; at limiting substrate concentrations the number of enzyme-substrate complexes formed is represented in the initial rate (as $v = k_{cat}[ES]$), and has a hyperbolic relationship to [S]. As the consecutive steps of enzyme 'activation' and enzyme-substrate complex formation, which both involve binding to substrate (in aggregated and monomeric forms respectively), are in equilibrium, a hyperbolic relationship between initial rates and substrate concentration would also be expected.

The ratio of the rate constants for lipase interfacial binding (or for the conformational change that may occur once the enzyme has bound to the interface) and the following catalytic steps may effect the overall kinetics observed and, consequently, the interpretation of kinetic constants. Three possible situations are considered, depending on the relative rates of these steps in the reaction mechanism:

(1) If the conformational change is fast in comparison to the catalytic steps, then the measured rate constants will represent the true catalytic constants.

(2) If the conformational change is slow compared to the catalytic steps, the measured constants will be influenced by the rate of this step. The equilibrium constant for isomerisation between the two states will determine the amount of 'active' enzyme available for catalysis at the interface and the 'apparent' values for k_{cat} and Km will reflect this step. Another possibility is that conversion of the enzyme-substrate complex (E*S) to products is fast, so that equilibrium between the two states is not reached. In this situation, the proportion of enzyme in the active bound state will not be determined by the equilibrium constant for this (conformational change) step and instead may vary with the substrate concentration (amount of interface) resulting in a non-hyperbolic relationship between the two. A similar mechanism to that described for the mnemonic model of kinetic co-operativity (above) may be involved, where at high substrate concentrations the active enzyme released at the end of the reaction remains in this active conformation bound to the interface. At low substrate concentrations the conformational change back to the closed, or, to a less active bound state may have time to occur. At high substrate concentrations, turnover may be so fast that the enzyme conformation does not have time to revert to the less active state.

Equilibrium is therefore not reached between E and E* and the measured rates show a positively co-operative relationship with increasing substrate concentration.

(3) If the rate of the enzyme conformational change and the catalytic constants are of the same order, then the reaction steps will remain in equilibrium. The resulting v vs. [S] plots can only be hyperbolic (as described above, single-site mechanisms cannot generate co-operativity of equilibrium binding, as the principle of microscopic reversibility would be violated).

The rate-determining step of a reaction changes with substrate concentration. This is true for enzymes that follow Michaelis-Menten kinetics (at low concentrations the rate is proportional to k_{cat}/Km and at saturating concentrations it is proportional to k_{cat}). The mechanism for Lipase 3 is believed to involve a conformational change (inferred from sequence alignment and homology modelling to lipases with known structures), that occurs before the enzyme binds to substrate in the formation of a Michaelis-complex. At low substrate surface areas, the conformational change may be rate limiting and at high surface areas the catalytic steps may determine the rate. If the rate of conversion to products is fast (high k_{cat}) then equilibrium in the steady state may not be reached and a sigmoidal plot of initial rate vs. [S] may be seen as the enzyme is able to remain in the more 'active' conformation at higher [S]. The conformational change could be the adsorption step itself, or a second isomerisation to a catalytically active form occurring after the enzyme has bound to the interface, such as that described in the kinetic model of Hult and Holmquist (1997) and shown in Figure 7.2.

Irregular kinetic curves (i.e. non-hyperbolic) have been reported for enzymes acting on lipid substrate (Gatt and Barenholz, 1973). However the deviations of v vs. [S] curves from Michaelis-Menten behaviour could be attributed to a change in the physical state of the substrate as its concentration is increased. In analysing these enzymes only soluble amphiphilic molecules were considered. These form true, molecular solutions at concentrations below the CMC (critical micellar concentration). Above the CMC the concentration of the monomers remains constant and the excess aggregates to form micelles. Deviation from the hyperbolic shape occurred if the transition from monomers to micelles occurred within the concentration range used in the experiment. A sigmoidal curve was predicted to occur in situations where the enzyme utilises substrate in the form of micelles more efficiently than monomers, which are utilised at a lesser rate or not at all (interfacial activation). This does not explain the results for the reaction of Lipase 3 with olive oil, as this substrate is composed entirely of long-chain triacylglycerols, which will

aggregate in water and in this case are converted to stabilised emulsion particles by sonication (and so all substrate molecules are in interfacial form).

This group (Gatt and Bartfai, 1977a and b) later presented a theoretical analysis of kinetics for enzymes interacting with lipid substrates. They simulated *v* versus S curves from rate equations that, although based on the Michaelis-Menten equation, were mostly were non-hyperbolic. One case considered was that part of the substrate adsorbs onto non-catalytic sites of the enzyme, or onto proteins of a non-pure enzyme preparation, thus reducing the quantity of free substrate able to react with the catalytic site of the enzyme. At a constant enzyme concentration the *v* vs. S curve would be sigmoidal. Also, as the molecular weight of a liposome may range from one to three orders of magnitude greater than the enzyme, situations may be encountered in which the enzyme is removed from the reaction mixture by adsorption onto the multi-molecular lipid substrate. In this case, increasing the concentration of the substrate will deplete the mixture of the free enzyme. An equation is derived for the portion of enzyme that can interact with substrate via its catalytic site showed that at high substrate concentrations the velocity decreases and an apparent substrate inhibition is observed.

The authors suggested that to be able to distinguish between these models and actual co-operativity of the enzyme mechanism, Hill plots be drawn at several protein concentrations (Gatt and Bartfai, 1977b). If the sigmoidal curves are due to co-operativity, the Hill coefficient will be a constant and not vary with enzyme concentration. If they are due to adsorption of the substrate onto enzyme, a Hill-like coefficient might be obtained, but it will vary and depend on protein concentration. Furthermore, *v* vs. E curves are usually linear with co-operative enzymes, whereas they might deviate from linearity in cases of substrate adsorption (Gatt and Bartfai, 1977b). In light of this, it was decided to repeat the initial rate curves using more than one enzyme concentration. This was carried out with the wild type lipase expressed in *Pichia pastoris* and the results are shown below (Figure 7.7).

From these results it can be seen that the Hill coefficient for the wild type lipase expressed in *Pichia pastoris* does not change significantly when different concentrations of enzyme are used (h = 2.9, 2.7 and 2.5 with 0.9 μg, 1.8 μg and 3.6 μg enzyme, respectively) (Figure 7.7c). It would therefore seem, from these results, that the co-operativity shown by the lipases is not due to enzyme or substrate depletion by adsorption between the enzyme and substrate at non-catalytic sites. These results provide support for the observed effect being due to mechanistic properties of the enzyme. In the following chapter a kinetic analysis of

Lipase 3 variants expressed and purified from *Aspergillus niger* by Danisco Ingredients (at laboratories in Brabrand, Denmark) is presented. It was thought that comparison of the two sets of results might provide further clues as to whether or not a mechanistic explanation can be given to the sigmoidal kinetics observed.

Figure 7.7 Analysis of kinetic curves, using three different concentrations of wild type Lipase 3 (from expression in *Pichia pastoris*). Assays were carried out using 1, 2 and 4 µl of 9.025 x 10^{-7} g μl^{-1} purified lipase (so that 1 E = 9.025 x 10^{-7} g, 2 E = 1.805 x 10^{-6} g and 4 E = 3.61 x 10^{-6} g of enzyme). (a) Activity in units (U: mmol min^{-1}) plotted against substrate concentration (in g l^{-1}). (b) The Lineweaver-Burk plot, from which values of V_{max} are taken. (c) The Hill plot, from which Hill coefficients are determined (equal to the slope at 50 % saturation of enzyme). (d) Plot of V_{max} in units (U) against enzyme concentration, showing a linear relationship between the two.

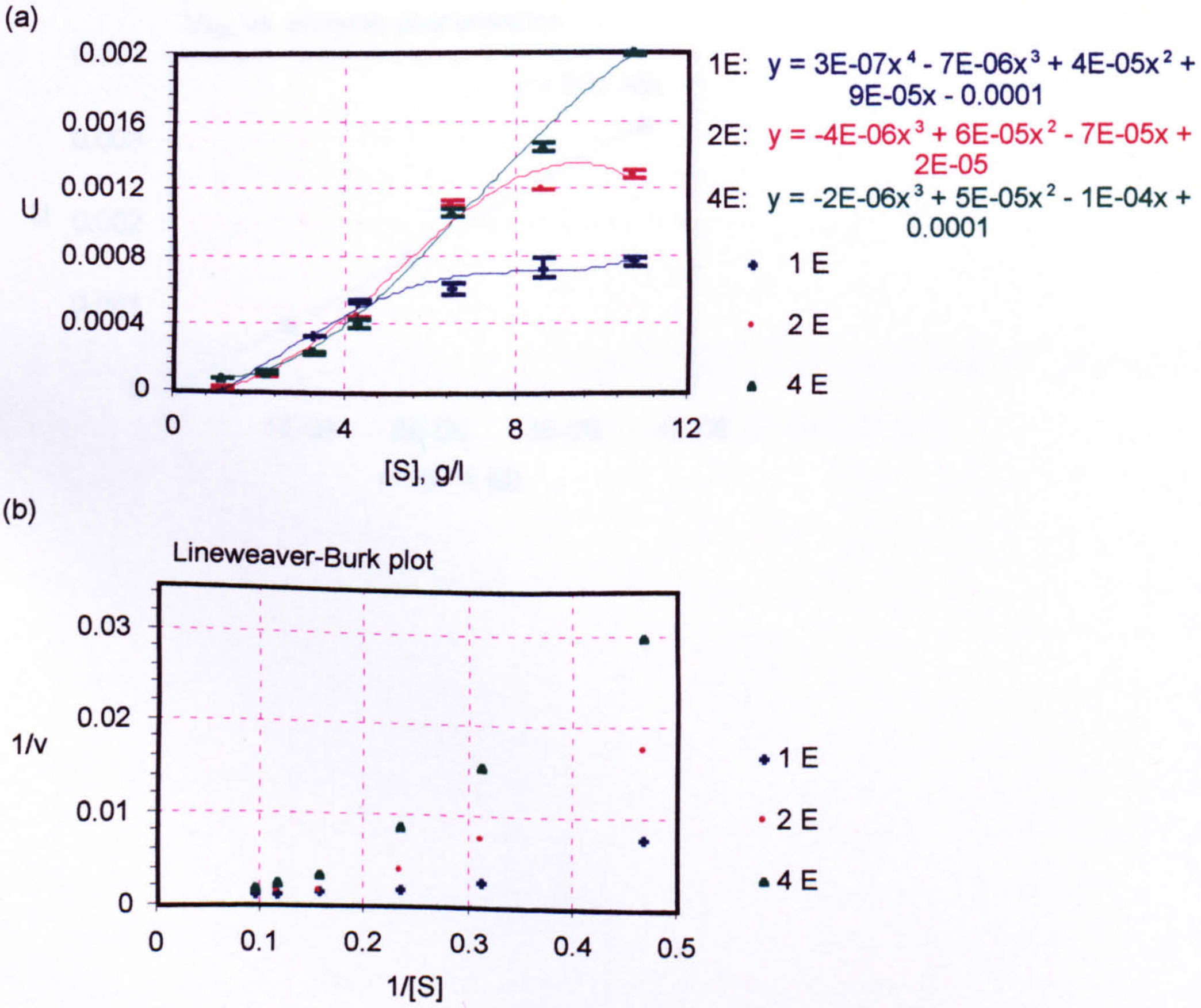

(c)

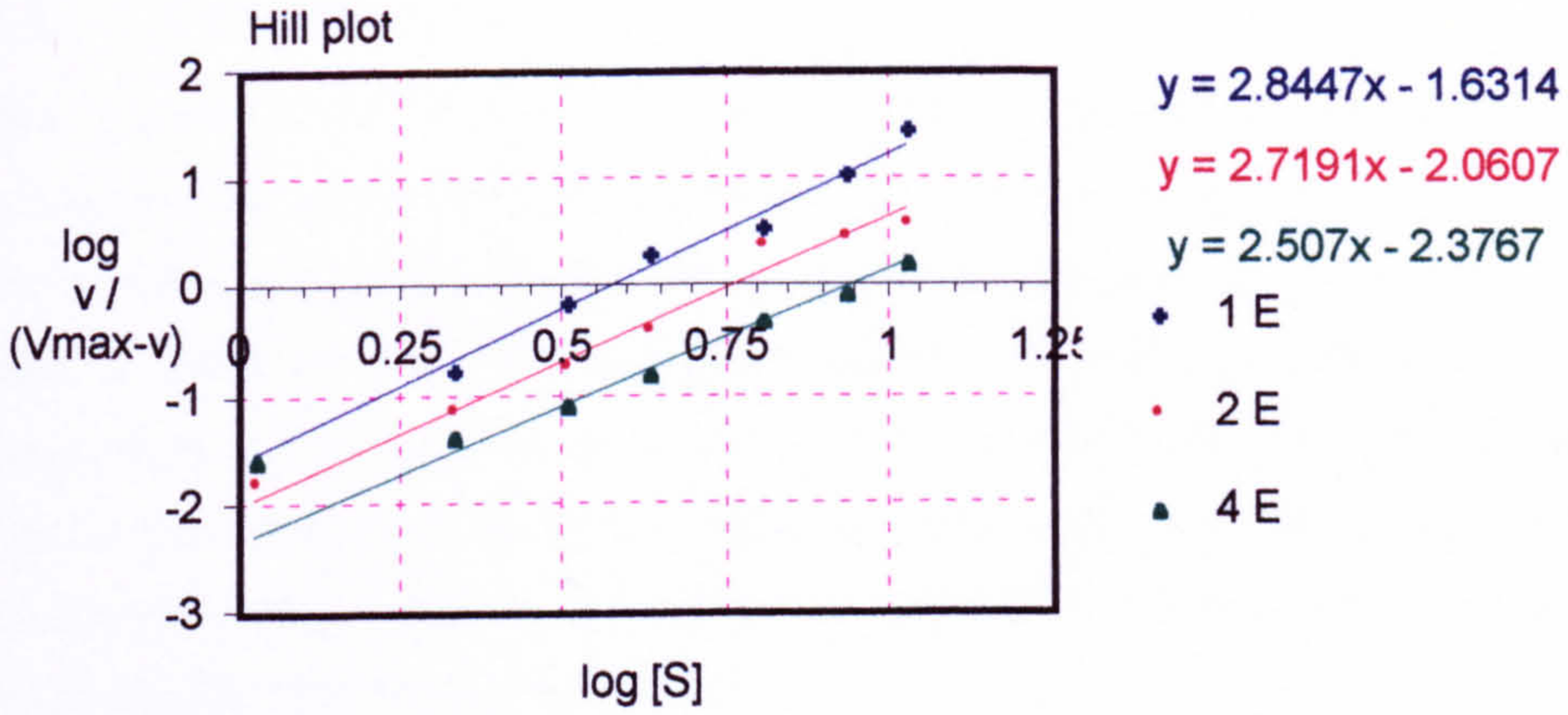
Hill plot
log v / (Vmax-v)
2
1
0
-1
-2
-3
0
0.25
0.5
0.75
1
1.25
log [S]
y = 2.8447x - 1.6314
y = 2.7191x - 2.0607
y = 2.507x - 2.3767
1 E
2 E
4 E

(d)

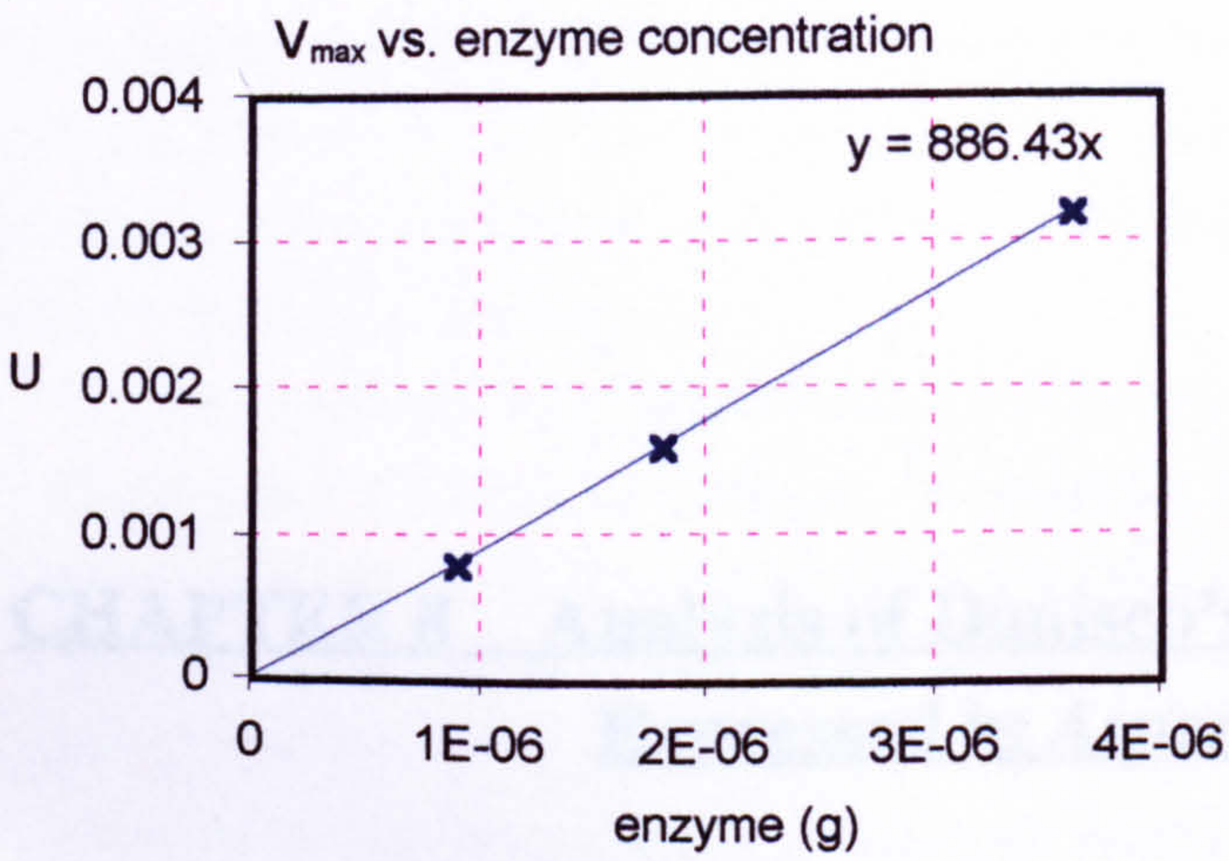
V_{max} vs. enzyme concentration
U
0.004
0.003
0.002
0.001
0
y = 886.43x
0
1E-06
2E-06
3E-06
4E-06
enzyme (g)

CHAPTER 8 Analysis of Danisco's 'Glycosylation' Mutants Expressed in *Aspergillus niger*

8.1 Introduction

The 'glycosylation' mutants of Lipase 3 were generated by site-directed-mutagenesis of a genomic DNA template as well as a cDNA template (for expression in *Pichia pastoris*). These were sent to Danisco where they were subsequently expressed in *Aspergillus niger* with a view to alleviate problems associated with glycosylation occurring on over-expression of Lipase 3 for industrial use. Danisco found that glycosylation at the mutated sites appeared to have been prevented (as indicated by SDS-PAGE) and activity levels of the enzyme were restored. In particular, the N59T N269Q double mutant was found to be the most effective in baking trials.

It was decided to follow up the kinetic analysis of lipase 'glycosylation' mutants expressed in *Pichia pastoris* with a similar analysis of the same mutants and wild type enzyme from expression using *Aspergillus niger* carried out by Danisco. The results of such an analysis could be useful for two reasons: -

1. Kinetic constants were determined for wild type and mutants of Danisco's Lipase 3 expressed in *Pichia pastoris* (previous chapter). It was noted for all of these lipases that initial reaction rates (v) plotted against interfacial surface area ($m^2\ l^{-1}$) of emulsified olive oil substrate gave sigmoidal curves, implying a co-operative mechanism. Hill plots, used to confirm co-operativity, also implied that this was the case and that the apparent co-operativity was positive (with values for the Hill coefficient, h, in the range 2 to 4). The observed effects could possibly be due to some post-translational modification from expression in *Pichia pastoris* leading to more than one isoform in the enzyme preparation with different kinetic properties. Alternatively, the enzymes isolated from the *Pichia* supernatants may not have been completely pure. To be able to eliminate these possibilities, it was decided to carry out the same experiments using the enzymes that had been expressed and purified by Danisco from *Aspergillus niger*.
2. A comparison of the derived kinetic constants for lipases expressed in *Pichia pastoris* and *Aspergillus niger* could be used to assess the effectiveness of using *Pichia* as an expression system for primary analysis of variants, prior to their industrial production from *Aspergillus niger*. Also, a comparison of the derived kinetic constants of the lipases expressed in both systems with the results of in-dough assays (next chapter) should aid prediction in the design and analysis of further lipase mutants with regard to their functionality in bread-making.

Purified proteins were obtained from Danisco. First of all, their specific activities were measured with olive oil emulsion substrate and then V_{max} and Km_{app} constants determined, again with olive oil emulsion substrate. Initial rates were measured using a pH-stat controller and emulsion particle sizes were measured by laser diffraction with a Mastersizer *S* for determination of total interfacial surface area.

Since carrying out lipase assays of the mutant and wild type lipases expressed in *Pichia pastoris* (results presented in Chapter 7) the laboratory moved location. For comparison of results obtained using the different equipment at the University of Nottingham with previous analyses carried out at the IFR (Institute of Food Research), the wild type lipase from expression in *Pichia pastoris* was also analysed for a second time.

8.2 Analysis of 'Glycosylation' Mutants Expressed in *Aspergillus niger*

8.2.1 Specific Activities

The specific activities of purified 'glycosylation' mutants and wild type Lipase 3 from Danisco (expressed in *Aspergillus niger)* were determined. At the substrate concentrations (or surface areas) used for these measurements, an increase in enzyme concentration resulted in a proportional increase in activity and increasing the substrate concentration did not alter the rate. With these conditions satisfied, substrate is presumed to be in excess, with catalysis occurring at the maximal rate. The specific activities with olive oil emulsion substrate are shown in Table 8.1. Assays were carried out at 37 °C and pH 7.3.

Table 8.1 Specific activities of Danisco's 'glycosylation' mutant enzymes (from *A. niger*) and wild type lipases (from *Pichia pastoris* and *A. niger*) with olive oil emulsion substrate. Activities were measured using a pH-stat controller. Three samples of each enzyme were assayed and standard deviations represent the variation in these measurements. Protein concentrations were determined from OD_{280} and OD_{260} values. *(U: mmol min^{-1}; stdevp: standard deviation).*

Lipase		Specific activity, U g^{-1}	*stdevp*
'Glycosylation' mutants (expressed in *A. niger*)	N59T	665	*± 21*
	N59T N269Q	462	*± 28*
	N59T N269T	263	*± 18*
	N269T	543	*± 36*
	N269Q	632	*± 23*
Wild type	*A. niger*	675	*± 4*
	Pichia	831	*± 20*

8.2.2 Kinetic Analysis

Initial reaction rates were measured over a range of interfacial areas using emulsified olive oil substrate. The effect of limiting substrate concentrations on initial rates (v) is illustrated in Figure 8.1. The values of Km_{app} (equal to surface area when v is at half maximal rate) and V_{max} (determined from Lineweaver-Burk plots) are shown in Table 8.2.

Figure 8.1 Effect of varying the surface area of an olive oil emulsion substrate on the activity of Danisco's 'glycosylation mutants' (expressed in *A. niger*) and wild type lipases (expressed in *Pichia pastoris* and *A. niger*). Initial rates were measured using substrate surface areas up to $V_{max,}$ using a pH-stat controller. Surface areas were calculated from emulsion particle sizes measured by laser diffraction using a Mastersizer *S*. Protein concentrations were determined from OD_{280} and OD_{260} values. *(U: mmol min^{-1}).*

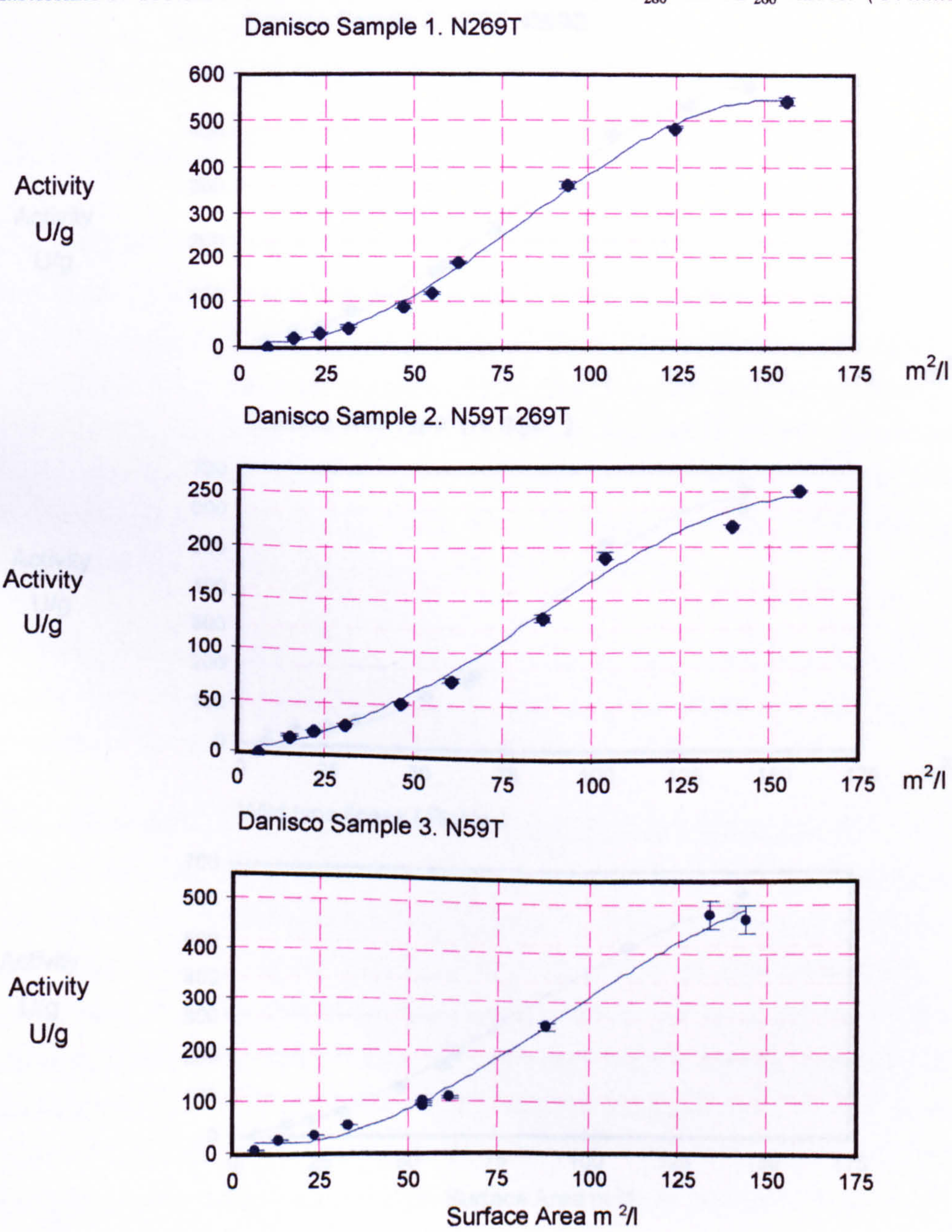

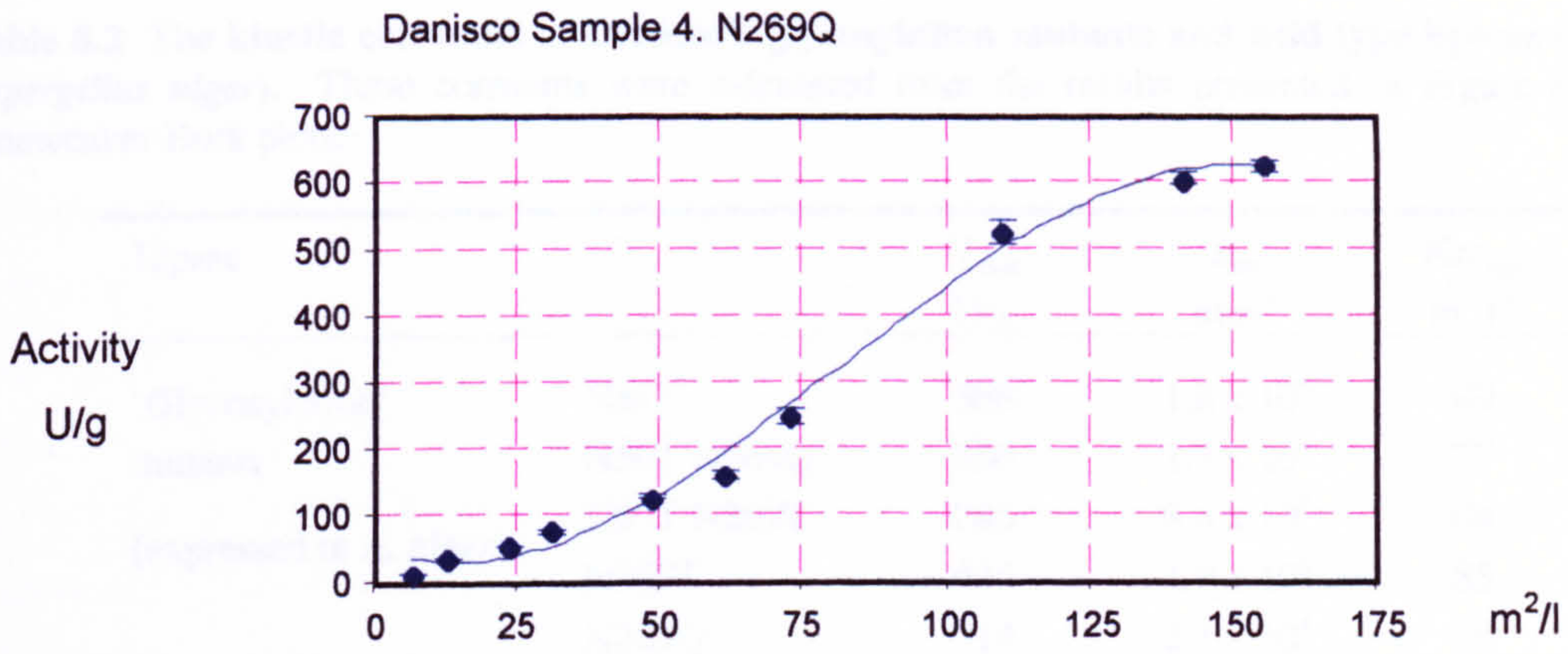
Danisco Sample 4. N269Q
Activity U/g
700
600
500
400
300
200
100
0
0 25 50 75 100 125 150 175
m²/l

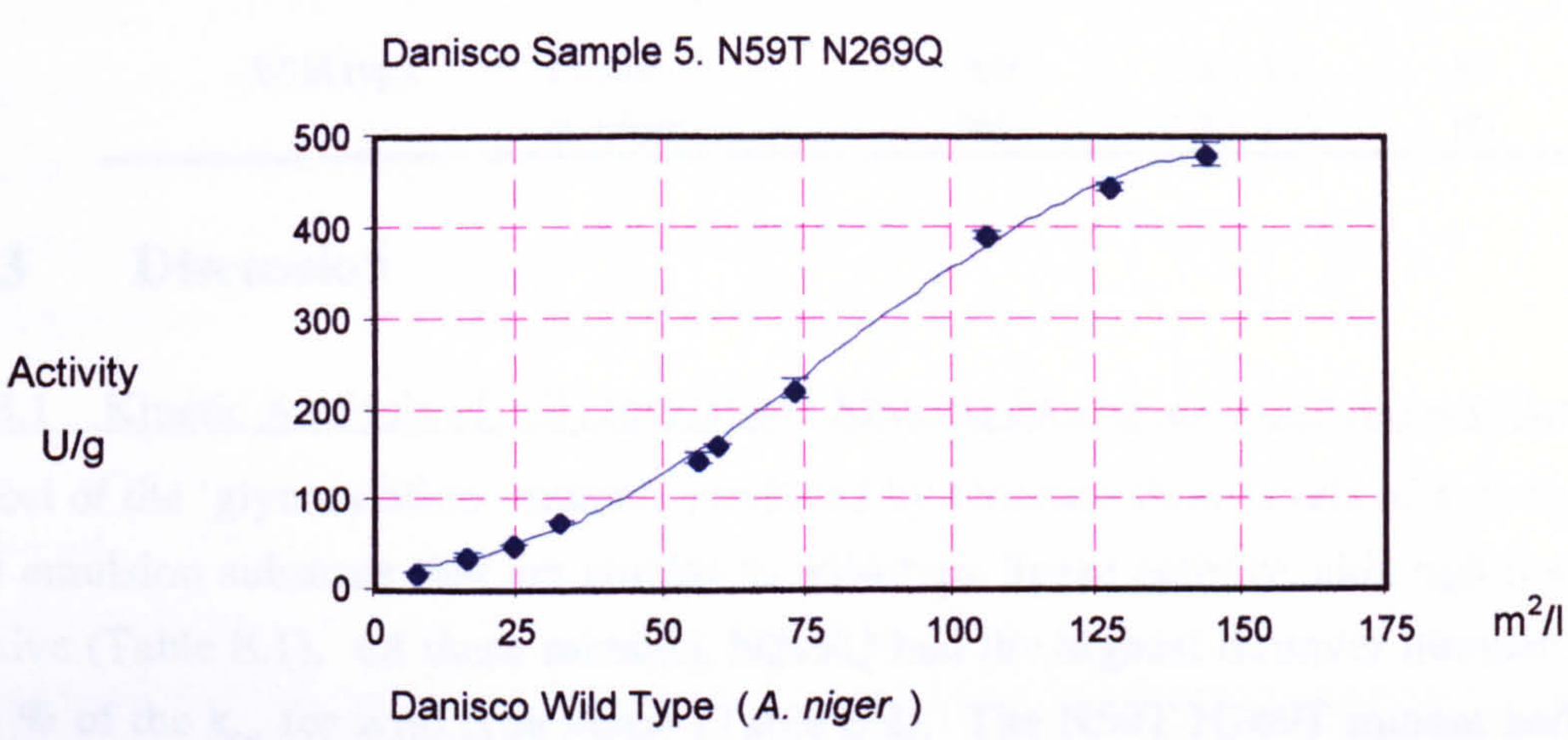
Danisco Sample 5. N59T N269Q
Activity U/g
500
400
300
200
100
0
0 25 50 75 100 125 150 175
m²/l
Danisco Wild Type (A. niger)
Activity U/g
700
600
500
400
300
200
100
0
0 25 50 75 100 125 150 175
m²/l
Wild type lipase (Pichia)
Activity U/g
700
600
500
400
300
200
100
0
0 25 50 75 100 125 150 175
Surface Area m²/l

Table 8.2 The kinetic constants of Danisco's glycosylation mutants and wild type lipases (expressed in *Aspergillus niger*). These constants were calculated from the results presented in Figure 8.1 and using Lineweaver-Burk plots.

Lipase		V_{max} U/g	k_{cat} min^{-1}	Km_{app} $m^2\ l^{-1}$
'Glycosylation' mutants (expressed in *A. niger*)	N59T	588	1.8×10^4	89
	N59T N269Q	556	1.7×10^4	77
	N59T N269T	286	8.6×10^3	84
	N269T	645	1.9×10^4	85
	N269Q	714	2.1×10^4	89
Wild type	*Pichia*	769	2.3×10^4	89
	A. niger	769	2.3×10^4	89

8.3 Discussion

8.3.1 Kinetic Analysis of 'Glycosylation' Mutants Expressed using *Aspergillus niger*

Most of the 'glycosylation' mutants produced by Danisco show levels of activity with olive oil emulsion substrate that are similar to wild-type lipase activity, although none are more active (Table 8.1). Of these mutants, N269Q had the highest turnover number, which was 91 % of the k_{cat} for wild type lipase (Table 8.2). The N59T N269T mutant had the lowest specific activity (equal to 39 % of the wild type specific activity) and the lowest turnover number (equal to 37 % the k_{cat} value for wild type). For the remaining 'glycosylation' mutants, activity levels were at least 70 % that of wild type.

The Km_{app} values of the mutant enzymes were all very similar to that of the wild type, ranging from 77 $m^2\ l^{-1}$ for N59T N269Q, to 89 $m^2\ l^{-1}$ for N59T and N269Q, which was also the value for the wild type enzyme (Table 8.2).

8.3.2 Analysis of Wild Type Lipase 3 Expressed using *Pichia pastoris*

A kinetic analysis of the wild type lipase from expression in *Pichia pastoris* had already been carried out (results presented in Chapter 7). This enzyme was analysed for a second time, along with the lipase variants from expression in *Aspergillus niger*, because the experimental work at this stage was being carried out in a different laboratory. The sonicator, Mastersizer and pH-stat, all necessary for the kinetic analysis with emulsified lipid substrate, were different from those used for the analysis of *Pichia* expressed lipases. In case of variations in results due to differences in equipment, the kinetic analysis of wild type lipase from *Pichia* was therefore repeated to enable comparison of results obtained in the different laboratories.

It was noted that the emulsions made using the sonicator at the University of Nottingham for analysis of the *Aspergillus* expressed lipases had a smaller particle size (average diameter = 0.43 μm ± 0.05) than the emulsions prepared in the same way at the IFR (average diameter = 0.90 μm ± 0.18). This resulted in the equivalent emulsions possessing higher surface areas. The assay results of the wild type lipase (from *Pichia pastoris*) carried out at the IFR were compared with the results obtained for this enzyme at the University of Nottingham, to see the effect of using emulsions with different sized particles on kinetic behaviour. The results are shown in Figure 8.2 and Figure 8.3. Figure 8.2 shows the results obtained at the IFR where the average particle diameter of the emulsions equalled 0.93 ± 0.22 μm. Figure 8.3 shows the results obtained at Nottingham where the average particle diameter of the emulsions used in an identical analysis of the *Pichia* expressed wild type lipase, was 0.43 ± 0.04 μm.

Despite the greater range of surface areas over which activities were measured for the emulsions with smaller particle sizes, the plot of initial rates against surface area did not look significantly different. When initial rates were plotted against substrate concentration expressed in g l^{-1}, the Km_{app} values were found to the same, irrespective of particle size (Figure 8.2b and Figure 8.3b). From both analyses of the wild type Lipase 3 expressed in *Pichia pastoris*, Km_{app} = 6 g l^{-1}. However, the Km_{app} values in terms of substrate surface area (m^2 l^{-1}) were different (Figure 8.2a and Figure 8.3a). These Km_{app} values (in m^2 l^{-1}) were higher for the emulsions with smaller particle sizes (and consequently greater emulsion surface areas). With small emulsion particles (where mean diameter = 0.4 μm), Km_{app} = 89 m^2 l^{-1} and with large emulsion particles (where mean diameter = 0.8 μm), Km_{app} = 33 m^2 l^{-1} (for wild type Lipase 3 expressed in *Pichia*).

These results indicate that substrate surface area (m^2 l^{-1}) does not determine lipase kinetic behaviour. Instead, the total amount of substrate present in the system, not just at the interface, influences the kinetic behaviour. A more suitable expression for substrate concentration when using bulk conditions such as lipid emulsion to determine kinetic constants would be in terms of its three-dimensional concentration (such as molarity or grams per litre), as this has proved to give consistent results regardless of the size of emulsion particles. This is in spite of the fact that lipase activity occurs at the lipid-water interface, (which is the reason that substrate surface area is generally considered when investigating lipase kinetics). As binding to the interface does not appear to be a slow (rate-limiting) step, the kinetic constants must therefore represent the mechanistic steps that

occur once the enzyme has bound to the interface. This is contrary to the findings of Benzonana and Desnuelle (1965) who, using bulk conditions, obtained a single Km value when substrate concentration was expressed as area/volume rather than as weight/volume and concluded that the apparent Km defined the binding affinity of the enzyme for the interface.

Figure 8.2 Effect of varying the amount of olive oil emulsion substrate on activity of wild type lipase expressed in *Pichia pastoris*, where average emulsion particle size = 0.93 μm. The olive oil emulsion is expressed in terms of (a) surface area (units: $m^2\ l^{-1}$) and (b) concentration (units: $g\ l^{-1}$). Average emulsion particle size = 0.93 ± 0.22 μm, from the measurement of duplicate samples taken from the 8 emulsions used. (Graph (a) is also presented in Chapter 7). *(U: mmol min^{-1}).*

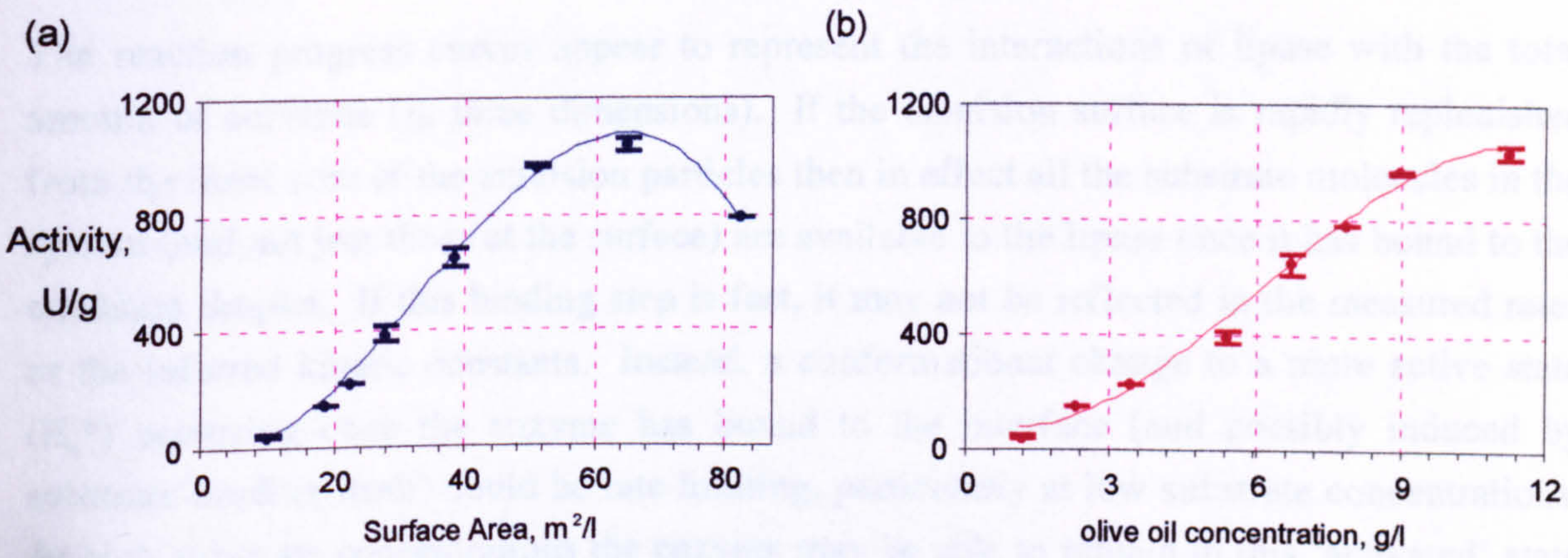

Figure 8.3 Effect of varying the amount of olive oil emulsion substrate on activity of wild type lipase expressed in *Pichia pastoris*, where average emulsion particle size = 0.43 μm. The olive oil emulsion is expressed in terms of (a) surface area (units: $m^2\ l^{-1}$) and (b) concentration (units: $g\ l^{-1}$). Average emulsion particle size = 0.43 ± 0.04 μm, from the measurement of duplicate samples taken from the 10 emulsions used. *(U: mmol min^{-1}).*

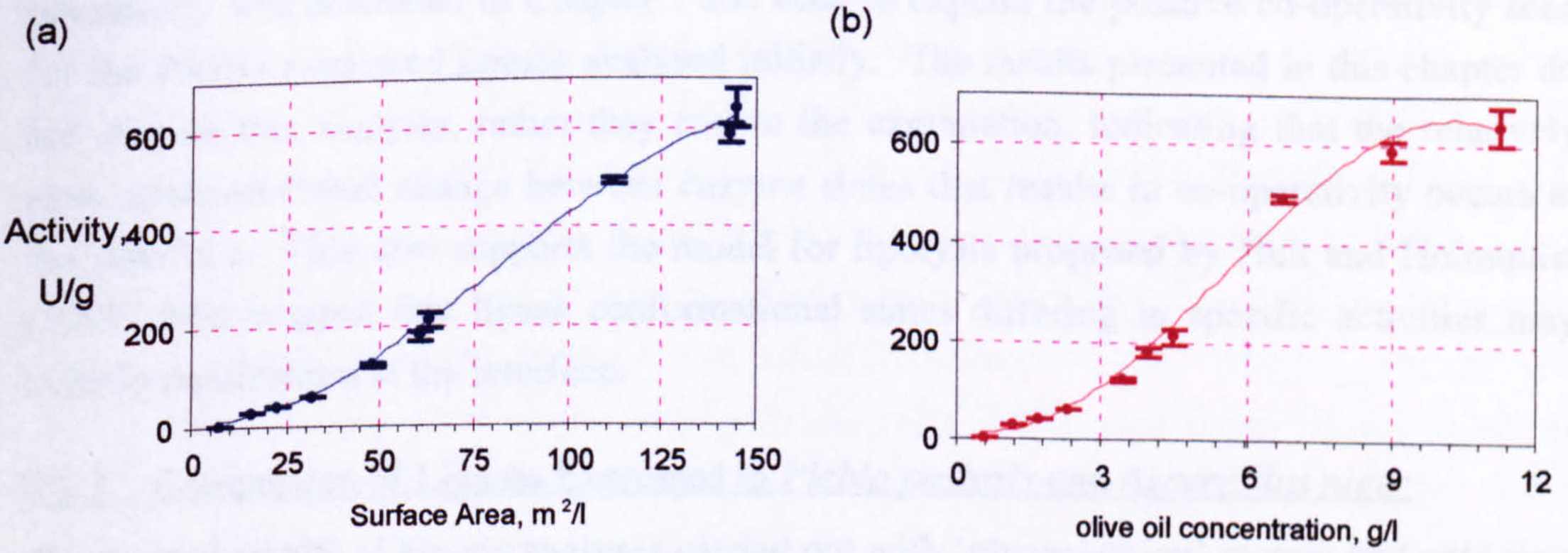

8.3.2.1 Sigmoidal kinetics

It was also noted that when activity is plotted against substrate concentration in grams per litre, the sigmoidal nature of the curves is not affected (Figure 8.2 and Figure 8.3). The shape of the curve is evidence of a co-operative mechanism (discussed in the previous chapter). As interfacial binding does not appear to influence the observed initial rates, the co-operativity must be due to steps occurring after enzyme adsorption to the interface. The model for lipase kinetics proposed by Hult and Holmquist (1997) (illustrated in Chapter 7, Figure 7.2) suggests that an 'active' enzyme conformation (E_a*) may be induced after the more general adsorption step to the lipid-water interface has occurred.

The reaction progress curves appear to represent the interactions of lipase with the total amount of substrate (in three dimensions). If the emulsion surface is rapidly replenished from the inner core of the emulsion particles then in effect all the substrate molecules in the system (and not just those at the surface) are available to the lipase once it has bound to the emulsion droplet. If this binding step is fast, it may not be reflected in the measured rates or the inferred kinetic constants. Instead, a conformational change to a more active state (E_a*) occurring once the enzyme has bound to the interface (and possibly induced by substrate binding itself) could be rate limiting, particularly at low substrate concentrations. At high substrate concentrations the enzyme may be able to remain in this 'activated' state and bind further substrate molecules provided that conversion of substrate to product (k_{cat}) is rapid and the conformational change to the less active form is relatively slow. Sigmoidal kinetic curves may then arise from the variation in the relative amounts of these conformational states with substrate concentration. This kinetic-mechanism for co-operativity was discussed in Chapter 7 and used to explain the positive co-operativity seen for the *Pichia* expressed lipases analysed initially. The results presented in this chapter do not dispute this analysis, rather they add to the explanation, indicating that the relatively slow conformational change between enzyme states that results in co-operativity occurs at the interface. This also supports the model for lipolysis proposed by Hult and Holmquist (1997) who suggest that lipase conformational states differing in specific activities may exist in equilibrium at the interface.

8.3.3 Comparison of Lipases Expressed in *Pichia pastoris* and *Aspergillus niger*

The overall results of kinetic analyses carried out with 'glycosylation' mutant and wild type Lipase 3 expressed in *Pichia pastoris* and *Aspergillus niger* are presented in Table 8.3. To compare the Km_{app} values for these two sets of mutants, they are shown in terms of olive oil

concentration (g l^{-1}) as this has been found to be constant despite the different particle sizes of the emulsions used.

Table 8.3 Kinetic constants for 'glycosylation' mutant and wild type Lipase 3 expressed in *Pichia pastoris* and *Aspergillus niger*. For comparison of Km_{app} constants, values are shown in g l^{-1}. (a) Kinetic analysis of 'glycosylation' mutants and wild type lipase from expression in *Pichia pastoris*, (these results are also presented in Chapter 7). (b) Kinetic analysis of 'glycosylation' mutants and wild type lipase expressed in *Aspergillus niger* by Danisco, and of wild type lipase expressed in *Pichia pastoris*. V_{max} values are also shown as percentages of the V_{max} of the wild type enzyme (*% w.t.*). *(U: mmol min^{-1}).*

(a)

	Lipase	V_{max} U g^{-1}	k_{cat} min^{-1}	Km_{app} g l^{-1}	V_{max} *% w.t.*
Pichia pastoris	N59T	1429	4.3×10^4	7.2	*114*
	N59T N269Q	1429	4.3×10^4	7.2	*114*
	N59T N269T	800	2.4×10^4	4.4	*64*
	N269T	1429	4.3×10^4	5.4	*114*
	N269Q	1250	3.8×10^4	4.8	*100*
	Wild type	1250	3.8×10^4	5.8	*100*

(b)

	Lipase	V_{max} U g^{-1}	k_{cat} min^{-1}	Km_{app} g l^{-1}	V_{max} *% w.t.*
Aspergillus niger	N59T	588	1.8×10^4	6.3	*76*
	N59T N269Q	556	1.7×10^4	5.0	*72*
	N59T N269T	286	0.9×10^4	5.4	*37*
	N269T	645	1.9×10^4	6.2	*84*
	N269Q	714	2.1×10^4	5.0	*93*
	Wild type	769	2.3×10^4	5.6	*100*
Pichia pastoris	Wild type	769	2.3×10^4	5.8	*100*

The assays carried out at the IFR for the *Pichia pastoris* expressed mutants gave higher V_{max} values than those obtained at the University of Nottingham for the *Aspergillus niger* expressed mutants. The V_{max} values for the *Pichia* expressed mutants were approximately twice as high as the *Aspergillus* expressed lipases from Danisco (Table 8.3a and b). This was also found to be the case for the wild type enzyme expressed in *Pichia pastoris*, which was analysed in conjunction with each set of lipases (from the two different expression systems), implying that this difference in activity levels is not real. The V_{max} for the wild type enzyme measured in conjunction with the other *Pichia* expressed lipases, equalled 1250 U g^{-1}. When a second kinetic analysis of this enzyme was carried out at the University of Nottingham, V_{max} was found to equal 769 U g^{-1} (which is also the V_{max} value for the wild type enzyme expressed using *Aspergillus niger*). The V_{max} and k_{cat} values for the two sets of lipases analysed are therefore comparable if considered in relation to the results for the wild type lipase expressed in *Pichia pastoris*.

The V_{max} values for the 'glycosylation' mutants and wild type enzymes expressed by *Pichia pastoris* and *Aspergillus niger* are shown in Table 8.3 as percentages of the V_{max} value for the *Pichia* expressed wild type. All the mutants show high levels of activity in comparison with the wild type level, although the mutants expressed in *Pichia* generally show higher activity levels compared to wild type (Table 8.3a). For both sets of 'glycosylation' mutants, the N59T N269T double mutant has the lowest activity compared to wild type and this mutant demonstrated less than half the activity level demonstrated by the wild type when expressed in *Aspergillus* (37 %).

The Km_{app} values for lipases expressed in *Pichia pastoris* ranged from 4.8 g l^{-1} for N269Q to 7.2 g l^{-1} for the N59T and N59T N269Q 'glycosylation' mutants. The value for the wild type enzyme expressed in *Pichia* was 5.8 g l^{-1}. The Km_{app} values for lipases expressed in *Aspergillus niger* ranged from 5.0 g l^{-1} for N269Q and N29T N269Q, to 6.2 for the N269T mutant and the value for the wild type was 5.6 g l^{-1}. Re-analysis of the wild type enzyme from expression in *Pichia* (carried out in parallel with the kinetic analysis of *Aspergillus* expressed lipases) again gave a value of 5.8 g l^{-1}, which is also very close to that of the *Aspergillus* expressed lipase (5.6 g l^{-1}). These results indicate that Km_{app} values can be compared when expressed in terms of total substrate concentration (in three dimensions), and that the values for the *Aspergillus* expressed lipases were very similar to those of the *Pichia* expressed enzymes.

8.3.3.1 Comparison of wild type enzymes

From the results shown in Table 8.3, for the wild type lipases, it can also be seen that the kinetic properties of the wild type lipase expressed in *Pichia pastoris* are virtually identical to those of the *Aspergillus niger* expressed enzyme from Danisco. The results from kinetic analysis of these two enzymes, carried out in the same laboratory conditions, show that values of V_{max} and k_{cat} are equal (Table 8.3b). Also, the values of Km_{app} for these enzymes are very close (5.6 g l^{-1} for *A. niger* expressed wild type and 5.8 g l^{-1} for the *Pichia* expressed wild type enzyme).

8.3.3.2 Co-operativity

When initial rates are plotted against substrate concentration, sigmoidal curves are obtained for the 'glycosylation' mutants and wild type lipase expressed by *Aspergillus niger* (Figure 8.1). This effect was also observed for the lipases expressed in *Pichia pastoris* (results presented in Chapter 7). It therefore seems unlikely that the sigmoidal nature of these

kinetic curves arises as a result of the expression system used, or from the presence of impurities in the enzymes preparations.

Table 8.4 Comparison of Hill coefficients for 'glycosylation' mutants and wild type Lipase 3, from expression in *Aspergillus niger* and *Pichia pastoris*.

Lipase	Hill coefficient	
	Expression system :-	
	Aspergillus niger	*Pichia pastoris*
N59T	3	3
N59T N269Q	3	3
N59T N269T	3	4
N269T	3	4
N269Q	4	3
Wild-type	3	3

Hill plots were drawn for the lipases expressed in *Aspergillus niger*. The Hill coefficients, equal to the gradients taken from the central regions of these plots, are presented in Table 8.4 and are compared to the values determined for the same enzymes expressed in *Pichia pastoris*. The wild type enzymes both had Hill coefficients of 3, as did most of the 'glycosylation' mutants. The exceptions were the *A. niger* expressed N269Q mutant and the *Pichia* expressed N59T N269T and N269T mutants, which had Hill coefficients of 4. Although the meaning of this coefficient in respect to the Lipase 3 mechanism is unclear (as Lipase 3 does not appear to possess more than one binding site and is monomeric), it does represent the degree of departure from simple Michaelis-Menten kinetics. The Hill coefficients shown in Table 8.4 indicate that the co-operative mechanism of the lipase variants is positive and that they all show approximately the same degree of departure from Michaelis-Menten saturation kinetics.

Figure 8.4 Hill plots for the wild type lipases expressed in *Pichia pastoris* and *Aspergillus niger*. The olive oil emulsion is expressed in terms of (a) surface area (units: $m^2\ l^{-1}$) and (b) concentration (units: $g\ l^{-1}$). *(U: mmol min^{-1}).* (Average emulsion particle size = 0.43 ± 0.04 μm). The initial rate data used in these plots is also represented in Figure 8.1 and Figure 8.3.

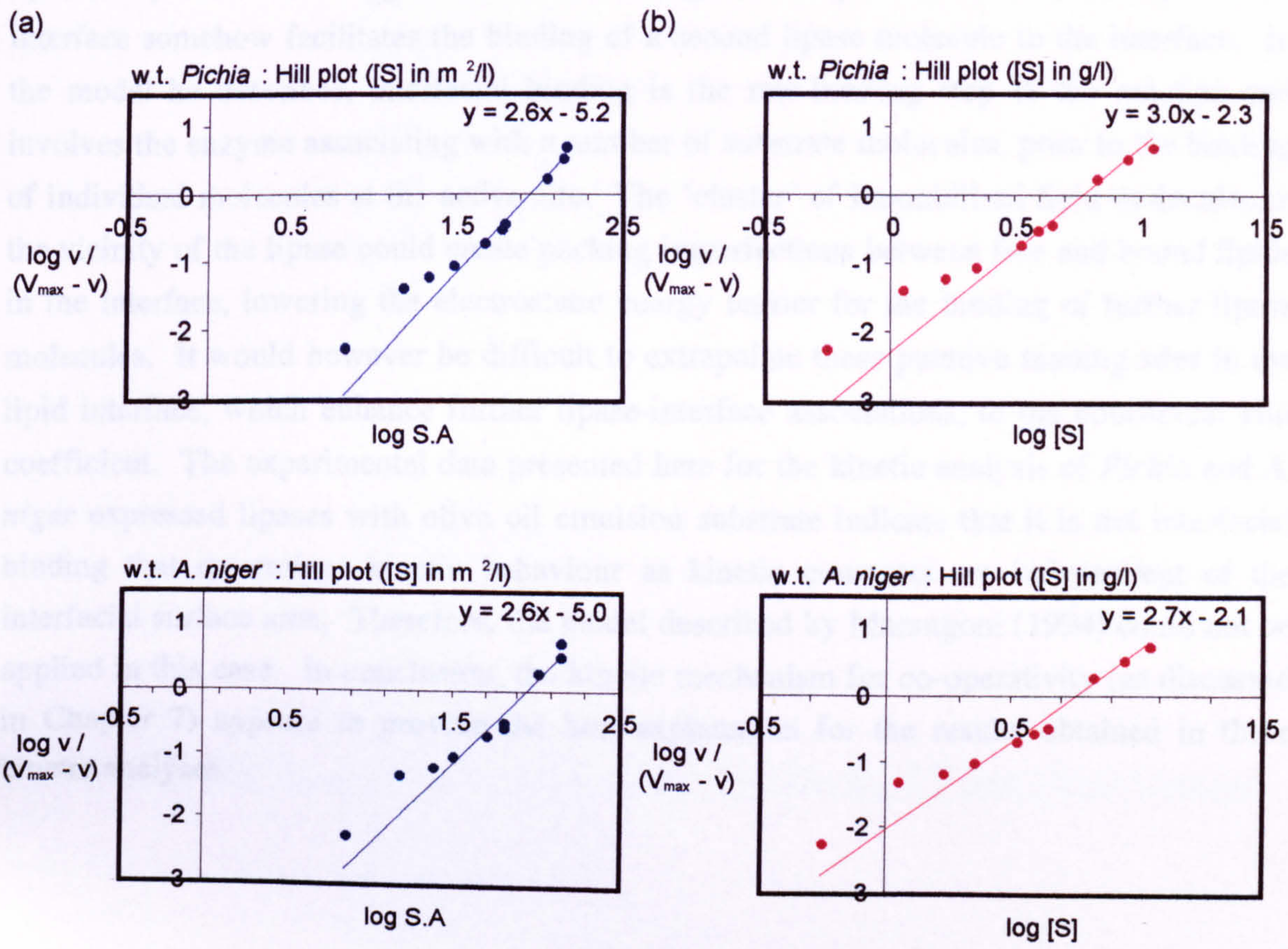

Emulsion surface area is proportional to substrate concentration in grams per litre only if the particle sizes in the emulsions used for a kinetic plot (of *v* against [S]) are approximately equal. If they are not, the degree of co-operativity observed may differ when initial rates are plotted against substrate surface area rather than substrate concentration as molarity or grams per litre. The non-hyperbolic nature of kinetic curves plotted against substrate concentration in grams per litre has already been noted (Figure 8.2 and Figure 8.3). The measure of co-operativity (Hill coefficient) was also found to be unaffected by the method chosen to express substrate concentration (surface area or grams per litre). This is illustrated in Figure 8.4, which also compares the results from the wild type lipases expressed in *Pichia* and *Aspergillus*. The gradients of the central linear regions of these plots (the Hill coefficient) are approximately equal for the two enzymes, and, as also seen for all the lipases analysed, are not affected by the choice of term for substrate concentration.

In an alternative kinetic model put forward by Marangoni (1994) to explain sigmoidal kinetic curves observed for lipases, interfacial binding itself was described as a co-operative process. He suggested that the binding of one lipase molecule to the lipid-water interface somehow facilitates the binding of a second lipase molecule to the interface. In the model he describes, interfacial binding is the rate-limiting step of the reaction and involves the enzyme associating with a number of substrate molecules, prior to the binding of individual molecules at the active site. The 'cluster' of immobilised lipid molecules in the vicinity of the lipase could create packing imperfections between free and bound lipids in the interface, lowering the electrostatic energy barrier for the binding of further lipase molecules. It would however be difficult to extrapolate these putative binding sites in the lipid interface, which enhance further lipase-interface associations, to the conceptual Hill coefficient. The experimental data presented here for the kinetic analysis of *Pichia* and *A. niger* expressed lipases with olive oil emulsion substrate indicate that it is not interfacial binding that determines kinetic behaviour as kinetic constants are independent of the interfacial surface area. Therefore, the model described by Marangoni (1994) could not be applied in this case. In conclusion, the kinetic mechanism for co-operativity (as discussed in Chapter 7) appears to provide the best explanation for the results obtained in these kinetic analyses.

CHAPTER 9 Results of Baking Trials and Final Discussion

9.1 Introduction

Danisco's Lipase 3 is an industrial enzyme of fungal origin, which has been developed for use in bread making to condition dough. A homology model of the three-dimensional structure of Lipase 3 was created and used to design mutants with a view to improved specific activity ('activity' mutants) and with decreased N-glycosylation ('glycosylation' mutants). A cDNA coding for Lipase 3 was isolated from *Aspergillus niger* RNA by RT-PCR and cloned into the pHIL-D2 vector to enable expression of the lipase in *Pichia pastoris*. Mutants were generated from the pHIL-D2 cDNA construct used as a template in the *dut⁻ ung⁻* method of site-directed-mutagenesis. The expression of Lipase 3 variants by secretion from *Pichia pastoris* yeast was established. The expressed enzymes were analysed by SDS-PAGE and activity assays including the olive oil emulsion assay, in which a pH-stat was used to detect and monitor the release of fatty acids. SDS-PAGE and MALDI-TOF MS indicated that mutants with altered N-glycosylation sites did have reduced glycosylation on secretion by *Pichia pastoris*. Activity assays implied that mutation of these sites did not significantly affect the specific activity of Lipase 3.

Lipases expressed in *Pichia pastoris* (wild type Lipase 3, plus 'glycosylation' and 'activity' mutants), and those expressed in *Aspergillus niger* (wild type and 'glycosylation' mutants only) all gave sigmoidal curves when initial rates were plotted against substrate concentration. Hill plots indicated a positive co-operative mechanism with Hill coefficients for these enzymes between 2 and 4. It is however difficult to postulate a mechanistic explanation for this observation as this lipase does not appear to possess multiple catalytic binding sites.

After the Lipase 3 variants had been expressed by *Pichia pastoris* and kinetic analyses carried out using the olive oil emulsion substrate, enzymes that demonstrated the highest activity levels were sent to Danisco Ingredients (in Brabrand, Denmark) for in-dough assays and baking tests to assess their effectiveness as bread additives.

9.2 Evaluation of Lipase Mutants Expressed by *Pichia pastoris* in Model Dough Systems and Baking Trials

The wild type and mutants of Lipase 3 from expression in *Pichia pastoris* had been analysed with olive oil emulsion substrate. The olive oil assay was thought to provide an indication of the level of lipase activity that would occur in dough systems, as oleic acid (C18:1, cis-9) is very similar in structure to the main fatty acid of acyl lipids in wheat,

linoleic acid (C18:2, cis-9,12). From the specific activities and kinetic constants measured for these enzymes with olive oil substrate it was decided that likely candidates for possible use in bread making were the T112D E114Q 'activity' mutant and the 'glycosylation' mutants, which all retained activities comparable to wild type. Supernatants of *Pichia* cultures that expressed these mutant lipases, plus the wild type enzyme were sent to Danisco Ingredients in Denmark and were evaluated in model dough systems and baking tests by Dr. Jørn Børch Søe using methods routinely carried out in his laboratory. The results presented here for the 'glycosylation' mutants expressed in *Pichia* are also presented in a Technical Note prepared for Danisco Ingredients by Dr. Jørn Bøch Søe: TN573, journal no. 2133.

9.2.1 'Glycosylation' mutants tested in dough and bread

9.2.1.1 Free fatty acid release in dough

Fatty acid formation in dough was measured when the 'glycosylation' mutant and wild type lipases were used in a bread recipe. The enzymes were added as *Pichia* supernatants to the flour at concentrations between 0 and 10000 LU kg^{-1} (where one lipase unit, LU, is defined as the quantity of enzyme that will liberate 1 μmol of butyric acid per minute when tributyrin is the triacylglycerol substrate). Fully proofed dough was frozen and ground. Free fatty acids were extracted using water-saturated butanol and analysed as copper salts in isooctane measured at 715 nm and quantified according to an oleic acid calibration curve (Kwon and Rhee, 1986). A clear correlation between enzyme dosage and fatty acid release was seen for all the tested enzymes, although the N269T and N59T N269T mutant enzymes gave a lower fatty acid response as a function of dosage compared with the other enzymes (Figure 9.1).

All the *Pichia* expressed lipases tested (wild type and 'glycosylation' mutants) were found to be active in dough systems. Most of the mutants showed the same level of activity as the wild type enzyme. The N269T single mutant and N59T N269T double mutant however were less active than the other lipase mutants. This had not been observed for the 'glycosylation' mutants expressed in *Aspergillus niger* when tested in dough and bread. Also, the wild type Lipase 3 from over-expression in *Aspergillus* showed very low activity. These differences could be due to different modes of glycosylation occurring in the two expression systems (*Pichia* and *Aspergillus*).

Figure 9.1 Fatty acid release in model dough with *Pichia* expressed lipase mutants. *Pichia* supernatants from expression of wild type and 'glycosylation' mutants of Lipase 3 were tested in model dough and the free fatty acids released were measured (experiments carried out by Danisco Ingredients). Lipases were added at concentrations of 500 – 10000 LUT kg^{-1} flour, where LU represents lipase units determined by activity measured with tributyrin substrate (LU = 1 μmol min^{-1}).

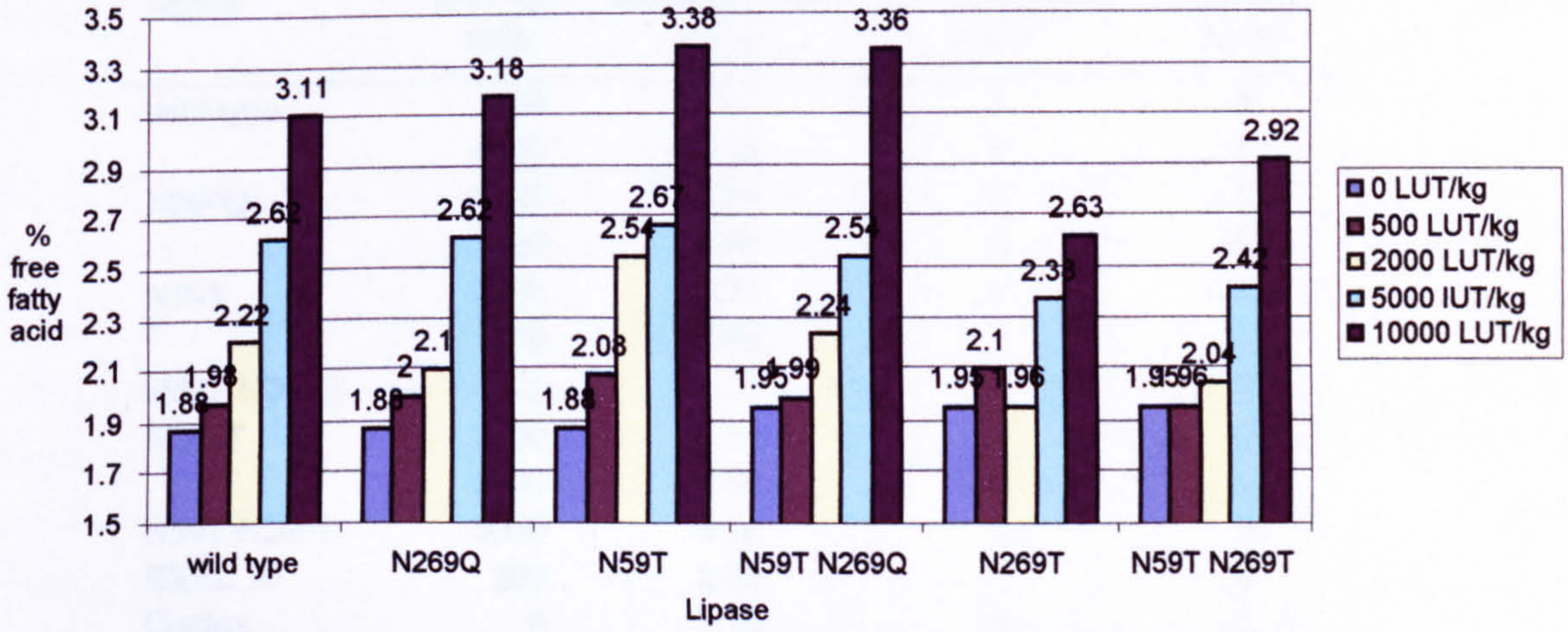

9.2.1.2 Baking tests

Based on the activity levels for the 'glycosylation' mutants in the model dough system, baking tests in hard crust rolls were carried out. The commercial product GRINDAMYL™ EXEL 16 was also tested as a reference. Samples of lipase were added to flour used in dough preparation to make hard crust rolls (2000 and 5000 LU kg^{-1}). As well as measuring the specific volumes of the rolls (ml g^{-1}), the extensibility and stickiness of the dough were evaluated after mixing and during moulding (on a scale of 1 to 10). The crumb structure was evaluated subjectively on a scale of 1 to 10 (from course to homogenous) and the crust and appearance were rated on a scale of 1 (coarse and gummy) to 10 (thin crust). These results are shown in Table 9.1.

For all the lipases tested, the extensibility and stickiness of the dough during mixing and moulding was no different from the control dough (score = 5), which had no added lipase. The crust and crumb structure both improved with added lipase and the observed effects were similar to those for the wild type lipase from *Pichia* (Table 9.1). No significant differences to the specific volume (ml g^{-1}) of the bread were seen on addition of lipase (Table 9.1). The effect of lipases was on the crust and crumb structure only, and did not result in any major changes to the bread volume.

Table 9.1 Results of baking experiments with *Pichia* expressed lipase variants and the GRINDAMYL™ EXEL 16 commercial enzyme. Crust and appearance were rated on a scale of 1 (coarse) to 10 (thin crust). Crumb structure was also evaluated on a scale of 1 (coarse) to 10 (homogenous). (Results obtained from Danisco Ingredients).

Lipase	LUT kg^{-1} flour	Specific volume $cm^3\ g^{-1}$	Crust/appearance score	Crumb score
wild type	2000	5.41	3	5
	5000	5.68	6	8
N269Q	2000	5.54	6	5
	5000	5.88	5	6
N59T	2000	5.77	4	4
	5000	5.85	7	7
N59T N269Q	4405	5.73	6	7
N269T	2000	5.50	4	6
	5000	5.69	6	6
N59T N269T	5000	5.39	6	7
EXEL 16	200	2.72	7	7
Control	0	5.78	2	2

The amounts of fatty acids released from these doughs, made using optimum dosages of the lipases were all of similar levels (Table 9.2) (although further testing is required for more accurate determination of optimum dosages). The N59T N269Q mutant showed slightly increased levels of released fatty acids over the levels measured for wild type enzyme. Again, levels of released fatty acids were all higher than those measured in control dough to which no lipase had been added and were also comparable to the result from a commercial product (EXEL 16).

Table 9.2 Analysis of free fatty acids in doughs used in baking tests with *Pichia* expressed lipases and GRINDAMYL™ EXEL 16 commercial lipase. Fully proofed dough from the baking tests (results shown in Table 9.1) was analysed for the presence of free fatty acids.

Lipase	LUT kg^{-1} flour	% free fatty acid
Wild type	2000	3.00
	5000	3.24
N269Q	2000	3.11
	5000	3.38
N269T	2000	2.98
	5000	3.31
N59T	2000	3.06
	5000	3.52
N59T N269Q	4400	3.98
N59T N269T	5000	3.21
EXEL 16	1000	2.74
Control	0	1.98

Overall, the baking tests in hard crust rolls gave very similar results with all the 'glycosylation' mutants expressed in *Pichia* and confirmed the typical lipase effect in bread in terms of improved stability and a fine homogenous crumb structure when compared to a control with no added lipase. The results also showed that using optimum dosages, the baking effects of the lipase 'glycosylation' mutants from *Pichia pastoris* were on a level with a commercial product GRINDAMYL™ EXEL 16.

9.2.2 The T112D E114Q 'activity' lipase mutant tested in dough and bread

The T112D E114Q double mutant expressed in *Pichia pastoris* was also tested in model dough and baking tests. The specific activity of this enzyme with olive oil emulsion substrate was 70 % of the wild type level. The effect on fatty acid formation in dough was tested using 0 – 10000 LU kg^{-1} flour of T112D E114Q and wild type enzymes (results are shown in Figure 9.2). The T112D E114Q mutant did not appear to be active in dough. Baking tests in hard crust rolls were also carried out with this mutant (Table 9.3). Extensibility and stickiness were the same as wild type levels, which were similar to control scores. The specific volumes also did not differ significantly from the control. The crust and crumb scores were found to be low; the mutant was no different from the control bread and the wild type showed only slight improvement at the dosage used in this test. Overall, the T112D E114Q mutant expressed in *Pichia* did not appear to be active in dough and did not have any dough-conditioning effect when used in baking tests. This was despite its relatively high specific activity with olive oil substrate (compared to the wild type level).

Figure 9.2 Fatty acid release in model dough with *Pichia* expressed wild type and T112D E114Q mutant lipase. *Pichia* supernatants from expression of wild type and T112D E114Q double mutant of Lipase 3 were used in model dough and the free fatty acids dough were measured. Lipase was added at concentrations of 500 – 10000 LUT kg^{-1} flour (LU = 1 μmol min^{-1}).

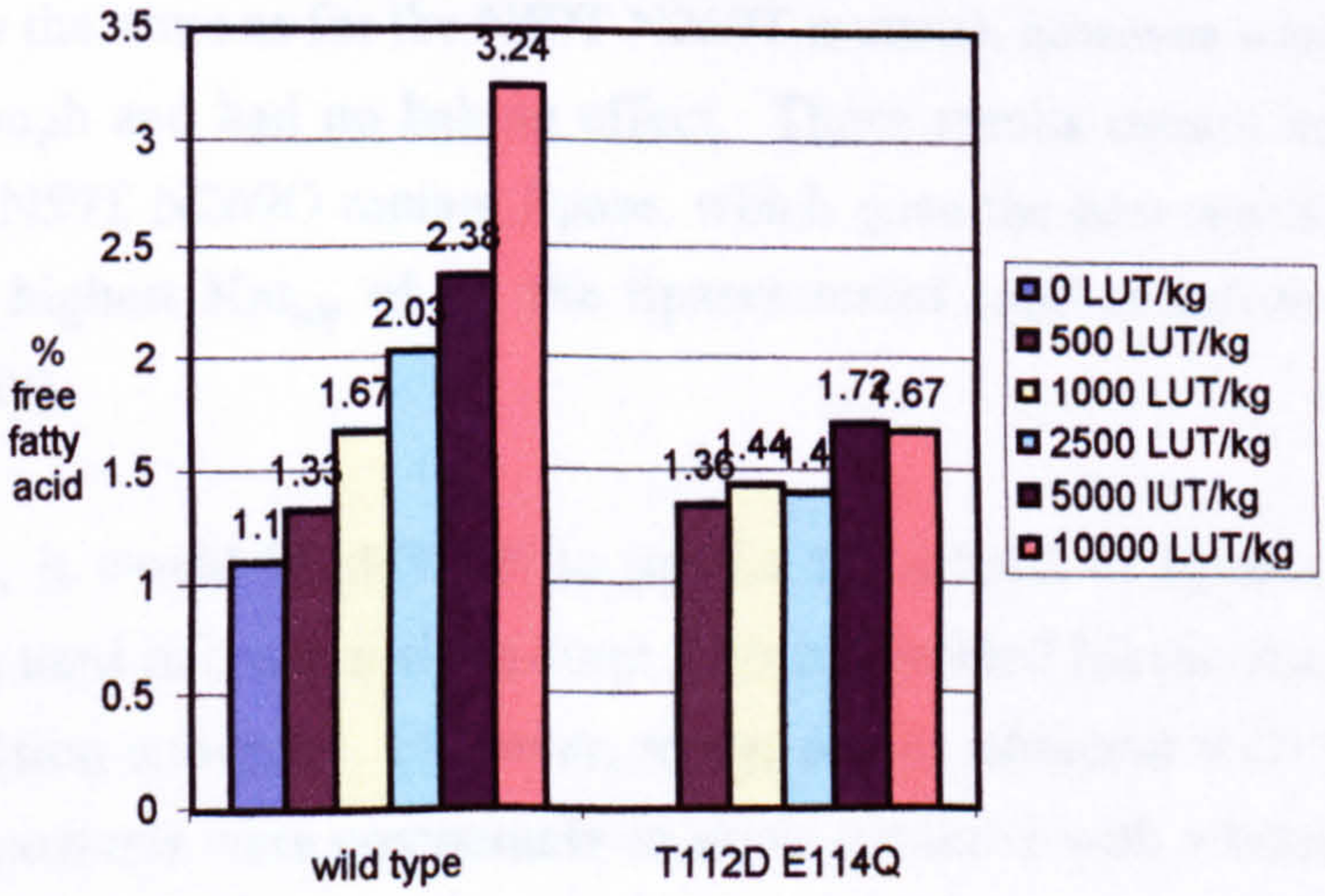

Table 9.3 Result of baking tests in hard crust rolls with wild type and T112D E114Q lipase mutant from expression in *Pichia pastoris*. (For explanation of scores see legend for Table 9.1).

Lipase	LUT kg^{-1} flour	Specific volume $cm^3\ g^{-1}$	Crust/appearance score	Crumb score
wild type	3000	5.46	3	4
T112D E114Q	3000	5.02	2	3
Control	0	5.12	2	2

9.2.3 The *Pichia pastoris* Yeast System for Expressing Lipase 3 Variants

When the specific activities of the mutant enzymes tested in bread were measured with olive oil substrate, all except the N59T N269T and N59T N269Q double 'glycosylation' mutants had high activities (at least 70 % the activity of the wild type enzyme). The two double mutants (N59T N269T and N59T N269Q) had specific activities that were half the level shown by the wild type. On kinetic analysis, the N59T N269Q mutant actually had a V_{max} value that was the same as wild type (these results are presented in Chapters 6 and 7). All of the 'glycosylation' mutants and the wild type enzyme from expression in *Pichia* were active in dough and when tested in bread the results obtained using optimum dosages were comparable to those of the commercial product. The N59T N269Q mutant was the most active in dough and also gave the very good results in the baking test, in terms of crust appearance and crumb structure. The N59T N269T double mutant, which had the lowest activity with olive oil, was also one of the least active of the 'glycosylation' mutants in dough (Figure 9.1), however the results in baking tests were not significantly different from those obtained with the remaining mutant enzymes (Table 9.1). The V_{max} for the T112D E114Q mutant with olive oil was 65 % the value for the wild type enzyme (and approximately the same as for the N59T N269T mutant), however was found to be virtually inactive in dough and had no baking effect. These results cannot be correlated to Km_{app} values as the N59T N269Q mutant lipase, which gave the best results in dough and bread tests had the highest Km_{app} of all the lipases tested (and therefore the lowest apparent binding affinity).

In conclusion, it would be difficult to predict the effects of lipases expressed in *Pichia pastoris* when used in bread making from their determined kinetic constants measured with olive oil emulsion substrate. However, as the results obtained with the lipases expressed using *Pichia pastoris* were comparable to those obtained with a commercial product, this system would be suitable for the production of Lipase 3 to be used in bread. The N59T

N269Q mutant in particular appears to be the most effective. Also, as N-glycosylation is prevented at both sites in this lipase mutant, over-glycosylation (N-linked) would be completely prevented on industrial scale production of this enzyme.

9.3 Future Work

9.3.1 Kinetic analysis

Alternative assay methods to the pH-stat technique may provide further information on the mechanism of lipase action. Also, a kinetic investigation of lipase variants using alternative methods to the pH-stat assay with olive oil substrate would indicate whether or not the sigmoidal kinetic curves (indicating co-operativity) are reproducible. One method used for measuring lipase activity is the monolayer method. This involves the use of a zero-order trough composed of a substrate reservoir and a reaction compartment containing the enzyme solution (Schmid and Verger, 1998). The two compartments, each covered with a monomolecular lipid film, are connected to each other by a narrow surface canal made in etched glass. A constant surface pressure of the film can be maintained automatically with a continuous supply of substrate. The rate of hydrolysis of lipid films spread at the air/water interface can be measured by monitoring one of several physicochemical parameters characteristic of the monolayer film (surface pressure, potential, area, etc.). Using the zero-order trough it is possible to obtain accurate pre-steady-state kinetic measurements with minimal perturbation from reaction products. Another method that has been used to study lipase kinetics of long-chain triacylglycerol hydrolysis is the 'oil-drop method' (Flipsen *et al.* 1996). The oil-water interfacial tension can be calculated from the drop profile. The decrease in interfacial tension can be related to lipase adsorption to an oil-drop and the hydrolysis of a long-chain triacylglycerol.

9.3.2 Glycosylation

The exact nature of glycan groups attached to lipases on secretion by *Pichia pastoris* cannot be determined from the results of mass spectrometry alone. An analysis of these oligosaccharide groups would therefore be useful. Oligosaccharides can be removed from glycoproteins enzymatically. Examples of such enzymes are peptide N-glycosidase (PNGase F) that cleaves Asn-linked oligosaccharides, O-glycosidase that cleaves Ser- and Thr-linked Gal (β 1,3) GalNAc (α 1) O-linked groups and N-acetylneuraminase (NANase II) that releases α 2-3 and α 2-6 N-acetylneuraminic acids (sialic acid). This can be followed by SDS-PAGE or mass spectrometry to compare intact glyco-protein with deglycosylated protein. Individual enzymes can be chosen to determine the type of

oligosaccharides present. Using kits that allow the isolation and profiling of N-linked oligosaccharides, the number of different N-linked oligosaccharides attached to a protein can be determined: for example, after enzymatic release, N-linked oligosaccharides can be fluorescently labelled, separated by SDS-PAGE and imaged using a UV transilluminator (Bio-rad literature for Glyco Analysis Kits, 1999). Each labelled and isolated N-linked oligosaccharide can then be structurally characterised by oligosaccharide sequencing, involving the sequential enzymatic digestion of a number of samples of the isolated oligosaccharides with exoglycosidases, followed by SDS-PAGE of digestion products and analysis using an imager.

9.3.3 Further Mutants of Lipase 3

Molecular modelling and site-directed-mutagenesis studies have been used to elucidate the roles of a number of key residues involved in the catalytic mechanisms of several lipases (Beer *et al.* 1996, Martinelle *et al.* 1996, Derewenda *et al.* 1994, Joeger and Haas, 1994, Holmquist *et al.* 1993). The results of such studies could be useful in the design of further mutants of Lipase 3, both in predicting the effects of proposed mutations and in the design of entirely new mutants with improved functions. For example, the Glu 87 residue in *Humicola lanuginosa* fungal lipase (also present in Lipase 3) and Arg 86 in the lipases of *Rhizomucor miehei* (*Rm*L) and *Rhizomucor delemar* (*Rd*L) have been demonstrated to play a role in stabilising the open enzyme via electrostatic interactions with the cortex of the protein (Martinelle *et al.* 1996, Peters *et al.* 1997, Norin *et al.* 1993). In particular, the positive Arg 86 residue of *Rm*L and *Rd*L interacts with a negative surface aspartate (Asp 61) (Peters *et al.* 1997). The lid tryptophan at position 89 of *Humicola lanuginosa* lipase (again, also in Lipase 3) and position 88 in *Rm*L appears to bind to the scissile acyl chain of an acylglycerol substrate, positioning it for catalysis. These two residues were targeted in the 'activity' mutants of Danisco's Lipase 3 (as E114Q and W116A mutations) and their functional roles were also discussed in Chapter 7. The roles of several other residues in lipases have been inferred from experimental and computational studies. In particular, the importance of two lid residues (Ser/Thr and Asn) present in fungal lipases that share high sequence homology with Lipase 3 have also been demonstrated and are described briefly below: -

(1) *Ser 83* The serine residue present at position 83 in *Humicola lanuginosa* lipase (and Lipase 3), and in *Rhizomucor miehei* lipase at position 82 is present in the hinge region of the lipase lid and forms part of the oxyanion hole (Derewenda *et al.* 1994, Joeger and Haas, 1994, Beer *et al.* 1996). The serine is orientated on opening to stabilise the

oxyanion intermediate (via the amide nitrogen and hydroxyl group of the side chain). In the lipases of *Rhizomucor oryzae* (*Ro*L) and *Rhizomucor delemar* (*Rd*L), the equivalent residue in this position is threonine (Thr 82 and Thr 83 respectively). Thr 83 Ser mutants of *Rd*L (Joeger and Haas, 1994) and *Ro*L (Beer *et al.* 1996) had 2 - 8 fold decreased activities. Although the serine hydroxyl group could partially substitute for the threonine hydroxyl group, it appeared that the difference in positioning of the side chains of the two amino acids was significant enough to reduce the specific activity of this mutant. Also, molecular dynamic simulations carried out for *Ro*L suggest that a serine in this position has a higher tendency to form a hydrogen bond to Asp 91 than to the oxyanion, compared with a threonine (believed to enhance the breakdown of the tetrahedral intermediate) (Beer *et al.* 1996).

(2) *Asn 92* An asparagine residue is present at position 92 in *Humicola lanuginosa* lipase (and Lipase 3). In *Rhizomucor oryzae* (*Ro*L) and *Rhizomucor miehei* (*Rm*L) lipases an aspartate is present in this position (Asp 91). From the crystal structures of inhibited *Rm*L and *Ro*L, Asp 91 is hydrogen bonded to the hydroxyl group of Ser 82/Thr 82 residues of the oxyanion hole, respectively (Beer *et al.* 1996). When the first tetrahedral intermediate forms, the Ser/Thr side chain re-orientates to hydrogen bond to the oxyanion. Reformation of the Thr-OH Asp-O^- hydrogen bond promotes the breakdown of the tetrahedral intermediate. Also, as Asp 91 is the only non-hydrophobic residue lying inside the fatty acid binding pocket of the open lipase, it could help to remove the negative fatty acid product from the binding pocket by unfavourable electrostatic interactions. An Asp 91 Asn mutant of *Ro*L was found to have 7.2 % residual wild type activity (Beer *et al.* 1996). The effect was explained by Asn forming a weaker hydrogen bond to Thr 82, which causes the breakdown of the first tetrahedral intermediate to be energetically less favourable because reformation of the hydrogen bond between Thr 82 and residue 91 (Asn) is less favourable than in the wild type. There is also a greater probability of Asn causing a conformation that blocks the hydrophobic pocket than Asp. A similar effect is seen for Thr 82 Ala/Val mutants of *Ro*L which were also generated; the mutated residue can no longer bind to Asp 91, which results in a destabilising effect as Asp 91 then blocks binding of fatty acid chains. These mutants have residual activities of 0.04 %.

In light of these observations, mutation of Asn 92 to Asp in Lipase 3 may result in improved specific activity as a stronger hydrogen bond between Asp 92 and Ser 83 of the oxyanion hole may promote the breakdown of the tetrahedral intermediate. A decrease in

Km could also be expected, as the stronger interaction with Ser 83 may reduce the possibility of this residue (Asp) blocking the hydrophobic pocket.

For this research project, the rational design of Lipase 3 mutants from a homology model to improve specific activity was not successful. A more effective method may be to generate mutants by random mutagenesis of the lipase gene followed by screening of expressed enzymes for those with improved properties. For successful engineering of an enzyme using this 'directed evolution' method, an established method of expression and secretion is required, as well as a suitable and efficient screening system for the desired properties. The rhodamine B plate assay of lipase activity may be used to rapidly screen *Pichia pastoris* transformants that secrete lipase, to detect those with enhanced activity. However an alternative method to spheroplast-generation must be used to transform the mutagenised DNA, as multiple integration into the *Pichia* genome can occur with this method (and so activity levels could not be reliably compared on rhodamine B plates). DNA sequencing can be used to identify mutations. Further improvements may be made by mutagenesis at the identified positions, or from additional rounds of random mutagenesis. Recently, evolutionary screening methods have been used to generate *Rhizomucor miehei* lipase mutants with modified properties from expression in *Pichia pastoris* (Gaskin *et al.* 1997).

For industrial production of Lipase 3, directed evolution involving random mutagenesis of the Lipase 3 gene may provide a quicker and simpler method for the generation of mutants with altered properties than the rational design of mutants from a homology model, provided an efficient screening procedure is used. In combination with computational studies of the Lipase 3 homology model structure and site-directed-mutagenesis of the lipase gene, altered residues may be identified and structural explanations obtained for the observed results. In this way, further light may be shed on the roles of individual residues in the mechanism of lipolysis, and in turn allow specific mutations to be made to give desired changes to enzyme characteristics.

APPENDIX A Materials, Media and Solutions

A1 Suppliers

Media components were purchased from Oxoid (Basingstoke, UK) except for Yeast Nitrogen Base, from Difco (Oxford, UK). Antibiotics and chemicals were purchased form Sigma and BDH (Poole, UK). Oligonucleotide primers were purchased from Life Technologies Inc. (Paisley, UK), as were molecular biology enzymes and reagents unless otherwise stated. The SDS-PAGE mini gel system, transblot apparatus and the Benchmark microplate reader were from Bio-Rad (Hemel Hempstead, UK). FPLC equipment and HiTrap columns were purchased from Amersham Pharmacia Biotech (Little Chalfont, UK). Thermal-Cyclers and ABI DNA Sequencer were from Perkin-Elmer (Warrington, UK). Sorvall Superspeed and Heraeus benchtop centrifuges are supplied by Kendro Laboratory Products Limited (Bishop's Stortford). The *Pichia pastoris* protein expression system (strain, vector, reagents etc.) is supplied by Invitrogen (Carlsbad, CA, USA). The pHM-290 pH-stat controller, microelectrodes and ABU901 autoburette were purchased from Radiometer (Crawley, UK).

A2 Strain Genotypes

A2.1 *E. coli* strains

SOLR *e*14$^-$(*mcr*A), Δ(*mcrCB-hsdSMR-mrr*)171, *sbcC*, *recB*, *recJ*, *uvrC*, *umuC* ::Tn5(kan^r), *lac*, *gyrA96*, *relA1*, *thi-1*, *endA1*, λ^R [F' *proAB*, *lac*I^{q}Z ΔM15, Tn*10*,(tet^r)] Su$^-$.

SURE *e*14$^-$(*mcr*A), Δ(*mcrCB-hsdSMR-mrr*)171, *sbcC*, *recB*, *recJ*, *uvrC*, *umuC* ::Tn5(kan^r), *uvrC*, *supE44*, *lac*, *gyrA96*, *relA1*, *thi-1*, *endA1* [F' *proAB*, *lac*I^{q}Z ΔM15, Tn*10*,(tet^r)]

CJ236 *dut*, *ung*, *thi*, *rel* A; pCJ105 (Cm^r).

TOP 10 F$^-$ *mcr*A Δ(*mrr-hsd*RMS-*mcr*BC) ϕ80*lac*ZΔM15, Δ*lac*X74, *rec*A1, *ara*D139,Δ(ara-leu)7697 galU *gal*K *rps* L (Str^R) *end*A1 *nup*G.

A2.2 *Pichia pastoris* Yeast Strain

GS115 *his 4*

A3 Media

A3.1 Bacterial Media

All bacterial media are made up in water and sterilised by autoclaving for 20 minutes.

Luria-Bertani Broth (L-Broth) (1 l)

10 g NaCl, 10 g tryptone, 15 g yeast extract, pH 7.

Luria-Bertani Agar (L-agar) (1 l)

10 g NaCl, 10 g tryptone, 5 g yeast extract, 15 g agar, pH 7.

SOB (1 l)

0.584 g NaCl, 20g tryptone, 5 g yeast extract, 0.186 g KCl, 2.465 g $MgSO_4$, 2.033 $MgCl_2$, pH 6.7 – 7.

A3.2 Stock Solutions for preparing Yeast Media

10 X D (dextrose) (100 ml)

20 g D-glucose in 100 ml water. Sterilise by autoclaving and store at room temperature.

10 X YNB (yeast nitrogen base) (100 ml)

14.4 g yeast nitrogen base without amino acids in 100 ml water. Filter sterilise, and store at 4 °C.

500 X B (biotin) (100 ml)

20 mg biotin in 100 ml water. Filter sterilise, and store at 4 °C.

100 X AA (amino acids) (100 ml)

500 mg each of L-glutamic acid, L-methionine, L-lysine, L-leucine and L-isoleucine in 100 ml water. Filter sterilise, and store at 4 °C.

10 X H (histidine) (100 ml)

400 mg L-histidine in 100 ml water. Filter sterilise, and store at 4 °C.

10 X GY (glycerol) (1 l)

Mix 100 ml glycerol with 900 ml water. Sterilise by autoclaving and store at room temperature.

10 X M (methanol) (100 ml)

5 ml methanol plus 95 ml water. Filter sterilise, and store at 4 °C.

A3.3 Yeast Media

YPD (1 l)

10 g yeast extract, 20 g peptone, 20 g D-glucose.
The yeast extract and peptone are dissolved in 900 ml water and autoclaved before adding 100 ml of 10 X D.

RDB (Regeneration Dextrose Base) plates (1 l)

186 g sorbitol, 20 g agar, 20 g D-glucose, 13.4 g yeast nitrogen base, 0.4 mg biotin, 50 mg each of L-glutamic acid, L-methionine, L-lysine, L-leucine and L-isoleucine.

186 g sorbitol and 20 g agar are mixed in 70 ml water and autoclaved, then cooled to 45 °C. To this, add a pre-warmed (45 °C) mixture of the following stock solutions: - 100 ml 10 X D, 100 ml 10 X YNB, 2 ml 500 XB and 10 ml 100 X AA, made up to 300 ml with water. Plates, poured immediately after mixing, can be stored at 4 °C.

RDHB (Regeneration Dextrose Base + Histidine) plates (1 l)

As for RDB, plus 40 mg L-histidine.

(10 ml 100 X H is included in the stock solutions added to the sorbitol and agar solution maintained at 45 °C).

RDB + 1 mM 3-AT (1 l)

As for RDB, plus 1 mM 3-amino triazole.

(1 ml 1 M 3-AT is included in the stock solutions added to the sorbitol and agar solution maintained at 45 °C).

RD (Regeneration Dextrose - top agar) (1 l)

As for RDB base plate (i.e. RDB, RDBH or RDB + 3-AT), except with 10 g agar.

MD (Minimal Dextrose) plates (1 l)

15 g agar, 20 g D-glucose, 13.4 g yeast nitrogen base, 0.4 mg biotin.

Mix 15 g agar with 800 ml water and autoclave. Cool to 60 °C, then add 100 ml 10 X YNB, 2 ml 500 X B and 100 ml 10 X D. Plates, poured immediately, can be stored at 4 °C.

MM (Minimal Methanol) plates (1 l)

15 g agar, 13.4 g yeast nitrogen base, 0.4 mg biotin, 5 ml methanol.

Prepared as for MD plates, 10 X M in place of 10 X D.

Rhodamine B plates (1 l)

20 g agar, 13.4 g yeast nitrogen base, 0.4 mg biotin, 5 ml methanol, 24 ml olive oil, 10 mg rhodamine B.

Mix 1 g agar in 40 ml water, autoclave and incubate at 55 °C. To this, add 5 ml 10 X YNB, 5 ml 10 X M, 0.1 ml 500 X B, 1.2 ml olive oil and 0.5 ml rhodamine B solution (1 mg ml^{-1} water). Shake vigorously and pour into 2 petri dishes immediately. Plates can be stored at 4 °C.

BMGY (Buffered Glycerol - complex Medium) (1 l)

10 g yeast extract, 20 g peptone, 0.1 M potassium phosphate buffer, pH 6, 13.4 g yeast nitrogen base, 0.4 mg biotin, 100 ml glycerol.

Mix 10 g yeast extract and 20 g peptone in 700 ml water and autoclave. Cool to room temperature before adding 100 ml 1 M potassium phosphate buffer pH6, 100 ml 10 X YNB, 2 ml 500 X B and 100 ml 10 X GY. Store at 4 °C.

BMMY (Buffered Methanol - complex Medium) (1 l)

10 g yeast extract, 20 g peptone, 0.1 M potassium phosphate buffer pH 6, 13.4 g yeast nitrogen base, 0.4 mg biotin, 5 ml methanol.

Prepare as for BMGY, adding 10 X M in place of 10 X GY.

A3.4 Media Additives

Chloramphenicol

A stock solution of 30 mg ml^{-1} is made up in 100% ethanol and stored at - 20 °C. The working concentration is 30 $\mu g\ ml^{-1}$.

Ampicillin

A stock solution of 50 mg ml^{-1} is made up in water, filter sterilised and stored at - 20 °C. The working concentration is 50 $\mu g\ ml^{-1}$.

Tetracycline

A stock solution of 5 mg ml^{-1} is made up in 100% ethanol is stored at - 20 °C. The working concentration is 5 $\mu g\ ml^{-1}$.

IPTG (isopropyl β-D thiogalactopyranoside)

A stock solution of 500 mM was made up in water and filter sterilised. For pBluescript vectors use 50 µl per 100 ml L-Agar.

Xgal (5-bromo 4-chloro 3-indolyl β - D - galactoside)

A stock solution of 250 mg ml^{-1} is made up in dimethylformamide. For pBluescript vectors, use 50 µl per 100 ml L-Agar.

A4 Solutions for Alkaline Lysis DNA Preparation

Solution A

50 mM glucose, 10 mM EDTA, 25 mM Tris, pH 8.
Sterilise by autoclaving.

Solution B

0.2 M NaOH, 1 % SDS.
Prepared when needed, from 10 % SDS and 10 M NaOH stock solutions.

Solution C

600 ml 5 M KOAc, 28.5 ml H_2O, 11.5 ml glacial acetic acid.
Sterilise by autoclaving.

T.E Buffer

10 mM Tris-HCl, pH 8, 1 mM EDTA pH 8.
Sterilise by autoclaving.

A5 Agarose Gel Electrophoresis Buffers

These buffers are prepared using distilled or reverse osmosis water.

TAE Buffer

40 mM Tris Acetate, 2 mM EDTA, pH 7.9.

TBE Buffer

40mM Tris Borate, 2 mM EDTA, pH 7.9.

A6 Restriction Digest Buffers

Life Technologies (Gibco) React 2

50 mM NaCl, 50 mM Tris-HCl, pH 8, 10 mM $MgCl_2$.

Life Technologies (Gibco) React 3

100 mM NaCl, 50 mM Tris-HCl, pH 8, 10 mM $MgCl_2$.

Promega Buffer C

50 mM KCl, 10 mM Tris-HCl, 7 mM $MgCl_2$, 1 mM DTT, pH 7.5

A7 Site-Directed-Mutagenesis Buffers

All of these buffers are filter sterilised and stored at – 20 °C in 1 ml aliquots.

10 X annealing buffer

0.2 M Tris-HCl pH 7.4, 0.02 M $MgCl_2$, 0.5 M NaCl.

T7 DNA Polymerase Dilution Buffer

20 mM potassium phosphate buffer, pH 7.4, 1 mM DTT, 0.1 mM EDTA and 50 % glycerol.

10 X synthesis buffer

5 mM each dNTP, 10 mM ATP, 100 mM Tris-HCl pH 7.4, 50 mM $MgCl_2$, 20 mM DTT.

A8 SDS-PAGE Solutions

5 X Running gel buffer (1 l)

7.5 g glycine, 15 g Tris, 5 g SDS in distilled water.

PBS (Phosphate Buffered Saline) (1 l)

0.14 M NaCl, 2.7 mM KCl, 10.1 mM Na_2HPO_4, 1.8 mM KH_2PO_4, pH 7.4.
Prepared from 10 X PBS (see below), made up in distilled water.

10 X PBS (1 l)

80 g NaCl, 2 g KCl, 18.1 g $Na_2HPO_4.2H_2O$, 2.4 g KH_2PO_4, pH 7.2-7.4

PBST (Phosphate Buffered Saline Tween)

1x PBS + 0.05 % (v/v) Tween 20.

APPENDIX B Lipase 3 cDNA Sequence

The coding strand of the cDNA clone for Danisco's Lipase 3 and translated amino acid sequence (as 3 letter codes). The 27 residue N-terminal signal sequence is included. The *Eco* RI restriction sites at either end of the sequence allowed the 1011bp fragment to be cloned into pCR-TOPO and pHIL-D2 vectors.

```
1                                                GAATTCGCCTCGATTGTTTGTATACCGCAAG

    Met Phe Ser Gly Arg Phe Gly Val Leu Leu Thr Ala Leu Ala Ala Leu Gly      17
32  ATG TTC TCT GGA CGG TTT GGA GTG CTT TTG ACA GCG CTT GCT GCG CTG GGT

    Ala Ala Ala Pro Ala Pro Leu Ala Val Arg Ser Val Ser Thr Ser Thr Leu      34
83  GCT GCC GCG CCG GCA CCG CTT GCT GTG CGG AGT GTC TCG ACT TCC ACG TTG

    Asp Glu Leu Gln Leu Phe Ala Gln Trp Ser Ala Ala Ala Tyr Cys Ser Asn      51
134 GAT GAG TTG CAA TTG TTC GCG CAA TGG TCT GCC GCA GCT TAT TGC TCG AAT

    Asn Ile Asp Ser Lys Asp Ser Asn Leu Thr Cys Thr Ala Asn Ala Cys Pro      68
185 AAT ATC GAC TCG AAA GAC TCC AAC TTG ACA TGC ACG GCC AAC GCC TGT CCA

    Ser Val Glu Glu Ala Ser Thr Thr Met Leu Leu Glu Phe Asp Leu Thr Asn      85
236 TCA GTC GAG GAG GCC AGT ACC ACG ATG CTG CTG GAG TTC GAC CTG ACG AAC

    Asp Phe Gly Gly Thr Ala Gly Phe Leu Ala Ala Asp Asn Thr Asn Lys Arg     102
287 GAC TTT GGA GGC ACA GCC GGT TTC CTG GCC GCG GAC AAC ACC AAC AAG CGG

    Leu Val Val Ala Phe Arg Gly Ser Ser Thr Ile Glu Asn Trp Ile Ala Asn     119
338 CTC GTG GTC GCC TTC CGG GGA AGC AGC ACG ATT GAG AAC TGG ATT GCT AAT

    Leu Asp Phe Ile Leu Glu Asp Asn Asp Asp Leu Cys Thr Gly Cys Lys Val     136
389 CTT GAC TTC ATC CTG GAA GAT AAC GAC GAC CTC TGC ACC GGC TGC AAG GTC

    His Thr Gly Phe Trp Lys Ala Trp Glu Ser Ala Ala Asp Glu Leu Thr Ser     153
440 CAT ACT GGT TTC TGG AAG GCA TGG GAG TCC GCT GCC GAC GAA CTG ACG AGC
```

Lys Ile Lys Ser Ala Met Ser Thr Tyr Ser Gly Tyr Thr Leu Tyr Phe Thr 170

491 AAG ATC AAG TCT GCG ATG AGC ACG TAT TCG GGC TAT ACC CTA TAC TTC ACC

Gly His Ser Leu Gly Gly Ala Leu Ala Thr Leu Gly Ala Thr Val Leu Arg 187

542 GGG CAC AGT TTG GGC GGC GCA TTG GCT ACG CTG GGA GCG ACA GTT CTG CGA

Asn Asp Gly Tyr Ser Val Glu Leu Tyr Thr Tyr Gly Cys Pro Arg Ile Gly 204

593 AAT GAC GGA TAT AGC GTT GAG CTG TAC ACC TAT GGA TGT CCT CGA ATC GGA

Asn Tyr Ala Leu Ala Glu His Ile Thr Ser Gln Gly Ser Gly Ala Asn Phe 221

644 AAC TAT GCG CTG GCT GAG CAT ATC ACC AGT CAG GGA TCT GGG GCC AAC TTC

Arg Val Thr His Leu Asn Asp Ile Val Pro Arg Val Pro Pro Met Asp Phe 238

695 CGT GTT ACA CAC TTG AAC GAC ATC GTC CCC CGG GTG CCA CCC ATG GAC TTT

Gly Phe Ser Gln Pro Ser Pro Glu Tyr Trp Ile Thr Ser Gly Asn Gly Ala 255

746 GGA TTC AGT CAG CCA AGT CCG GAA TAC TGG ATC ACC AGT GGC AAT GGA GCC

Ser Val Thr Ala Ser Asp Ile Glu Val Ile Glu Gly Ile Asn Ser Thr Ala 272

797 AGT GTC ACG GCG TCG GAT ATC GAA GTC ATC GAG GGA ATC AAT TCA ACG GCG

Gly Asn Ala Gly Glu Ala Thr Val Ser Val Val Ala His Leu Trp Tyr Phe 289

848 GGA AAT GCA GGC GAA GCA ACG GTG AGC GTT GTG GCT CAC TTG TGG TAC TTT

Phe Ala Ile Ser Glu Cys Leu Leu Stop 297

899 TTT GCG ATT TCC GAG TGC CTG CTA TAA CTAGACCGACTGTCAGATTAGTGGACGGGAG

957 AAGTGTACATAAGTAATTAGTATATAATCAGAGCAACCCAGTGGTGGTGATGGTGGAATTC

References

Ainslie, G. R. Jr., Shill, J. P. and Neet, K. E. (1972) Transients and Cooperativity. A slow transition model for relating transients and cooperative kinetics of enzymes. The Journal of Biological Chemistry. **247**:7088-7096

Autio, K. and Laurikainen, T. (1997) Relationships between flour/dough microstructure and dough handling and baking properties. Trends in Food Science and Technology. **8**: 181-185

Beer, H. D., Wohlfahrt, G., McCarthy, J. E. G., Schomburg, D. and Schmid, R. D. (1996) Analysis of the catalytic mechanism of a fungal lipase using computer-aided design and structural mutants. Protein Engineering. **9**: 507-517

Belitz, H. D. and Grosch, W. (Eds.) (1987) Food Chemistry. Springer-Verlag, Berlin, Heidelberg. (1st Edition; translation from the German second edition).

Belitz, H. D. and Grosch, W. (Eds.) (1999) Food Chemistry. Springer-Verlag, Berlin, Heidelberg. (2nd Edition).

Benzonana, G. and Desnuelle, P. (1965) Etude cinétique de l'action de la lipase pancréatique sur des triglycérides en émulsion. Essai d'une enzymologie en milieu hétérogène. Biochimica et Biophysica Acta. **105**:121-136

Bernstein, F. C., Koetzle, T. F., Williams, G. J. B., Meyer, E. F., Jr, Brice, M. D., Rodgers, J. R., Kennard, D., Shimanouchi, T. and Tasumi, M. (1997) The Protein Data Bank: a computer-based archival file for macromolecular structures. Journal of Molecular Biology. **112**:535-542

Bio-rad Literature (1999) Glycoprotein and Carbohydrate Analysis. www.bio-rad.com

Björkling, F., Godtfredsen, S. E. and Kirk, O. (1991) The future impact of industrial lipases. Trends in Biotechnology. **9**:360-363

Blow, D. (1990) More of the catalytic triad. Nature. **343**:694-695

Bradford, M. M. (1976) A rapid and sensitive method for the quantitation of microgram quantities of protein utilising the principle of protein-dye binding. Analytical Biochemistry. **72**: 248-254

Brady, L., Brzozowski, A. M., Derewenda, Z. S., Dodson, E., Dodson, G., Tolley, S., Turkenburg, J. P., Christiansen, L., Huge-Jensen, B., Norskow, L., Thim, L. and Menge, U. (1990) A serine protease triad forms the catalytic centre of a triacylglycerol lipase. Nature. **343**: 767-770

Brenner, S. (1988) The molecular evolution of genes and proteins: a tale of two serines. Nature **334**: 528-530

Brockerhoff, H. and Jensen, R. G. (eds.) (1974) Lipases *in* 'Lipolytic Enzymes'. Academic press, New York. pp 25-27

Brockman, H. L. (1984) in 'Lipases' (Borgstrom, B, and Brockman, H. L, eds.). Elsevier Science Publisher B. V, Amsterdam, The Netherlands. pp 13 - 29

Brzozowski, A. M., Derewenda, U., Derewenda, Z. S., Dodson, G. G., Lawson, D. M., Turkenburg, J. P., Bjorkling, F., Huge-Jensen, B., Patkar, S. A. and Thim, L. (1991) A model for interfacial activation in lipases from the structure of a fungal lipase-inhibitor complex. Nature. **351**: 491-494

Carrière, F., Withers-Martinez, C., van Tilbeurgh, H., Roussel, A., Cambillau, C. and Verger, R. (1998) Structural basis for the substrate selectivity of pancreatic lipases and some related proteins. Biochimica et Bioiphysica Acta **1376**:417-432

Chang, R-C., Chen, J. C., and Shaw, J-F. 1996) Studying the Active Site pocket of *Staphylococcus hyicus* Lipase by Site-Directed Mutagenesis. Biochemical and Biophysical Research Communications. **229**:6-10

Clare, J. J., Rayment, F. B., Ballantine, S.P., Sreekrishna, F. and Romanos, M.A. (1991) High-level expression of tetanus toxin fragment C in *Pichia Pastoris* strains containing multiple tandem integrations of the Gene. Biotechnology. **9**: 455-460

Clare, J. J., Romanos, M. A., Rayment, F. B., Roweder, J. E., Smith, M. A., Payne, M. M., Sreekrishna, K. and Henwood, C. A. (1991) Production of mouse epidermal growth factor in yeast: high-level secretion using *Pichia pastoris* strains containing multiple gene copies. Gene. **105**:205-212

Cornish-Bowden, A. and Cardenas, M. L. (1987) Co-operativity in Monomeric Enzymes. Journal of Theoretical Biology. **124**:1-23

Cregg, J. M., Vedvick, T. S. and Raschke, W. C. (1993) Recent Advances in the Expression of Foreign Genes in *Pichia pastoris*. Biotechnology. **11**:905-910

Creighton, T. E (1993) Proteins: Structures and Molecular Properties. W. H. Freeman and Company, New York. (2nd Edition) pp 91-93; 253-258; 368-374; 396-403

Cygler, M. and Schrag, J. D. (1997) Structure as Basis for Understanding Interfacial Properties of Lipases. Methods in Enzymology. **284**:3-27

Cygler, M., Grochulski, P. Kazlauskas, R. J., Schrag, J. D., Bouthillier, F., Rubin, B., Serreqi, A. N. and Gupta, A. K. (1994) A structural basis for the chiral preferences of lipases. Journal of the American Chemical Society. **116**: 3180-3186

Dente, L., Cesareni, G. and Cortese, R. (1983) pEMBL: a new family of single stranded plasmids. Nucleic Acids Research. **11**:1645-1655

Derewenda, U., Brzozowski, A. M., Lawson, D. M. and Derewenda, Z. S. (1992) Catalysis at the interface: The anatomy of a conformational change in a triglyceride lipase. Biochemistry. **31**: 1532-1541

Derewenda, U., Swenson, L., Green, R., Wei, Y., Dodson, G. G., Yamaguchi, S., Haas, M. J. and Derewenda, Z. S. (1994) An unusual buried polar cluster in a family of fungal lipases. Nature Structural Biology. **1**: 36-47

Derewenda, U., Swenson, L., Wei, Y., Green, R., Kobos, P. M., Joerger, R., Haas, M. J. and Derewenda, Z. S. (1994) Conformational lability of lipases observed in the absence of an oil-water interface: crystallographic studies of enzymes from the fungi *Humicola lanuginosa* and *Rhizopus delemar*. Journal of Lipid Research. **35**: 524-534

Desnuelle, P. (1972) The Lipases *in* 'The Enzymes Vol. VII' 3rd Edition (Boyer P D, ed.). Academic press, New York. pp 575-615

Dotto, G. P., Enea, V. and Zinder, N. D. (1981) Functional analysis of bacteriophage f1 intergenic region. Virology. **114**:463-473

Dugi, K. A., Dichek, H. L., Talley, G. D., Brewer, H. B. and Santamarina-Fojo, S. (1992) Human lipoprotein lipase: The loop covering the catalytic site is essential for interaction with lipid substrates. The Journal of Biological Chemistry. **267**: 25086-25091

Egloff, M., Marguet, F., Buono, G., Verger, R., Cambillau, C. and van Tilbeurgh, H. (1995) The 2.46 Å Resolution Structure of the Pancreatic Lipase-Colipase Complex Inhibited by a C11 Alkyl Phosphonate. Biochemistry. **34**: 2751-2762

Ferrato, F., Carrière, F., Sarda, L. and Verger, R. (1997) A Critical Reevaluation of the Phenomenon of Interfacial Activation. Methods in Enzymology. **286**:327-347

Fersht, A. L. (1985) Enzyme Structure and Mechanism. W. H Freeman and company, New York. (2nd Edition) pp 27-28, 47-78, 98-106, 265-278

Gan, Z., Ellis, P.R. and Scholfield, J. D. (1995) Gas Cell Stabilisation and Gas Retention in Wheat Bread Dough. Journal of Cereal Science. **21**: 215-230

Gaskin, D. J. H., Bovagnet, A. H., Turner, N. A. and Vulfson, E. N. (1997) Directed evolution of an industrially important enzyme. Biochemical Society Transactions. **23**:15S

Gatt, S. and Barenholz, Y. (1973) Enzymes of Complex Lipid Metabolism. Annual Review of Biochemistry. **42**:61-90

Gatt, S. and Bartfai, T. (1977) Rate Equations and Simulation Curves for Enzymatic Reactions Which Utilize Lipids as Substrates. I. Interaction of Enzymes With the Monomers and Micelles of Soluble, Amphiphilic Lipids. Biochimica et Biophysica Acta. **488**:1-12

Gatt, S. and Bartfai, T. (1977) Rate Equations and Simulation Curves for Enzymatic Reactions Which Utilize Lipids as Substrates. II. Effect of Adsorption of the Substrate or Enzyme on the Steady-State Kinetics. Biochimica et Biophysica Acta. **488**:13-24

Godfrey, T. (1996) Baking. Industrial Enzymology. Eds. Godfrey, T. and West, S. Macmillan Press Ltd., 25 Eccleston Place, London. (2nd Edition) Ch. 2.5: pp 89-101

Grochulski, P., Bouthillier, F., Kazlauskas, R. J., Serreqi, A. N., Schrag, J. D., Ziomek, E. and Cygler, M. (1994) Analogs of reaction intermediates identify a unique substrate binding site in *Candida rugosa* lipase. Biochemistry. **33**: 3494-3500

Guex, N. and Peitsch, M. C. (1997) SWISS-MODEL and the Swiss-PdbViewer: An environment for comparative protein modelling. Electrophoresis **18**:2714-2723. (http://www.expasy.ch/spdbv/mainpage.htm)

Haalck, L., Paltauf, F., Pleiss, J., Schmid, R. D., Spener, F. and Stadler, P. (1997) Stereoselectivity of Lipase from *Rhizopus oryzae* toward Triacylglycerols and Analogs: Computer-Aided Modeling and Experimental Validation. Methods In Enzymology. **284**:353-376

Haas, M. J., Cichowicz, D. J. and Bailey, D. G. (1992) Purification and Characterization of an Extracellular Lipase from the Fungus *Rhizopus delemar*. Lipids. **27**: 571-576

Hellinga, H. W. (1998) Computational protein engineering. Nature Structural Biology. **5**:525-527

Hjorth, A., Carrière, F., Cudrey, C., Woldike, H., Boel, E., Lawson, D. M., Ferrato, F., Cambillau, C., Dodson, G. G., Thim, L. and Verger R. (1993) A structural domain (the lid) found in pancreatic lipases is absent in the guinea pig (phospho)lipase. Biochemistry. **32**: 4702-4707

Holmquist, M. Tessier, D. C. and Cygler, M. (1997) Identification of Residues Essential for Differential Fatty Acyl Specificity of *Geotrichum candidum* Lipases I and II. Biochemistry. **36**:15019-15025

Holmquist, M., Martinelle, M., Clausen, I. G., Patkar, S., Svendsen, A., and Hult, K. (1994) Trp89 in the lid of *Humicola lanuginosa* lipase is important for efficient hydrolysis of tributyrin. Lipids. **29**: 599-603

Holzwarth, H. C., Pleiss, J. and Schmid, R. D. (1997) Computer-aided modelling of stereoselective triglyceride hydrolysis catalyzed by *Rhizopus oryzae* lipase. Journal of Molecular Catalysis B-Enzymatic. **3**:73-82

Honig, B. and Nicholls, A. (1995) Classical Electrostatics in Biology and Chemistry. Science. **268**:1144-1149

Hult, K. and Holmquist, M. (1997) Kinetics, Molecular Modeling, and Synthetic Applications with Microbial Lipases. Methods in Enzymology. **286**:386-405

Iwai, M., Tsujisaka, Y. and Fukumoto, J (1964) Studies on lipase III. Effect of calcium ion on the action of the crystalline lipase of *Aspergillus niger*. Journal of General Applied Microbiology. **10**:87-93

Iwai, M. and Tsujisake, Y. (1984) Fungal lipase in in 'Lipases' (Borgstrom, B, and Brockman, H. L, eds.). Elsevier Science Publisher B. V, Amsterdam, The Netherlands. pp 451-452

Inoue, H., Nojima, H. and Okayama, H. (1990) Gene **96**:23-28

Jackson, S., E. and Fersht, A. R. (1993) Contribution of long-range electrostatic interactions to the stabilisation of the catalytic transition state of the serine protease subtilisin BPN'. Biochemistry. **32**:13909-13916

Jaeger, K-E. and Reetz, M. T. (1998) Microbial lipases form versatile tools for biotechnology. Trends in Biotechnology. **16**:396-402

Jennens, M. L. and Lowe, M. E. (1994) A Surface Loop Covering the Active Site of Human Pancreatic Lipase Influences Interfacial Activation and Lipid Binding. The Journal of Biological Chemistry. **269**:25470-25474

Jensen, O. N., Shevchenko, A. and Mann, M. (1996) Protein analysis by mass spectrometry. Protein Structure, A Practical Approach. Ed. Creighton, T. E. IRL Press, Oxford University Press, Oxford. pp 29-57

Joerger, R. D. and Haas, M. J. (1994) Alteration of chain length selectivity of a *Rhizopus delemar* lipase through site-directed mutagenesis. Lipids. **29**: 377-384

Kazlauskas, R. J. (1994) Elucidating structure-mechanism relationships in lipases: prospects for predicting and engineering catalytic properties. Trends in Biotechnology. **12**:464-472

Kazlauskas, R. J., Weissfloch, A. N. E., Rappaport, A. T. and Cuccia, L. A. (1991) A Rule To Predict Which Enantiomer of a Secondary Alcohol Reacts Faster in Reactions Catalyzed by Cholesterol Esterase, Lipase from *Pseudomonas cepacia*, and Lipase from *Candida rugosa*. Journal of Organic Chemistry. **56**:2656-2665

Kornfeld, R. and Kornfeld, S. (1985) Assembly of Asparagine-Linked Oligosaccharides. Annual Review of Biochemistry. **54**:631-664

Kuchner, O. and Arnold, F. (1997) Directed evolution of enzyme catalysts. Trends in Biotechnology. **15**:523-530

Kunkel, T. A., Roberts, J. D. and Zakour, R. A. (1987) Methods in Enzymology (ed. Wu, R.) **154**: 367-382

Kwon, D. Y. and Rhee, J. A. (1996) A Simple and Rapid Colorimetric Method for Determination of Free Fatty Acids for Lipase Assay. Journal of the American Oil Chemists Society. **63**:89

Lawson, D. M., Brzozowski, A. M., Rety, S., Verma, C. and Dodson, G. G. (1994) Probing the nature of substrate binding in *Humicola lanuginosa* lipase through X-ray crystallography and intuitive modelling. Protein Engineering. **7**: 543-550

Lienhard, G. E. (1973) Enzymatic catalysis and transition-state theory. Science. **180**:149-154

Longhi, S., Mannesse, M., Verheij, H. M., Haas, G. H. de., Egmond, M., Knoops-Mouthuy, E. and Cambillau, C. (1997) Crystal structure of cutinase covalently inhibited by a triglyceride analogue. Protein Science. **6**: 275-286

Lookene, A., Groot, N. B., Kastelein, J. J. P., Olivecrona, G. and Bruin, T. (1997) Mutation of Tryptophan Residues in Lipoprotein Lipase. The Journal of Biological Chemistry. **272**:766-772

Mannesse, M. L., Cox, R. C., Koops, B. C., Verheij, H. M., Haas, G. H. de., Egmond, M. R., van der Hijden, H. T. W. M. and Vlieg, J. de. (1995) Cutinase from *Fusarium solani pisi* hydrolyzing triglyceride analogues. Effect of acyl chain length and position in the substrate molecule on activity and enantioselectivity. Biochemistry. **34**: 6400-6407

Marangoni, A. G. (1994) Enzyme Kinetics of Lipolysis Revisited: The Role of Lipase Interfacial Binding. Biochemical and Biophysical Research Communications. **200**:1321-1328

Martinelle, M. and Hult, K. (1994) Kinetics of triglyceride lipases *in* 'Lipases: Their Structure, Biochemistry and Application'. (Wooley, P. and Petersen, S, eds.). Cambridge University Press, Cambridge. pp 159-180

Martinelle, M., Holmquist, M., Clausen, I. G, Patkar, S. Svendsen, A. and Hult, K. (1996) The role of Glu87 and Trp89 in the lid of *Humicola lanuginosa* lipase. Protein Engineering. **9**: 519-524

Martinez, C., Geus, P. De., Lauwereys, M., Matthyssens, G. and Cambillau, C. (1992) *Fusarium solani* cutinase is a lipolytic enzyme with a catalytic serine accessible to solvent. Nature. **356**: 615-618

Matsudaira, P. (1987) Sequence from picomole quantities of proteins electroblotted onto polyvinylidene difluoride membranes. Journal of Biological Chemistry. **262**:10035-10038

Monfort, A., Blasco, A., Sanz, P. and Prieto, J. A. (1999) Expression of *LIP1* and *LIP2* Genes from *Geotrichum* species in Baker's yeast Strains and Their Application to the Bread-making Process. Journal of Agricultural and Food Chemistry. **47**:803-808

Montesino, R., Garcia, R., Quintero, O. and Cremata, J. A. (1998) Variation in N-Linked Oligosaccharide Structures on Heterologous Proteins Secreted by the Methylotrophic yeast *Pichia pastoris*. Protein Expression and Purification. **14**:197–207.

Neet, K. E. (1995) Cooperativity in Enzyme Function: Equilibrium and Kinetic Aspects. Methods in Enzymology. **249**:519-567

Neet, K. E. and Ainslie, R. (1980) Hysteretic Enzymes. Methods in Enzymology. **64**:192-226

Neet, K. E., Keenan, R. P. and Tippett, P. S. (1990) Observation of a Kinetic Slow Transition in Monomeric Glucokinase. Biochemistry. **29**:770-777

Norin, M., Olsen, O., Svendsen, A., Edholm, O. and Hult, K. (1993) Theoretical studies of *Rhizomucor miehei* lipase activation. Protein Engineering. **6**:855-863

Norin, M., Haeffner, F., Achour, A., Norin, T. and Hult, K. (1994) Computer modeling of substrate binding to lipases from *Rhizomucor miehei*, *Humicola lanuginosa*, and *Candida rugosa*. Protein Science. **3**:1493-1503

Ollis, D. L., Cheah, E., Cygler, M., Dijkstra, B., Frolow, F., Franken, S. M., Harel, M., Remington, S. J., Silman, I., Schrag, J., Sussman, J. L., Verschueren, K. H. G. and Goldman, A. (1992) The α/β hydrolase fold. Protein Engineering. **5**:197-211

Orengo, C. A., Michie, A. D., Jones, S., Jones, D. T., Swindells, M. B. and Thornton, J.M. (1997) CATH - A Hierarchic Classification of Protein Domain Structures. Structure. **5**:1093-1108 (http://www/biochem.ucl.ac.uk/bsm/cath/CATH.html)

Peters, G. H., Toxvaerd, S., Olsen, O. H. and Svendsen, A. (1997) Computational studies of the activation of lipases and the effect of a hydrophobic environment. Protein Engineering. **10**:137-147

Petersen, M. T. N., Martell, P., Petersen, E. I., Drabløs, F. and Petersen, S. B. (1997) Surface and Electrostatics of Cutinases. Methods in Enzymology. **284**:130-154

Pleiss, J. Fischer, M. and Schmid, R. D. (1998) Anatomy of lipase bindings sites: the scissile fatty acid binding site. Chemistry and Physics of Lipids. **93**:67-80

Poldermans, B. and Schoppink, P. (1999) Controlling the Baking Process and Product Quality with Enzymes. Cereal Foods World. **44**: 132-135

Prompers, J. J., Groenewegen, A., Hilbers, C. W. and Pepermans, H. A. M. (1999) Backbone Dynamics of *Fusarium solani pisi* Cutinase Probed by Nuclear Magnetic Resonance: The lack of Interfacial Activation Revisited. Biochemistry. **38**:5315-5327

Reetz, M. T. and Jaeger, K. E. (1998) Overexpression, immobilisation and biotechnological application of *pseudomonas* lipases. Chemistry and Physics of Lipids. **93**:3-14

Reetz, M. T. and Jaeger, K. E. (1999) Superior biocatalysts by directed evolution. Topics in Current Chemistry. **200**:31-57

Rogalska, E., Cudrey, C., Ferrato, F. and Verger, R. (1993) Stereoselective hydrolysis of triglycerides by animal and microbial lipases. Chirality. **5**:24-30

Russel, M., Kidd, S. and Kelley, M. R. (1986) An improved filamentous helper phage for generating single-stranded plasmid DNA. Gene. **45**: 33-338

Sali, A. and Blundell, T. L. (1993) Comparative Protein Modelling by Satisfaction of Spatial Restraints. Journal of Molecular Biology. **234**: 779-815

Sambrook, J., Fritsch, E. F. and Maniatis, T. (1989) Molecular Cloning: A laboratory manual, (2nd Edition) Plainview, New York: Cold Spring Harbor Laboratory Press. 1.25.

Sanger, F. S., Nicklen, S. and Coulson, A. R. (1977) DNA sequencing with chain-terminating inhibitors. Proceedings of the National Academy of Sciences of the United States of America. **74**: 5463-5467

Sarda, L. and Desnuelle, P. (1958) Action de la lipase pancréatique sur les esters en émulsion. Biochimica et Biophysica Acta. **30**: 512-521

Sarda, L., Marchis-Mouren, G. and Desnuelle, P. (1957) Sur les interactions de la lipase pancréatique avec les triglycérides. Biochimica et Biophysica Acta. **24**: 425-427

Scheib, H., Pleiss, J., Stadler, P., Kovac, A., Potthoff, A. P., Haalck, L., Spener, F., Paltauf, F. and Schmid, R. D. (1998) Rational design of *Rhizopus oryzae* lipase with modified stereoselectivity toward triradylglycerols. Protein Engineering. **11**:675-682

Schmid, R. D. and Verger, R. (1998) Lipases: Interfacial Enzymes with Attractive Applications. Angewandte Chemie. **37**: 1608-1633

Schrag, J. D. and Cygler, M. (1997) Lipases and α/β Hydrolase fold. Methods in Enzymology. **284**:85-107

Schrag, J. D., Li, Y., Wu, S. and Cygler, M. (1991) Ser-His-Glu triad forms the catalytic site of the lipase from *Geotrichum candidum*. Nature. **351**: 761-764

Sheffield, P. J., Bhat, K. M., Owen, J. O., Perry, B., Sumner, I. G. and Warwicker, J. (1995) Increased activity of porcine pancreatic phospholipase A_2 by designed long-range electrostatic stabilisation of the transition state. Biochemical and Biophysical Research Communications. **216**:778-784

Si, J. Q. (1996) New Enzymes for the Baking Industry (Ingredients). Food Technology Europe. March/April:60-64

Si, J. Q. (1997) Synergistic Effect of Enzymes for Breadbaking. Cereal Foods World. **42**: 802-807

Small, D. M. (1968) A Classification of Biologic Lipids Based upon Their interaction in Aqueous Systems. The Journal of the American Oil Chemists' Society. **45**:108-117

Sokolofsky. (1990) Neurospora Newsletter. **37**: 41

Stadler, P., Kovac, A., Haalck, L., Spener, F. and Paltauf, F. (1995) Stereoselectivity of microbial lipases. The substitution at position sn-2 of triacylglycerol analogs influences the stereoselectivity of different microbial lipases. European Journal of Biochemistry. **227**:335-343

Storer, A. C. and Cornish-Bowden, A. (1977) Kinetic Evidence for a 'Mnemonical' Mechanism for Rat Liver Glucokinase. Biochemistry Journal. **165**:61-19

Thirstrup, K., Verger, R. and Carrière, F. (1994) Evidence for a Pancreatic Lipase Subfamily with New Kinetic Properties. Biochemistry. **33**: 2748-2756

van Tilbeurgh, H., Egloff, M. P., Martinez, C., Rugani, N., Verger, R. and Cambillau, C. (1993) Interfacial activation of the lipase-procolipase complex by mixed micelles revealed by X-ray crystallography. Nature. **362**: 814-820

Verger, R and de Haas, G. H. (1976) Interfacial enzyme kinetics of lipolysis. Annual Review of Biophysics and Bioengineering. **5**: 77-117

Verger, R. (1980) Enzyme Kinetics of Lipolysis. Methods in Enzymology. **64**:340-392

Verger, R (1984) Pancreatic lipase in 'Lipases' (Borgstrom, B, and Brockman, H. L, eds.). Elsevier Science Publisher B. V, Amsterdam, The Netherlands. P 85

Verger, R., Mieras, M. C. E., and de Haas, G. H. (1973) Action of phospholipase A_2 at Interfaces. The Journal of Biological Chemistry. **11**: 4023-4034

Vulfson, E. N. (1994) in Lipases: their structure, biochemistry and application. Cambridge University Press. pp 271-288

Wang, Y. J., Sheu, J. Y., Wang, F. F. and Shaw, J. F. (1987) Lipase-Catalyzed Oil Hydrolysis in the Absence of Added Emulsifier. Biotechnology and Bioengineering. **31**: 628-633

Warburg, O. and Christian W. (1941) Isolierung und Kristallisation des Gärungsferments Enolase. Biochemika Zeitung. **310**: 384 - 421

Warshel, A. (1978) Energetics of enzyme catalysis. Proceedings of the National Academy of Sciences of the United States of America. **75**: 5250-5254

Warshel, A. (1981) Calculations of Enzymatic Reactions: Calculations of pKa, Proton Transfer Reactions, and General Acid Catalysis Reactions in Enzymes. Biochemistry. **20**: 3167-3177

Warshel. A., Naray-Szabo, G., Sussman, F., and Hwang, J.-K. (1989) How Do Serine Proteases Really Work? Biochemistry. **28**:3629-3637

Warwicker, J. and Watson, H. C (1982) Calculation of the Electric Potential in the Active Site Cleft due to α-Helix Dipoles. Journal of Molecular Biology. **157**:671-679

Winkler, F. K., D'Arcy, A. and Hunziker, W. (1990) Structure of human pancreatic lipase. Nature. **343**: 771-774

Yamaguchi, S., Takeuchi, K., Mase, T., Oikawa, K., McMullen, T., Derewenda, U., McElhaney, R. N., Kay, C. M., and Derewenda, Z. S. (1996) the consequences of engineering an extra disulfide bond in the *Penicillium camembertii* mono- and diglyceride specific lipase. Protein Engineering. **9**:789-795